Tübinger Hörforschungszentrum
Molekulare Hörphysiologie

in Zusammenarbeit mit

der Radiologischen Universitätsklinik Tübingen
Abteilung Diagnostische und Interventionelle Neuroradiologie

und

der Universitätsklinik für Psychiatrie und Psychotherapie
Tübingen, Abteilung Allgemeine Psychiatrie und
Psychotherapie mit Poliklinik

# Tinnitus with and without hyperacusis subclassified based on audiometry, gamma oscillations and haemodynamics

**Inaugural-Dissertation**
**zur Erlangung des Doktorgrades**
**der Humanwissenschaften**

**der Medizinischen Fakultät**
**der Eberhard Karls Universität**
**zu Tübingen**

**vorgelegt von**

**Wertz, Jakob**

**2024**

| | |
|---|---|
| Dekan: | Professor Dr. Bernd Pichler |
| 1. Berichterstatter: | Professorin Dr. M. Knipper-Breer |
| 2. Berichterstatter: | Professorin Dr. D. Thorwarth |
| Tag der Disputation: | 19.12.2023 |

# TABLE OF CONTENTS

# LIST OF FIGURES

# LIST OF TABLES

# LIST OF APPENDICES

# LIST OF ABBREVIATIONS

| Abbreviation | Description |
|---|---|
| 1/2/3...22 | NIRS optode montage |
| AAN | Ascending auditory nuclei |
| ANF | Auditory Nerve Fibre |
| ABR | Auditory brainstem response |
| AC | Auditory cortex |
| AC-I | Primary auditory cortex |
| AF | Auditory nerve fibres |
| AFz | EEG electrode montage (ground) |
| BA | Brodmann area |
| BB-chirp | Broadband chirp |
| BOLD | Blood oxygenation level-dependent |
| C | Control |
| CN | Cochlear nucleus |
| DL | Dorsolateral |
| EDPTs | Estimated distortion-product thresholds |
| EEG | Electroencephalography |
| EHF | Extended high-frequency |
| FDR | False discovery rate |
| fMRI | Functional magnetic resonance imaging |
| fNIRS | Functional near-infrared spectroscopy |
| GHS | Goebel-Hiller-Score |
| HF-chirp | High-frequency chirp |
| HKI | Hyperacusis inventory |
| HL | Hearing level |
| IC | Inferior colliculus |
| ICA | Independent component analysis |
| Ins | Insula |
| IPL | Inter-peak-latencies |
| LDL | Loudness discomfort levels |
| LF-chirp | Low-frequency chirp |

| Abbreviation | Description |
|---|---|
| LH | Left hemisphere |
| M | Medial |
| Mam. Body | Mammillary body |
| MGB | Medial geniculate body |
| MOC | Medial olivocochlear bundle |
| MTG | Middle temporal gyrus |
| nHL | Normalised hearing level |
| NIRS | Near-infrared spectroscopy |
| OLSA | Oldenburger Satztest |
| PFC | Prefrontal cortex |
| PO | Parietal operculum |
| PTA | Pure tone audiogram |
| PTA4 | Pure tone audiometry threshold average 0.5 – 4 kHz, better ear |
| PTA-EHF | Pure tone audiometry threshold average 11.2 – 16 kHz, better ear |
| PTA-HF | Pure tone audiometry threshold average 6 – 10 kHz, better ear |
| PTA-T | Pure tone audiometry threshold at tinnitus frequency |
| Quart | Quartile |
| RH | Right hemisphere |
| ROI | Region of interest |
| rs | Resting-state |
| rs-fMRI | Resting-state-fMRI |
| rs-fMRI-bfc | Resting-state-fMRI-based functional connectivity |
| SD | Standard deviation |
| SL | Sensation level |
| SOC | Superior olivary complex |
| SPL | Sound pressure level |
| STG | Superior temporal gyrus |
| T | Patients with Tinnitus |
| TD | Tinnitus duration |
| TH | Patients with Tinnitus and co-occurrent hyperacusis |

# 1. INTRODUCTION

## 1.1. Definition and aetiology of tinnitus & hyperacusis

Tinnitus, a symptom caused by a malfunction of the auditory system, is the conscious perception of sound in the absence of an external acoustic source (Knipper et al., 2020). With about one in seven adults (14.7 %) reporting symptoms, the prevalence of tinnitus in Europe is very high (Biswas et al., 2022). About 9 % of adult Germans report suffering from tinnitus occasionally (Statista, 2017). Tinnitus patients miss more than twice as much time from work as the average German employee. Apart from the individual burden for every single patient, the resulting high socioeconomic costs also demonstrate the urgency of research in the tinnitus field. There are numerous proposed causes for tinnitus like (i) severe noise exposure, (ii) ototoxic medication, (iii) infection or disease of the middle ear or tympanic membrane, (iv) Meniere's syndrome, (v) brain aneurysm, (vi) acoustic nerve tumour, or (vii) damage to the IHC/OHC (Biswas et al., 2023; Manche et al., 2016; Baguley et al., 2013; Kim et al., 2015). Causal treatment (in clinical routine) is very challenging, considering the neurophysiological basis of tinnitus development is poorly understood, and the hypothetical causes of tinnitus are still highly controversial. Due to the vast number of patients suffering from tinnitus, numerous therapeutic approaches have been introduced to relieve and cure tinnitus. Despite all these therapies, there is still no or insufficient evidence for most treatments (Hesse et al., 2022). The sole evidence-based therapeutic interventions recommended in the clinical guidelines are counselling and psychotherapeutic behavioural therapy, focusing on managing and coping with tinnitus rather than directly treating the tinnitus. From a scientific point of view and also for many patients, this situation is not acceptable since these techniques are only helpful for some.

To study tinnitus cure or relief, a precise classification and definition of tinnitus subtypes is essential: According to the International statistical classification of diseases ICD 10, tinnitus is categorised as tinnitus aurium (H93.1) and pulsatile tinnitus (H93.A, with subcategories unilateral (right, left), bilateral, and unspecified ear). The pulsatile and typically objectively measurable tinnitus is usually caused by audible vascular or muscular noises (Lockwood et al., 2002; Sismanis, 2003). In the presented thesis, only idiopathic tinnitus aurium was investigated; patients with pulsatile tinnitus were referred to the study physician for further treatment. Tinnitus is further divided into acute and chronic tinnitus. The S3 guideline chronic tinnitus (AWMF Register No. 017/064, as of September 2021) defines chronic tinnitus as tinnitus with a duration of at least three months. At the same time, the transitions between acute and chronic are referred to as "not static, but fluid"

(Hesse et al., 2022). For this research, however, precisely this transition period is of interest; we, therefore, include acute tinnitus subjects with a tinnitus duration (TD) of more than one month. The actual burden of a patient with tinnitus is highly variable. It can be determined as a severity score and is recommended to evaluate therapy indication and success (Hesse et al., 2022). In particular, a high tinnitus burden leads to a substantial loss in quality of life and an enormous socioeconomic burden (Kleinjung and Langguth, 2020; Haider et al., 2018; Michikawa et al., 2010; Hebert et al., 2013; Pattyn et al., 2016). As shown, tinnitus is not a uniform clinical entity but instead manifests in many rather distinct types. Since tinnitus burden particularly increases with comorbidities, diagnosis to identify the individually relevant concomitant symptoms is generally recommended according to clinical guidelines. This is of particular importance in tinnitus patients with hyperacusis, in whom high distress levels were found (Schecklmann et al., 2014; Vielsmeier et al., 2016). As animal studies also provided promising hints (Mohrle et al., 2019), we focus in the following studies on this comorbidity. Hyperacusis and other sound hypersensitivities have recently received more attention in research. Even in the clinic until now, only hyperacusis is included in the ICD 10 under "Other abnormal auditory sensations" (H93.23). Hyperacusis is defined as an increased sensitivity to sound wherein moderate sounds are perceived as too loud or even painful (Baguley, 2003) thought to be related to increased amplification of auditory signals in central auditory pathways (Norena, 2011). This sensitivity is only a matter of the physical properties of the sounds, the meaning of the sound and the context in which it occurs must be irrelevant (Jastreboff and Jastreboff, 2015). As there was no better explanation until now, it has been assumed that the increased sensitivity is related to an increased amplification of auditory signals in the central auditory pathways (Norena, 2011).

Compared to tinnitus, noise hypersensitivity is still a rather new topic of research. In particular, the separation of hyperacusis from other noise hypersensitivities is not yet understood. The known hypersensitivities are still in the process of clinical classification. Therefore, the classification used in the three papers presented in the present thesis was not the same. Approximately 90 % of hyperacusis patients report additional tinnitus (Aazh et al., 2014), whereas only about 40 % of tinnitus patients report additional hyperacusis (Baguley, 2003). Therefore, we can deduce that hyperacusis and tinnitus are strongly correlated, while tinnitus can also regularly occur independently. This correlation emphasises the relevance of the subsequent study of tinnitus subgroups separated into tinnitus only and with concomitant hyperacusis. However, since this distinction has been assessed in a minimal number of clinical studies, this may be one of the main reasons for the prevailing contradictory concepts about the pathophysiology and the neuronal

correlate of tinnitus. These contradictions could be one of the critical factors why causal tinnitus therapies have not been developed to date (Knipper et al., 2021).

## 1.2. Tinnitus – What is known so far? What is our hypothesis?

While it is generally accepted that tinnitus is linked to increased spontaneous firing rates following the deafferentation of auditory nerves (Bauer et al., 2007; Roberts et al., 2010; Weisz et al., 2006; Milloy et al., 2017; Guest et al., 2017; Gilles et al., 2016), it remains highly controversial how elevated spontaneous activity is translated to the tinnitus percept. While some studies suggest that after cochlear deafferentation, a homeostatic increase in neural gain generates central hyper-excitability (as a faulty compensatory mechanism), leading to tinnitus (Shore et al., 2016; Roberts and Salvi, 2019; Norena, 2011; Schaette and Kempter, 2012; Marks et al., 2018; Schaette and McAlpine, 2011; Yang and Bao, 2013; Yang et al., 2011; Noreña, 2015), more recent studies predict tinnitus develops when the reduced auditory input fails to increase neural gain, due to diminished stimulus-evoked responses (Rüttiger et al., 2013; Singer et al., 2013; Zeng, 2013; Hofmeier et al., 2018; Mohrle et al., 2019; Berlot et al., 2020; Zeng, 2020).

Based on the literature and previous work, we are convinced that a co-morbidity of tinnitus and hyperacusis obscure the identification of actual neural correlates leading to tinnitus. Consequently, the numerous efforts to develop advanced therapeutic concepts for tinnitus, whether through electric stimulation (Zeng et al., 2019), bimodal neuromodulation (Conlon et al., 2019; Conlon et al., 2020; Marks et al., 2018), or pharmacological treatments (Beebe Palumbo et al., 2015; Cederroth et al., 2018) have been hampered by our current lack of knowledge about the actual neural correlates of tinnitus. It has already been suggested that concomitant conditions such as hearing loss or hyperacusis contribute to the confounding effects due to superposition (Sedley, 2019). Therefore, in more recent studies, the groups were consistently matched to their hearing threshold, and patients with hyperacusis were excluded (Berlot et al., 2020; Joo et al., 2020). In the first publication reported here, we demonstrated that T- and TH-group, with clinically normal PTAs, can be discriminated by differing ABR latency and peak-to-peak amplitude, as well as by functional connectivity and haemodynamic auditory responses in the cortex (Hofmeier et al., 2021). Both are involved in attentional processes and their correlated acoustic contrast amplification (Knipper et al., 2020). As reviewed by Knipper (Knipper et al., 2020), γ-oscillations, which showed to be increased in chronic tinnitus [>30-45 Hz] (Weisz and Langguth, 2010), have recently been attributed an important role in tinnitus pathogenesis due to their connection to altered fast auditory processing and consequently modified

corticofugal feedback loops. Fast auditory fibre activity, correlated with tinnitus development (Knipper et al., 2021; Knipper et al., 2020), promotes inhibition of parvalbumin-positive (PV+) interneurons, linked to oscillatory activity in the γ-band (Ibarra et al., 2021; Pellegrini et al., 2021; Chen et al., 2017). Following this model (Knipper et al., 2020), the reduction in fast auditory fibre activity should lead to a reduction in central tonic PV+ interneuron activity in tinnitus, resulting in a reduced sharpness of central tonal representations and a reduction in stimulus-induced gamma oscillations. Whereas, in tinnitus with hyperacusis, the stimulus-evoked responses may more likely increase across a broad frequency range due to increased central amplification. As far as the author can tell, there were no approaches differentiating tinnitus with or without the co-occurrence of hyperacusis using a multimodal setting of combined audiometry, functional imaging, and oscillation assays. Thus, a clear distinction of neural correlates for disease forms is a prerequisite for the stated goal of successful, individualised therapy.

## 1.3. The scientific aims and objectives of the present thesis

The main scientific aim was to clarify the pathophysiological mechanisms behind tinnitus and the frequently occurring comorbidity hyperacusis. A first goal was to confirm the effects of tinnitus described by previous studies of our research group (Hofmeier et al., 2018; Mohrle et al., 2019), in a new cohort of participants. Tinnitus biomarkers in humans are reduced suprathreshold ABR waves (wave V), a reduction of stimulus-evoked BOLD fMRI responses in auditory areas, and changes in the fMRI resting-state network (functional connectivity). The biomarkers were considered for both T- and TH-subgroups to show the importance of the differentiation between tinnitus with and without hyperacusis. A factor that has remained untouched until now but is relevant to many treatment recommendations (Hesse et al., 2022) is the tinnitus duration. Therefore, this thesis aimed to disclose whether differences in audiometric/tinnitus characteristics as a function of tinnitus duration can improve individual therapy recommendations for the tinnitus subgroups.

To examine the proposed PV+ framework (Knipper et al., 2020) described above, the questionnaires, audiometry, and fMRI responses were repeated in the new cohort to determine whether the observations from the previous studies hold. As the conditions were met, we can conclude that we have obtained a comparable set of tinnitus subgroups. In order to extend this multimodal approach, we simultaneously measured EEG and fNIRS to validate our previous findings based on altered BOLD fMRI responses (Knipper et al., 2020).

# 2. MATERIAL AND METHODS

## 2.1. Ethical proposal

All studies presented in this document have been approved by the Ethics Committee of the University Hospital Tübingen and the University of Tübingen (Faculty of Medicine).

Preceding applications:

- 444/2014BO2 - 'Funktionelle MR-Tomographie zur Darstellung der Hirnaktivität und der Hörbahn bei Tinnitus-Patienten und Vergleichspersonen I' (2014)
- 264/2016BO1 - 'Funktionelle MR-Tomographie zur Darstellung der Hirnaktivität und der Hörbahn bei Tinnitus-Patienten und Vergleichspersonen II' (2016-2017)

Subsequent applications:

- 391/2018BO2 - 'Funktionelle MR-Tomographie zur Darstellung der Hirnaktivität und der Hörbahn bei Tinnitus-Patienten und Vergleichspersonen III' (2019)
- 092/2020BO2 - 'Messung von spontanen und ereignis-evozierten Hirnströmen bei Tinnitus und Hyperakusis-Patienten und Vergleichspersonen' (2020)
- 383/2021BO2 - 'Funktionelle Darstellung der Hirnaktivität und der Hörbahn bei Tinnitus-Hyperakusis Patienten und Vergleichspersonen mit Hilfe Bildgebender/ Audiologischer Verfahren IV' (2021)

In addition, the study was registered at the German Clinical Trial Register as DRKS0006332. All study participants were informed about risks, data protection and study procedure prior to the examinations. Written informed consent was obtained from each participant. Participants received an allowance for their participation. All methods were used in accordance with the "Declaration of Helsinki" of the World Medical Association for Ethics in Human Research. The methods and the inclusion and exclusion criteria were defined in advance.

## 2.2. Examination procedure

The study examinations were divided into three days. On the first day, written informed consent and approval by the ethics committee were obtained at the Department of Otolaryngology in Tübingen. Subsequently, ear examination, tympanometry and pure tone audiometry (PTA) were performed to verify the inclusion and exclusion criteria (**Appendix A**). After inclusion in the study, participants completed the remaining examinations, including auditory brainstem response (ABR), questionnaires, and speech intelligibility testing. Functional magnetic resonance imaging (fMRI) measurements were performed on the second day at the Department of Diagnostic and Interventional Neuroradiology in Tübingen. Participants were required to agree to an additional written informed consent for fMRI by the medical radiology assistant prior to the measurement. On the third day, combined electroencephalography (EEG) and functional near-infrared spectroscopy (fNIRS) was performed at the Department of Psychiatry and Psychotherapy in Tübingen. Each of the three visits lasted about two hours. All procedures are listed in **Table 1**. Participants received an expense allowance of 20€ for each day of the trial (total 60€).

***Table 1: Examination overview***

| Examination day 1 | Examination day 2 | Examination day 3 |
|---|---|---|
| ○ Clarification/privacy policy<br>○ Check for inclusion/exclusion criteria<br>○ Ear examination<br>○ Questionnaires<br>• Goebel-Hiller-Score<br>• Hyperakusis-Inventar<br>○ Audiological diagnostic<br>• Pure tone audiometry<br>• Bone conduction Hearing thresholds<br>• Air conduction Hearing threshold<br>• Loudness discomfort level (LDL)<br>• Tympanometry<br>• Tinnitus localisation<br>• Tinnitus suppression<br>• Auditory brainstem response<br>•Speech audiogram (Freiburger, OLSA)<br>○ Blood sample collection | ○ Clarification and instructions<br>○ Structural image acquisition<br>○ Task-evoked MRI measurements<br>• Broadband chirp stimulus<br>• High-frequency chirp stimulus<br>• Low-frequency chirp stimulus<br>• Music piece stimulus<br>○ Resting-state | ○ Combined EEG/fNIRS<br>• Active Frequency Discrimination Learning Paradigm<br>• Resting-state |

## 2.3. Recruitment of study participants

### 2.3.1. Recruitment of participants

The rare occurrence of some of the tinnitus subgroups (especially the TH-group) surveyed without other clinical disorders, such as presbycusis or misophonia, complicates recruitment of the aimed subject numbers for the randomised controlled trial. In order to acquire as many subjects as possible, e-mails were sent to the University Hospital Tübingen mailing list (for older patients) and the university mailing list (for younger patients). In addition, the ENT clinic involved in the study referred potential participants to the working group.

Because tinnitus is often associated with concurrent disorders, it was not possible to measure a representative sample of the population, as the exclusion of further disorders (**Appendix A**) is considered more important.

### 2.3.2. Study inclusion and exclusion criteria

The studies (Hofmeier et al., 2018; Hofmeier et al., 2021; Wertz et al., 2023) recruited participants with and without tinnitus between the age of 18 and 70. According to the clinical definition, patients were required to have normal to mild hearing loss at most (as described in the respective results section or below 20 dB threshold loss between 0.25 kHz and 4 kHz and 40 dB threshold loss between 4 kHz and 10 kHz). In order to be able to carry out the questionnaires and the measurement clarifications in a comparable manner, the subjects had to be native German speakers and must not have any other diseases of the hearing system (e.g., Meniere's disease, acoustic trauma, deafness, or a hearing aid supply, **Appendix A**). In addition, contradictions for fMRI measurements, neurological disorders, pregnancy, medications, and drug or alcohol abuse were excluded. Patients with tinnitus had to have permanent tinnitus for more than four weeks, not have participated in any tinnitus therapy for six months, and not have a decompensated tinnitus to prevent associated psychiatric comorbidities (see GHS questionnaire).

A central problem encountered in research is the need for more reliable objectifiable parameters for noise hypersensitivity, as it is a subjective phenomenon with many subtypes (Jastreboff and Jastreboff, 2023). The high overlap of hyperacusis with phonophobia, recruitment, or misophonia is a major challenge in research on this topic. This aspect was given special attention in the recruitment by asking participants if there were any particularly unpleasant sounds or noises for them (“Stören Sie bestimmte Töne

oder Geräusche?"), and we specifically addressed examples such as the sound of, e.g., chewing, eating, smacking, clicking a pencil, rubbing styrofoam or chalk on a blackboard ("Stören Sie Geräusche wie Kauen, Schmatzen, Kuli klicken, Reiben von Styropor oder Kreide auf einer Tafel?"). If one of the answers were positive, we excluded the subjects from the study.

### 2.3.3 Hyperacusis group classification

#### According to Hyperakusis-Inventar (HKI)

The HKI questionnaire classifies subjects with hyperacusis at an HKI score < 12 (Fischer, 2013). Control and tinnitus subjects below the cut-off value get assigned to the C- and T-groups, respectively, whereas patients above the value are placed in the TH-group.

#### According to HKI & (Goldstein and Shulman, 1996)

To assess the grade of hyperacusis, Loudness discomfort level (LDL) were measured at 0.25, 0.5, 1, 2, 4, and 6 kHz (Goldstein and Shulman, 1996) and the Hyperacusis questionnaire (Hyperacusis Inventory (HKI)) was administered (Fischer, 2013) in all participants. The HKI and LDL methods classify subjects into four hyperacusis severity quartiles (for LDL, see **Table 2**; for HKI, see Methods 2.4.1) with an additional hyperacusis cut-off value at HKI score > 12 (Goldstein and Shulman, 1996; Berthold-Scholz, 2013).

***Table 2: Hyperacusis classification***
*Hyperacusis classification according to (Goldstein and Shulman, 1996). The Dynamic Range is calculated for each frequency from LDL minus PTA.*

| Hyperacusis | Dynamic Range | Loudness discomfort level |
|---|---|---|
| None | 60 dB or greater in all frequencies | 95 dB or greater in all frequencies |
| Mild | 50-55 dB at any frequency | 80-90 dB at two or more frequencies |
| Moderate | 40-45 dB at any frequency | 65-75 dB at two or more frequencies |
| Severe | 35 dB or less at any frequency | 60 dB or lower at two or more frequencies |

For the control group, we specify an HKI burden below the cut-off value and a none or mild burden measured by LDLs. We specify a moderate/ severe burden as measured by LDL combined with a mild to severe HKI burden for subjects with tinnitus we include in the TH-group. Also included are subjects with a mild burden, as measured by the LDLs,

combined with a moderate to severe HKI burden. The remaining tinnitus patients with a lower LDL burden than severe were included in the T-group.

## 2.4. Questionnaires

### 2.4.1. Hyperacusis questionnaire – Hyperacusis Inventar (HKI)

In order to separate the tinnitus groups according to the comorbidity of hyperacusis, we used the so-called Hyperacusis Inventory (HKI) as a hyperacusis questionnaire (**Appendix B**). This questionnaire combines items from the German noise sensitivity questionnaire (Nelting et al., 2002) and the French hyperacusis questionnaire (Khalfa et al., 2002), resulting in a high sensitivity for complaints caused by hyperacusis and a low correlation with tinnitus and hearing threshold loss (Fischer, 2013). The test consists of 9 items with four response options (always true, often true, sometimes true, never true, with 3, 2, 1, or 0 points for the possible responses). With a maximum score of 27, a cut-off value of $> 11$ points is defined for the presence of hyperacusis based on the reported sensitivity and specificity of the test (Fischer, 2013). Additionally, based on the HKI classification by Berthold-Scholz, the subjects were divided into four hyperacusis severity quartiles (none = 0-8, mild = 9-13, moderate = 14-18, and severe = 19-27, (Berthold-Scholz, 2013)).

### 2.4.2. Tinnitus questionnaire – Goebel-Hiller-Score (GHS)

The German version of the clinically used tinnitus questionnaire, the Goebel-Hiller-Score (GHS), was used to classify the level of distress caused by tinnitus (Goebel and Hiller, 1994). The GHS consists of 52 test items with three response options (applicable, partially applicable, and not applicable, with 2, 1, or 0 points for the possible responses). The questions are categorised into the sub-scores: emotional distress, cognitive distress, intrusiveness, auditory perception difficulties, sleep disturbances, and somatic complaints. To determine severity, the total scores are quartered into mild (0-30), moderate (31-46), severe (47-59), and very severe (60-84). Decompensated tinnitus, often associated with psychiatric comorbidities, is considered when the score exceeds 46 (below 46 points, the tinnitus is considered compensated) (Goebel and Hiller, 1994).

## 2.5. Audiological diagnostic

### 2.5.1. Macroscopic ear examination

The ears are examined by an ENT doctor in a macroscopic ear examination (General Inspection and Otoscopy) prior to the measurements. During the examination, special attention is paid to discharge, inflammation, foreign bodies, stenoses, cerumen, and scars. During this procedure, the ear canal and the tympanic membrane were cleaned from wax and inspected to exclude external canal anomalies or tympanic membrane pathologies.

### 2.5.2. Tympanometry

The tympanometry was performed using the AT235 (Interacoustics, Middelfart, Denmark) with 226 Hz and 300 daPa. Tympanometry is used to detect middle ear-related issues. All subjects without normal middle ear pressure and average static compliance in the tympanometry were discussed in more detail with the study physician.

The specified parameters are Ear canal volume, Static compliance (SC, "is the greatest amount of acoustic energy absorbed by the middle ear system (the vertical peak of the tympanic tracing)" (Onusko, 2004)), and Tympanometric peak pressure (TTP, the ear canal pressure at which the peak of the tympanogram occurs (Margolis et al., 2000)).

### 2.5.3. Pure tone audiometry (PTA) – Hearing thresholds in air and bone conduction

With assistance provided by the audiologists of the Department of Otorhinolaryngology, Head and Neck Surgery, Tübingen, Germany, the individual pure tone pitch and loudness were determined. The measurements were performed in a soundproof chamber (Industrial Acoustics, Niederkruchten, Germany) with the audiometer (AT1000, Auritec, Medizindiagnostische Systeme GmbH, Hamburg, Germany) and the on-ear headphones (AT 1350 A, Beyerdynamic, Heilbronn, Germany). For high frequencies above 10 kHz, the over-ear headphones (HDA 300, Sennheiser, Wedemark, Germany) are used. The frequencies measured with this setup include 0.125, 0.25, 0.5, 1, 2, 3, 4, 6, 8, 10, 11.2, 12.5, 14, and 16 kHz.

First, the air conduction hearing thresholds were measured at all frequencies. In order to exclude air conduction hearing loss, the bone conduction hearing thresholds are then measured at the frequencies (0.25, 0.5, 1, 2, 4, and 6 kHz) using the B71W (RADIOEAR, Middelfart, Denmark) bone transducer. In the following, when PTA is mentioned, we

always refer to PTA air conduction, as bone conduction was solely tested to exclude air conduction hearing loss.

In clinical settings, PTA thresholds are commonly employed to derive a standardised measure, referred to as PTA4, which captures hearing thresholds for specific frequencies, important in the context of speech understanding (0.5, 1, 2, and 4 kHz) (von Gablenz and Holube, 2015). Additionally, we applied this method to the high-frequency range (PTA-HF), which considers thresholds at 6, 8, and 10 kHz, and to the extended high-frequency range (PTA-EHF), which includes 11.2, 12.5, 14, and 16 kHz.

### 2.5.4. Uncomfortable level or loudness discomfort level (LDL) thresholds in air conduction

LDLs were determined for each ear individually at frequencies of 0.25, 0.5, 1, 2, 4, and 6 kHz. The patient was instructed to report the point at which the sound presented through the audiometer's headphones became uncomfortable - not painful but unpleasant. The measurement did not exceed a loudness level of 115 dB HL to avoid hearing damage. The difference between the pure tone threshold and the LDL is referred to as the dynamic range (DR).

### 2.5.5. Tinnitus localisation

Using the two-alternative forced choice (2AFC) recursive matching method, the frequency closest to the tinnitus is first identified, and then the matching tinnitus loudness is determined with 1 dB accuracy. In this method, a series of acoustic sinus stimuli were presented to the patient, and they were asked to indicate whether the tinnitus was higher/lower in pitch or louder/quieter after each stimulus. The procedure was repeated to obtain the most accurate determination of tinnitus frequency and loudness (Vernon and Fenwick, 1984).

### 2.5.6. Tinnitus suppression

In the tinnitus suppression measurement, the subject is presented with pure tones at various frequencies (0.125, 0.25, 0.5, 1, 2, 3, 4, 6, 8, and 10 kHz). For each frequency, the intensity of the stimulation is gradually increased by an audiologist until the patient reports a suppression of their tinnitus (Feldmann, 1971).

### 2.5.7. Speech audiogram – Oldenburger Satztest (OLSA) & Monosyllabically speech understanding test “Freiburger Wörtertest”

The German "Oldenburger Satztest" speech audiogram (OLSA) is a standardised test to evaluate the ability to perceive and understand speech in noise. The test is performed in the Department of Otorhinolaryngology, Head and Neck Surgery, Tübingen, and involves the presentation of speech stimuli with and without background noise via on-ear headphones (AT 1350 A, Beyerdynamic, Heilbronn, Germany). The speech reception threshold is assessed by repeating random five-word sentences in German by OLSA. The resulting data comprehensively assesses the individual's speech recognition abilities in noisy conditions (HörTechgGmbH, 2012; Wagener et al., 1999). The subject is asked to repeat a series of these sentences, and the dB level at which they are able to repeat 50 % of the words correctly is considered as their speech reception threshold. The OLSA test uses standardised speech stimuli and consists of two phases. The first phase involves presenting speech signals to both ears without background noise. The second phase involves presenting speech signals to one ear while simultaneously presenting speech-shaped noise at 65 dB to the opposite ear.

Prior to the switch to OLSA, the monosyllabic (noun) speech understanding test ('Freiburger') was utilised for speech audiometry (Hoth, 2016).

### 2.5.8. Supra-threshold Auditory Brainstem Response (ABR)

#### ABR Measurement setup – Audera GSI

The auditory evoked brainstem response (ABR) measurement is derived ipsilaterally with the GSI Audera (Grason-Stadler, Eden Prairie, USA) device and stimulated via Telephonics TDH 39p headphones (Telephonics 296D000-4, C16396, Farmingdale, USA).

Measurements were performed with four electrodes (Neuroline 720, Ambu, Bad Nauheim, Germany) at predetermined positions according to the international 10-20 electrode system (Jasper, 1958). Before placing the electrodes, the skin of the subject was cleaned with medical abrasive paper (Red Dot Trace Prep, 3M, Canada) and alcohol (Softasept N, B. Braun SE, Deutschland) to ensure the electrode impedance was always below five kΩ (GND: Fpz; Inverting input (-): hairline; Non-inverting input (+): mastoid at stimulus-administration point).

The auditory brainstem response (ABR) was recorded in response to broadband acoustic click stimuli with a duration of 100 milliseconds with alternating polarity. Stimuli were presented at sound pressure levels from 25 to 75 dB SPL in 10-decibel increments. The repetition rate of the click stimuli was 11.1 Hz, with a total of 2000 repetitions. The ABR signals were bandpass filtered between 150 and 3000 Hz (-24dB/Oct Butterworth high-pass filter; lowpass: -40 dB/oct linear phase low-pass filter). The electrode impedance was maintained at less than five kΩ, and the impedance difference between two individual electrodes should not exceed two kΩ (Hofmeier et al., 2018).

### ABR Measurement setup – Brain Vision – actiCHamp Plus 64 System

The auditory evoked brainstem response (ABR) measurement is derived ipsilaterally with the amplifier (actiCHamp Plus, Brainproducts, Germany) and the preamplifier (Bipolar amplifier EP-PreAmp gain factor of 50, Brain Products, Munich, Germany) according to the manufacturer specifications with a sampling rate of 50 kHz. There is a deviation only in the ABR electrode placement to achieve better comparability to the old measurement system.

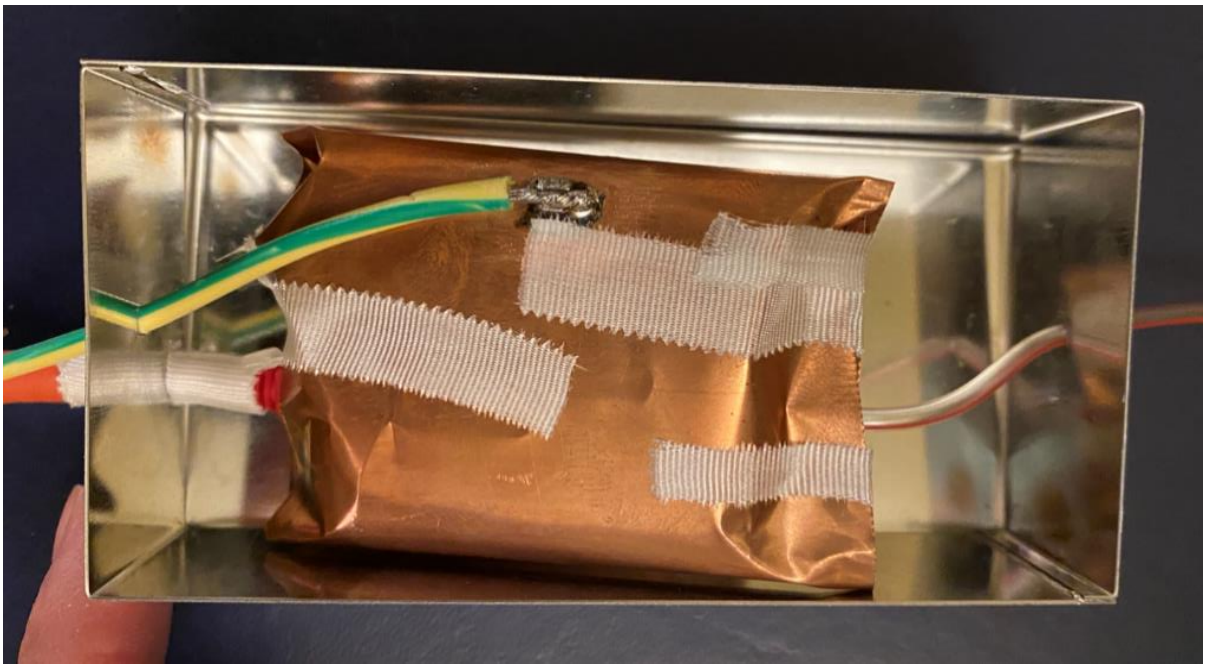

***Figure 1:*** *ER2 in electromagnetic shielding with grounded µ-metal.*

The ABR was recorded in response to broadband acoustic click stimuli presented with 65 to 85 dB SPL in 10 dB steps, a high-frequency chirp (HF-chirp) with a range of 12-20 kHz and a low-frequency chirp (LF-chirp) with a range of 0.25-3 kHz. The stimuli were presented at a repetition rate of 11.1 Hz with 3000 repetitions of alternating polarity at a sampling rate < 44.1 kHz. The acoustic stimulation is generated via the sound card

(Scarlett 8i6 3rd Gen, Focusrite, United Kingdom) and the shielded (Grounded μ-metal and steel; kindly provided by the AG Verhulst see **Figure 1**) in-ear headphone transducers (ER-2, Etymotic Research Inc, USA) with foam ear-tips (ER1-14A (13mm), Etymotic Research Inc, USA).

To ensure temporal precision of the triggers, the SPDIF trigger output of the sound card is transmitted via DA Converter (D1C6064, Oehlbach, Deutschland), a custom-designed trigger box. The trigger box is constructed from an electrical comparator that triggers the actiCHamp when the input signal exceeds 50 mV, reducing the trigger jitter to the microsecond range.

### Supra-threshold ABR analysis

At each stimulus level, the different components of the ABR waveform were tested for latency and amplitude group differences. Wave determination was accomplished by bandpass filtering (30-2000 Hz with a Hamming windowed first-order FIR filter), inverting, averaging the results, and then attributing the waveform to the stimulus onset. The most prominent positive peak, occurring typically at 5-6 ms after stimulus onset, was determined as wave V. Subsequently, waves I and III were selected in the range of 2, respectively, 4 ms seconds before wave V. The peak-to-peak amplitude between positive and trailing negative deflections defined the wave amplitudes. We selected the latencies of positive peaks for wave measurements. ABR wave amplitudes, latencies, and inter-peak-latencies (IPL) were determined for individual ears and then averaged for the participant's left and right ears. Wave V to I amplitude ratios smaller than one and larger than five were excluded from the analysis since these outliers misaligned the midpoints toward non-represented data ranges.

## 2.6. Functional magnetic resonance imaging (fMRI) – PrismaFit

The fMRI image acquisition was performed on a 3-Tesla scanner (Prisma Fit, Siemens, Germany) with a 64-channel head-neck coil. For the acoustic stimulation, we used special MRI-suitable over-ear headphones (CONFON HP-SC 03, MR Confon GmbH, Magdeburg, Germany). Four different auditory stimuli were generated during scanning using stimulus presentation software (Neurobehavioral Systems software, Neurobs, Berkeley, USA; Panasonic-SC-PMX5 Amplifier, Panasonic Marketing Europe GmbH, Hamburg, Germany). During the data acquisition phase, we acquired structural, task-evoked, and resting-state fMRI images.

### 2.6.1. Structural MRI image acquisition – T1-weighted whole brain – Experimental design

The anatomical whole brain images measured initially are necessary to align the functional fMRI images to the anatomical origin in a pre-processing step to eliminate artefacts of the head movements. We used the Magnetization Prepared RApid Gradient Echo (MPRAGE) sequence for T1-weighted three-dimensional structural volumes consisting of 192 slices for each dimension (coronal, sagittal, and axial view).

According to (Hofmeier et al., 2018), the parameters for structural image acquisition were: repetition time (TR) = 2300 ms; acquisition time (TA) = 3.5 min; field of view (FOV) = 240 mm; bandwidth = 200 Hz/pixel; slice thickness = 0.94 mm; inversion time (TI) = 900 ms; slice distance = 3.7 mm; echo time (TE) 2.1 ms.

### 2.6.2. Task-evoked fMRI measurements – Experimental design

The task-evoked functional images were obtained using a T2* weighted echo-planar sequence with an alternating block design containing eight off-blocks and seven on-blocks, with a total of 150 images. This echo-planar sequence is timed by cardiac gating to avoid distortion due to brain pulsation artefacts in the brain due to the heartbeat-related blood flow. This step was developed to detect small blood oxygen level-dependent (BOLD) changes in hearing-specific brainstem regions. Therefore, a pulse oximeter (finger plethysmograph) detected the subject's heart rate, and the scanner synchronised it with the image acquisition timing. Due to the short time window between two heartbeat cycles during cardiac gating, we limited the brain scan to ten coronal slices covering the brainstem and the auditory cortex. According to (Hofmeier et al., 2018), parameters for structural image acquisition were: repetition time (TR) = 2000-3000 ms (cardiac-gated); flip angle (FA) = 90°; field of view (FOV) = 290 mm; matrix size = 64 x 64; slice number = 10 coronal slices; slice thickness = 2.5 mm; slice gap = 1.25 mm; images = 150; slice distance = 3.7 mm; echo time (TE) = 35 ms.

The evoked fMRI experiment comprised four different stimulations. First, a pop-rock song ("Closer to the Edge", Leto, J., 2010) without cardiac gating was presented to test the setup and verify the fMRI responses. Then, if everything was satisfactory, cardiac gating was applied to measure the same song, followed by chirps in high-, low-, and broad-band frequencies. The utilised chirps have the highest power within the frequency range of 12-20 kHz (HF-chirp), 0.25-3 kHz (LF-chirp), and 0.3-25 kHz (BB-chirp). According to (Hofmeier et al., 2018), the chirps were designed to stimulate the basilar membrane to

achieve simultaneous excitation in the targeted frequency range (Stapells and Picton, 1981).

### 2.6.3. Resting-state fMRI measurements – Experimental design

In a period of awake rest lasting 5 or 10 minutes, a gradient echo planar imaging sequence was used to acquire resting-state functional images for the whole brain, including the brainstem. Subjects were told to keep their eyes closed and stay alert without any specific task to perform. Earplugs were provided to all subjects to minimize noise during the scan. According to (Hofmeier et al., 2018), the rs-fMRI measurement parameters were: echo time (TE) 35 ms, repetition time (TR) 2 s, number of slices 40 with 25 % gap, field of view (FOV) 190 x 190 mm² with a matrix of 64 x 51, which was interpolated to 64 x 64, pixel bandwidth 1954 Hz/px, that covered the whole brain and relevant brainstem areas: cochlear nucleus (CN), superior olivary complex (SOC), inferior colliculus (IC) and the medial geniculate body (MGB).

### 2.6.4. fMRI data analysis for task-evoked measurements

All pre-processing steps were performed in MATLAB (version R2019b, MathWorks Inc., Natick, USA) using the Statistic Parametric Mapping (SPM) toolbox (version 12, Welcome Trust Centre for Neuroimaging, UCL, London, UK, (Josephs et al., 1997)). Each subject's structural and functional images were reoriented according to the origin of the MNI coordinate system on the anterior commissure (AC) and the y-axis alignment through the posterior commissure (PC). The utilised heartbeat-triggered image acquisition generally causes a non-constant repetition time (TR), leading to a significant signal variance and a possible obscured BOLD signal. Therefore, in the next step, the TR image correction, the images are corrected to a virtual TR of 2 s to reduce signal variance. Based on a T1 estimate in each pixel of all 150 images measured with variable TR values, a hypothetical signal intensity for a fixed TR of 2 s was estimated by an exponential fit (Hofmeier et al., 2018; Hofmeier et al., 2021; Guimaraes et al., 1998). After TR correction, functional images were co-registered, normalised to the Montreal Neurological Institute (MNI) template, and smoothed with a Gaussian kernel of 5 mm (FWHM). Following the segmentation of the anatomical images into white matter (WM), grey matter (GM), and cerebrospinal fluid (CBF), a WM mask was created and used for a WM regression to avoid interfering noise from GM and CBF. The SPM toolbox's general linear model was used for the individual subject-level analysis based on the experimental block design as a first statistical step. The general linear model result was acquired using contrast vectors to produce statistical

parametric maps. Next, we utilised the SPM toolbox's second-level specification independent two-sample t-test to conduct the group analysis for the predefined ROIs (**Table 3**).

***Table 3: Predefined fMRI ROIs in MNI coordinates***

*The predefined ROIs in MNI coordinates for fMRI analysis were used from: [1] (Muhlau et al., 2006), [2] (Amunts et al., 2020b) and (Amunts et al., 2020b), [3] (Hofmeier et al., 2018), [4] (Lacadie et al., 2008), [5] (Horing et al., 2019), [6] (Lancaster et al., 2000), and [7] (Mai et al., 2016).*

| **Task-evoked predefined ROIs** | | | | |
|---|---|---|---|---|
| *Brain Region* | *MNI Coordinates (in mm)* | | | *Radius (in mm)* |
| *(Brodmann Area)* | *X* | *Y* | *Z* | |
| *Subcortical Regions:* | | | | |
| CN-R/CN-L[1] | ±10 | -39 | -45 | 3 |
| SOC-R/SOC-L[1] | ±13 | -35 | -41 | 3 |
| IC-R/IC-L[1] | ±6 | -33 | -11 | 3 |
| MGB-R/MGB-L[1] | ±17 | -24 | -2 | 3 |
| *Primary Auditory Cortex Regions:* | | | | |
| BA41-R/BA41-L[2] | 49/-48 | -13/-20 | 5/7 | 3 |
| BA41A-R/BA41A-L[2] | 53/-52 | -3/-8 | -2/2 | 3 |
| BA41P-R/BA41P-L[2] | ±40 | -25/-30 | 10/11 | 3 |
| BA42-R/BA42-L[3] | ±64 | -22 | 9 | 3 |
| BA42A-R/BA42A-L[3] | ±60 | -18 | 10 | 3 |
| BA42P-R/BA42P-L[3] | ±56 | -25 | 12 | 3 |
| *Temporal Regions / Sound Identification Regions:* | | | | |
| BA22A-R/BA22A-L[3] | ±54 | -6 | -6 | 3 |
| BA22P-R/BA22P-L[3] | ±67 | -27 | 3 | 3 |
| BA21A-R/BA21A-L[3] | ±66 | -13 | -5 | 3 |
| BA21P-R/BA21P-L[3] | ±66 | -22 | -5 | 3 |
| Hipp-R/Hipp-L[4] | 28/-29 | -22/-19 | -14/-15 | 3 |
| BA13P-R/BA13P-L[2] | 37/-38 | -17/-19 | 6/5 | 3 |
| *Somatosensory/Pain Regions:* | | | | |
| $PO_1$-R/ $PO_1$-L[5] | ±59 | -23 | 25 | 3 |
| $PO_2$-R/ $PO_2$-L[5] | ±58 | -14 | 18 | 3 |
| DpIns-R/DpIns-L[5] | 40/-41 | -21 | 19 | 3 |
| Mam.-Body-R/Mam.-Body-L[6] | 4/-2 | -12 | -14 | 3 |
| **Resting-state additional predefined ROIs** | | | | |
| *Brain Region* | *MNI Coordinates (in mm)* | | | *Radius (in mm)* |
| *(Brodmann Area)* | *X* | *Y* | *Z* | |
| *Emotional Regions* | | | | 3 |
| BA13A-R/BA13A-L[2] | 32/-33 | 26/23 | 1/2 | 3 |
| Amyg-R/Amyg-L[4] | 21/-24 | -1/0 | -22/-21 | 3 |
| *Temporo-frontal Attentional Regions* | | | | |
| BA45-R/BA45-L[4] | 46/-47 | 26/27 | 7/6 | 3 |
| BA46-R/BA46-L[4] | 43/-46 | 38 | 12/8 | 3 |
| BA47-R/BA47-L[4] | 38/-40 | 30/31 | -12/-13 | 3 |
| BA9M-R/BA9M-L[7] | ±7 | 50 | 30 | 3 |
| BA9DL-R/BA9DL-L[7] | ±50 | 14 | 32 | 3 |

### 2.6.5. fMRI data analysis for resting-state measurement

As with the task-evoked analysis, the subject's structural and functional images were set to the centre of the anterior commissure with SPM12, the axial plane aligned to the AC-PC line, and the head reoriented if necessary to have the mid-sagittal plane split the brain into the two hemispheres. Afterwards, rs-fMRI was further processed with dpabi DPARSF Advanced Edition v 4.5 (Yan et al., 2016) with the following settings: Time Point = 150; TR (s): 2; Slice Timing; Slice Number: 40; Slice Order: [1:2:39 2:2:40]; Reference Slice: 20; Realign; T1 Coreg to Fun; New Segment + DARTEL; Nuisance Covariates Regression (Polynomial trend: 1); Head Motion model: Friston 24; Head motion scrubbing regressors; Filter (Hz): 0.01 ~ 0.1; Normalise using EPI templates (Bounding Box: [-90 -126 -72;90 90 108], Voxel Size [3 3 3]); Smooth by DARTEL (FWHM: [5 5 5]); Default mask (SPM 5 apriori mask – threshold at 50 %); Extract ROI time courses (**Table 3**).

After pre-processing, the MATLAB function *corrcoeff()* was used to calculate Pearson correlation coefficients for each pairwise ROI time course combination in every subject. Afterwards, the quantity of significant positive ($p < .05$) rs-fMRI BOLD correlations among pre-determined ROI clusters was calculated for C-, T- and TH-group (subcortical regions to MGB; MGB to AC-I; AC-I to sound identification regions; AC-I to emotional regions; AC-I to attention regions; AC-I to anxiety regions; Pain regions to emotional regions; Pain regions attention regions; Pain regions to the anxiety regions, see **Table 3**). Due to minor sample sizes in the last cohort, we adjusted the analysis and calculated the frequency of significant positive ($p < .05$) rs-fMRI BOLD correlations among pre-determined ROI clusters for C-, T- and TH-group (subcortical regions to MGB; MGB to AC-I; AC-I to BA45, BA46, BA47; AC-I to BA9M, BA9DL; AC-I to BA21, BA22, BA39, BA40) for C-, T- and TH-group.

## 2.7. Electroencephalography (EEG) and functional Near-infrared spectroscopy (fNIRS) combined measurement

### 2.7.1. EEG & fNIRS – Experimental design

Simultaneous EEG and fNIRS recordings were obtained with a specialised cap integrating both sensor types. EEG signals were recorded at a sampling rate of 1 kHz using 21 passive electrodes, positioned according to the international 10-20 system (Jasper, 1958), with FCz as the reference and AFz as the ground electrode (**Figure 2**, grey disks). To maintain optimal signal quality, electrode impedances were kept below five kΩ. The recording

system consisted of a 32-channel DC amplifier and the Vision Recorder data acquisition software (Brain Products, Munich, Germany). The concentration changes of oxygenated and deoxygenated haemoglobin ((de)oxy-Hb) were measured by a continuous wave, multichannel NIRS system (ETG-4000 Optical Topography System; Hitachi Medical Co., Japan) with a temporal resolution of 10 Hz using two 22-channel optode arrays covering the left and right fronto-temporo-parietal head areas (12x6 cm each; inter-optode distance: 30 mm; s (**Figure 2**, red/blue disks).

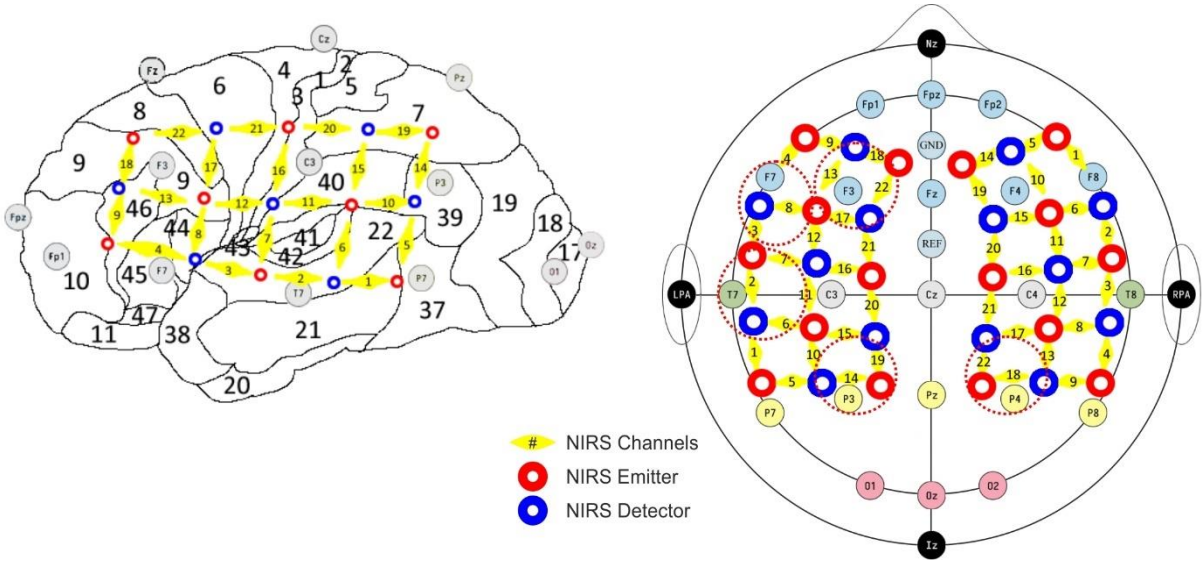


***Figure 2**: Electrode and optode arrangement. Sampling encompassed the auditory cortex, temporo-parietal, ventrolateral prefrontal, and dorsolateral prefrontal areas (**Table 4**).*

Acoustic stimulation was generated via the sound card (Scarlett 4i4, Focusrite, United Kingdom) and presented through the Monitor Speaker (Model MSP5, Yamaha Corporation, Japan). To ensure temporal precision of the triggers, the electrical signal of the sound card is transmitted via a y-cable to the loudspeaker and a custom-designed trigger box. The trigger box is constructed from an electrical comparator that triggers the EEG and NIRS when the input signal exceeds 50 mV, reducing the trigger jitter to the microsecond range.

### 2.7.2. Two-tone Discrimination Paradigm (TDP) and resting-state Paradigm

EEG and fNIRS were recorded simultaneously while the subjects remained seated with their eyes open in front of a computer screen and were instructed to fixate on a cross in the centre of the computer screen. During the tone discrimination task, subjects were exposed to two distinct pure tone frequencies with a sampling rate of 44.1 kHz, each 250 ms long and separated by 250 ms intervals. Each sinusoidal stimulus was designed with 10 ms continuous amplitude attenuation (cosine slope) at the beginning and end to avoid

click artefacts in the loudspeaker. The task was to identify which stimuli were higher/lower in pitch and reply by keystroke. This task's difficulty was constantly adapted to the individual performance by adjusting the frequencies to a correct response in 3 out of 4 trials. The auditory stimuli were generated at a sensation level (SL) of 65 dB (above the individual hearing level (HL)). In order to realize the dB SL stimulation, individual PTAs of the measured frequencies of the respective better ear are interconnected via stepwise linear interpolation ("Piecewise linear interpolation"). Based on this curve, the hearing loss between the measured frequencies is interpolated. To check the PTA thresholds, study participants were instructed to adjust the reference frequency and the tinnitus frequency until their subjective perceptions were equal.

The paradigm consisted of these two stimulus frequency ranges: (i) the first centred at 1 kHz, referred to as fRef; (ii) the second centred at the individual's tinnitus frequency, referred to as fTin (for controls 6 kHz based on the average tinnitus frequency in (Hofmeier et al., 2018). For subjects with low tinnitus (< 2.5 kHz), the mean tinnitus frequency (6 kHz) was presented as the reference stimulus.

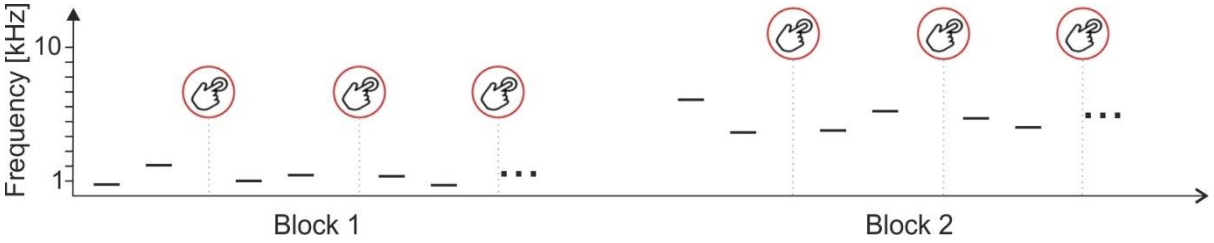


***Figure 3:*** *Illustration of the two-tone discrimination paradigm (TDP).*

Randomised (± ¼ octave), a tone was generated around fTin and fRef. 500 ms after the start of the first stimulus, a second stimulus was presented one semitone (f*2)/12) higher or lower. After the second stimulus, the subjects were instructed to indicate as fast as possible by mouse click whether the second tone was higher or lower than the first (**Figure 3**). The second stimulus also varied (± 0.5 dB) in loudness to prevent subjects from detecting the loudness and not the frequency. To analyse the slow BOLD data of the NIRS without too much superposition of the signals of successive runs, the inter-trial interval (ITI) was randomised 1.2 ± 0.2 s, resulting in a mean epoch length of ~2.5-3 s (to be able to analyse thoroughly without superposition, an ITI of > 10-12 s would have to be implemented, but this would be unacceptable for the required number of trials and the boredom of the subject). We acquired six blocks of 20 trials for each of the two centre frequencies, providing a total of 240 stimulus pairs, followed by 8 min of awake rest with eyes open.

All EEG electrodes and fNIRS channels were cleaned and pre-processed in the first analysis step. However, five region of interest (ROI) were determined for the final group analysis based on the EEG resting-state differences (**Table 4**).

***Table 4: Regions of interest***
*Regions of interest with their respective Brodmann areas, EEG electrodes, and fNIRS channel configurations. fNIRS channel positions according to (Metzger et al., 2016), (Amunts et al., 2020a), and (Amunts et al., 2020b). BA, Brodmann Area.*

| Brain Region | Brodmann Area | EEG Electrode | fNIRS Channel right | fNIRS Channel left |
|---|---|---|---|---|
| Auditory cortex | BA41, 42 & BA22 | T7, T8 | 3, 7, 8 | 2, 6, 7 |
| Temporo-parietal areas | BA39, 40 & ventral BA7 | P3, P4 | 18, 22 | 14, 19 |
| Ventrolateral prefrontal areas | BA44, 45, 46 | F7, F8 | 1, 5, 6 | 4, 8, 9 |
| Dorsolateral prefrontal areas | Dorsolateral BA9 | F3, F4 | *10, 14, 15, 19* | *13, 17, 18, 22* |

### 2.7.3. EEG pre-processing

The code for the EEG pre-processing was written in MATLAB using the functions of the EEGLab toolbox (Delorme and Makeig, 2004) and official MATLAB toolboxes (Wavelet Toolbox v6.1, Statistics and Machine Learning Toolbox v12.3, Signal Processing Toolbox v9.0, Parallel Computing Toolbox v7.6, Curve Fitting Toolbox v 3.7).

#### Import EEG data, epoch, and electrode information

First, the ".eeg" files saved by the amplifier were imported into EEGLAB using the toolbox FileIO. The epoch and channel information were imported and stored in the raw data structure in the next step. The epoch number, session number, frequency of the first tone, frequency of the second tone, difference, difficulty, response, and reaction time are stored for each epoch. Electrodes are positioned and named according to the international 10-20 system.

#### Filtering of the EEG data

To remove linear trends, high-pass filtering of the data is often necessary. To obtain ICA decompositions of good quality, it is also recommended to filter the data high at ~ 1 Hz (Klug and Gramann, 2021). To overcome the phase shift and artefact vulnerability of

conventional high-pass filters, the low-frequency drifts in the EEG data were removed using the MATLAB toolbox NoiseTools (robustly remove trend function:

*nt_detrend(EEG.data, order, w, basis, thresh, niter, wsize)). w: weights = 1; basis: 'polynomials'; thresh: threshold for outliers = 3 SD; niter: number of iterations = 1; wsize: window size for local detrending = 50 sample points* (de Cheveigne and Arzounian, 2018).

Thereby, continuous EEG data were cut into 50 sample windows, and all points below a threshold of 3 standard deviations were included in the linear fit detrending. As a result, the frequencies below ~3 Hz were filtered out without frequency-dependent phase shift or jump artefact smearing.

### Resampling of the EEG data

To save memory and disk space, the data was down-sampled using *resample()* from the MATLAB Signal Processing toolbox. Prior to the resampling, a low-pass filter with half the resampling frequency was applied to the data to avoid aliasing effects. Frequency to resample = 500 Hz; Anti-aliasing filter cut-off = 0.8x500; Anti-aliasing filter transition band-width = 0.2x500.

### Epoching of the EEG data

In order to analyse event-related EEG dynamics of continuously recorded data, we extracted data epochs time-locked to the stimulus event. This study used epoch boundaries from 0.5 seconds before to 2 seconds after the first auditory stimulus began. To pre-process EEG TDP and resting-state as similar as possible, epochs with the exact boundaries applied to the resting-state data. These epochs were slightly jittered to reduce periodic artefacts such as line noise (at 5 kHz sample points, the maximum jitter is 0.1 seconds, *randi([1 500],1)*).

### Artefact rejection in the EEG data

At first, the epoched EEG data were manually screened in the time domain (**Figure 4**). In this process, the entire data set was screened for open and flat channels (**Figure 4**, left), which were deleted and interpolated from the surrounding channels. After that, the epochs to be removed were preselected based on variance and a visual inspection was performed to ensure that artefacts such as muscle artefacts or jumps were removed (**Figure 4**, right).

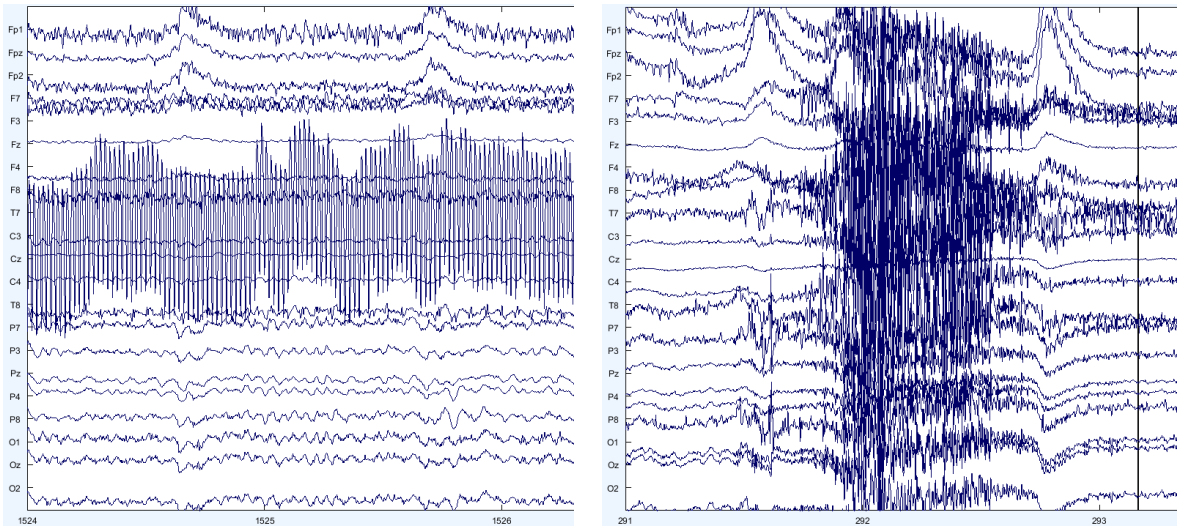


***Figure 4:*** *EEG time domain examples for open channel and muscle/movement artefacts.*

Up to 10 % of channels or 10 % of epochs were removed, but subjects were excluded if more data must be removed.

## Independent Component Analysis (ICA) based on the Infomax optimisation algorithm

Within this study, we applied ICA to identify and remove further artefacts (i.e. muscle artefacts, eye blinks, or eye movements) embedded in the data without removing the affected data regions. ICA is a computational method for blind source separation, i.e. a technique to separate a multivariate signal composed of linearly mixed sources into statistically maximally independent components (Hyvarinen and Oja, 2000). In mathematical terms, the ICA calculates the weight matrix W for the EEG data X to obtain the maximum independent components U.

$$U = W X$$

We used the ICA function of (Delorme and Makeig, 2004) based on the Infomax algorithm of Tony Bell in an extended version of (Lee et al., 1999) to extract also sub- and super-gaussian sources (e.g., line noise). After the ICA, the time domain of the independent components was visually monitored for faults missed in the first cleaning cycle. If, for example, an artefact was detected in all independent components of an epoch, this epoch was removed from the data prior to the ICA, and subsequently, the ICA was recalculated. This approach is recommended since, for data containing too many types of noise, unique data features will degrade the ICA results and produce component maps that contain many single-channel or noisy components.

Artefact removal with ICA in the EEG data

After computing the independent components and determining the component dipoles (dipfit v4.3), the components were classified using the EEGLAB plugin iclabel (Pion-Tonachini et al., 2019). Based on this trained artificial neural network architecture, the percentage probability of assigning each component to one of the seven artefact categories (brain muscle, eye, heart, line noise, channel noise, or other) was estimated. The classification worked well with solid artefacts like blinking (**Figure 4, 5**, see electrodes: Fp1, Fpz, Fp2). Due to the limitation of the number of independent components to the number of measuring electrodes, it frequently occurred that the ICA failed to separate artefacts from brain activity. To determine whether artefact rejection must be performed again, each component was reviewed in the time domain, frequency domain, and for spatial effects of the scalp activity.

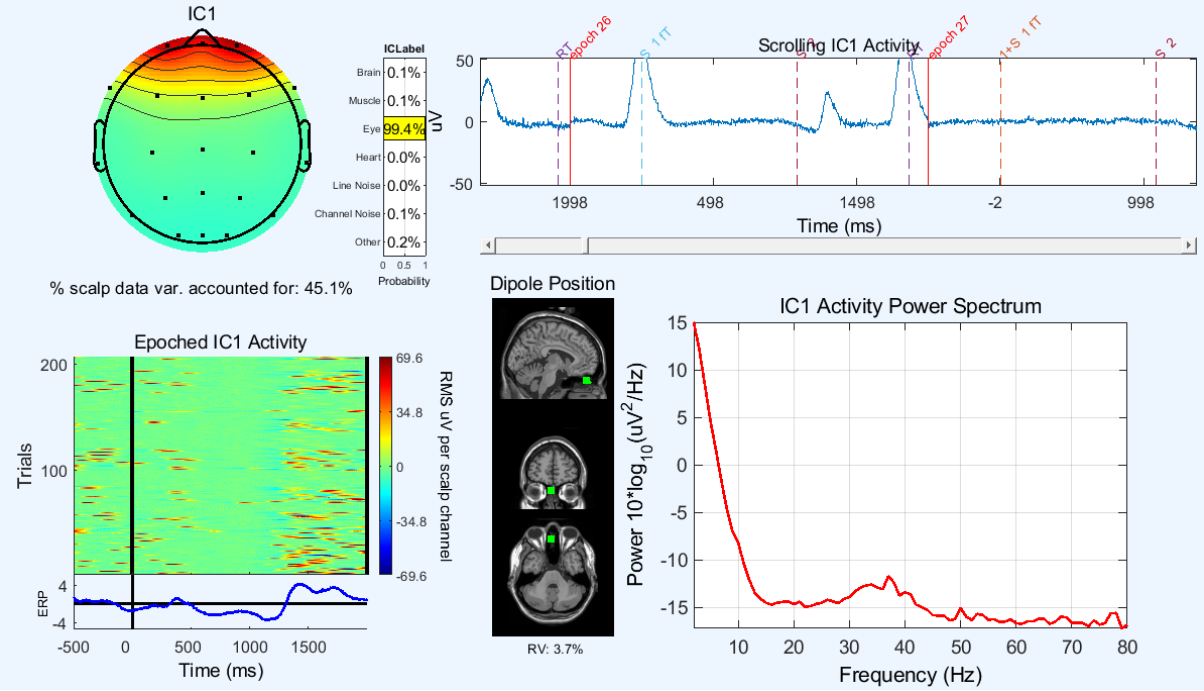


***Figure 5:*** *Example of an independent component (eye blinking).*

After selecting the highly artefact-contaminated components, they were subtracted from the EEG data. We obtained the cleaned EEG channel data X by zeroing out the components (row in U) to be deleted and applying the inverse transformation of the weight matrix W.

$$X = W^{-1} U$$

### Reference to the “Average Reference” in the EEG data

The common reference electrode used in our setup was placed at FCz (**Figure 2**). Typical recording references are the mastoids (A1/TP9 and A2/TP10 in the 10-20 electrode System) or the average reference. The mastoids had to be discarded as a reference because the electrodes provided highly artefactual recordings in more than 40 % of the subjects. If, in future studies, mastoids should be measured successfully in all subjects, the mastoid electrodes must be taped separately to the head. They should not be integrated into the EEG cap because different head shapes have significantly varying contact pressure, especially at the mastoid. After careful consideration, we have chosen to implement the average reference method. This involves subtracting the average potential of all electrodes from each channel. Thus, we do not have to exclude subjects whose reference electrode drifts over several epochs. Furthermore, we achieve better comparability with the numerous other EEG studies that use this reference.

## 2.7.4. EEG analyses

### Time/frequency decomposition – Continuous wavelet transform (CWT)

Compared to conventional methods such as the short-time Fourier transform (STFT), the advantage of the CWT method is superior frequency-dependent resolution. Like all linear time-frequency transformations, the wavelet transform is also affected by the uncertainty principle of Küpfmüller; therefore, it is not possible to localise an event with high accuracy in time and frequency at the same time. Thus, there is only a trade-off between good temporal resolution and good resolution in the frequency domain.

Time-frequency decomposition was applied to pre-processed EEG channels using complex Morlet wavelet transforms with a length of 1.2 cycles (**Figure 6**, left) at the lowest frequency of 4 Hz and linear increase up to 29.85 cycles (**Figure 6**, right) at the highest frequency of 199 Hz. The technique used here, with the number of cycles increasing with frequency, provides improved frequency resolution at high and low frequencies compared to the standard wavelet approach that uses a constant cycle length (Delorme and Makeig, 2004; Grossmann and Morlet, 1984; Kronland-Martinet et al., 1987). To process the amount of data, only 200 time points for 199 frequencies were calculated for each of the 2.5 ms epochs.

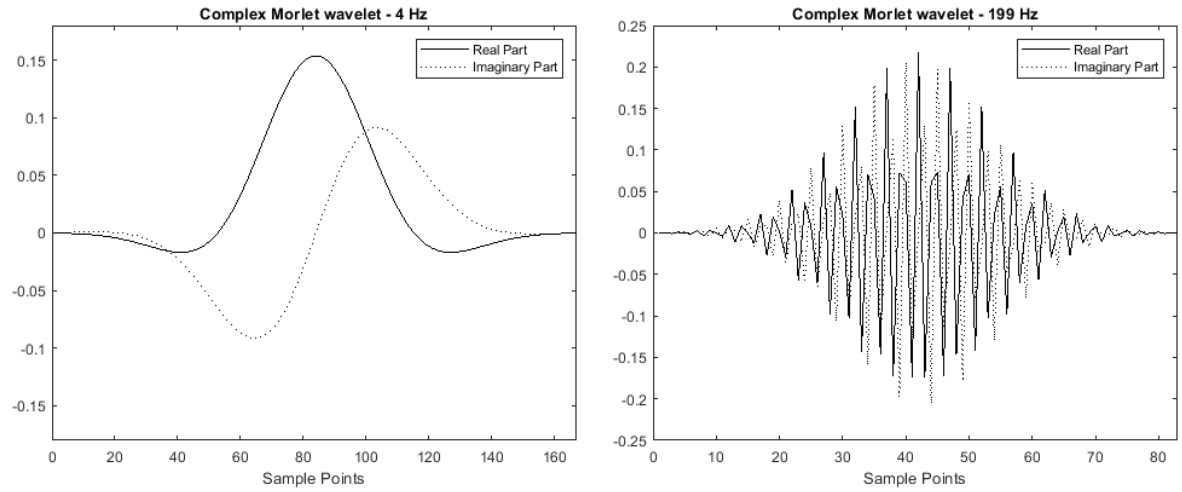


***Figure 6:*** *Complex Morlet wavelets (1.2 cycles at 4 Hz and 29.85 cycles at 199 Hz).*

After computing the wavelets, the scalar product between each wavelet and all 200-time points of the EEG epoch is calculated. This is applied to all epochs and all 21 channels to obtain the imaginary and real parts of all time-frequency points and to calculate amplitude and phase information. Power and phase were calculated:

*Power = alltfX.*conj(alltfX); % power for wavelets  newtimef() Line 1212*
*Angle = alltfX./ sqrt(alltfX .* conj(alltfX)); % ITC newtimef() Line 1195*

According to the established EEG analysis method, the calculated power points were grouped in theta, alpha, beta, low gamma, gamma, high gamma, and very high gamma frequency blocks (**Table 5**) for baseline, first stimulus, pause, a second stimulus, and post-stimulus phase. These time-frequency blocks were further sorted and averaged by performance (discrimination difficulty, wrong answer, correct answer) and stimulation frequency (fRef or fTin).

***Table 5: Frequency bands***
*Frequency bands of the EEG analysis in Hz.*

| Frequency band | Frequency [Hz] |
|---|---|
| Theta | >4 bis<8 |
| Alpha | >8 bis <13 |
| Beta | >13 bis <21 |
| Low gamma | >21 bis <40 |
| Gamma | >40 bis <60 |
| High gamma | >60 bis <120 |
| Very high gamma | >120 bis <200 |

## 1/f power-law function – Power normalisation

The difficulty with the empirical observation that power frequency-specific activity decreases as frequency increases (following a 1/f power-law function) is that it underweights higher frequencies, which are of particular interest. To address this problem, we have opted for power normalisation for individual patients (each computed frequency band of each subject was transformed individually for each epoch). For EEG power data with mean $\bar{X}$ and standard deviation S the z-score of a data point x is:

$$z - score = \frac{x - \bar{X}}{S}$$

## EEG single-trial analysis – Resting-state

Complementary to conventional EEG analysis, we were particularly interested in the single-trial information of the dataset. Due to our experimental design, the participant is not exposed to monotonic/ repetitive auditory stimulation in each epoch (as in ABR). Therefore, we do not benefit from averaging across many epochs as in conventional EEG/ABR analysis. For this reason, we computed the significant oscillation events for each electrode of each patient with a version of the oevent.py toolbox translated into MATLAB (Neymotin et al., 2022). The cwt-transformed time-frequency data were normalised by median power for each epoch. A local maximum filter (3 x 3 window) was applied to the transformed data to detect power peaks in the spectrogram. In order to detect peaks in the wavelet transform spectrogram, a local maximum filter (16x16-pixel window) was applied to the normalised data, and all points exceeding the threshold (3 x median) in frequency were determined as maxima. Time and frequency thresholds are defined before/after and above/below the peak to determine the event limits around the estimated peaks. Time (minT, maxT) and frequency span (minF to maxF) are defined as the point where the power value is less than half the maximum event amplitude and less than four times the median threshold (**Figure 7**). Based on the parameter duration (number of cycles, cycle>3) and the frequency range (log(maxF/minF), Foct < 1.5), further too-small events were excluded. After excluding the first oscillation events, overlapping events were merged when the bounding box overlap area in the spectrogram was > 50 % of the area of each event (Neymotin et al., 2022).

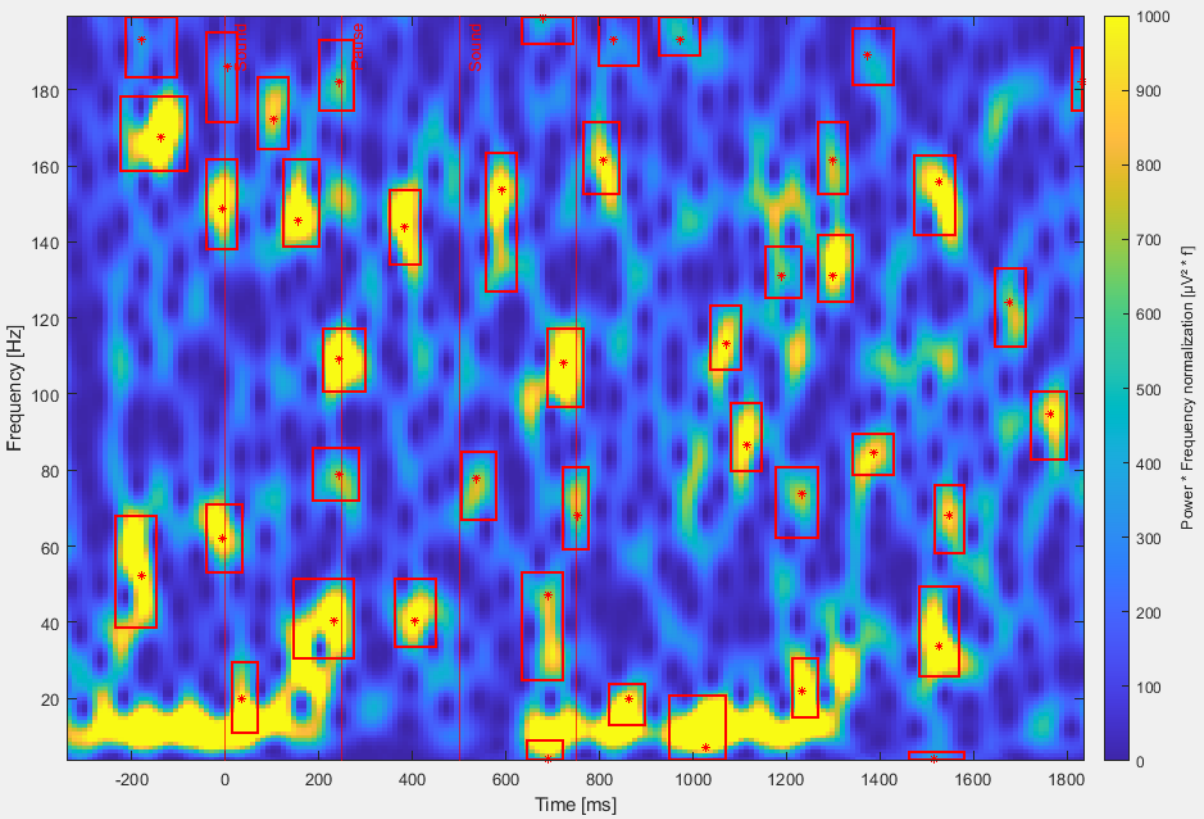


***Figure 7:*** *Oscillation events with bounding box. Individual single trial (TP2, electrode "T8", epoch 133) cwt plot illustrating the method for the selection of significant oscillation events. The cwt power of each epoch was normalized to the median, and events were distinguished according to length, frequency width, and intensity.*

### 2.7.5. fNIRS pre-processing

The code for the fNIRS pre-processing was written in MATLAB using the in-house toolbox "NIRS brain AnalyzIR" (Santosa et al., 2018).

#### Import of fNIRS data, block, and channel information

First, the ETG4000 files were imported into MATLAB using the "ETG4000 Export Tool" (*nirsexport()*) and saved as oxy- and deoxy-Hb. Because of the rapid event-related design, the paradigm is too dynamic for the deconvolution of the haemodynamic responses for each epoch; the epoch information was discarded, and the block information (fTin and fRef) was saved for the final block analysis. Since the NIRS toolbox is not as widely adopted as the EEG toolbox, the explicit functions employed are listed below.

### Artefact rejection of the fNIRS data

During the artefact rejection process for fNIRS traces, all channels are manually screened in the time domain. If there are any Not a Number values (NaNs) or noisy epochs, they are removed as required. Afterwards, open and deleted channels are interpolated using nearby channels.

*F = F.setProperty('function_handle',@NAfilt.interpolateChannel); % arithmetic mean*

### Filtering of the fNIRS data

Band-pass filtering (0.001-0.1 Hz) is performed to remove slow linear trends and other physiological noise, such as heartbeat (1-1.5 Hz), respiration (0.2-0.5 Hz), and Mayer waves (0.1 Hz; low-frequency blood pressure fluctuation components).

*F = NirsDataFunctor('function_handle', @bandpass, 'parameters', {[0.01 0.5], 10, 'old'}, 'input_names', {'oxy.tddr', 'deoxy.tddr'}, 'output_names', {'oxy.bpf', 'deoxy.bpf'});*

### Motion correction of the fNIRS data – Temporal Derivative Distribution Repair (TDDR)

Based on robust regression, the Temporal Derivative Distribution Repair TDDR method (Fishburn et al., 2019) is utilised for motion correction, effectively removing baseline shifts and spike artefacts.

*F = NirsDataFunctor('function_handle', @(X)TDDR(X,10), 'input_names', {'oxy.raw', 'deoxy.raw'}, 'output_names', {'oxy.tddr', 'deoxy.tddr'});*

Finally, the resulting signal was visually inspected, and trials with dominant artefacts were manually removed.

## 2.8. Statistical analysis

For the statistical tests, MATLAB programming system (version R2020a, MathWorks Inc., Natick, USA), PRISM 8 (GraphPad Software, Boston, USA), and R (The R Foundation for Statistical Computing, Vienna, Austria) were used for evaluation. Unless otherwise noted, statistical significance was tested at the level of $\alpha = 5$ %. The level of significance is illustrated in the figures with symbols or shaded areas (not significant (ns.); $p > 0.05$; * $p \leq 0.05$; ** $p < 0.01$; *** $p < 0.001$). Generally, the Shapiro-Wilk or Levene test was utilised to test for normality. Unless otherwise specified, mean and standard deviation were used to present normally distributed data, while median and quartiles were used for non-normally distributed data.

ROIs with reduced or enhanced evoked BOLD fMRI signal data are presented as significant ($p < 0.05$, FDR corrected **Figure 14, 15**, (Hofmeier et al., 2021)) differences in defined brain region activity. The second level specification independent two-sample t-test of the Statistical Parametric Mapping (SPM) toolbox was used to perform the group analysis. Three different contrasts were calculated in the analysis (T- vs C-group; TH- vs C-group; TH- vs T-group). For functional connectivity between defined ROIs in rs-fMRI (**Figure 19, 20**, (Hofmeier et al., 2021)), data are presented as significant ($p < 0.05$, FDR corrected) positive or negative correlation coefficients. In order to compare the number of connectivity between areas of interest among the groups, the data are simplified. The correlation values between the ROIs are divided into three subgroups by a one-sample *t*-test (not significantly different from zero, significantly positive, and significantly negative). To compare the connectivity between two areas in an analysis of variance, the number of significant correlations from each ROI of the first area to all ROIs of the second area is counted. Due to the non-parametric and repeated measures data, an align-and-rank transformation is performed with the ARTool (Wobbrock et al., 2011) before the variances of the groups are analysed. Afterwards, a repeated measures analysis of variance of the aligned rank transformed data is performed in R using the ARTool library.

```
m <- art(sig_Corr ~ Group + Error(ROI), data = data)
```

If the ANOVA shows a significant effect, a post-hoc comparison is performed. The contrasts in ART within a single factor (Group – levels: C-, T- and TH-group) may be computed with estimated marginal means (EMMs)/ least-squares means in R using the emmeans library (Confidence level used: 0.95; p value adjustment: Tukey method for comparing a family of 3 estimates).

```
emmeans(artlm(m, "Group"), pairwise ~ Group).
```

# 3. RESULTS

## 3.1. Paper I: Functional biomarkers that distinguish between tinnitus with and without hyperacusis (Hofmeier et al., 2021)

### 3.1.1. Recruitment & hyperacusis classification

The first trial consisted of 93 participants. Their hearing thresholds did not exceed 20 dB at each frequency from 0.125 kHz to 3 kHz and 40 dB at each frequency from 4 to 10 kHz in the PTA (**Figure 11**, (Hofmeier et al., 2021)). To ensure homogeneity of groups, age, sex, and handedness were considered and presented in **Appendix C.** For sub-classification, 50 tinnitus patients were recruited and categorised either as T-group (mean age 29.73 ± 7.86 years, age range 20-50 years) or TH-group (mean age 26.95 ± 6.94 years, age range 18-57 years) based on the HKI score (as shown in **Figure 8**, (Hofmeier et al., 2021)). The C-group consisted of 43 subjects (mean age 26.51 ± 5.83 years, age range 18-45 years) who did not have tinnitus and hyperacusis (Hofmeier et al., 2021).

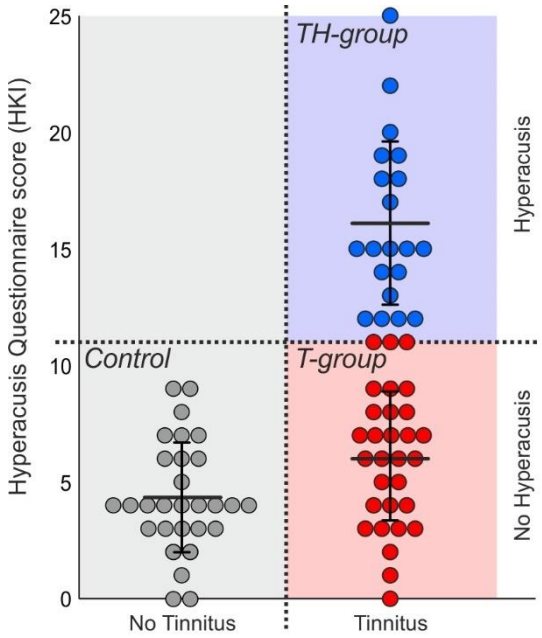


***Figure 8:*** *Hyperacusis questionnaire total score (HKI). The figure represents the mean ± SD between C- (n = 29, grey), T- (n = 30, red), and TH-group (n = 20, blue). Modified according to (Hofmeier et al., 2021).*

In total, we were able to include the 43 healthy controls and, out of 50 tinnitus subjects, 30 patients in the T-group and 20 in the TH-group.

### 3.1.2. Tinnitus description and tinnitus distress assessed with the tinnitus questionnaire – Goebel-Hiller Score (GHS)

In addition to the HKI, patients completed the GHS tinnitus questionnaire, which assessed various aspects of tinnitus severity, including laterality, emotional and cognitive distress, intrusiveness, and auditory difficulty. The TH-group had significantly higher total GHS scores than the T-group (T-group = 13.87 ± 10.32; TH-group = 28.6 ± 12.03; Mann-Whitney-U test p = < 0.001***; **Figure 9A**, (Hofmeier et al., 2021)). 80 % of participants in the TH-group experienced bilateral tinnitus, while 5 % reported it as unilateral in their right ear and 15 % in their left ear. In the T-group, 60 % experienced tinnitus in both ears, with 23.3 % reporting it in their right and 16.6 % in their left ear (**Appendix D**).

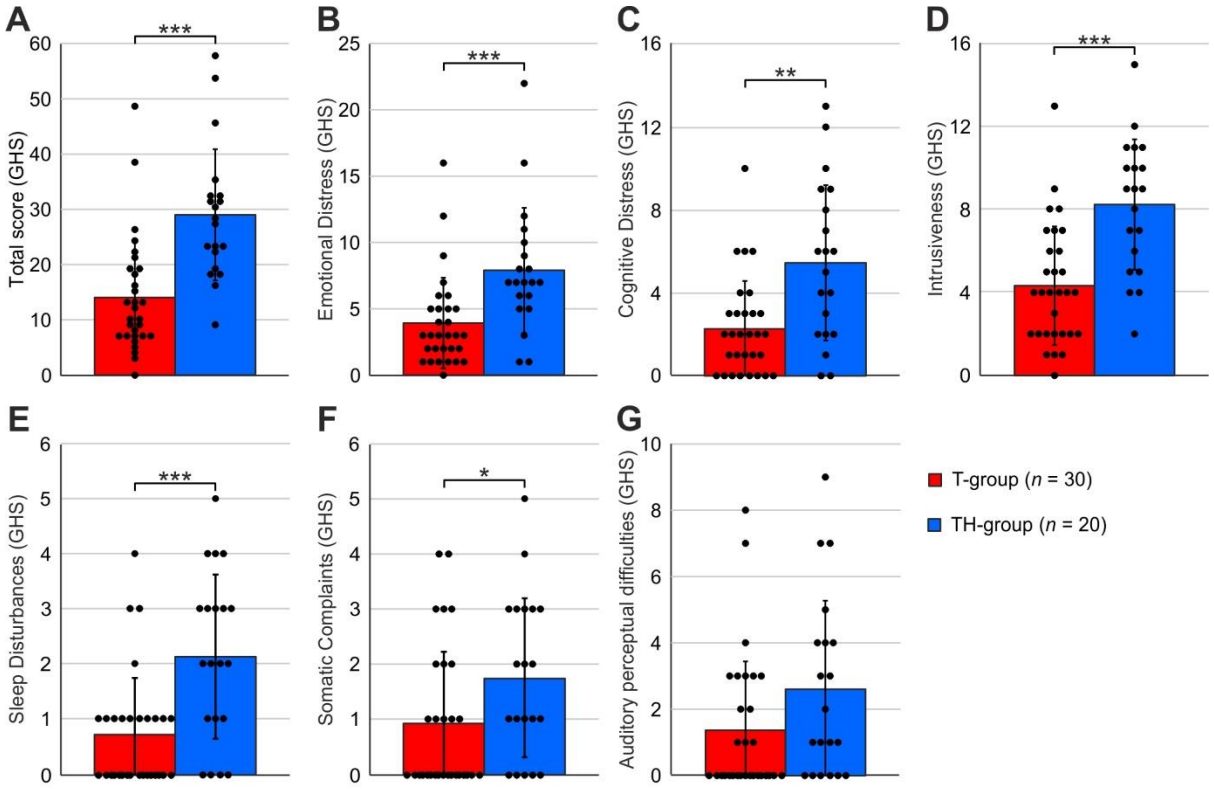


***Figure 9:*** *Scores for the tinnitus distress questionnaire (GHS). The bar charts illustrate the comparison of the tinnitus questionnaire mean ± SD between T- (n = 30, red) and TH-group (n = 20, blue). Modified according to (Hofmeier et al., 2021).*

Even according to the GHS questionnaires sub-scores, the TH-group scored significantly worse than the T-group in emotional distress (T-group = 3.93 ± 3.47; TH-group = 7.9 ± 4.83; p = < 0.001***), cognitive distress (T-group = 2.27 ± 2.35; TH-group = 5.45 ± 3.845; p = 0.002**), intrusiveness (T-group = 4.33 ± 2.9; TH-group = 8.25 ± 3.23; p = < 0.001***), sleep disturbance (T-group = 0.73 ± 1.05; TH-group = 2.15 ± 1.53; p = 0.001**), and somatic complaints (T-group = 0.93 ± 1.31; TH-group = 1.75 ± 1.48; p = 0.033*; **Figure 9B-F**, (Hofmeier et al., 2021)).

For each participant, the two-tailed Pearson correlation between the GHS sub-scores and loudness of tinnitus percept (dB hearing level (HL)) was depicted for the right and left ear, but no significant correlations were found (**Appendix E** (A-F), (Hofmeier et al., 2021)). Among all the sub-scores, the auditory perception difficulties score was the only one that showed no significant differences (**Appendix E** (G), (Hofmeier et al., 2021)). However, we observed increased auditory perceptional difficulty scores in patients with self-rated tinnitus loudness ≤ 15 dB HL in the TH-group but not in the T-group (**Figure 10A-C**, (Hofmeier et al., 2021)).

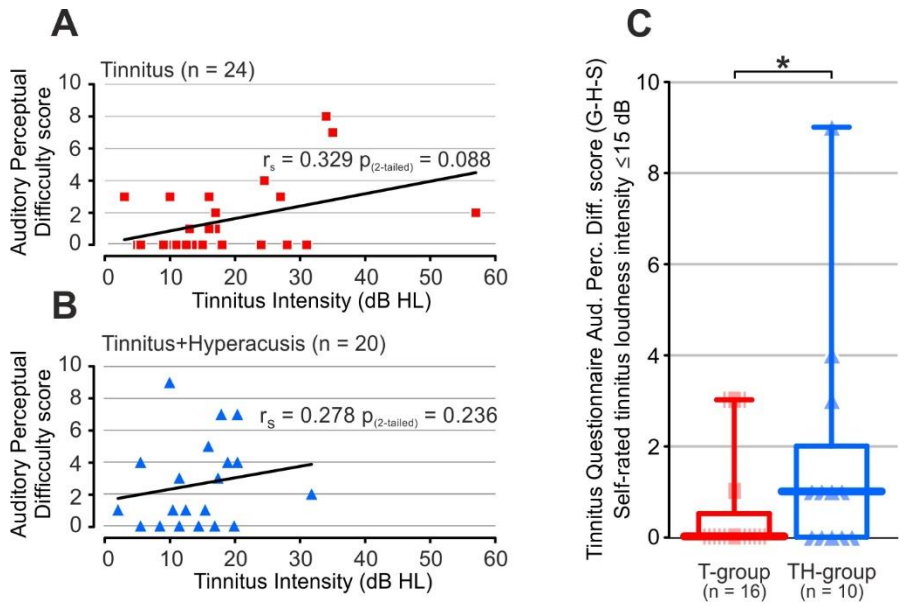


***Figure 10:*** *Auditory perception difficulties GHS sub-score. Two-tailed Pearson correlation between the auditory perception difficulties GHS sub-score and tinnitus loudness for T- (A) and TH-group (B). Auditory perceptional difficulty scores for patients with self-rated tinnitus loudness ≤ 15 dB HL. Modified according to (Hofmeier et al., 2021).*

**To summarise**, based on the GHS score and tinnitus laterality, the TH-group exhibited more significant distress than the T-group, even at low tinnitus levels.

### 3.1.3. Audiological evaluation

#### Hearing threshold differences – Pure Tone Audiometry (PTA)

To assess whether the differences in cognitive distress and annoyance between the T- and TH-group are also reflected in differences in hearing loss, we measured the hearing function by PTA. Based on the PTA measurements, there were no significant group differences in hearing thresholds between 0.125 and 10 kHz for both the right and left ears (Mann-Whitney-U test, $p > 0.5$; **Figure 11A-C**, (Hofmeier et al., 2021)).

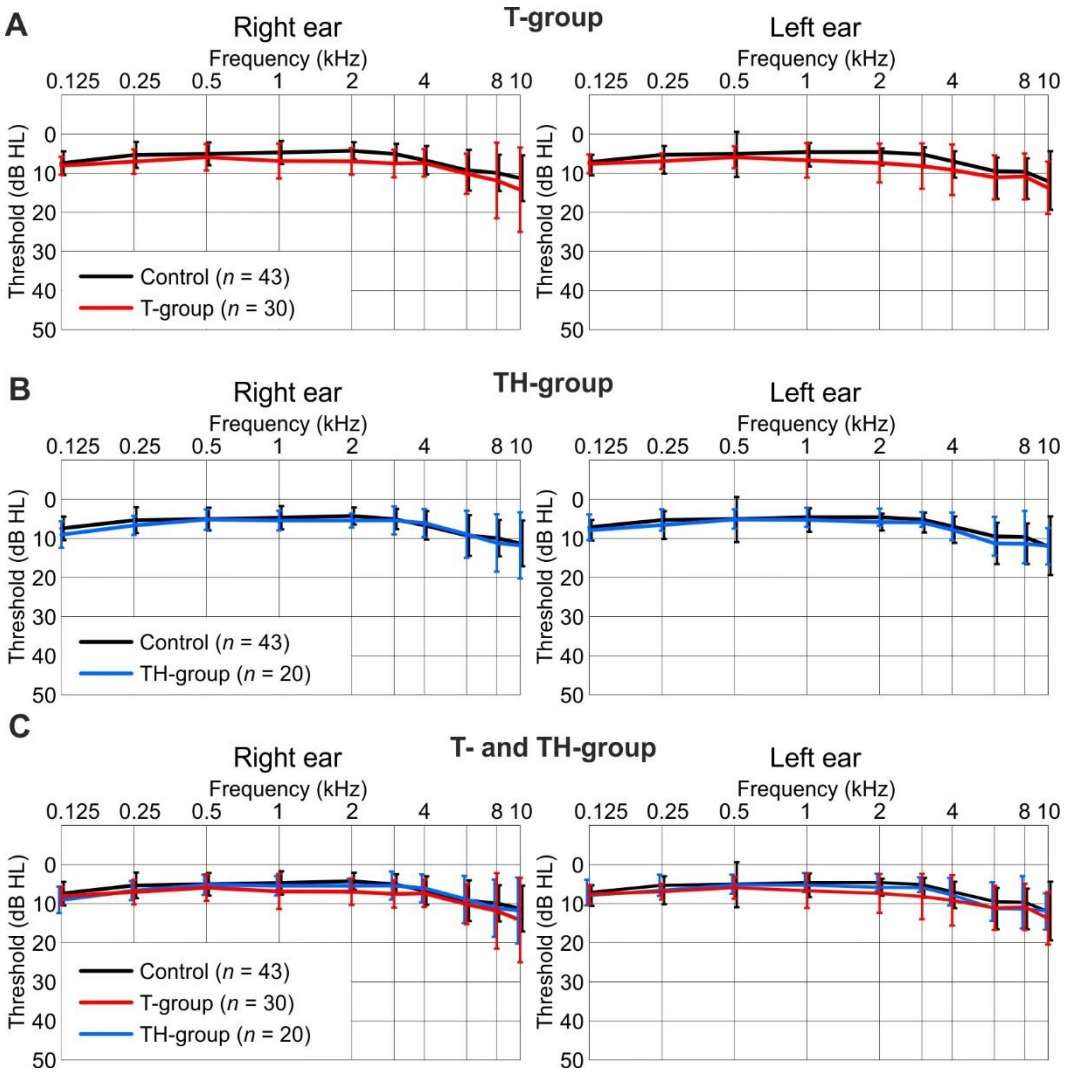


***Figure 11:*** *Pure tone audiometry (as mean ± SD) for the C- (n = 43, black), T- (n = 30, red), and TH-group (n = 20, blue), separated for the right and left ear. Mann-Whitney-U test was used to check for group differences. (A) T- compared to the C-group, (B) TH- compared to the C-group, (C) T- compared to TH- and C-group. dB, decibel; HL, hearing level; kHz, kilohertz; SD, Standard Deviation. Modified according to (Hofmeier et al., 2021).*

**In summary,** the results obtained from the PTA measurement indicate no significant variations in the hearing threshold.

Identification of difference in supra-threshold sound-induced ABR wave amplitude & latency

The ABR waves I to VI were assessed by applying click stimuli from 25 to 75 dB normalised hearing level (nHL) in 10 dB steps (**Figure 12**, (Hofmeier et al., 2021)). These supra-threshold ABR waves were attributed to specific neural activities generated in the auditory nerve (Wave I), cochlear nucleus (Wave III), superior olivary complex (Wave V), and inferior colliculus output or medial geniculate body (Wave VI). The results of the RM two-way ANOVA indicated significant peak-to-peak group effects for waves III ($p = 0.0199$) and V ($p = 0.0044$), while there was a trend towards significance for wave VI ($p = 0.0535$; **Figure 12A-C**, upper panel, (Hofmeier et al., 2021); for details of statistical results, see **Table 6**). For latencies, the results of the RM two-way ANOVA indicated significant group effects for wave V ($p < 0.0001$) and close to significant effects for wave I ($p = 0.0674$) and III ($p = 0.0869$; **Figure 12A-C**, lower panel, (Hofmeier et al., 2021); for details of statistical results, see **Table 6**).

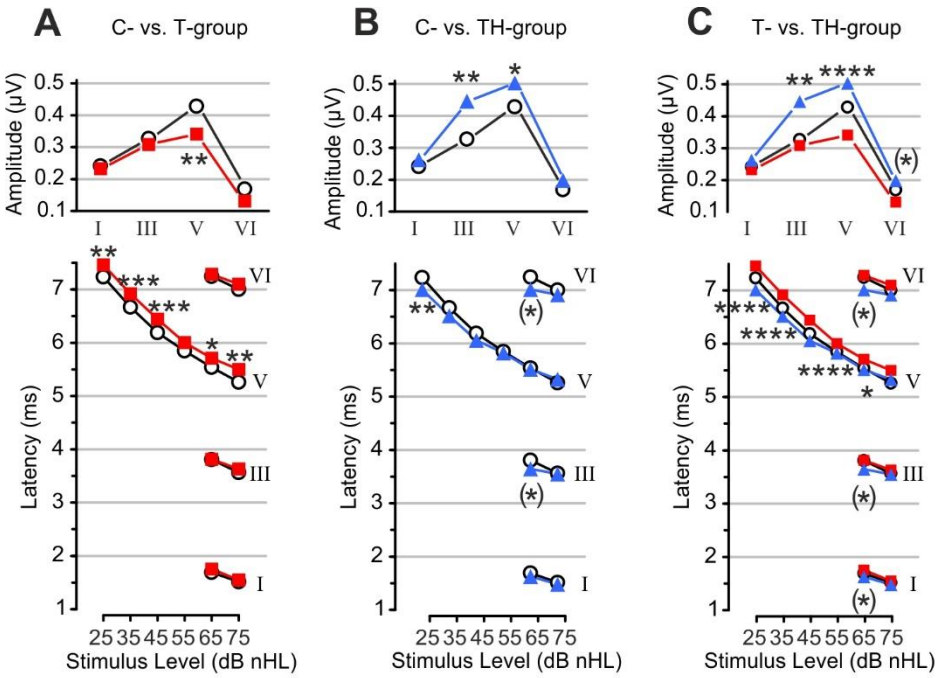


***Figure 12:*** *Supra-threshold ABR wave amplitude changes and latency shifts. ABR wave I, III, V, and VI amplitude at 75 dB nHL (upper panels) and latency as a function of stimulus level (lower panels) for (A) C- (n = 43, grey) and T-group (n = 30, red), (B) C- and TH-group (n = 20, blue), and (C) T- and TH-group. Differential responses in waves I, III and VI were observed and shown for 65 and 75 dB nHL stimuli. Modified according to (Hofmeier et al., 2021).*

At 75 dB nHL, the T-group showed significantly lower amplitude and delayed latency of ABR wave V, along with significantly elevated IPL between I-V compared with the control group (Holm-Šídák's post-hoc test $p = 0.0027$); **Figure 13B**, (Hofmeier et al., 2021)). In contrast, the TH-group showed a significantly higher ABR wave III and V amplitude than

controls, while no significant variations were observed in IPL (**Figure 13B**, (Hofmeier et al., 2021)). According to this direct comparison, the TH-group demonstrated a notable decrease in wave V latency across all volume levels, combined with significantly higher ABR wave III and V amplitude at 75 dB nHL (**Figure 12C**, (Hofmeier et al., 2021)).

In the next step, we examined the amplitude ratio between ABR wave V and I. This is a conventional measure of central neural gain, which is still presumed to be elevated in individuals experiencing tinnitus. In our cohort, one-way ANOVA also indicates differences in the ABR wave ratio V/I at 75 nHL ($p = 0.038$). However, we observed significantly lower ratios for the T- compared to the C-group (Holm-Šídák's post-hoc test $p = 0.0498$), while no differences were observed for the TH-group (**Figure 13A**, (Hofmeier et al., 2021)).

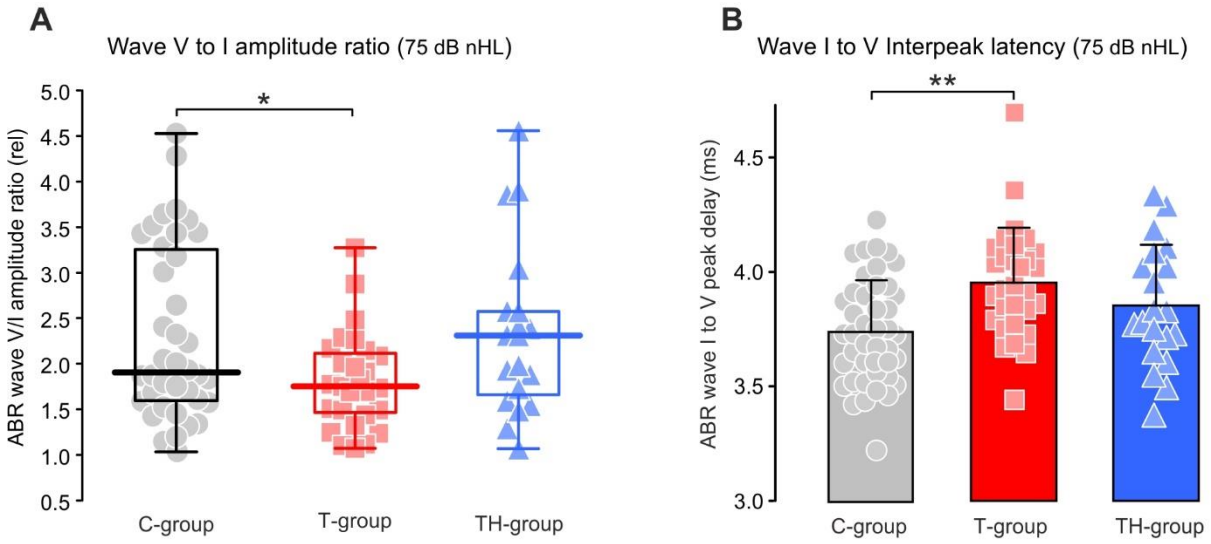


***Figure 13:*** *Neural gain and interpeak latency at 75 dB nHL. The box plots in (A) display the median, quartiles, and range of ABR gain (wave ratio V/I) for C- (n = 43, grey), T- (n = 30, red), and TH-group (n = 20, blue). The bar graphs in (B) show the mean ± SD of Interpeak Latency (IPL) between the peaks of ABR waves I and V. Modified according to (Hofmeier et al., 2021).*

**In summary,** despite similar hearing thresholds, participants in the T-group exhibited significantly reduced and delayed ABR waves III-VI; in particular, their reduced neural gain (ABR wave V/I) distinguished them from control subjects. In contrast, the TH-group displayed higher ABR amplitudes upon exposure to high sound levels, along with a tendency towards shorter ABR latencies.

***Table 6: ABR statistics***

*ABR Latency and suprathreshold amplitude (p values). Modified according to (Hofmeier, Wolpert et al. 2018).*

| | Level | **ABR wave amplitude (µV)** mean±SD (n) | | | Holm-Sidak's multiple comparisons test (adjusted p value) | | |
|---|---|---|---|---|---|---|---|
| | nHL (dB) | C | T | TH | C - T | C - TH | T - TH |
| **Wave I** 2-way RM ANOVA group: p=0.3824 F(2,88)=0.9720 | 75 | 0.24±0.121 (43) | 0.23±0.086 (30) | 0.26±0.119 (20) | 0.6838 | 0.6838 | 0.5612 |
| | 65 | 0.15±0.082 (42) | 0.14±0.076 (30) | 0.18±0.105 (19) | 0.7880 | 0.5215 | 0.5215 |
| **Wave III** 2-way RM ANOVA group: p=0.0199 F(2,89)=4.097 | 75 | 0.33±0.153 (43) | 0.31±0.186 (30) | 0.45±0.175 (20) | 0.5186 | 0.0052 | 0.0024 |
| | 65 | 0.23±0.156 (42) | 0.18±0.093 (30) | 0.24±0.093 (20) | 0.4103 | 0.6668 | 0.4103 |
| **Wave V** 2-way RM ANOVA group: p=0.0044 F(2,87)=5.784 | 75 | 0.43±0.174 (43) | 0.34±0.115 (30) | 0.5±0.177 (20) | 0.0031 | 0.0578 | < 0.0001 |
| | 65 | 0.34±0.122 (43) | 0.29±0.105 (30) | 0.35±0.112 (20) | 0.211 | 0.7953 | 0.211 |
| | 55 | 0.28±0.114 (43) | 0.27±0.095 (30) | 0.32±0.111 (19) | 0.6765 | 0.3439 | 0.3039 |
| | 45 | 0.27±0.105 (42) | 0.24±0.085 (30) | 0.31±0.13 (19) | 0.3506 | 0.3506 | 0.0883 |
| | 35 | 0.25±0.168 (41) | 0.19±0.115 (30) | 0.27±0.103 (19) | 0.1256 | 0.6976 | 0.1256 |
| | 25 | 0.21±0.104 (42) | 0.18±0.068 (30) | 0.23±0.106 (19) | 0.4206 | 0.6466 | 0.4113 |
| **Wave VI** 2-way RM ANOVA group: p=0.0535 F(2,83)=3.033 | 75 | 0.17±0.097 (41) | 0.13±0.106 (30) | 0.2±0.12 (19) | 0.2377 | 0.2481 | 0.0658 |
| | 65 | 0.15±0.097 (41) | 0.11±0.065 (30) | 0.15±0.114 (17) | 0.1861 | 0.8202 | 0.188 |
| | Level | **ABR wave amplitude (µV)** mean±SD (n) | | | Holm-Šídák's multiple comparisons test (adjusted p value) | | |
| | SPL (nHL) | C | T | TH | C - T | C - TH | T - TH |
| **Wave I** 2-way RM ANOVA group: p=0.0674 F(2,88)=2.782 | 75 | 1.52±0.155 (43) | 1.54±0.126 (30) | 1.48±0.145 (20) | 0.5571 | 0.5571 | 0.2803 |
| | 65 | 1.69±0.176 (42) | 1.76±0.186 (30) | 1.63±0.183 (19) | 0.1763 | 0.1763 | 0.021 |
| **Wave III** 2-way RM ANOVA group: p=0.0869 F(2,89)=2.511 | 75 | 3.56±0.189 (43) | 3.63±0.148 (30) | 3.55±0.100 (20) | 0.5061 | 0.8026 | 0.5061 |
| | 65 | 3.81±0.384 (42) | 3.81±0.200 (30) | 3.65±0.109 (20) | 0.9292 | 0.0422 | 0.0422 |
| **Wave V** 2-way RM ANOVA group: p<0.0001 F(2,88)=10.53 | 75 | 5.26±0.219 (43) | 5.50±0.238 (30) | 5.33±0.2 (20) | 0.0027 | 0.4952 | 0.0753 |
| | 65 | 5.54±0.261 (43) | 5.71±0.237 (30) | 5.52±0.17 (20) | 0.0446 | 0.7114 | 0.0446 |
| | 55 | 5.84±0.276 (43) | 6.00±0.237 (30) | 5.82±0.243 (19) | 0.0707 | 0.8223 | 0.079 |
| | 45 | 6.19±0.273 (42) | 6.45±0.317 (30) | 6.06±0.239 (19) | 0.0006 | 0.1135 | < 0.0001 |
| | 35 | 6.67±0.359 (42) | 6.92±0.407 (30) | 6.51±0.235 (19) | 0.0009 | 0.0611 | < 0.0001 |
| | 25 | 7.24±0.373 (42) | 7.46±0.412 (30) | 7.01±0.331 (19) | 0.0031 | 0.0061 | < 0.0001 |
| **Wave VI** 2-way RM ANOVA group: p=0.1121 F(2,83)=2.247 | 75 | 7±0.327 (41) | 7.1±0.379 (30) | 6.91±0.209 (19) | 0.5239 | 0.5239 | 0.2592 |
| | 65 | 7.25±0.359 (41) | 7.29±0.463 (30) | 7.01±0.319 (17) | 0.5991 | 0.0956 | 0.0655 |

### 3.1.4. Sound-evoked BOLD fMRI responses

Acoustically evoked BOLD fMRI responses were recorded from anatomically predefined ROIs (**Table 3**, upper panel), statistically compared by two-sample t-tests, and plotted as Δ t-values of statistical parametric maps averaged for the groups. Significant (FDR-corrected, $p < 0.05$) differences were highlighted as bold bars. The depicted bar graphs represent the BOLD signal in response to binaural stimulation with (i) rock music in yellow, (ii) LF-chirp in green, (iii) HF-chirp in red, and (iv) BB-chirp stimuli in blue (**Figure 14-16**, (Hofmeier et al., 2021)). The areas being investigated include both subcortical and cortical regions of the ascending auditory pathway, as well as regions involved in sound identification and pain processing.

#### Sound-induced BOLD fMRI response for subcortical regions

One of the most striking observations was a significant reduction of the evoked response in auditory brainstem regions (such as the SOC and partly CN) for T- and TH- compared to the C-group, especially in response to music and LF-chirp stimuli (**Figure 14** yellow and green, (Hofmeier et al., 2021)). Since this is observed in both subgroups, we considered this a tinnitus-specific pattern. However, in the TH-group, evoked BOLD signals to LF-chirp stimuli were elevated from the MGB upwards (**Figure 14** green, (Hofmeier et al., 2021)).

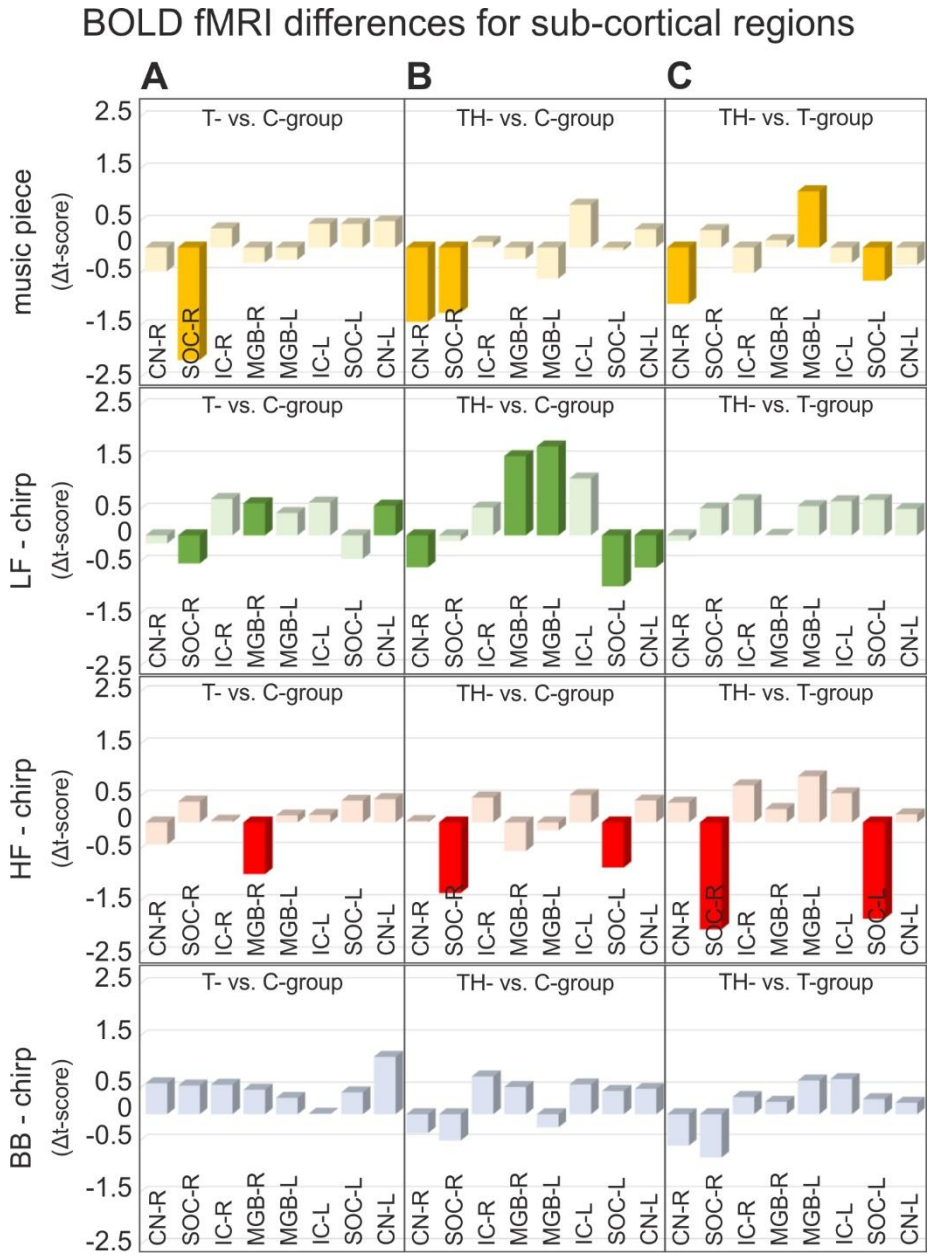


***Figure 14:*** *Task-evoked fMRI group differences for subcortical regions in C- (n = 43), T- (n = 30), and TH-group (n = 20). Differences for significant (two-sample t-test, p < 0.05, FDR corrected) task-evoked BOLD activity (reduced or enhanced as Δ t-score compared to the respective group notified within each panel) for the predefined brain areas (see* ***Table 3****) Activity differences between (A) C- and T-group, (B) C- and TH-group, (C) T- and TH-group evoked by rock music (yellow), LF-chirp (green), HF-chirp (red), and BB-chirp (blue). CN, cochlear nucleus; FDR, False discovery rate; SOC, superior olivary complex; IC, Inferior colliculus; MGB, medial geniculate body; L, left; R, right. Modified according to (Hofmeier et al., 2021).*

## Sound-induced BOLD fMRI response for auditory cortex regions

In the primary auditory cortex (AC-I) and the primary core region of the Broca Area, comprising the anterior and posterior AC-I in Heschl's gyrus of the superior temporal gyrus Brodmann area 41 (BA41A, P), as well as in the lateral superior temporal gyrus (BA42A, P), the LF-chirp stimuli induced a dominant enhanced BOLD fMRI response in the TH-

group (**Figure 15B** green, (Hofmeier et al., 2021)). In contrast, all BOLD responses were reduced in the T-group (**Figure 15A** green, (Hofmeier et al., 2021)). Moreover, all stimuli types induced reduced BOLD responses in the T-group and enhanced BOLD responses in the TH-group (**Figure 15A-C**, (Hofmeier et al., 2021)).

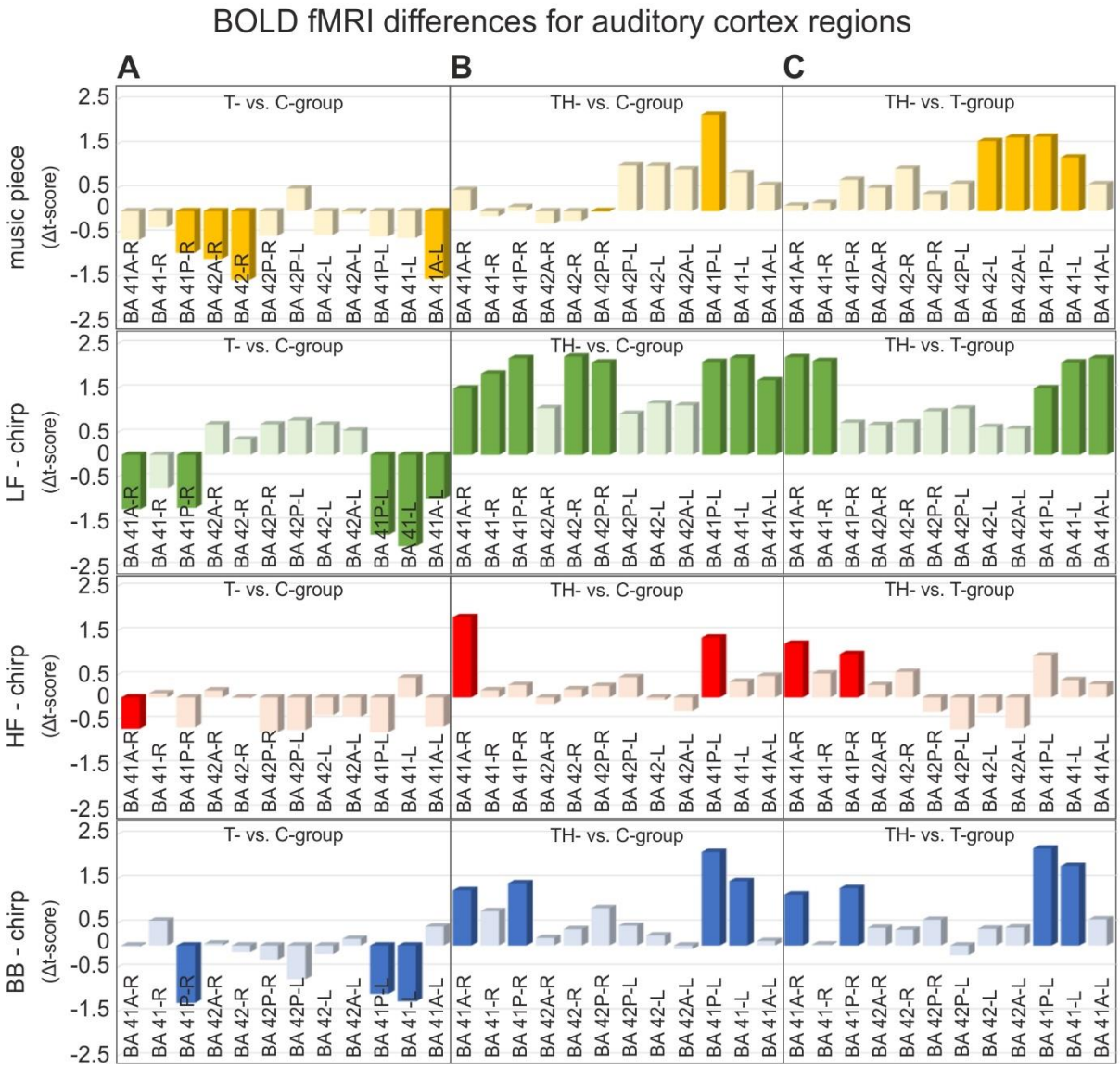


***Figure 15:*** *Task-evoked fMRI group differences for auditory cortex regions in C- (n = 43), T- (n = 30), and TH-group (n = 20). Differences for significant (two-sample t-test, p < 0.05, FDR corrected) task-evoked BOLD activity (reduced or enhanced as Δ t-score compared to the respective group notified within each panel) for the predefined brain areas (see **Table 3**). Activity differences between (A) C- and T-group, (B) C- and TH-group, (C) T- and TH-group evoked by rock music (yellow), LF-chirp (green), HF-chirp (red), and BB-chirp (blue). A, anterior; BA, Brodmann area; FDR, False discovery rate; L, left; P, posterior; R, right. Modified according to (Hofmeier et al., 2021).*

Sound-induced BOLD fMRI response for sound identification regions

This distinct group-specific AC-I BOLD fMRI pattern, with reduced T-group responses but enhanced TH-group responses, was also observable in regions responsible for sound identification (**Figure 16**, (Hofmeier et al., 2021)). Exclusively, HF-chirp stimuli evoked responses were reduced also in the TH-group (**Figure 16B**, (Hofmeier et al., 2021)).

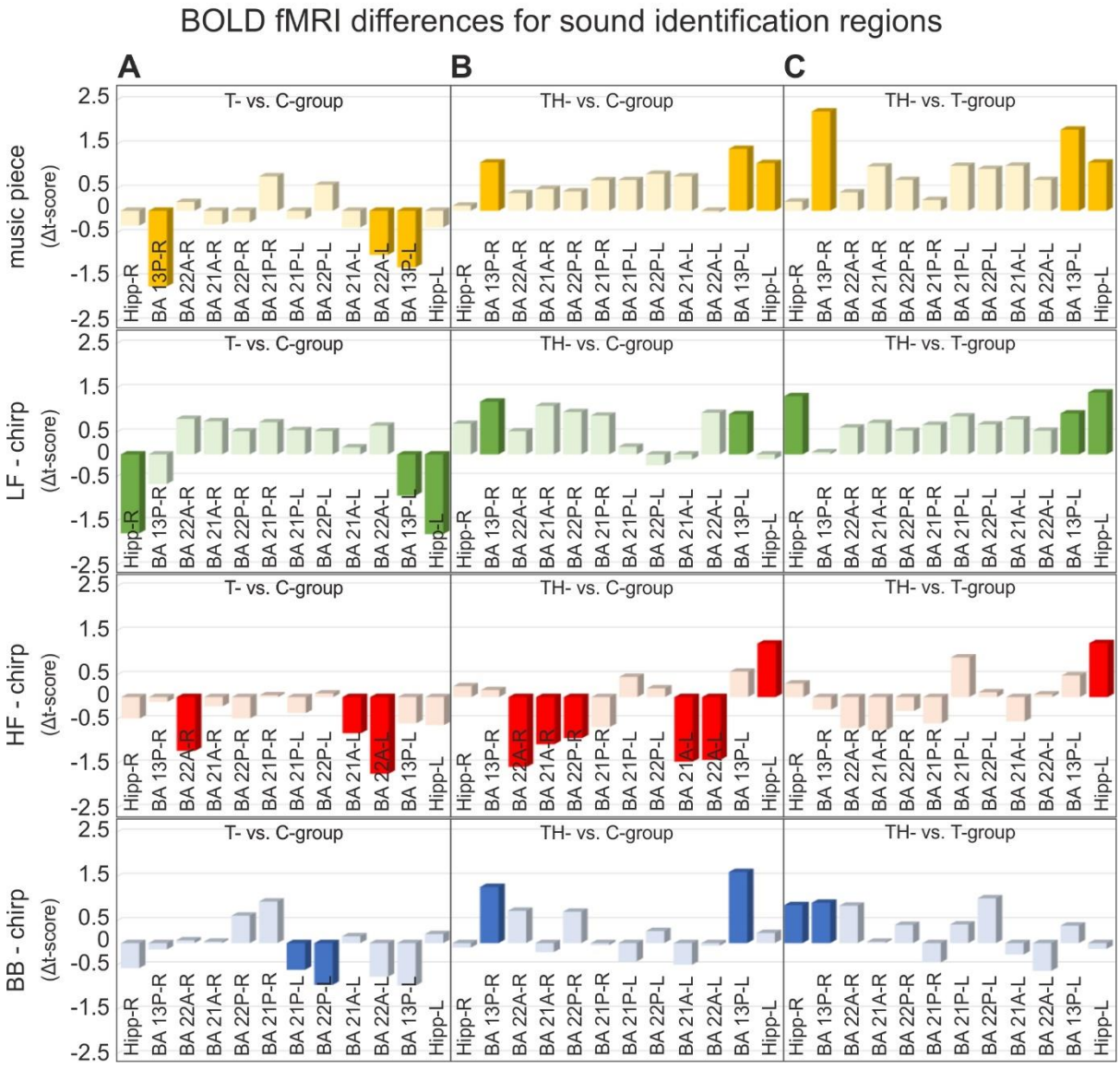


***Figure 16:*** *Task-evoked fMRI group differences for sound identification associated regions in C- (n = 43), T- (n = 30), and TH-group (n = 20). Differences for significant (two-sample t-test, p < 0.05, FDR corrected) task-evoked BOLD activity (reduced or enhanced as Δ t-score compared to the respective group notified within each panel) for the predefined brain areas (see **Table 3**). Activity differences between (A) C- and T-group, (B) C- and TH-group, (C) T- and TH-group evoked by rock music (yellow), LF-chirp (green), HF-chirp (red), and BB-chirp (blue). A, anterior; BA, Brodmann area; FDR, False discovery rate; Hipp, hippocampus; L, left; P, posterior; R, right. Modified according to (Hofmeier et al., 2021).*

Thus, the posterior insula (BA13P), known to be responsible for sound detection, and the hippocampus, known to be accountable for auditory skill formation and memory-dependent auditory perception, induced enhanced BOLD fMRI responses to music, LF-chirp, and BB-chirp stimuli in the TH-group, whereas all stimuli elicited reduced BOLD fMRI responses in the T-group **(Figure 16, (Hofmeier et al., 2021)).**

Only the superior temporal gyrus BA22 and the multimodal region of BA21, as part of Wernicke`s reception/understanding system, were significantly reduced in T- and TH-group (**Figure 16** red, (Hofmeier et al., 2021)), indicating the HF-chirp stimuli responses in these Wernicke`s regions as characteristic for tinnitus.

### Sound-induced BOLD fMRI response for pain regions

Finally, we focused on pathways related to fear and pain, including the mammillary body (Mam. Body). This region of the limbic system state-dependent regulates the insular and peri-insular regions, especially the dorsal posterior insula (DpIns) and the regions of the postcentral gyrus with the parietal operculum (PO1, PO2). It has been documented that these areas become active after experiencing painful stimulation.

Increased BOLD signals were found in the Mam. Body in response to BB-chirp stimuli in both the T-group and the TH-group (**Figure 17** blue, (Hofmeier et al., 2021)). For music stimuli, we observed reduced BOLD fMRI signals in the DpIns and both parietal operculum regions ($PO_1$, $PO_2$) in the T- compared to the C-group. This reduced response was no longer found in the TH-group, particularly in the PO regions, leading to significant group differences (**Figure 17C** yellow, (Hofmeier et al., 2021)).

**In summary**, significant results were found, which were consistent across all stimuli: the T-group was characterised by reduced BOLD responses to all stimuli in subcortical (SOC) and AC-I (BA41, BA42) regions, regions of sound identification (posterior insula, hippocampus, BA21, BA22) and pain association (DpIns, $PO_1$, $PO_2$; **Figure 14-16A**, (Hofmeier et al., 2021)). On the other hand, as characteristic of the TH-group, enhanced BOLD fMRI activity, particularly in response to LF-chirp stimuli, was found in the MGB, the AC-I, and regions of sound identification, including changed activities in pain-receptive regions (**Figure 14-16B, C**, (Hofmeier et al., 2021)).

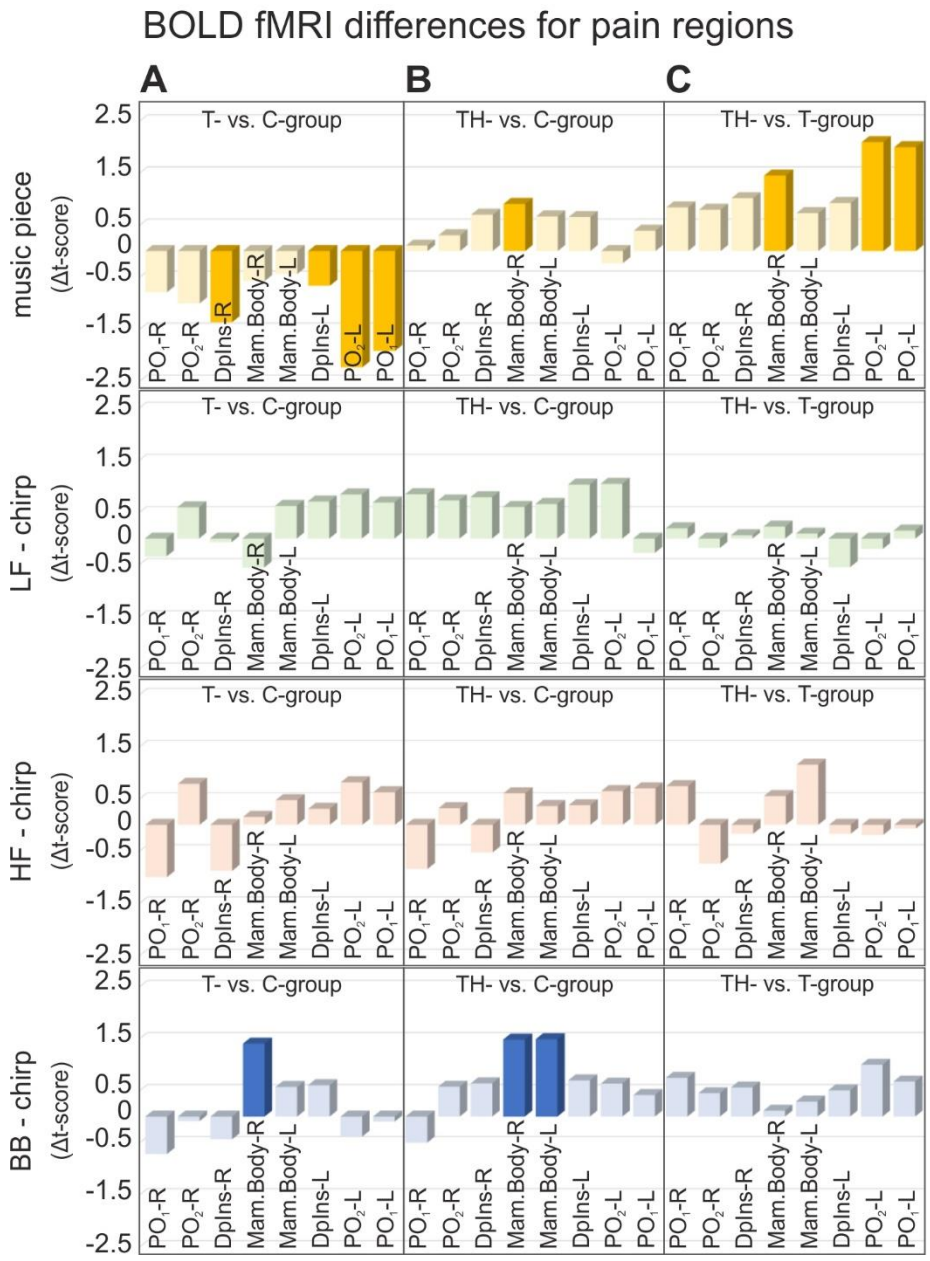


***Figure 17:*** *Task-evoked fMRI group differences for pain-associated regions in C- (n = 43), T- (n = 30), and TH-group (n = 20). Differences for significant (two-sample t-test, p < 0.05, FDR corrected) task-evoked BOLD activity (reduced or enhanced as Δ t-score compared to the respective group notified within each panel) for the predefined brain areas (see* ***Table 3****). Activity differences between (A) C- and T-group, (B) C- and TH-group, (C) T- and TH-group evoked by rock music (yellow), LF-chirp (green), HF-chirp (red), and BB-chirp (blue). A, anterior; BA, Brodmann area; DpIns, Dorsal Posterior Insula; FDR, False discovery rate; L, left; Mam. Body, mammillary body; P, posterior; PO, parietal operculum; R, right. Modified according to (Hofmeier et al., 2021).*

### 3.1.5. Resting-state BOLD fMRI connectivity

Previous findings suggested that task-evoked BOLD fMRI activity and behavioural performance may be correlated with a higher level of synchronous, positive fMRI activity at rest. To assess whether the differences in the evoked BOLD fMRI responses in the T-

and TH-groups are reflected in differences of BOLD activity at rest (rs-fMRI), positive and negative BOLD signals were assessed between predefined ROIs (**Table 3**). These overall correlations were depicted for defined ROI in the left and right hemisphere (**Figure 18A, Figure 19-21**, lower panel, (Hofmeier et al., 2021)) and distinguished for individual groups as positive or negative correlations (**Figure 18A**, left and right panel, **Figure 19-21**, lower panel, (Hofmeier et al., 2021)).

Resting-state BOLD fMRI connectivity – Number of correlations and correlation strength

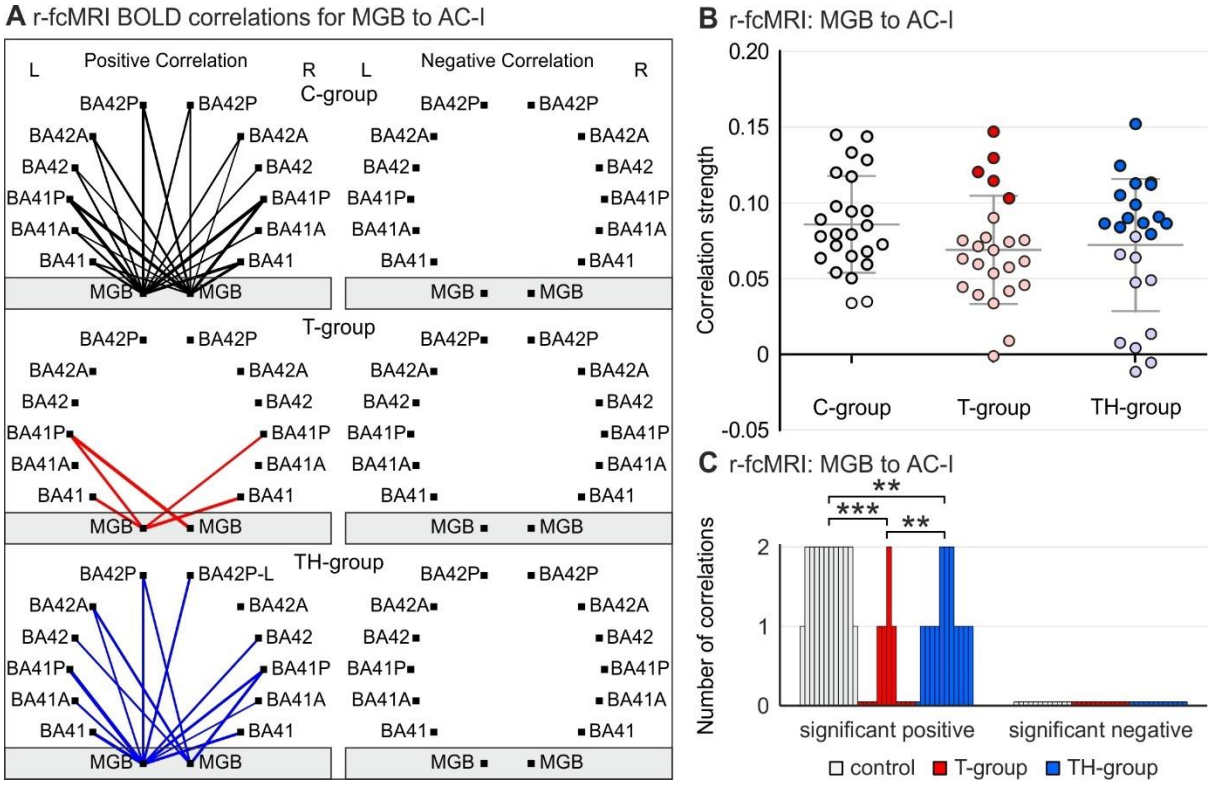


***Figure 18:*** *Illustration of methods for evaluating qualitative and quantitative group differences of rs-fMRI correlations. The patterns in (A) show the amount of significant nonzero (one-sample t-test p < 0.05, FDR corrected) rs-fMRI BOLD correlations of the scatterplot (B), divided into positive and negative correlations for the different groups. In the scatterplot (B), each data point represents the group mean of the correlation strength between two coordinates of the considered predefined ROI groups (in this example, MGB and the AC-I (BA41; BA41A; BA41P; BA42; BA42A; BA42P)). Mean ± SD shown for C- (n = 43, grey), T- (n = 30, red), and TH-group (n = 20, blue). Significantly, nonzero values are highlighted. The bar chart (C) shows the amount of significant nonzero rs-fMRI BOLD correlations of (A). For the group comparisons, the data is Align and Rank Transformed (ARTool), and the variance is determined with repeated measures ANOVA. BA, Brodmann area; FDR, False discovery rate. Modified according to (Hofmeier et al., 2021).*

Number of correlations (**Figure 18A, 19-21A-C**, (Hofmeier et al., 2021)) and correlation strength (**Figure 18B**, (Hofmeier et al., 2021)) of significantly connected interregional functional pathways were analysed separately. Group differences between correlation strengths were insignificant (shown for MGB to AC-I in **Figure 18B**, (Hofmeier et al.,

2021)). In contrast, there was a significant difference in the number of correlations between the groups (**Figure 19-21**, upper panel, (Hofmeier et al., 2021)). As a characteristic sign, the number of correlations between nearly all identified networks were lowered for both the T- and TH-group compared to controls (**Figure 19-21**, (Hofmeier et al., 2021)).

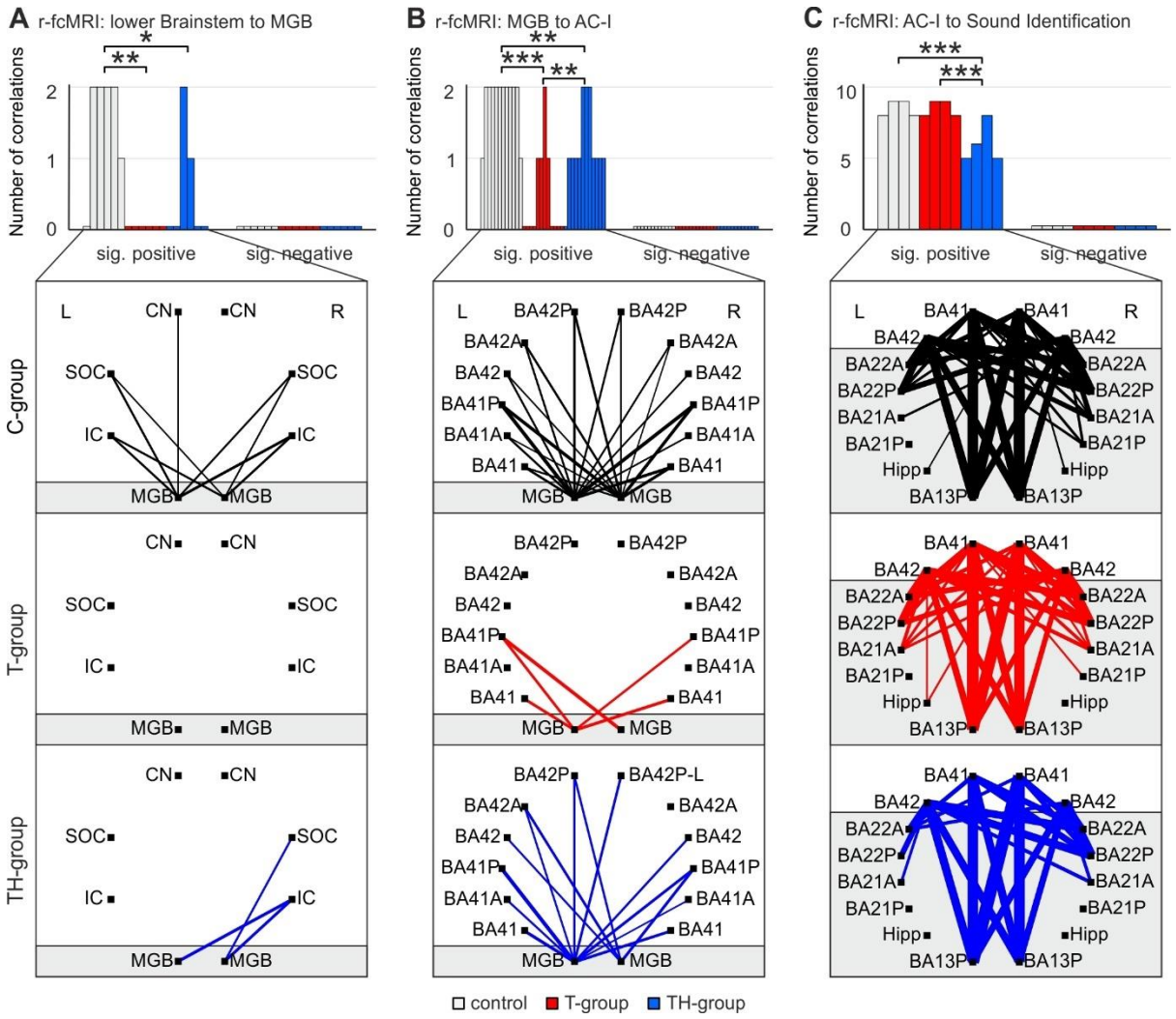


***Figure 19:*** *Qualitative and quantitative group differences in rs-fMRI correlations within the ascending auditory pathway. Graphs (A-C) show the amount of significant nonzero (one-sample t-test p < 0.05, FDR corrected) rs-fMRI BOLD correlations, divided into positive correlations and negative correlations for the distinct groups. C- (n = 43, grey/black), T- (n = 30, red), and TH-group (n = 20, blue). The thickness of the lines in the lower column corresponds to the correlation strength. Connectivity between (A) Lower Brainstem (CN, SOC, IC) and the MGB, (B) MGB and the AC-I (BA41; BA41A; BA41P; BA42; BA42A; BA42P), (C) AC-I and the Sound Identification Network (BA21A; BA21P; BA22A; BA22P; Hipp; BA13P). AC-I, auditory cortex; BA, Brodmann area; BOLD, blood oxygenation level depended; CN, cochlear nucleus; FDR, False discovery rate; Hipp, hippocampus; IC, inferior colliculus; MGB, medial geniculate body; ROI, region of interest; SOC, superior olivary complex. Modified according to (Hofmeier et al., 2021).*

Significant reductions in positive rs-fMRI correlations were observed in auditory-specific and associated regions in the T-group, with the TH-group showing comparatively less

reduction. This is displayed for the functional connectivity (i) between the MGB and subcortical auditory regions such as the CN, SOC, and IC (**Figure 19A**, (Hofmeier et al., 2021)), (ii) between MGB and the anterior AC-I regions BA41 and BA42 (**Figure 19B**, (Hofmeier et al., 2021)), (iii) between the AC-I and regions controlling emotional distress, particularly the amygdala (**Figure 20A**, (Hofmeier et al., 2021)), and (iv) between the AC-I and the attention-controlling regions BA45 and BA46 (**Figure 20B**, (Hofmeier et al., 2021)).

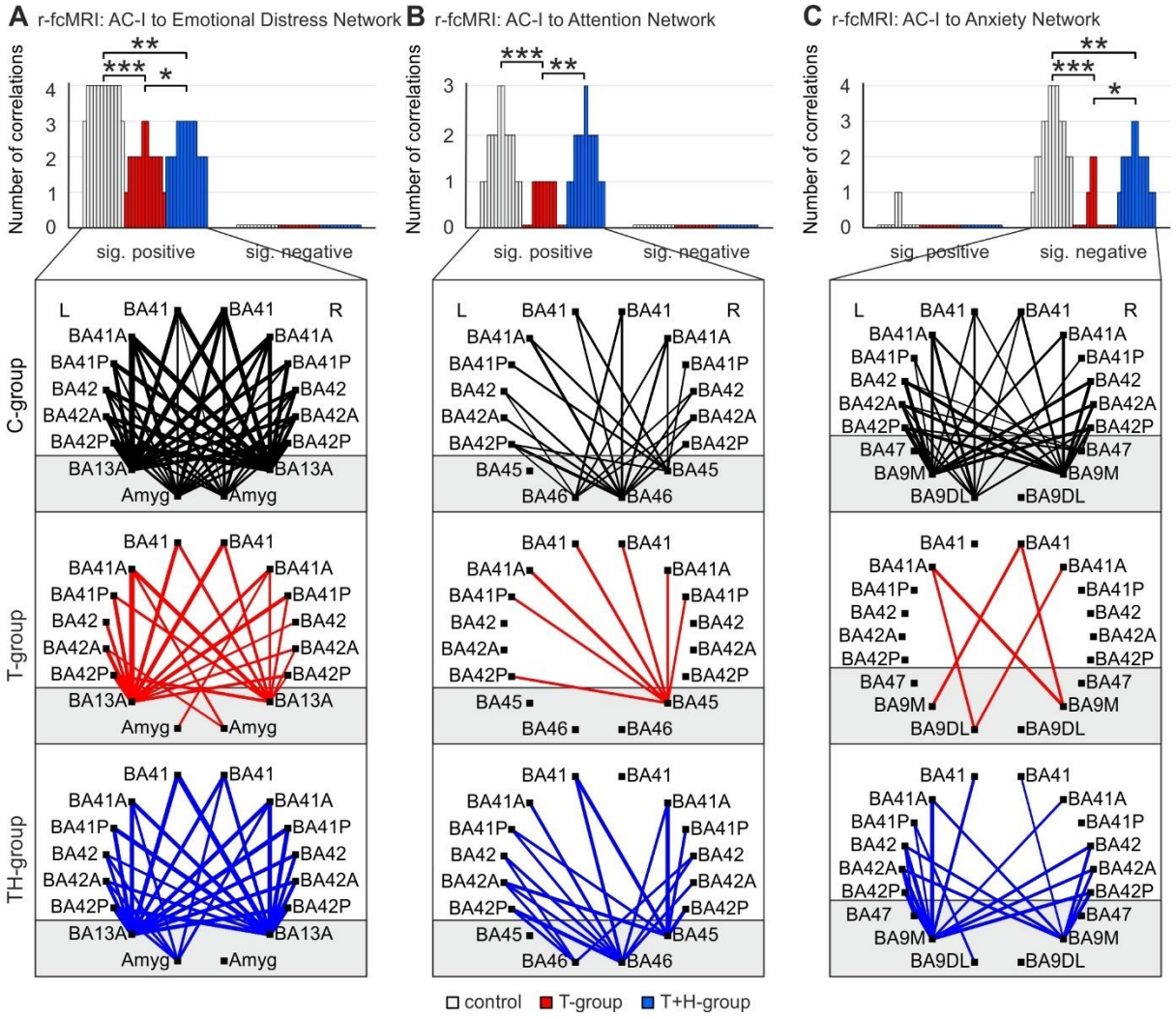


***Figure 20:*** *Qualitative and quantitative group differences in rs-fMRI correlations of auditory cortex networks. Functional connectivity between (A) AC-I (BA41; BA41A; BA41P; BA42; BA42A; BA42P) and the Emotional Distress Network (BA13A; Amyg), (B) AC-I and the Attention Network (BA45; BA46), (C) AC-I and the Anxiety Network (BA47; BA9M; BA9DL). Amyg, amygdala; AC-I, primary auditory cortex; DL, dorsolateral; M, medial; ROI, region of interest. Modified according to (Hofmeier et al., 2021).*

This challenges the hypothesis that reduced evoked BOLD fMRI in subcortical auditory regions in both the T- and TH-group (**Figure 14**, (Hofmeier et al., 2021)) may be reflected in a reduced number of positive correlations between subcortical and cortical auditory regions and associated regions (**Figure 19A, B, 20A, B, 21A**, (Hofmeier et al., 2021)). The

number of correlations between the primary AC-I (BA41, 42) and associated BA21, 22 regions (sound identification), were reduced in the TH- but not in the T-group (**Figure 19C**, (Hofmeier et al., 2021)).

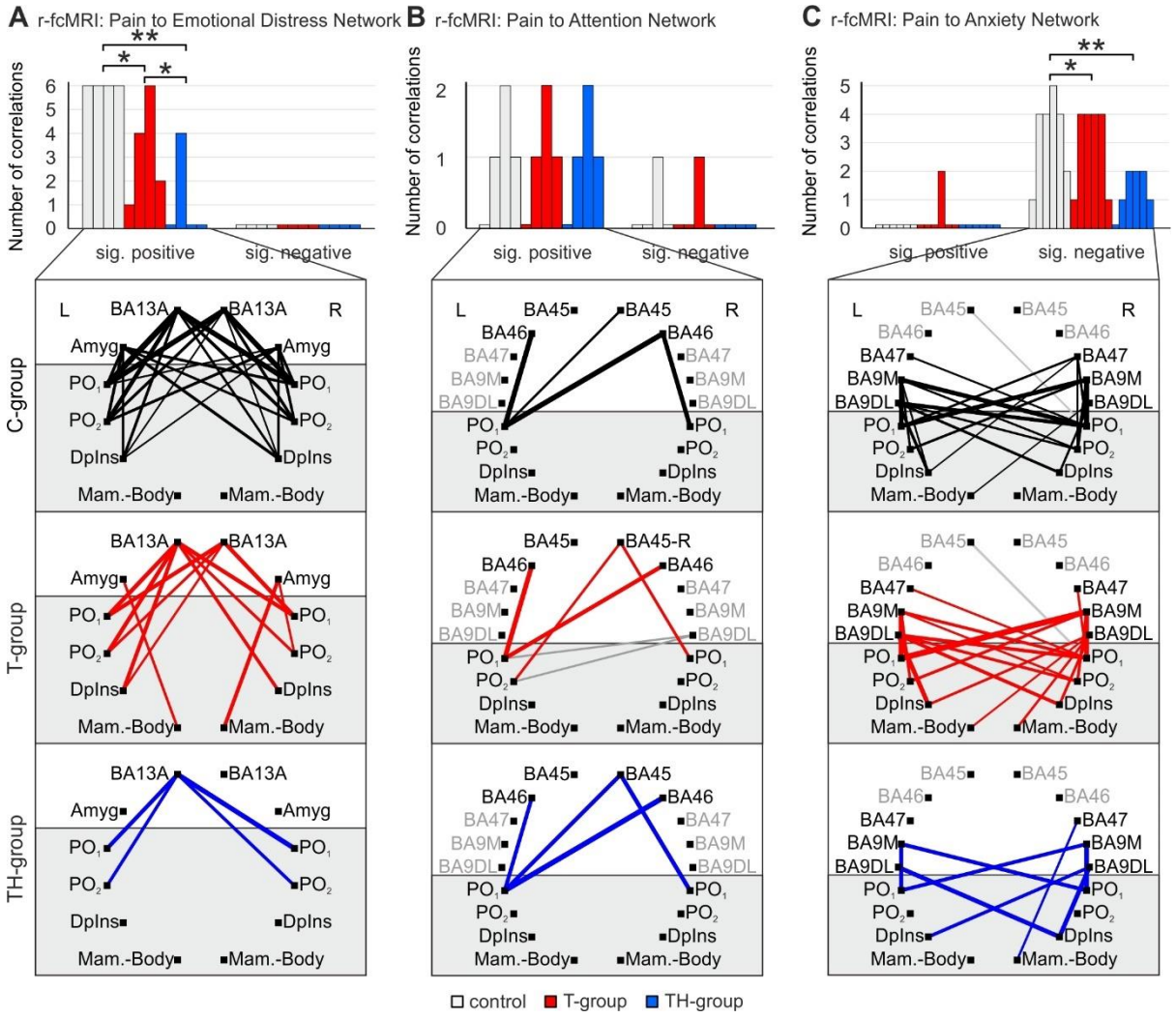


***Figure 21:*** *Qualitative and quantitative group differences in rs-fMRI correlations of pain networks. Functional connectivity between (A) the Pain Network (PO1; PO2; DpIns; Mam. Body) and the Emotional Distress Network, (B) the Pain Network and the Attention Network, and (C) the Pain Network and Anxiety Network. Amyg, amygdala; DpIns, dorsal posterior Insula; Mam, mammillary; PO, parietal operculum; ROI, region of interest. Modified according to (Hofmeier et al., 2021).*

The number of significantly anti-correlated (negative) functional connections was low in our analysis, indicating synchronised neuronal activity and homogeneous haemodynamic responses: The number of negative rs-fMRI correlations between the AC-I and fronto-parietal BA9 and BA47 regions was lower in the T- than in the TH-group, but both groups were less correlated than controls (**Figure 20C**, (Hofmeier et al., 2021)). Also, significantly fewer negatively correlated connections were found between the pain network and the fronto-parietal BA9 and BA47 regions in both T- and TH-groups compared to the C-group (**Figure 21C**, (Hofmeier et al., 2021)). This indicates that in the C group, the number of

negative correlations of AC-I to anxiety regions (**Figure 20C**, (Hofmeier et al., 2021)), pain to anxiety regions (**Figure 21C**, (Hofmeier et al., 2021)), and vice versa was higher than in the T- and TH-group. The connectivity between AC-I and the attention network was significantly weakened, but only in the T-group (**Figure 20B**, (Hofmeier et al., 2021)).

**In summary**, we revealed fewer positive correlations between (sub-)cortical and associated auditory regions in the T-group and a less reduced number in the TH-group (**Figure 19A, B, 20A**, (Hofmeier et al., 2021)). On the other hand, there was a significantly reduced number of positive correlations in AC-I to sound identification regions and in pain to emotional regions in the TH-group but a less reduced number in the T-group (**Figure 19C, 21A**, (Hofmeier et al., 2021)).

## Identified T- and TH-group specific biomarkers

**In recap**, the most characteristic functional biomarkers of the T-group were (i) delayed and reduced ABR wave V, (ii) reduced evoked BOLD fMRI responses in the MGB, AC-I, BA13P and hippocampus, particularly for HF-chirp stimuli, and (iii) reduced positive connectivity between subcortical auditory regions and the AC-I (**Figure 22**, red, (Hofmeier et al., 2021)).

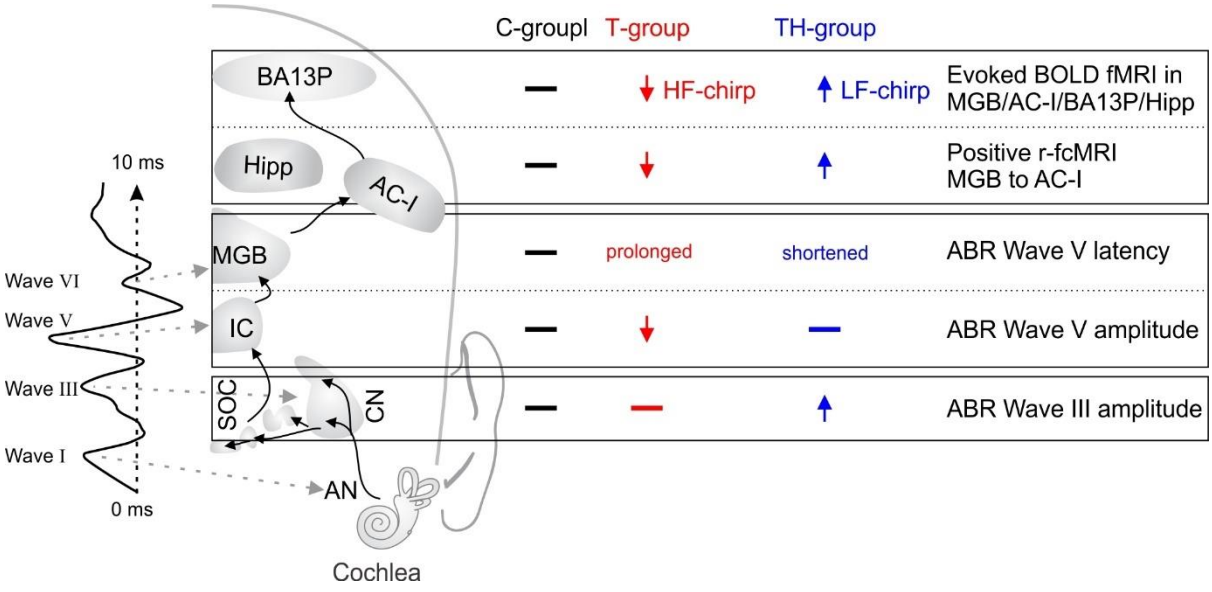


***Figure 22:*** *Overview of the characteristic functional biomarkers discriminating the T- and TH-groups (rs-fMRI, evoked fMRI, ABR wave amplitude and latency). Wave I, III, V, and VI represent distinct ABR wave components. Horizontal bar: unchanged; down arrow: smaller; Up arrow: larger/more. ABR, auditory brain response; AC-I, auditory cortex; AN, auditory nerve; BA, Brodmann area; BOLD, blood oxygenation level-dependent; CN, cochlear nucleus; Hipp, hippocampus; IC, inferior colliculus; LF, low frequency; MGB, medial geniculate body; SOC, superior olivary complex. Modified according to (Hofmeier et al., 2021).*

These characteristics can be differentiated from those in the TH-group. Specifically, they have an (i) enhanced ABR wave III and V in response to high sound intensity, (ii) elevated evoked BOLD fMRI responses in the MGB, AC-I, BA13P, and hippocampus, particularly for LF-Chirp stimuli, and (iii) less reduced positive connectivity between subcortical auditory regions and the AC-I (**Figure 22**, blue, (Hofmeier et al., 2021)).

## 3.2. Paper II: Co-occurrence of hyperacusis accelerates with tinnitus burden over time and requires medical care (Refat et al., 2021)

### 3.2.1. Recruitment and sub-group classification

Of the 96 participants, 43 healthy individuals could be designated to the control group (age: 26.5 ± 5.8 years, between 18-45 years, 20 men and 23 women). Among the remaining 53 patients, 33 patients complained of tinnitus without co-occurrence of hyperacusis (age: 32.6 ± 11.5 years, between 20 and 61 years, 22 men and 11 women, T-group), and the HKI classified 20 with co-occurrence of hyperacusis (age: 26.9 ± 6.9 years, between 18 and 49 years, 6 men and 14 women, TH-group).

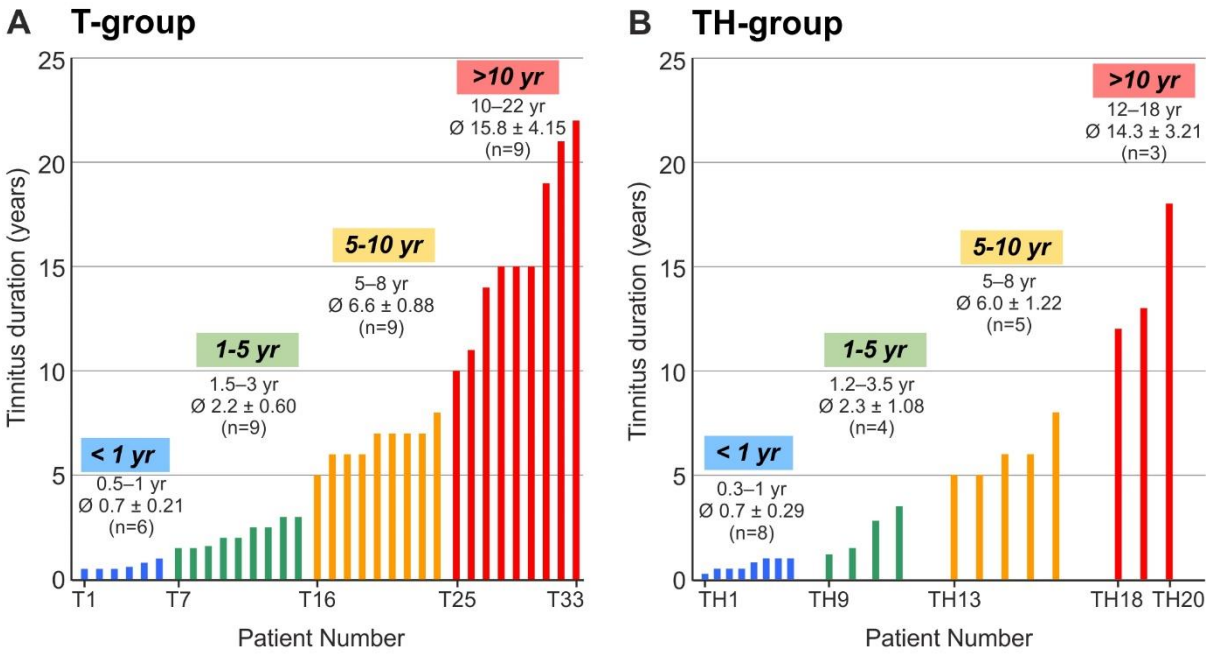


***Figure 23:*** *Distribution of participants according to the tinnitus duration. (A) Thirty-three participants with tinnitus (T1 to T33) were classified into four tinnitus duration groups of up to one year (< 1 yr), between one and five years (1-5 yr), between five and ten years (5-10 yr), and ten years and more (> 10 yr). (B) Twenty participants with tinnitus and hyperacusis (TH1 to TH20) were classified accordingly. Groups were colour-coded by blue, green, yellow, and red concerning tinnitus duration throughout this manuscript. Yr, years. Modified according to (Refat et al., 2021).*

In accordance with the inclusion criteria, the hearing threshold did not exceed 20 dB at any frequency from 0.125 to 3 kHz and did not exceed 50 dB at any frequency from 4 to 10 kHz. The participants were split into four groups according to their tinnitus duration (TD): (I) less than one year, (II) one to five years, (III) five to ten years, and (IV) more than ten years (**Table 7**, **Appendix F**, **Figure 23**, (Refat et al., 2021).

***Table 7: Tinnitus duration***
*Distribution of tinnitus duration (TD) in years.*

| | T-group | | | | TH-group | | | |
|---|---|---|---|---|---|---|---|---|
| TD [year] | **0.5-1** | **1-5** | **5-10** | **> 10** | **0.5-1** | **1-5** | **5-10** | **> 10** |
| n | 6 | 9 | 9 | 9 | 8 | 4 | 5 | 3 |
| mean age | 35.2 | 34.1 | 29 | 33.1 | 29 | 24.2 | 27 | 25 |

### 3.2.2. Tinnitus description and tinnitus distress assessed with the tinnitus questionnaire – Goebel-Hiller Score (GHS)

To obtain in-depth insights into whether tinnitus perception differs between the groups, we analysed tinnitus frequency, loudness and distress (GHS) between the four tinnitus duration groups for T- and TH-group (**Figure 24, 25**, (Refat et al., 2021); for individual data, see **Appendix G**). The frequency of the tinnitus perception did not significantly change with TD in the T- ($p = 0.070$; **Figure 24A**, (Refat et al., 2021)) or the TH-group ($p = 0.534$; **Figure 24B**, (Refat et al., 2021)). The frequency also did not differ between the groups (T-group: below one year (5.93 ± 3.17 kHz), one to five years (5.43 ± 3.18 kHz), five to ten years (7.19 ± 2.76 kHz), more than ten years (5.61 ± 2.4 kHz); TH-group below one year (5.96 ± 1.84 kHz), one to five years (6.39 ± 3.52 kHz), five to ten years (4.75 ± 3.45 kHz), more than ten years (6 ± 4.15 kHz).

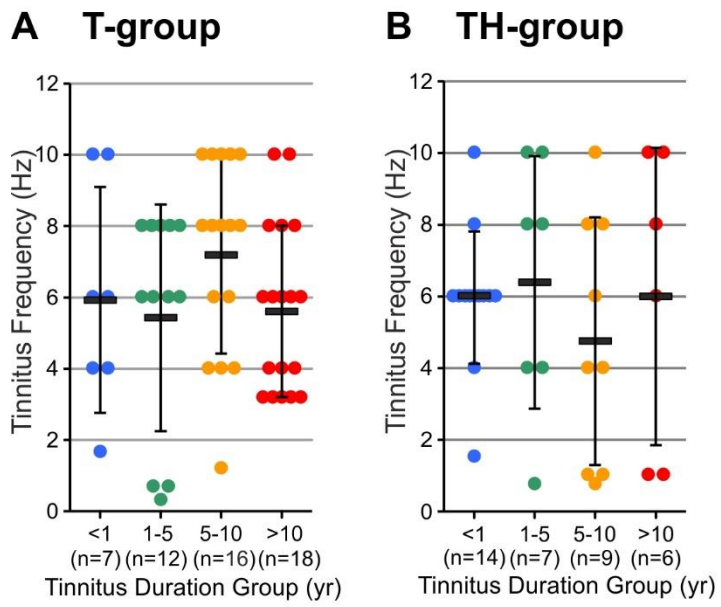


***Figure 24:*** *Tinnitus frequency according to the tinnitus duration. Subjectively matched T- (A) and TH-subgroups (B) tinnitus frequency. Modified according to (Refat et al., 2021).*

The T-group's subjective tinnitus level (loudness) decreased over time (**Figure 25A**, (Refat et al., 2021)). The loudness was significantly greater for a tinnitus duration below five years than for tinnitus durations longer than five years (< 5 years, 26.9 ± 15.8 dB, n = 19; > 5 years, 16.1 ± 11.7 dB, n = 34; **p = 0.005; **Figure 25A**, (Refat et al., 2021)). In contrast, in the TH-group, the tinnitus loudness increased with tinnitus duration (< 5 years, 12 ± 7.2 dB, n = 21; > 5 years, 16.9 ± 8 dB, n = 15; *p = 0.015; **Figure 25B**, (Refat et al., 2021)). To observe the continuous change of tinnitus loudness over time, tinnitus loudness (in dB HL) was plotted as a function of tinnitus duration for T- and TH-group. Linear regression indicated decreasing tinnitus loudness for the T-group (*p = 0.018; **Figure 25A**, (Refat et al., 2021)). No significant increase for tinnitus patients with the co-occurrence of hyperacusis was found (p = 0.111; **Figure 25B**, (Refat et al., 2021)).

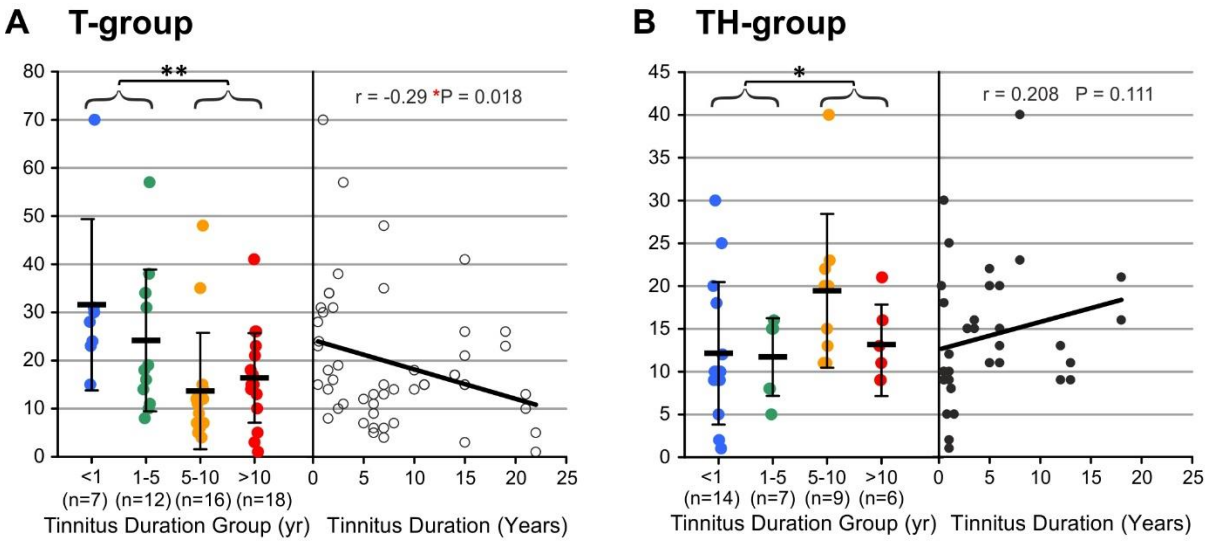


***Figure 25:*** *Tinnitus loudness according to the tinnitus duration. The loudness of the tinnitus percept over tinnitus duration in the T- (A) and TH-group (B). Modified according to (Refat et al., 2021).*

**In summary**, individual tinnitus frequency remained constant in both T- and TH-groups. In parallel, the individual tinnitus loudness decreased over tinnitus duration in the T-group but increased in the TH-group.

## Tinnitus burden remained constant over time but accelerated significantly with the co-occurrence of hyperacusis

The assessment of the tinnitus distress score (GHS) did not show any significant changes in the total score over time in either the T- (**Figure 26A**, (Refat et al., 2021)) or the TH-group (**Figure 26B**, (Refat et al., 2021)). Despite the fact that the T-group had a higher perceived tinnitus loudness than the TH-group (**Figure 25**, (Refat et al., 2021)), the total tinnitus distress score was significantly higher in the TH- than in the T-group (Mann-

Whitney-U test $p < 0.001$; **Figure 26**, (Refat et al., 2021)). These differences further imply that the GHS tinnitus score differs between groups from the acute stage onwards. These remarkably similar GHS scores across tinnitus duration may be related to the differences between groups we observed in the HKI as a function of tinnitus duration (**Figure 27**, (Refat et al., 2021)). Thus, we identified a significant increase in hyperacusis related complaints (HKI) over time in the T-group (**Figure 27A**, (Refat et al., 2021), *p = 0.03; n = 33) but not in the TH-group (**Figure 27B**, (Refat et al., 2021), p = 0.174, n = 20).

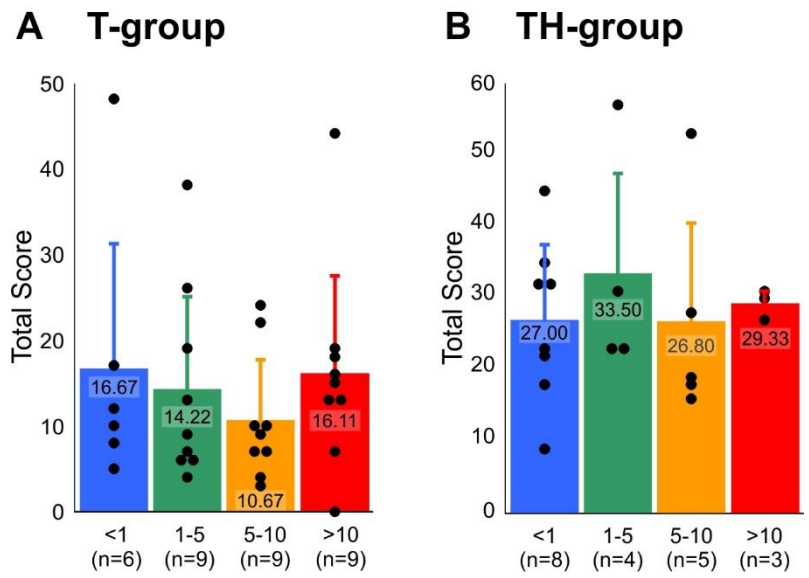


***Figure 26:*** *Tinnitus distress according to the tinnitus duration. The Goebel-Hiller tinnitus questionnaire total score over tinnitus duration in the T- (A) and TH-group (B). Modified according to (Refat et al., 2021).*

This indicates that specific characteristics of hyperacusis are more likely to occur over time. Hyperacusis percept significantly increases in the participants with tinnitus with the longer persistence of their tinnitus (in years), determined by the hyperacusis questionnaire score (HKI).

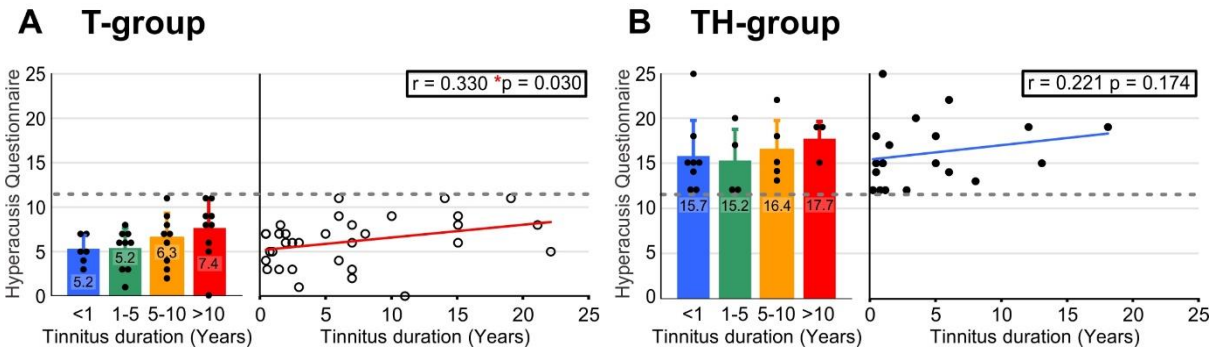


***Figure 27:*** *Hyperacusis questionnaire (HKI) according to the tinnitus duration. Hyperacusis burden (HKI) over tinnitus duration in the T- (A) and TH-group (B). Modified according to (Refat et al., 2021).*

**In summary**, we observed no clear trend in tinnitus duration in relation to distress, but a positive significant correlation for hyperacusis burden in the T-group assessed by HKI.

Individuals in the T-group shift from unilateral to bilateral tinnitus over time, while the TH-group experiences bilateral tinnitus from early on

As time passes, the likelihood of developing hyperacusis and experiencing tinnitus in both ears increases significantly. Thus, in the T-group, the tinnitus percept was unilateral, primarily in individuals with a short tinnitus duration of < 1 year (**Figure 28A**, (Refat et al., 2021)). During experiencing tinnitus, however, the tinnitus percept shifted to an utterly bilateral sensation (Chi-Square Test, **p = 0.002). In contrast, in the TH-group, a bilateral experience of tinnitus dominated from the beginning, with a steadily increasing proportion (Chi-Square Test, p = 0.816; **Figure 28B**, (Refat et al., 2021)). Based on the findings, most tinnitus patients transition from unilateral to bilateral tinnitus, this shift generally occurs within a maximum of 10 years. TH patients, in contrast, usually have bilateral tinnitus from very early stages.

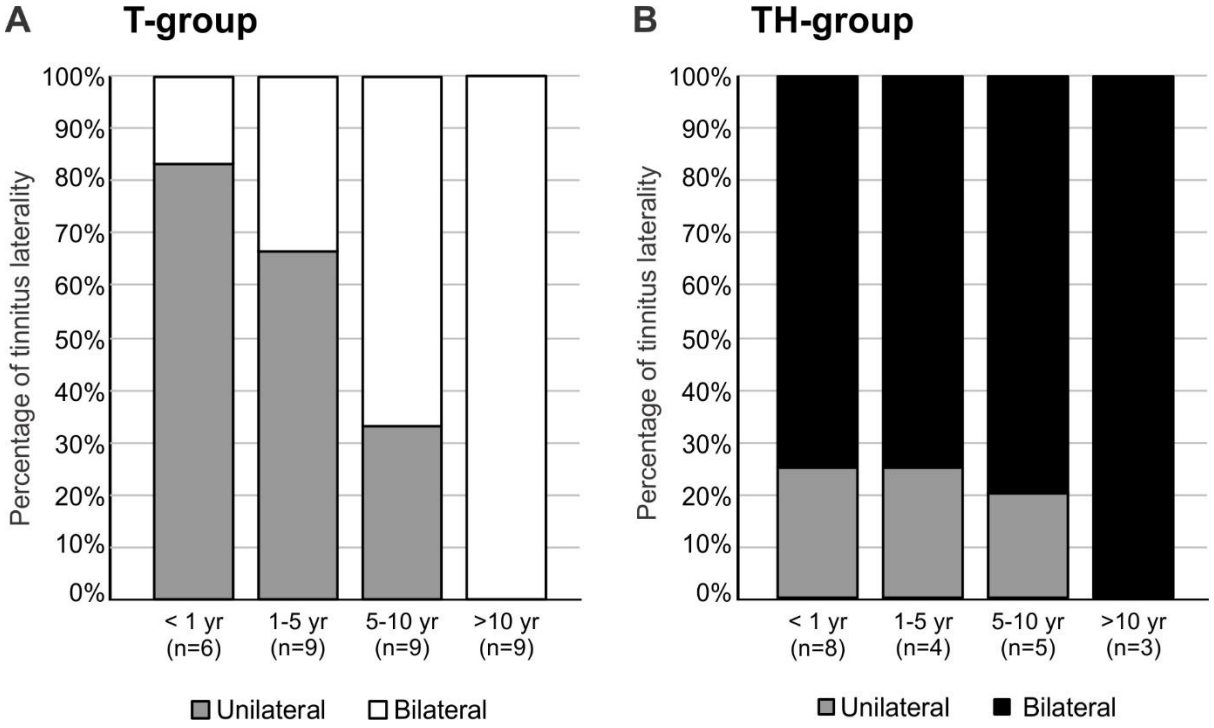


***Figure 28:*** *Tinnitus laterality according to the tinnitus duration. The bar charts show the distribution of unilateral (grey) and bilateral (black/white) tinnitus for the T- (A) and TH-groups (B) divided for the TD sub-groups. Modified according to (Refat et al., 2021).*

**In summary,** long-term tinnitus patients tend to have bilateral tinnitus irrespective of the subgroup. However, bilaterality in the TH-group is apparent initially, while bilaterality steadily increases over time in the T-group.

### 3.2.3. Audiological evaluation

#### Hearing thresholds do not differ – Pure Tone Audiometry (PTA)

To investigate whether the hearing thresholds of the T- and TH-groups differed from those of the control group, we again examined hearing function with a pure tone audiogram up to 10 kHz. The thresholds of the C-group are shown as ± 1 SD shaded in grey, and the T- and TH-groups are divided into four groups according to the tinnitus duration and depicted as mean. Kruskal-Wallis test did not find statistically significant differences in hearing thresholds (0.125-10 kHz) between the four tinnitus duration groups in the T- (**Figure 29A**, (Refat et al., 2021)) and the TH-group (**Figure 29B**, (Refat et al., 2021)).

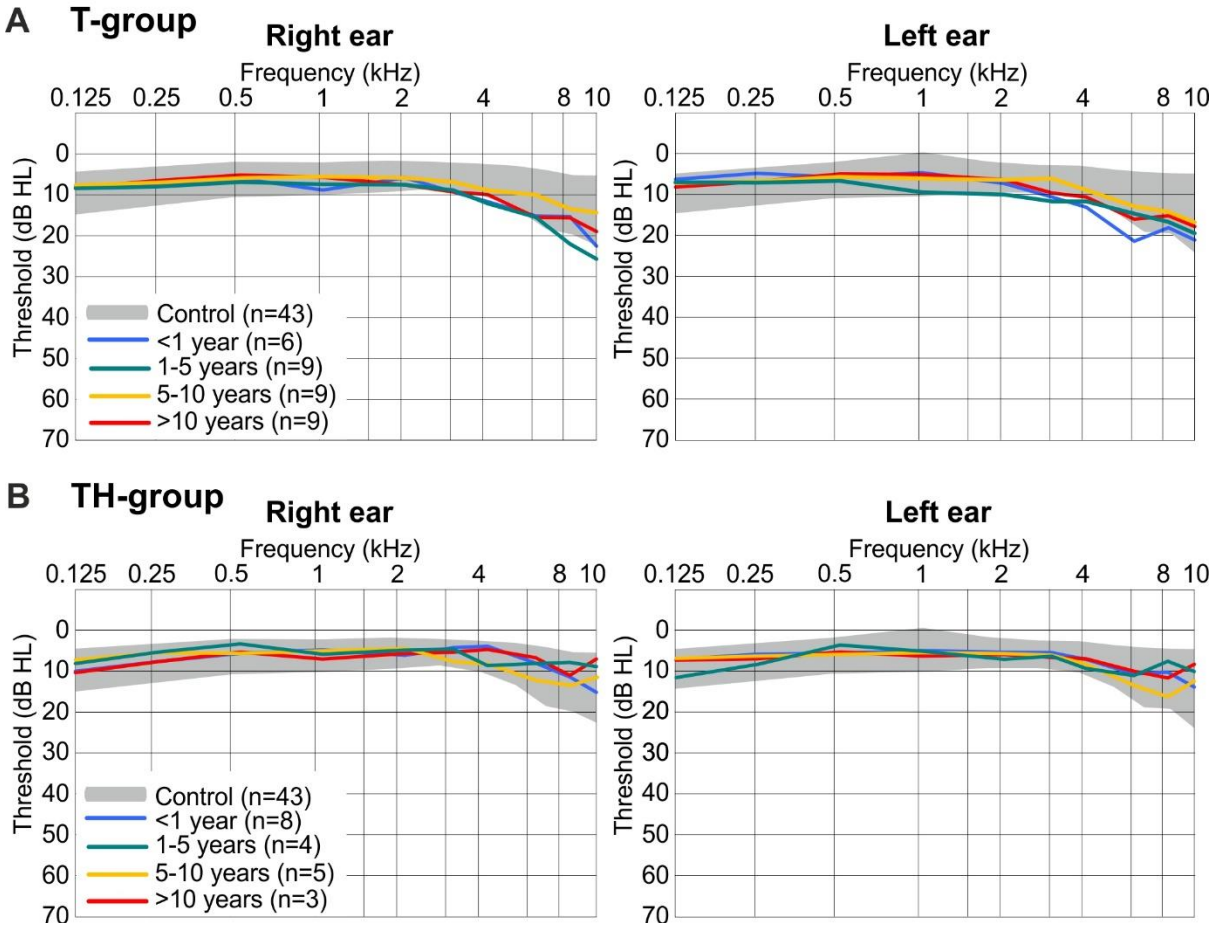


***Figure 29:*** *Pure Tone Audiometry (PTA) hearing threshold according to the tinnitus duration. C-group thresholds are shaded in grey as ± 1 SD, and T- (A) and TH-subgroups (B) are shown as mean in blue, green, yellow, and red. Modified according to (Refat et al., 2021).*

**In summary**, we observed no disparity in hearing thresholds between the tinnitus subgroups and controls, and therefore, we cannot attribute the subsequent audiometric measurements to any changes in hearing thresholds.

## Identification of difference in supra-threshold sound-induced ABR wave amplitude and latency

In comparison to hearing thresholds, ABR waves elicited by 25–75 dB nHL broadband click stimuli showed remarkable group differences (**Figure 30**, (Refat et al., 2021), for detailed statistics, see **Table 8**). Regarding peak-to-peak amplitudes, we present the loudest stimulation (75 dB nHL click) since most waves could be determined (**Figure 30A, C**, (Refat et al., 2021)). Compared to the C-group, we found significantly reduced wave I ($p = 0.0441$) and V ($p = 0.0058$; **Figure 30A**, (Refat et al., 2021)) amplitudes and prolonged wave V latency ($p < 0.0001$; **Figure 30B**, (Refat et al., 2021)) in the overall T-group. On the other hand, we observed significantly increased wave III and V ($p = 0.0055$; **Figure 30C**, (Refat et al., 2021)) combined with prolonged wave V latencies ($p < 0.0001$; **Figure 30D**, (Refat et al., 2021)). These group changes occur without evident gradual changes dependent on tinnitus duration. Nevertheless, some notable statistical differences were found within the T- and TH-groups. In the T-group, those with tinnitus for less than five years had lower wave I amplitudes, while those with tinnitus over five years had a significantly higher ABR wave I than the C-group ($p = 0{,}0148$; **Figure 30A**, (Refat et al., 2021)). We observed that wave III exhibited a similar but not statistically significant trend (**Figure 30A**, (Refat et al., 2021)). This effect is not evident in the TH-group, as all age groups tend to be at or above the control level. This may indicate that in the T-group, over time, the lower auditory brain regions (ABR waves I to III) generate advanced amplification (brainstem gain), possibly related to the increased likelihood of hyperacusis.

The ABR peak latencies were presented as a function of stimulus intensity across the stimulation levels 25 to 75 dB nHL (**Figure 30B, D**, (Refat et al., 2021), for detailed statistics, see **Table 8**). In the T-group, 2-way ANOVA demonstrated significantly delayed ABR wave peaks, especially for latencies of ABR wave V across all stimulus levels ($p < 0.0001$; **Figure 30B**, (Refat et al., 2021)). Also, a significant group difference was observed in ABR wave VI ($p = 0.0177$; **Figure 30B**, (Refat et al., 2021)), but no significant differences were found in the post-hoc tests (**Table 8**). These group changes occur with gradual wave V amplitude changes dependent on tinnitus duration, most pronounced for tinnitus durations above five years and elevated stimulation levels ($p = 0.0032$; **Figure 30B**, (Refat et al., 2021)). In stark contrast, for the TH-group, 2-way ANOVA demonstrated significantly shortened ABR wave V latencies ($p = 0.0055$; **Figure 30D**, (Refat et al., 2021)), especially for low stimulus levels, where increased tinnitus duration was associated with shorter waves ($p = 0.0167$; **Figure 30D**, (Refat et al., 2021)).

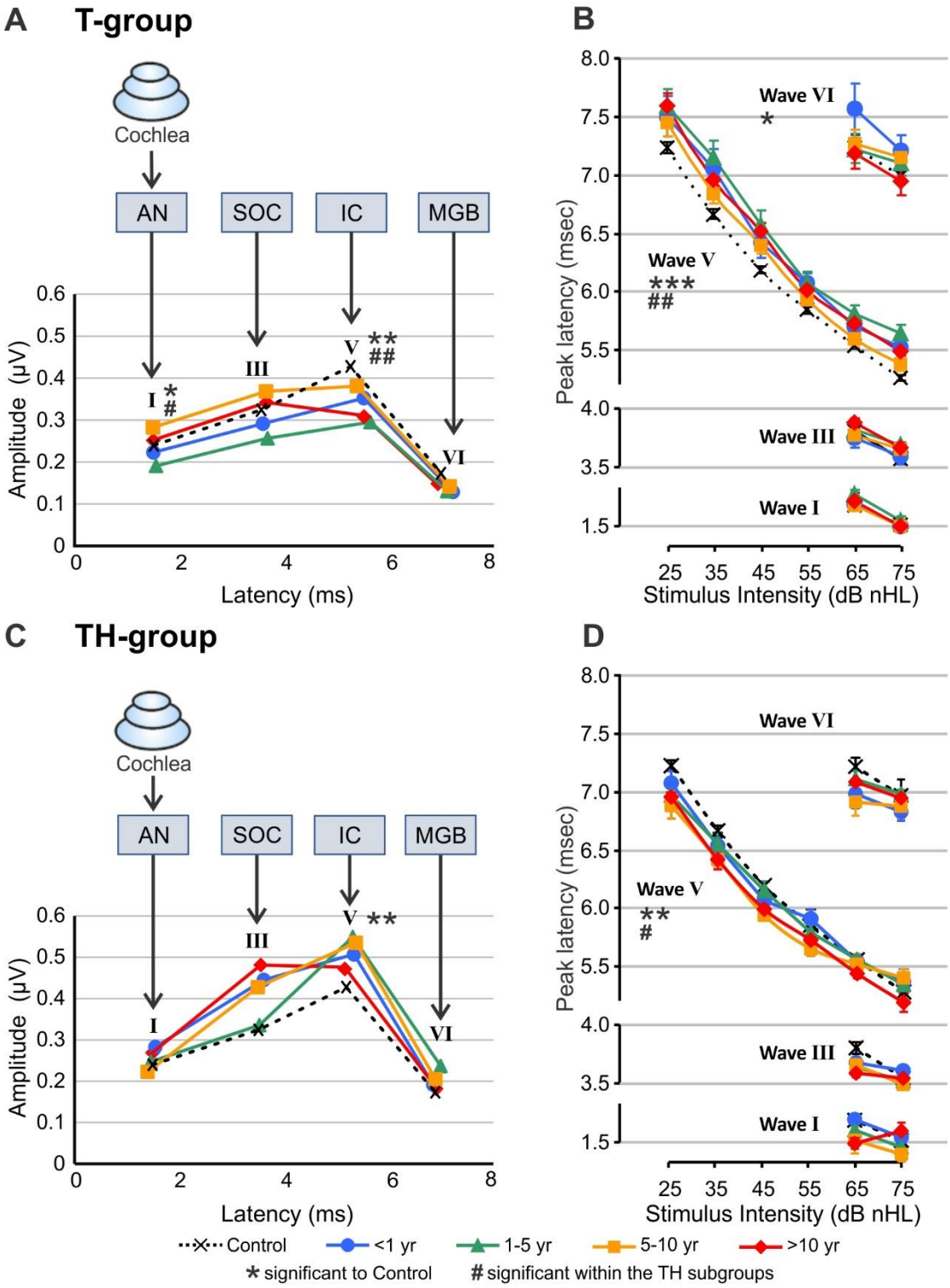


***Figure 30:*** *Supra-threshold ABR wave peak-to-peak amplitude and latency according to the tinnitus duration of T- (A, B) and TH-subgroups (C, D). The amplitudes of ABR waves I, III, V, and VI for 75 dB nHL (A, C) were categorised according to tinnitus duration (coloured) and compared to controls (black). Peak latency as a function of stimulus intensity for ABR waves ranging from 25-75 dB nHL (B, D). AN, auditory nerve; SOC, superior olivary complex; IC, inferior colliculus; MGB, the medial geniculate body. Modified according to (Refat et al., 2021).*

**In summary**, ABR wave V remains reduced and delayed in T-Subgroups, and ABR wave III and V remain enhanced and shortened in TH-Subgroups.

***Table 8: ABR statistics II***

*Statistical significance of ABR wave amplitude and latency differences. Only p values < 0.05 are reported. * p < 0.05, ** p < 0.01, *** p < 0.001 **** p<0.0001 in post-hoc Holm-Šídák's multiple comparison test. 75, 65, 55, 45, 35, 25 dB nHL stimulus level. |--- * ---| significant difference in post-hoc Holm-Šídák's multiple comparison tests between groups. TD, tinnitus duration [years]. Modified according to (Refat et al., 2021).*

| **Study Group**<br>Δ source of variation | 2-way ANOVA | | | pairwise comparisons | | |
|---|---|---|---|---|---|---|
| **T-group** | *wave* | *p Value* | *TD <1* | *TD 1-5* | *TD 5-10* | *TD >10* |
| ABR amplitude | I | **0.0441** | | | | |
| Δ to Control | III | 0.2500 | | | | |
| | V | **0.0058** | | 75*** | | 75** |
| | VI | 0.2651 | | | | |
| ABR latency | I | 0.3485 | | | | |
| Δ to Control | III | 0.5095 | | | | |
| | V | **<0.0001** | 75* 35** 25* | 75*** 65* 55* 45*** 35**** 25*** | 25* | 75* 45** 35** 25*** |
| | VI | **0.0177** | | | | |
| ABR amplitude | I | **0.0148** | | |--- * ---| | | |
| Δ duration | III | 0.0865 | | | | |
| | V | 0.2108 | | | | |
| | VI | 0.7673 | | | | |
| ABR latency | I | 0.2694 | | | | |
| Δ duration | III | 0.1444 | | | | |
| | V | **0.0032** | | | | |
| | VI | 0.0741 | | | | |
| **TH-group** | *wave* | *P* | *<1* | *1-5* | *5-10* | *>10* |
| ABR amplitude | I | 0.5008 | | | | |
| Δ to Control | III | 0.6225 | | | | |
| | V | **0.0057** | | | | |
| | VI | 0.2159 | | | | |
| ABR latency | I | **0.0522** | | | | |
| Δ to Control | III | 0.7149 | | | | |
| | V | **0.0055** | | | 25* | |
| | VI | 0.4370 | | | | |
| ABR amplitude | I | 0.5223 | | | | |
| Δ duration | III | 0.5250 | | | | |
| | V | 0.0881 | | | | |
| | VI | 0.2208 | | | | |
| ABR latency | I | 0.2694 | | | | |
| Δ duration | III | 0.1660 | | | | |
| | V | **0.0167** | | | | |
| | VI | 0.5311 | | | | |
| **Study Group**<br>Δ source of variation | | | | 2-way ANOVA and pairwise comparison | | |
| **T- vs. TH-group** | *wave* | | *TD <1* | *TD 1-5* | *TD 5-10* | *TD >10* |
| ABR amplitude | I | | 0.0712 | 0.1350 | 0.2287 | 0.6539 |
| Δ T vs TH | III | | **0.0182** 75* | **0.0573** | 0.7065 | **0.0498** 75* |
| | V | | **0.0002** 75* | **0.0002** (0.047) 75**** | **0.0002** 75** | **<0.0001** 75* 45* 25* |
| | VI | | **0.0054** 65* | 0.1175 | 0.1540 | 0.6557 |
| ABR latency | I | | 0.6801 | **0.0016** 65** | **0.0209** | 0.301 (0.020) 65* |
| Δ T vs TH | III | | 0.7997 | **0.0010** 75* 65* | **0.0006** 75** 65* | **0.0007** 65** |
| | V | | **<0.0001** 45* 35** 25* | **<0.0001** 35** 25** | **<0.0001** 45** 35** 25*** | **<0.0001** 45*** 35*** 25**** |
| | VI | | **0.0021** 65* | 0.5216 | 0.0100 | 0.8685 |

Central output to reduced auditory input (neural gain) remained reduced in the T-group and increased in the TH-group across the tinnitus duration

To determine the gain along the ascending auditory pathway, "neural gain" (ABR wave V/I) and "brainstem gain" (ABR wave III/I) are determined by dividing the respective waves for each individual. 75 dB nHL evoked ABR wave ratio V/I (**Figure 31A–C**, (Refat et al., 2021)) and III/I (**Figure 31D-F**, (Refat et al., 2021)) are presented for T- and TH-group (**Figure 31A, D**, (Refat et al., 2021)) and for the tinnitus duration subgroups (**Figure 31B, C, E, F**, (Refat et al., 2021)).

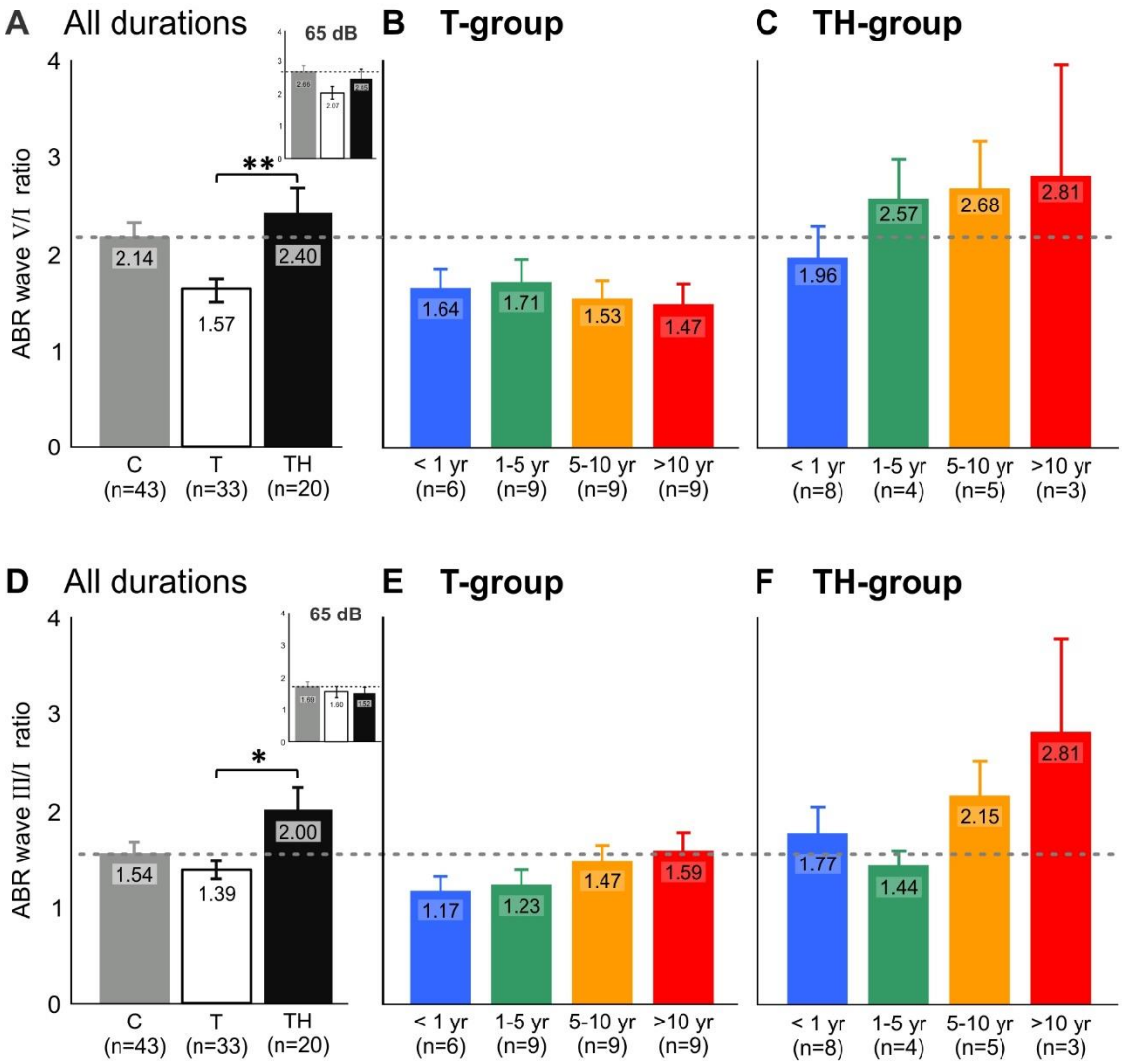


***Figure 31:*** *ABR wave gain (V/I and III/I ratio) according to the tinnitus duration. Peak-to-peak amplitude ratio wave V/I (A-C) and wave III/I (D-E) for 75 dB nHL click stimulus-evoked ABR responses of C- (grey), T-(white), TH-(black), and the subgroups categorised and coloured according to the tinnitus duration (B, C, E, F). The horizontal dashed line marks the mean value of the controls. The inserts display the response for 65 dB nHL clicks (A, D). Modified according to (Refat et al., 2021).*

Compared to the T-group, a robust enhanced 75 dB evoked brainstem (ABR wave ratio III/I, p = 0.026; **Figure 31D**, (Refat et al., 2021)) and neural gain (ABR wave ratio V/I, p = 0.001; **Figure 31A**, (Refat et al., 2021)) was observed in the TH-group. However, this cannot be observed for lower stimulation levels (**Figure 31A, D** insert, (Refat et al., 2021)), suggesting that gain changes in TH-groups only occur at higher simulation levels. In comparison to the C-group (dotted line), we observed an increase in the gain (ABR wave III/I and ABR wave V/I) for the T- and TH-groups with increasing tinnitus duration (**Figure 31C, E, F**, (Refat et al., 2021)); only ABR wave V/I remained continuously reduced for all tinnitus duration T-subgroups (**Figure 31B**, (Refat et al., 2021)). For the T-group, we observed the increase of ABR wave III (**Figure 30A**, (Refat et al., 2021)) with tinnitus duration in the rise of the ABR wave III/I ratio over tinnitus duration (**Figure 31E**, (Refat et al., 2021)).

**In summary**, neural central gain (ABR wave V/I ratio) decreased in the T-group, while ABR wave III/I and ABR wave V/I ratio increased in the TH-group with advancing tinnitus duration. Over time, the T-group displayed a tendency for the ABR wave V/I ratio to become more reduced, while the ABR wave III/I ratio appeared to be less diminished. These trends challenge the concept of increasing hyperacusis characteristics in tinnitus patients as tinnitus duration persists.

## 3.3. Paper III: "Differential cortical activation patterns through sub-classifying tinnitus with and without hyperacusis based on audiometry, gamma oscillations, and hemodynamics" (Wertz et al., 2023)

The last study was designed to validate objective markers to distinguish between tinnitus with and without hyperacusis identified in the previous studies (Hofmeier et al., 2018; Hofmeier et al., 2021; Refat et al., 2021). In addition to the approaches utilised in the previous studies, the focus was on identifying changes in brain oscillations and haemodynamic responses in an expanded cohort. 86 participants aged 18-57 were included using the previously described inclusion and exclusion criteria (**Appendix H, Table 9** Total cohort). Additionally, more stringent subclassification criteria for hyperacusis were applied using the hyperacusis questionnaire HKI and the loudness discomfort level (LDL).

***Table 9: Demographic group information***

*Group information of included Participants for age and gender. EEG, Electroencephalography; EHF, extended high frequency; rs-fMRI, resting-state functional magnetic resonance imaging.*

| Group | Age [years] | | | Participants [n] | | |
|---|---|---|---|---|---|---|
| | **Mean** | **Min** | **Max** | **n** | **female** | **male** |
| Total cohort | | | | | | |
| Control | 27.6 | 19 | 45 | 39 | 22 | 17 |
| T-group | 30.5 | 20 | 51 | 30 | 10 | 20 |
| TH-group | 32 | 20 | 57 | 17 | 12 | 5 |
| Gr1 – Subjects included in EHF Audiometry | | | | | | |
| Control | 27.6 | 22 | 39 | 22 | 13 | 9 |
| T-group | 33.5 | 20 | 55 | 18 | 6 | 12 |
| TH-group | 33.7 | 20 | 57 | 11 | 9 | 2 |
| Gr2 – Subjects included in rs-fMRI | | | | | | |
| Control | 28.5 | 23 | 36 | 12 | 7 | 5 |
| T-group | 32.75 | 22 | 55 | 15 | 5 | 11 |
| TH-group | 38.8 | 24 | 57 | 6 | 5 | 1 |
| Gr3 – Subjects included in EEG | | | | | | |
| Control | 28 | 23 | 36 | 13 | 8 | 5 |
| T-group | 32.2 | 22 | 55 | 11 | 5 | 6 |
| TH-group | 37.8 | 27 | 57 | 5 | 5 | |

### 3.3.1. Recruitment & hyperacusis classification

Among these 86 participants (for age, gender, and handedness, see **Appendix H, Table 9**), 30 reported tinnitus without hyperacusis (T-group), and 17 tinnitus patients fulfilled the criteria for the co-occurrence of hyperacusis (TH-group, see Methods 2.3.3). The remaining 39 participants were included in the control group (C-group). According to the exclusion criteria (see Methods 2.3.2), hearing thresholds in the PTAs did not exceed 20 dB at any frequency from 0.125 to 3 kHz and 40 dB at any frequency from 4 to 10 kHz.

Not the entire cohort of participants was available for all measurement sessions. Thus, the extended high-frequency PTA (PTA-EHF) up to 16 kHz could only be measured in a subgroup of 22 control subjects (C-group), 18 patients with tinnitus without the concomitant presence of hyperacusis (T-group), and 11 patients in whom tinnitus occurred with hyperacusis (TH-group, **Table 9**, Gr1). In the second session, the fMRI measurement, a total of 12 C, 15 T, and 6 TH subjects from the total cohort participated (**Table 9**, Gr2). In the last session, with simultaneous EEG and fNIRS recording,13 C, 11 T, and 5 TH patients could be included (**Table 9**, Gr3). Still, most participants in the subgroups overlapped (**Table 9**). After conducting a Kruskal-Wallis test, it was found that the TH-group was significantly increased in the HKI in the total cohort and the Gr3 subgroup (**Figure 32A, I**, (Wertz et al., 2023), for detailed statistics, see **Table 10**). Due to the revised hyperacusis classification, patients in the T-group with an HKI above 11 and patients in the TH-group with an HKI below 11 were also identified (**Figure 32I**, (Wertz et al., 2023)). However, the classification has been improved overall, as patients with self-described hyperacusis, which failed to reach the cut-off value in the HKI, were repeatedly encountered in the survey.

### 3.3.2. Tinnitus description and tinnitus distress assessed with the tinnitus questionnaire – Goebel-Hiller Score (GHS) – Elevated distress in tinnitus subjects with co-morbid hyperacusis

In addition to the HKI, the GHS tinnitus score was employed to assess tinnitus severity, emotional distress, cognitive distress, self-experienced intrusiveness, auditory perceptual difficulty, sleep disturbance, and somatic complaints (**Figure 32B-H, J-P**, (Wertz et al., 2023), for detailed statistics, see **Table 10**).

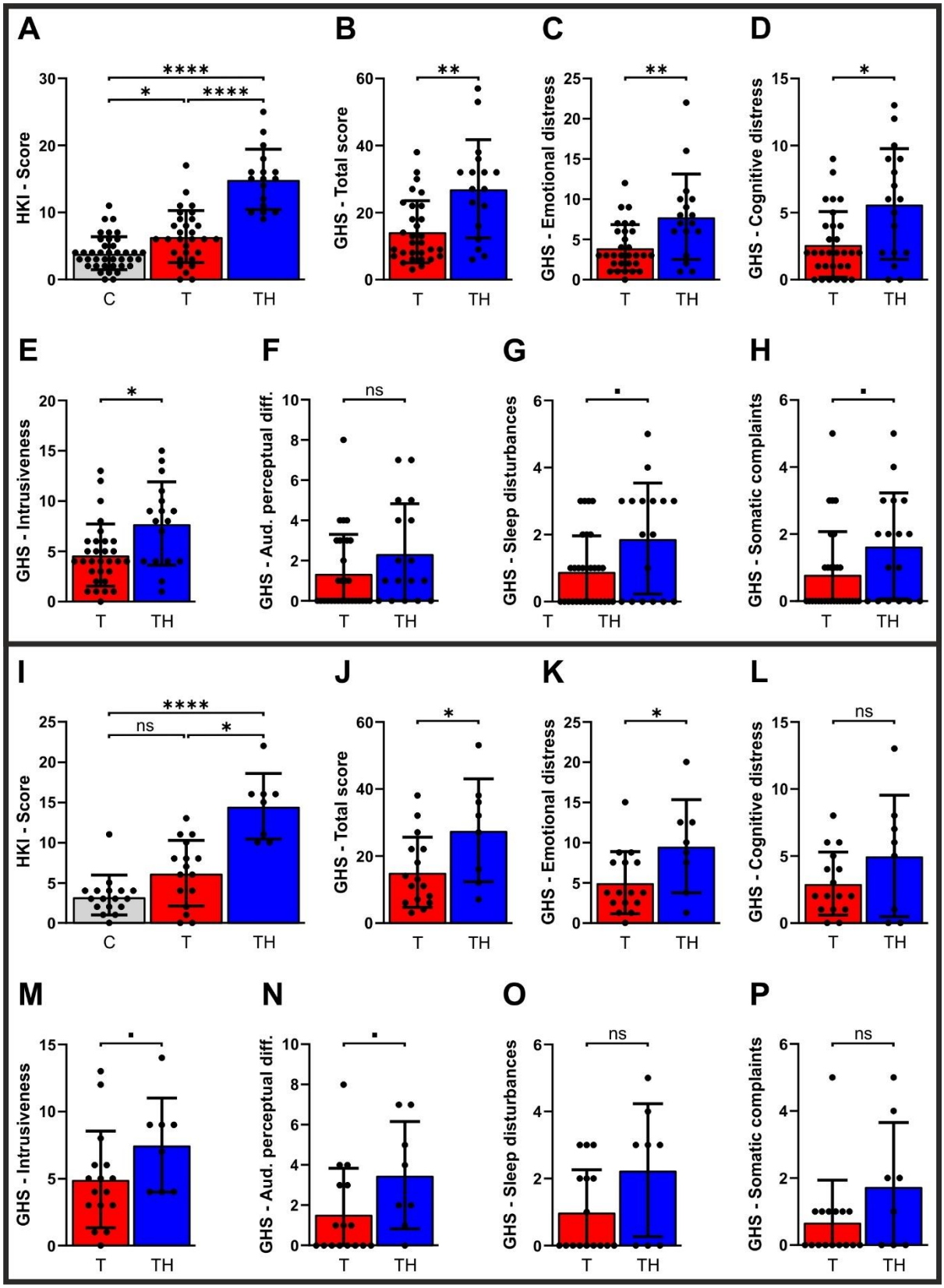


***Figure 32:*** *Tinnitus distress and hyperacusis questionnaire scores. The bar charts represent mean ± SD for (A; I) hyperacusis questionnaire (HKI) score, (B-H, J-P) tinnitus distress (GHS) scores between C- (grey), T- (red), and TH-group (blue). Figures (A-H) show the total cohort and (I-P) a subset of EEG-measured patients. GHS, Goebel and Hiller Score; HKI, Hyperakusis-Inventar; SD, standard deviation. Modified according to (Wertz et al., 2023).*

Noteworthy, GHS total and sub-score differences in the Gr3 subgroup of 41 participants (**Figure 32J-P**, (Wertz et al., 2023)) did not differ from those in the total cohort of 86 participants (**Figure 32B-H**, (Wertz et al., 2023)), as both cohorts exhibited significant group differences in HKI and GHS total scores.

***Table 10: Questionnaire statistics***

*Tinnitus and hyperacusis questionnaire (p values). Auditory perceptual diff., Auditory perceptual difficulties; KWT, Kruskal-Wallis test; MC, Multiple Comparison; $TH_n$, number of tinnitus patients with Hyperacusis; $T_n$, number of tinnitus patients.*

| Questionnaire | Test | Test Statistic | p value |
|---|---|---|---|
| (A) HKI | KWT | H (2) = 41.58 | p < 0.0001 |
| | Dunn's MC test | C- (mean rank = 29,0 n = 39) and T-group (mean rank = 440, n = 30) | p = 0.0397 |
| | | C- (mean rank = 29,0 n = 39) and TH-group (mean rank = 75.6, n = 17) | p < 0.0001 |
| | | T- (mean rank = 44,0 n = 30) and TH-group (mean rank = 75.7, n = 17) | p < 0.0001 |
| (B) Total score | 2-tailed Mann–Whitney-U test | U = 117.5 $T_n$ = 30 $TH_n$ = 17 | p = 0.0018 |
| (C) Emotional distress | | U = 133.5 | p = 0.0059 |
| (D) Cognitive distress | | U = 145 | p = 0.0129 |
| (E) Intrusiveness | | U = 142.5 | p = 0.011 |
| (F) Auditory perceptual diff. | | U = 186 | p = 0.1095 |
| (G) Sleep disturbances | | U = 172.5 | p = 0.056 |
| (H) Somatic complaints | | U = 173 | p = 0.0503 |
| (I) HKI | KWT | H (2) = 19.13 | p < 0.0001 |
| | Dunn's MC test | C- (mean rank = 13.7, n = 17) and T-group (mean rank = 21.2, n = 16) | ns. |
| | | C- (mean rank = 13.7, n = 17) and TH-group (mean rank = 36.0, n = 8) | p < 0.0001 |
| | | T- (mean rank = 21.2, n = 16) and TH-group (mean rank = 36.0, n = 8) | p = 0.012 |
| (J) Total score | 2-tailed Mann–Whitney-U test | U = 117.5 $T_n$ = 30 $TH_n$ = 17 | p = 0.0018 |
| (K) Emotional distress | | U = 133.5 | p = 0.0059 |
| (L) Cognitive distress | | U = 145 | p = 0.0129 |
| (M) Intrusiveness | | U = 142.5 | p = 0.011 |
| (N) Auditory perceptual diff. | | U = 186 | p = 0.1095 |
| (O) Sleep disturbances | | U = 172.5 | p = 0.056 |
| (P) Somatic complaints | | U = 173 | p = 0.0503 |

A higher tinnitus severity was observed in the TH- compared to the T-group, irrespective of whether total or sub-scores were considered (**Figure 32B-H, J-P**, (Wertz et al., 2023)), with significance reached in the total score, as previously reported. Regardless of the small cohort size used in the third study, the distress caused by tinnitus was reproducibly more significant in tinnitus patients with co-occurrence of hyperacusis.

### 3.3.3. Audiological evaluation

Hearing threshold differences – Pure Tone Audiometry (PTA) – No T and TH specific differences in extended high-frequency hearing threshold up to 16 kHz

As described in the methods, PTAs in the subgroup Gr1 (22 C, 18 T, and 11 TH) were measured for frequencies between 0.125 and 16 kHz. Again, it was confirmed that the TH-group, in contrast to the C- or T-group, showed decreased LDL over the 0.25-6 kHz frequency range (**Figure 33A**, lower panel, (Wertz et al., 2023)). The PTA4, accounting for PTA thresholds at 0.5, 1, 2, and 4 kHz, the PTA-HF, accounting for thresholds at 6, 8, and 10 kHz, and the PTA-EHF, including thresholds in the extended high frequency ranges at 11.2, 12.5, 14, and 16 kHz, were plotted for the C-, T-, and TH-group (**Figure 33B**, (Wertz et al., 2023)). Due to the inhomogeneous group variance, a non-parametric mixed effects analysis had to be performed, which indicated a statistical trend ($F(2, 48) = 2.77$, $p = 0.0727$). Nevertheless, the Holm-Šídák multiple comparison tests revealed no significant group differences, although the threshold increases in the EHFs for the T- and even more pronounced for TH-group were evident (**Figure 33B**, (Wertz et al., 2023)). However, the tendential differences in the EHF region are lost when we normalise the groups for age (**Figure 33C**, (Wertz et al., 2023)).

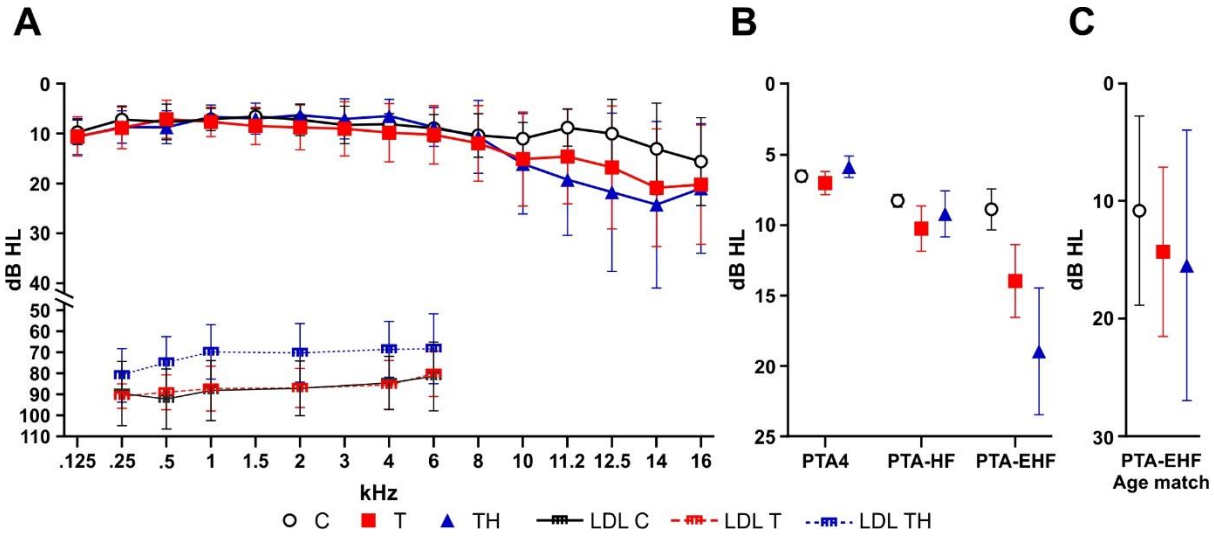


***Figure 33:*** *Hearing sensitivity thresholds for the left and right ear determined by PTA (mean ± SD) for C (n = 22, black), T- (n = 18, red), and TH-group (n = 11, blue). (A) PTA, LDL, (B) PTA4, PTA-HF, PTA-EHF, and (C) PTA-EHF thresholds for an age-matched subgroup C- (n = 5, black), T- (n = 5, red), and TH-group (n = 5, blue). dB, decibel; HL, hearing level; PTA, pure tone audiometry; PTA-EHF, PTAs in extended high frequencies (better ear of 11.2-16 kHz); PTA-HF, PTAs in medium frequencies (better ear of 6-10 kHz); PTA4, PTAs in low frequencies (better ear of 0.5,1,2,4 kHz); SD, standard deviation; LDL, loudness discomfort level. Modified according to (Wertz et al., 2023).*

**In summary**, no significant group differences were found for hearing thresholds up to 16 kHz, regardless of whether the entire group or an age-matched subgroup was considered.

## Influence of comorbid hyperacusis on tinnitus loudness and subsequent differences in tinnitus distress and hearing threshold within the tinnitus frequency

The information provided is crucial for the subject's ability to accurately differentiate frequencies in our active auditory tone discrimination task, involving acoustic stimulation within and outside the range of tinnitus frequency. We observed significant positive correlations between the individual tinnitus loudness and PTA-HF (**Figure 34B**, (Wertz et al., 2023)) and PTA-T thresholds of the individual tinnitus frequency (**Figure 34D**, (Wertz et al., 2023)) in the T-, but not in the TH-group. In addition, slight correlations were found between PTA4 and PTA-EHF (as shown in **Figure 33A, 34A, C**, (Wertz et al., 2023)) in the T-, but not in the TH-group. Furthermore, a significant rise in correlation within the T-group for PTA-HF, particularly when we restrict our analysis to tinnitus subjects whose tinnitus frequency falls within the PTA-HF spectrum, became apparent (**Figure 34E**, (Wertz et al., 2023)). This suggests that threshold elevations play a dominant role within the frequency range associated with tinnitus.

We hypothesised that the loudness of tinnitus in the TH-group does not correlate with the PTA-T threshold since distress in TH subjects is already higher even at low tinnitus volume. After analysing the correlation to the different GHS scores, we discovered that not only the total score (**Figure 34F**, (Wertz et al., 2023)) but also the sub-scores, including emotional distress (**Figure 34G**, (Wertz et al., 2023)), intrusiveness (**Figure 34H**, (Wertz et al., 2023)), and auditory perceptual difficulties (**Figure 34I**, (Wertz et al., 2023)), were all positively correlated with tinnitus loudness in the T-group. In comparison, the TH-group showed mostly uncorrelated parameters, except emotional distress, which had a negative correlation (**Figure 34G**, (Wertz et al., 2023)).

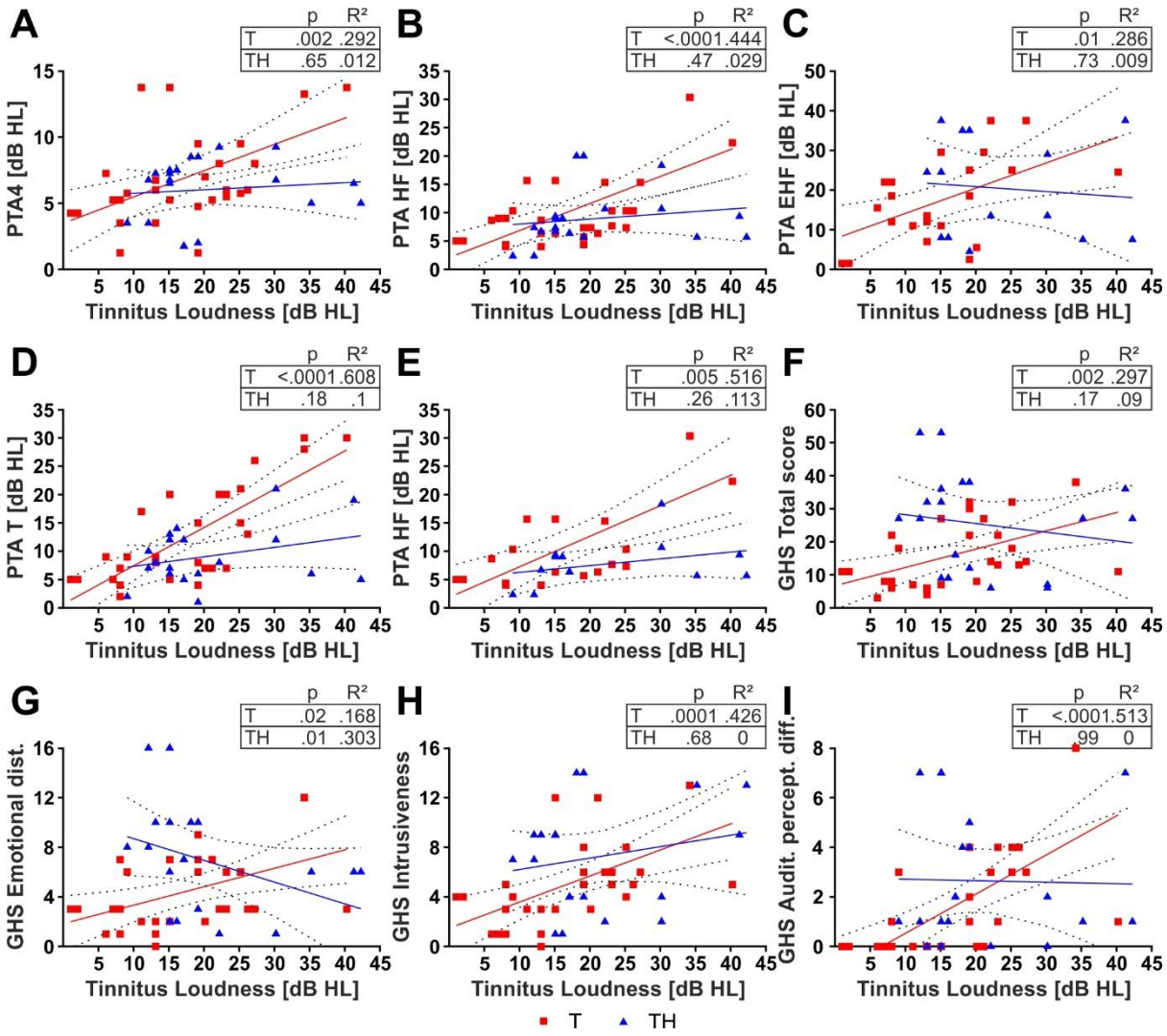


***Figure 34:*** *Correlation between tinnitus loudness and GHS/ hearing thresholds for T- (red) and TH-group (blue). Two-tailed Pearson correlation between tinnitus loudness and (A) PTA4, (B) PTA-HF, (C) PTA-EHF, (D) PTA-T, and (E) PTA-HF in subjects with individual tinnitus in the range of 6-10 kHz. Two-tailed Spearman correlation between tinnitus loudness and (F) GHS total score, (G) GHS emotional distress, (H) GHS intrusiveness, and (I) GHS auditory perceptual difficulties. dB, decibel; GHS, Goebel and Hiller Score; HL, hearing level; PTA, pure tone audiometry threshold; PTA EHF, PTAs in extended high frequencies (better ear of 11.2-16 kHz); PTA MF, PTAs in medium frequencies (better ear of 6-10 kHz); PTA T, PTAs in individual tinnitus frequency; PTA 4, PTAs in low frequencies (better ear of 0.5,1,2,4 kHz). Modified according to (Wertz et al., 2023).*

Next, we hypothesised that the variation of GHS sub-scores correlation to tinnitus loudness between T and TH was solely caused by the groups' perceived tinnitus loudness. Therefore, we again analysed the GHS auditory perceptual difficulty scores of both groups, focusing only on subjects with low tinnitus loudness levels ≤ 15 dB HL (**Figure 34I, 35A**, (Wertz et al., 2023)). Indeed, it is evident that, particularly in the TH-group, even individuals with low tinnitus loudness experience a more significant perceived distress of auditory perception difficulty ($U = 38$, $p = 0.0016$). The PTA corrected LDL threshold showed a significant positive correlation with individual tinnitus loudness perception in the T-group but not in the TH-group. In accordance with tinnitus loudness and distress,

the PTA-adjusted LDL threshold showed a significant positive correlation with individual tinnitus loudness perception in the T- but not in the TH-group (**Figure 35B**, (Wertz et al., 2023)). The reported correlations to tinnitus loudness are even more relevant, as a Mann-Whitney-U test revealed significantly higher PTA-threshold-corrected tinnitus loudness in the TH-group (U = 162, p = 0.0157; **Figure 35C**, (Wertz et al., 2023)).

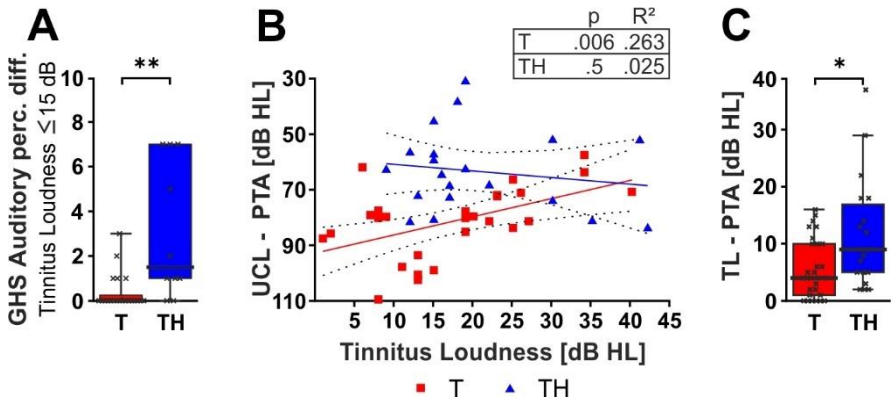


***Figure 35:*** *Auditory perceptual difficulty, loudness discomfort, and tinnitus loudness. The box plot (A) shows the median, range (whiskers), and quartiles (box) of the GHS auditory perceptual difficulty (Aud. Perc. Diff.) sub-score for patients with self-rated tinnitus loudness ≤ 15 dB HL. (B) Two-tailed Spearman correlation between tinnitus loudness and the dynamic range (PTA-LDL). The box plot (C) shows the median, range (whiskers), and quartiles (box) of the tinnitus loudness corrected for PTA threshold for T- (red) and TH-group (blue). dB, decibel; GHS, Goebel and Hiller Score; HL, hearing level; PTA, pure tone audiometry threshold; LDL, loudness discomfort level. Modified according to (Wertz et al., 2023).*

**In summary**, these results again reveal differences between tinnitus subgroups, particularly concerning how individual tinnitus loudness disturbed the patients, as evidenced by a strong correlation with PTA T thresholds and GHS distress scores.

## T and TH subjects showed differential effects on suprathreshold ABR amplitude and latency

Since our motivation was to validate the T- and TH-specific characteristics described above. We focused on reproducing the effects of differential auditory brainstem response behaviour with ABR waves. Based on a two-way ANOVA, a significant group difference has been found in ABR wave amplitudes evoked at a stimulus level of 85 dB SPL ($F(2,227) = 10.4$, $p < 0.0001$). Agreeing with prior findings, Holm-Šídák's multiple comparison tests demonstrated significantly reduced wave V amplitude in the T- (mean = 0.34 ± 0.07, nEars = 28) compared to the C-group (mean = 0.44 ± 0.156, nEars = 36, p = 0.003; **Figure 36A**, (Wertz et al., 2023)). Concurrently, two-way ANOVA revealed significant prolonged peak latencies in ABR waves I, III, and V of the T- and TH-group ($F (2, 228) = 10.34$, $p = < 0.0001$; **Figure 36B**, (Wertz et al., 2023)). Holm-Šídák's multiple comparison tests displayed significant prolonged ABR wave I latencies in the T- (nEars = 27) compared to

the C-group (nEars = 35, $p < 0.01$) and in the TH- (nEars = 16) compared to the C-group ($p = 0.04$). Also, for ABR wave III, we found significantly prolonged responses in the T- (nEars = 27) compared to the C-group (nEars = 36, $p < 0.01$) and in the TH- (nEars = 16) compared to the C-group ($p = 0.03$).

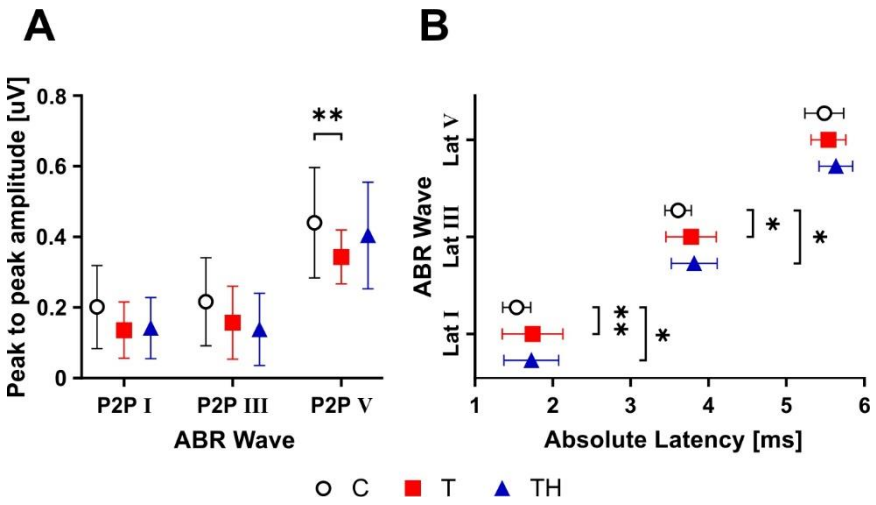


***Figure 36:*** *Supra-threshold ABR wave peak-to-peak amplitude changes and latency shifts. ABR wave I, III, and V peak-to-peak (P2P) amplitude (A) and latency (B) at 85 dB SPL. ABR, auditory brainstem response; Lat, latency; P2P, peak-to-peak. Modified according to (Wertz et al., 2023).*

**In summary**, the findings reproduced differential amplitude reduction of ABR wave V and elongation of the ABR wave I and III latencies for the T- and less the TH-group. However, we were not able to confirm a decrease in ABR wave V or III latency previously observed in the TH-group (Hofmeier et al., 2021).

## No speech discrimination threshold differences between groups

Previous studies have highlighted the impact of tinnitus on language comprehension. As our own research has also identified differences in BOLD fMRI responses within the language processing regions (Hofmeier et al., 2018), we conducted the "Oldenburger Satztest" (OLSA), a German matrix sentence test. We analysed the speech reception threshold in both quiet and fixed noise conditions to determine if differing audiometric parameters (**Figure 34-36**, (Wertz et al., 2023)) impact other aspects of auditory processing, such as speech understanding. However, no differences in OLSA thresholds could be identified, regardless of whether the test was in quiet (**Appendix I** (A), (Wertz et al., 2023)) or noise conditions (**Appendix I** (B), (Wertz et al., 2023)). **In summary**, individuals experiencing tinnitus, with or without hyperacusis, exhibited no differences in speech reception thresholds utilised by OLSA. However, noticeably higher variability of OLSA thresholds may require further investigation.

### 3.3.4. Resting-state BOLD fMRI connectivity

Aiming to validate the T- and TH-specific rs-fMRI connectivity characteristics described above, we focused on the differential weakening of synchronous auditory neural BOLD responses reflected in reduced and delayed ABR waves (**Figure 36**, (Wertz et al., 2023)).

In the third cohort, we analysed the frequency of significant correlations between prespecified ROIs (**Table 3**), prioritising cortical regions, consistent with our EEG and fNIRS analysis (**Figure 2**, **Table 4**, (Wertz et al., 2023)). We are ultimately interested in biomarkers providing personalised information, so we investigated whether the regions are significantly connected for each individual subject. The frequencies of positively correlated connections were defined for each subject within the C-, T-, and TH-groups in (i) brainstem regions as the CN, SOC, IC to the MGB (**Figure 37A, 38A**, (Wertz et al., 2023)); (ii) the MGB to the AC-I regions (BA41, 42; **Figure 37B, 38B**, (Wertz et al., 2023)); (iii) the AC-I to middle temporal (BA21, 22) and the temporo-parietal junction or Wernicke area (BA39, 40; **Figure 37C, 38C**, (Wertz et al., 2023)); (iv) the AC-I to regions of the attention/stress-regulating networks: part of the ventrolateral prefrontal network, including inferior frontal gyrus (BA45 and BA47), a part of the dorsolateral prefrontal cortex (BA46; **Figure 37D, 38D**, (Wertz et al., 2023)); (v) the AC-I to the dorsolateral and medial BA9 (BA9DL, 9M) prefrontal cortex regions involved in distress regulation (**Figure 37E, 38E**, (Wertz et al., 2023)).

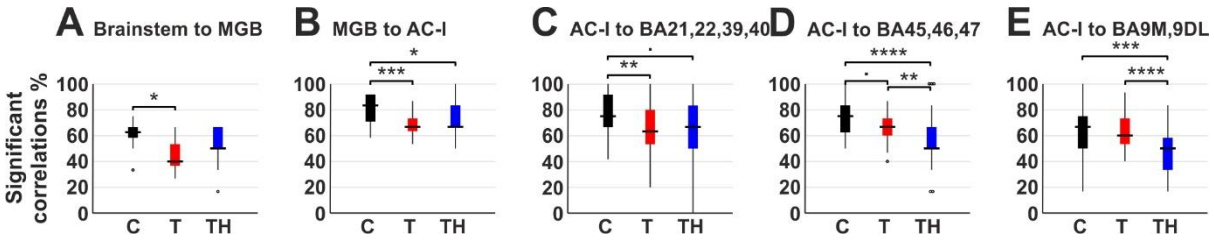


***Figure 37:*** *Frequency of significant positive rs-fMRI correlations. The boxplots display the frequency of significant positive rs-fMRI BOLD correlations between predefined ROIs in (A) subcortical regions and MGB, (B) MGB and AC-I, (C) AC-I and temporo-parietal cortex (BA21, 22, 39, 40), (D) AC-I and ventrolateral prefrontal cortex (BA45, 46, 47), (E) AC-I and anterior mesial and dorsolateral prefrontal cortex (BA9M, 9DL) for C- (n = 12, black), T- (n = 15, red), and TH-group (n = 6, blue). Regarding the management of the family-wise error rate, the p values obtained from the Kruskal-Wallis test were adjusted by Bonferroni correction. AC-I, primary auditory cortex; BA, Brodmann area; BOLD, blood oxygenation level depended; DL, dorsolateral; M, medial; MGB, medial geniculate body; ROI, region of interest. Modified according to (Wertz et al., 2023).*

In general, we again noticed that positive correlations occurred less frequently in the T- compared to the C-group. This trend was less evident in TH-group connections specific to auditory regions (**Figure 37, 38**, (Wertz et al., 2023)). The significant reduction of the T-group in brainstem regions to the MGB ($p = 0.015$; **Figure 37A, 38A**, (Wertz et al., 2023)), MGB to AC-I ($p = 0.0009$; **Figure 37B, 38B**, (Wertz et al., 2023)), and AC-I to Wernicke (p

= 0.0016; **Figure 37C, 38C**, (Wertz et al., 2023)) has been confirmed by Dunn's multiple comparison tests. When comparing the T-to the C-group, there was only a slight decrease in connectivity frequency between AC-I and the ventrolateral prefrontal networks (**Figure 37D, 38D**, (Wertz et al., 2023)) or distress-related dorsolateral prefrontal networks (**Figure 37E, 38E**, (Wertz et al., 2023)).

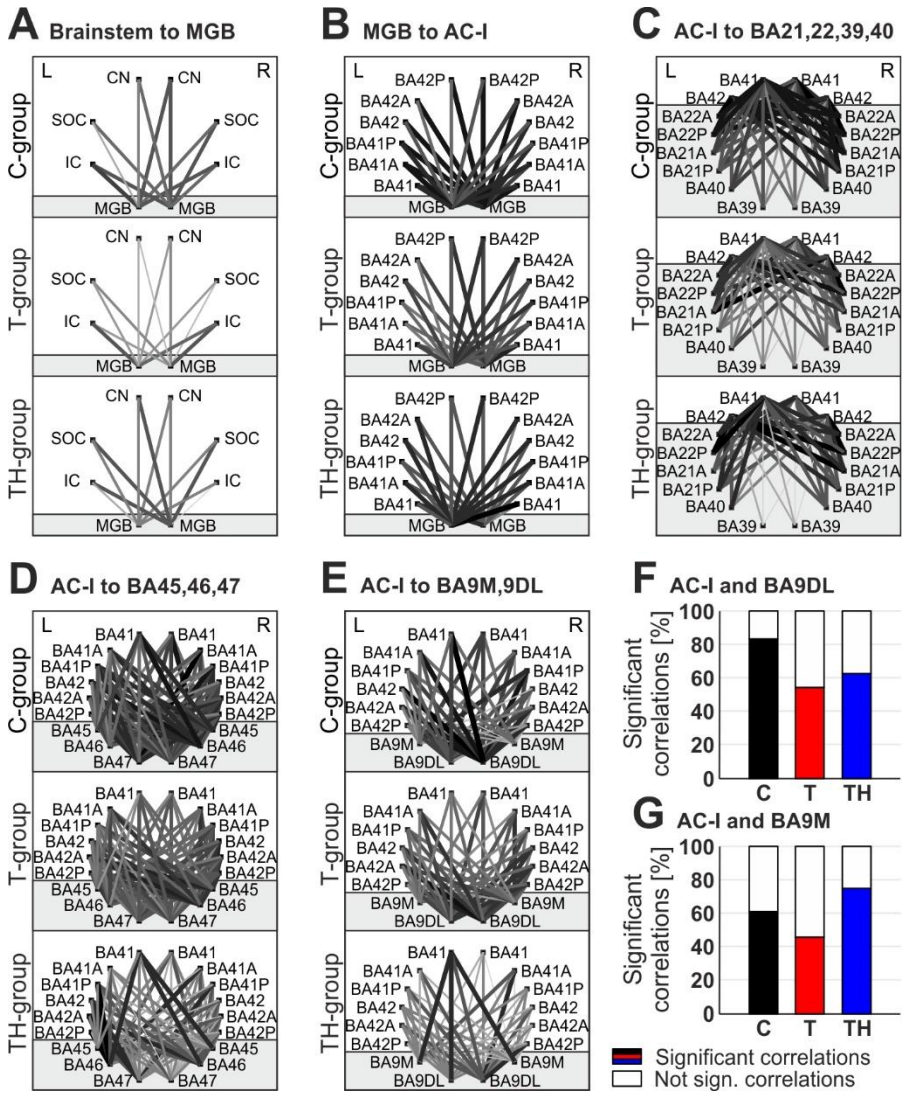


***Figure 38:*** *Frequency patterns of significant positive rs-fMRI correlations. The patterns in (A-E) show the frequency of significant positive (p < .05) rs-fMRI BOLD correlations between predefined ROIs for C- (n = 12, grey), T- (n = 15, red), and TH-group (n = 6, blue). The thickness and colour of lines correspond to the correlation strength. The patterns show the frequency of significant positive correlations between (A) subcortical regions and MGB, (B) MGB and AC-I, (C) AC-I and BA45, BA46, BA47, (D) AC-I and BA9M, BA9DL, (E) AC-I and BA21, BA22, BA39, BA40. Fisher exact probability test shows descriptive group differences in the frequency of significant positive (p < .05) rs-fMRI BOLD correlations between (F) AC-I-L and BA9DL (p = 0.122) and (G) AC-I-L and BA9M (p = 0.298). AC-I, primary auditory cortex; BA, Brodmann area; BOLD, blood oxygenation level depended; DL, dorsolateral; L, left hemisphere; M, medial; MGB, medial geniculate body; R, right hemisphere; ROI, region of interest. Modified according to (Wertz et al., 2023).*

However, Dunn's multiple comparison tests indicated that the TH-group had a significantly more prominent decrease in connection frequency, most evident from AC-I to

BA45, 46, and 47 (C-TH $p < 0.0001$, T-TH $p = 0.0014$; **Figure 37D**, (Wertz et al., 2023)), and from AC-I to BA9M and 9DL (C-TH $p = 0.0002$, T-TH $p < 0.0001$; **Figure 37E**, (Wertz et al., 2023)). Upon analysing the frequencies between the left AC-I and the medial prefrontal cortex (BA9M) or the dorsolateral prefrontal cortex (BA9DL) separately, we found that the frequency of correlations to BA9DL for both T- and TH-groups decreased in comparison to the C-group. Notably, the correlations to BA9M increased in the TH-group but not in the T-group (**Figure 38G**, (Wertz et al., 2023)).

**In summary**, our analysis found evidence for a significant decline in network connection between ROIs in the ascending auditory pathway up to the AC and associated cortical regions, including the extended Wernicke region, especially in the T-group. For the TH-group, there was a significant decrease in connectivity to the dorsolateral and ventrolateral prefrontal cortex regions.

### 3.3.5. Resting-state and two-tone discrimination evoked EEG and fNIRS recordings – Altered haemodynamic responses and gamma oscillations

To assess brain oscillations during active auditory perception, we conducted a two-tone pitch discrimination task to compare T- and TH-groups with control subjects. As stated in the methods section, participants listen to two frequency blocks: (i) stimuli close to the individual tinnitus frequency or 6 kHz for control subjects, and (ii) stimuli close to a reference frequency of 1 kHz. We subsequently recorded a resting-state in simultaneous EEG and fNIRS measurement to evaluate brain oscillations at rest. The EEG analysis focused on cortical oscillations, particularly in the gamma frequency band, and differentiated between ongoing, evoked, and induced oscillations.

Meanwhile, the fNIRS examination provided haemodynamic concentration changes of oxy-Hb and deoxy-Hb in the brain's temporal, parietal, and frontal regions (**Figure 2**, **Table 4**, (Wertz et al., 2023)). Initially, we conducted a single trial event analysis of the resting-state EEG analysis on all channels to identify the ROIs, revealing distinct ongoing oscillation patterns in gamma bands for subsequent analysis (**Figure 40-45A**, (Wertz et al., 2023)). We did not report differences for lower oscillations, as no group effects were found, probably due to the pre-processing being optimised for gamma-band oscillations. For the analysis, the frequencies are separated into three bands (**Appendix J-M**, (Wertz et al., 2023), green headings indicate significant differences): low gamma (21-40 Hz, left panel), mid gamma (41-60 Hz, mid panel), and high gamma (61-120 Hz, right panel). The fNIRS responses are presented as group average maps (**Figure 39**, (Wertz et al., 2023)): The upper row contains both oxy- (first and third row) and deoxy-Hb maps (second and

fourth row) for reference stimuli (fRef, first and second row) and for tinnitus/test stimuli (fTin, third and fourth row).

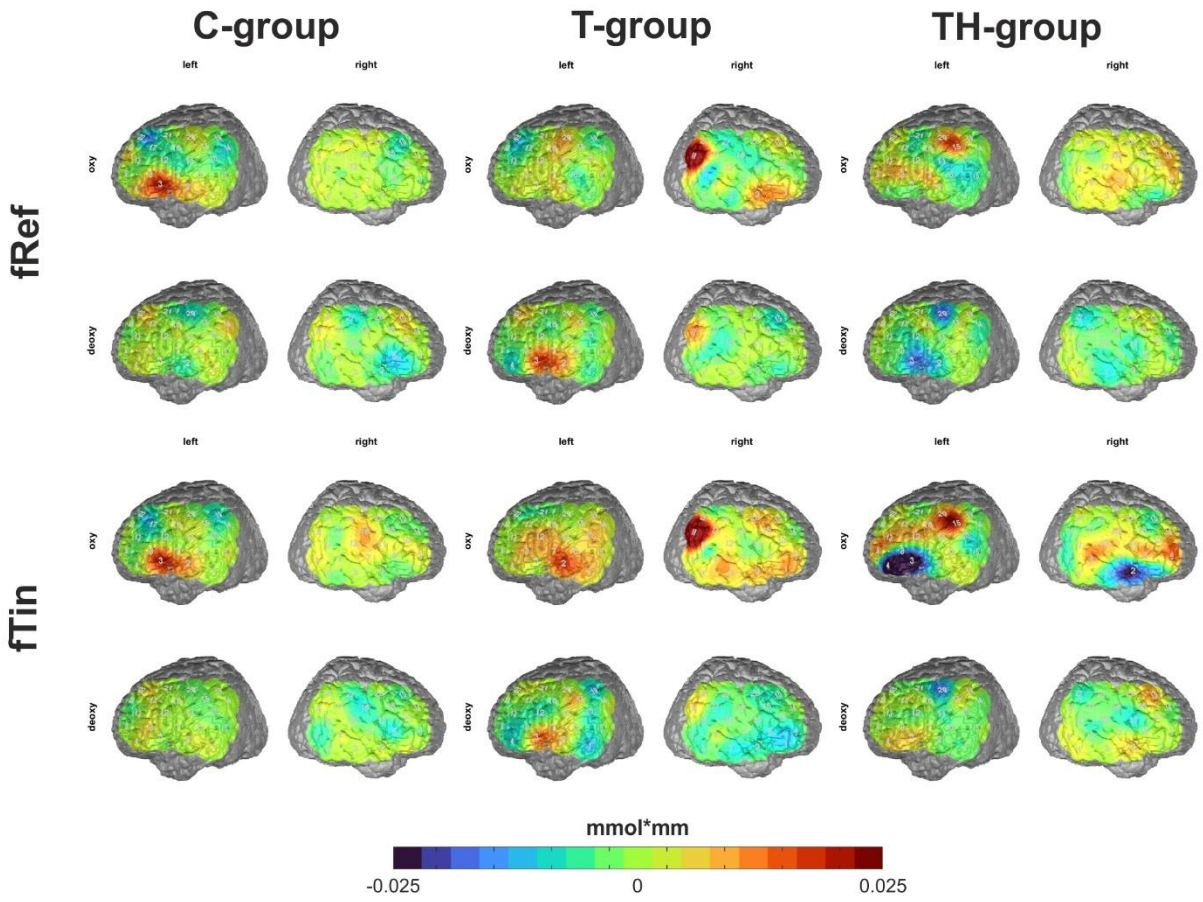


***Figure 39:*** *Haemodynamic fNIRS maps for reference and tinnitus frequency stimulation. Concentration changes of oxygenated and deoxygenated haemoglobin for the two 22-channel optode arrays covering the left and right fronto-temporo-parietal head areas. Deoxy, deoxygenated haemoglobin; fRef, reference frequency stimulation; fTin, tinnitus frequency stimulation; oxy, oxygenated haemoglobin. Modified according to (Wertz et al., 2023).*

The main objective of the EEG and fNIRS analysis was to compare the ROIs previously identified in resting-state EEG and rs-fMRI (**Appendix J-M**, **Figure 37**, (Wertz et al., 2023)). Immediately, it became apparent that all significant group differences in EEG and fNIRS could be attributed almost exclusively to the left hemisphere (**Figure 40-45**, (Wertz et al., 2023)).

### The left temporal region – Auditory cortex

In the left temporal region, we accumulate signals from the auditory cortex (BA41, 42 and BA21, 22; NIRS channels 2, 6, 7; electrode T7; **Figure 2**, **Table 4**, (Wertz et al., 2023)) during both active auditory perception and resting-state. During the latter, we observed a significant increase in high gamma [61-120 Hz] ($p = 0.018$), as well as an elevated trend

in low gamma [21-40 Hz] events (p = 0.08) in the T- compared to the C-group (**Figure 40A**, (Wertz et al., 2023)).

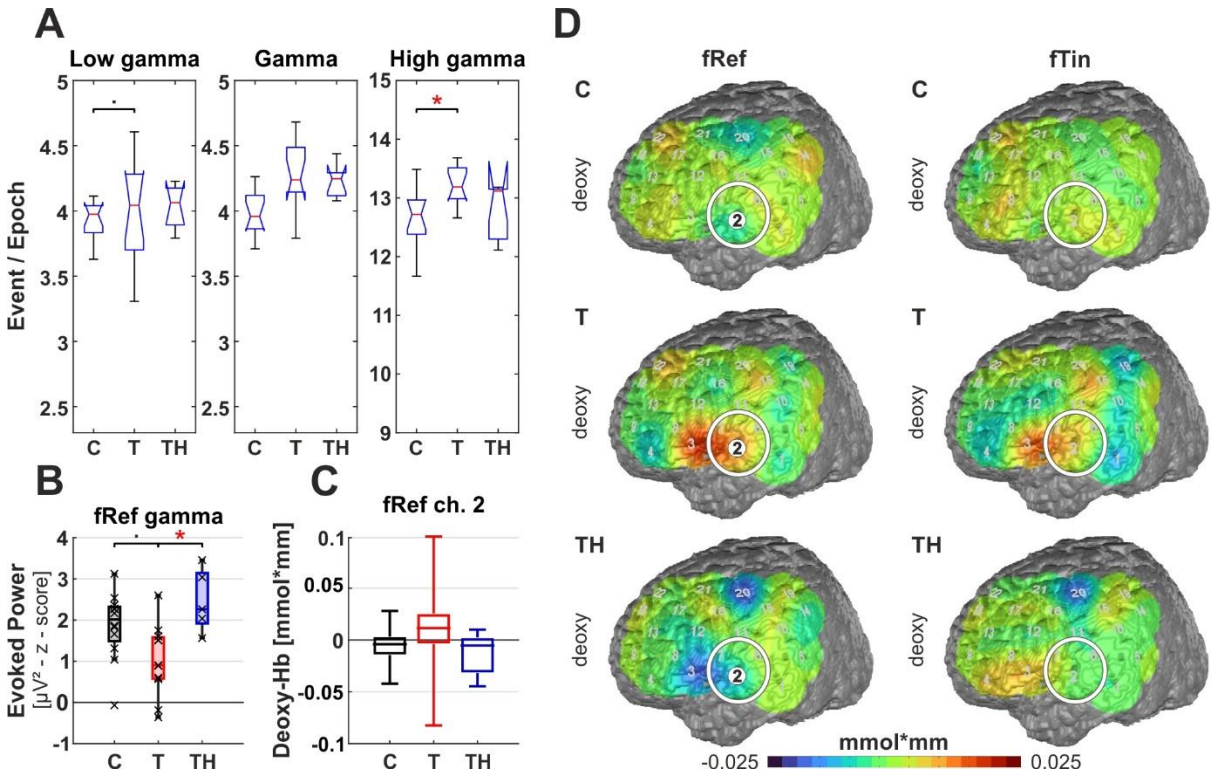


***Figure 40:*** *Oscillations and haemodynamic activity from the region of interest "T7": Box plots display median, quartiles, and range of measures derived from signals recorded at the T7 electrode for C- (n = 12), T- (n = 15), and TH-group (n = 6). (A) Spontaneous oscillation events per epoch at different gamma frequency ranges. The left panel represents the low gamma [21-40 Hz], the centre panel represents (mid) gamma [41-60 Hz], and the right panel represents the high gamma [61-120 Hz] band. (B) Evoked gamma [41-60 Hz] power, left and right plots comparing responses to stimulation with fRef and fTin. (C) fNIRS deoxy-Hb response to fRef stimulation in the left channel 2: Box plots display median, quartiles, and 5-95 percentile. (D) fNIRS deoxy-Hb changes in response to fRef (left column) and fTin (right column). The white circle highlights the region of interest on the pseudo colour maps, which represent simple group averages of (here only) deoxy-Hb concentration in mmol*mm; in subsequent figures, we combine oxy- and deoxy-Hb plots with identical scaling. Deoxy, deoxygenated haemoglobin; fRef, reference frequency stimulation; fTin, tinnitus frequency stimulation; oxy, oxygenated haemoglobin. Modified according to (Wertz et al., 2023).*

In combination with these increased (high) gamma resting-state events, we found reduced evoked gamma power [41-60 Hz] for stimulation of the reference frequency (fRef) in T-, compared to the TH-group (p = 0.021), but only a trend between C- and T-group (p = 0.055; **Figure 40B**, (Wertz et al., 2023)). Accompanied by the differences in EEG, the T-group tended to increased NIRS deoxy-Hb (warm colours) responses and increased variance in the left temporal region when exposed to fRef. The Kruskal-Wallis test indicated a trend (p = 0.06) with an effect size of d = 0.75 (**Figure 40C**, (Wertz et al., 2023)). In contrast, the TH-group experienced a rather reduction in deoxy-Hb (cool colours) in the temporal cortex when exposed to the fRef.

**In summary**, the findings support our prediction that T-group individuals exhibit increased spontaneous gamma oscillations but reduced evoked gamma oscillations in the AC. Notably, the effects evoked by fRef are more pronounced than for fTin, which is also indicated by the increased deoxy-Hb responses, implying highly variable but reduced metabolic activation in and over the AC-I.

### The parieto-temporal junction – TPJ

In the right parieto-temporal junction, the only exception of our left hemispheric results, we gather signals from the right hemisphere homologue of the Wernicke area and the more ventral parts of the posterior parietal cortex (BA7, 39, 40; NIRS channels 13, 17, 18, 22; electrode P4; **Figure 2**, **Table 4**, (Wertz et al., 2023)). In the T-group, we observed a prominent increase in spontaneous oscillatory events in the low gamma band [21-40 Hz]. Kruskal-Wallis test showed a significant group difference ($p = 0.006$; post-hoc: $p = 0.029$; **Figure 41A**, (Wertz et al., 2023)) with the largest effect size (Cohen's $d = 1.258$) in the data. There were no significant differences in evoked gamma among the groups, nor were there any trends. However, the TH-group displayed tendentially reduced induced high gamma power compared to the T-group ($p = 0.065$; **Figure 41B**, (Wertz et al., 2023)). Compared to C- and TH-group, the T-group showed a substantial stimulus evoked increase in oxy-Hb activation in the right temporo-parietal cortex, corresponding to BA39, 40, and potentially the ventral end of BA7 (**Figure 41C**, (Wertz et al., 2023)).

**In summary**, the T-group shows significantly increased spontaneous oscillatory events paired with increased evoked oxy-Hb response in the right parieto-temporal junction, indicating a possible imbalance in their attentional mechanisms.

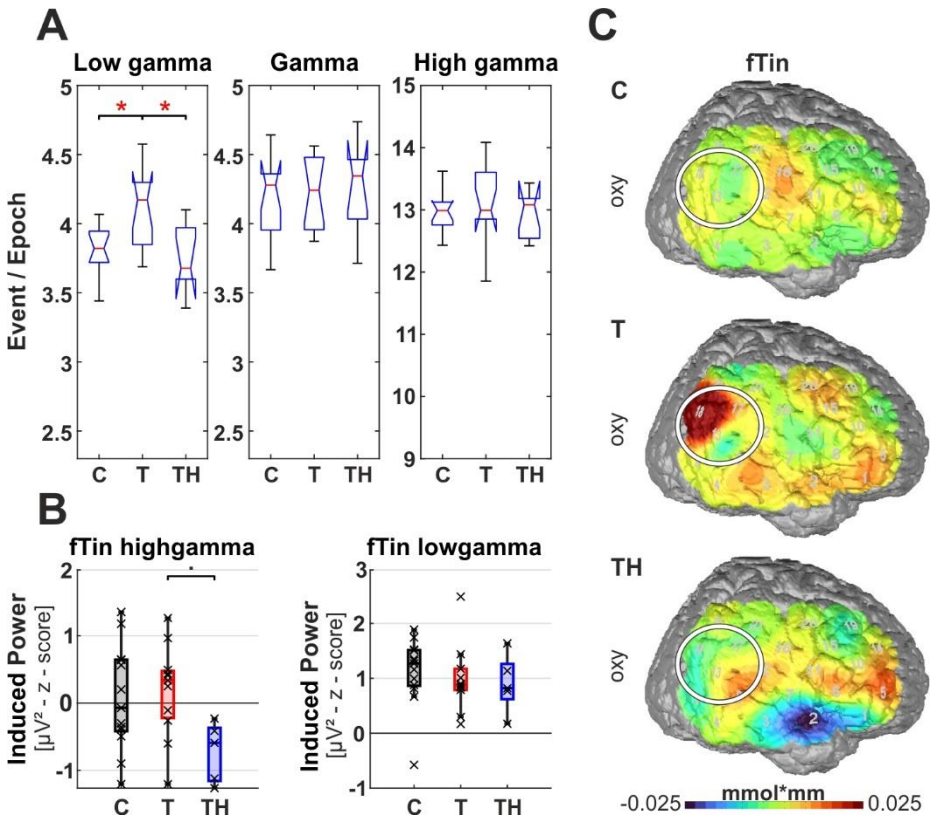


***Figure 41:*** *Oscillations and haemodynamic activity from the region of interest "P4": Box plots display median, quartiles, and range of measures derived from signals recorded at the P4 electrode for C- (n = 12), T- (n = 15), and TH-group (n = 6). (A) Spontaneous oscillation events per epoch at different gamma frequency ranges. The left panel represents the low gamma [21-40 Hz], the centre panel represents (mid) gamma [41-60 Hz], and the right panel represents the high gamma [61-120 Hz] band. (B) Induced gamma power in response to fTin stimulation, left and right plots comparing high [61-120 Hz] and low [41-60 Hz] gamma. (C) fNIRS oxy-Hb changes in response to fTin. Deoxy, deoxygenated haemoglobin; fRef, reference frequency stimulation; fTin, tinnitus frequency stimulation; oxy, oxygenated haemoglobin. Modified according to (Wertz et al., 2023).*

The left parieto-temporal junction corresponds to Wernicke's area (BA39, 40; NIRS channels 10, 14, 15, 19; electrode P3; **Figure 2**, **Table 4**, (Wertz et al., 2023)). For the Wernicke's area, we found varying differences in the resting-state, with significantly reduced oscillatory events in the low gamma band [21-40 Hz] in TH- compared to the C-group ($p = 0.017$; **Figure 42A**, (Wertz et al., 2023)) with a robust effect size ($d = 0.975$). However, for the mid gamma [41-60 Hz], we found increased events in the TH-group ($p = 0.07$), accompanied by increased fTin-evoked mid gamma (**Figure 42A**, (Wertz et al., 2023)). While at the right parieto-temporal junction, distinct patterns occurred in the T-group, at the left Wernicke's area, the TH-group displayed altered responses. Also, channel 14's haemodynamic response indicated a potential decrease in fTin-evoked deoxy-Hb in the TH-group. This effect was statistically significant in a Kruskal-Wallis test ($p = 0.046$, effect size $d = 0.833$, post-hoc: $p = 0.069$; **Figure 42C, D**, left panel, (Wertz et al., 2023)).

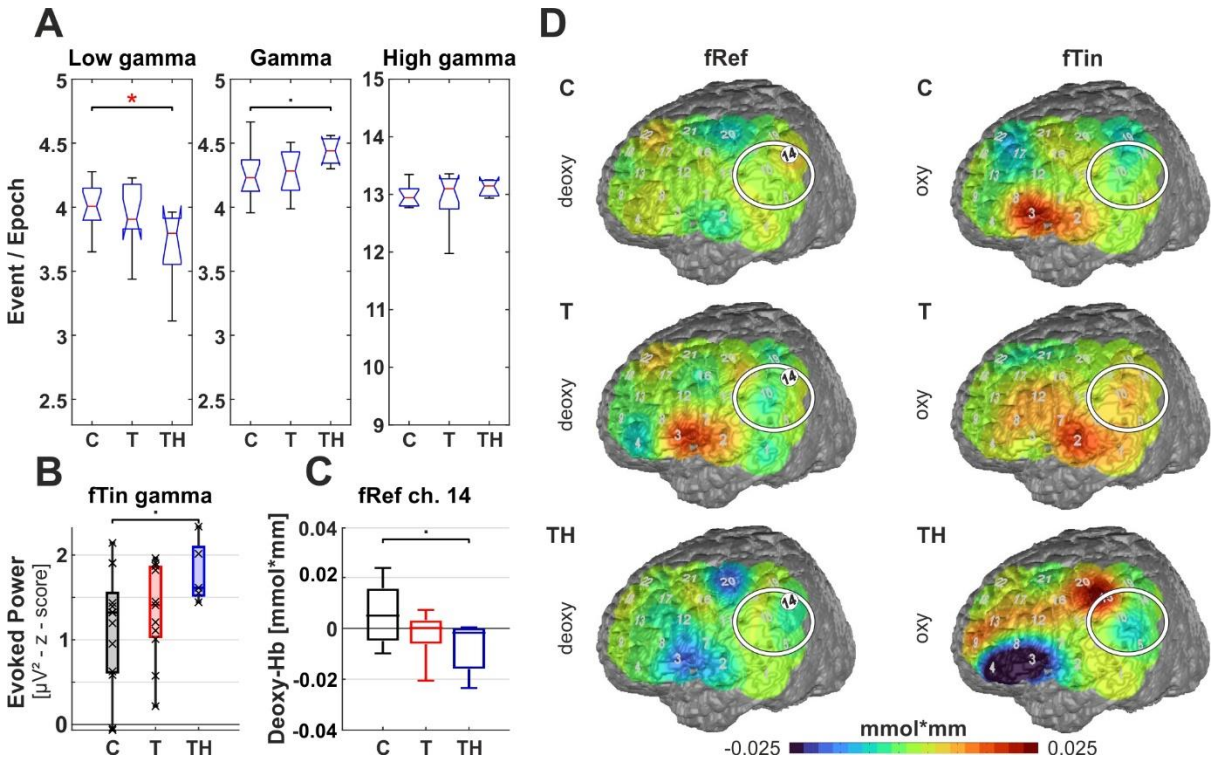


***Figure 42:*** *Oscillations and haemodynamic activity from the region of interest "P3": Box plots display median, quartiles, and range of measures derived from signals recorded at the P3 electrode for C- (n = 12), T- (n = 15), and TH-group (n = 6). (A) Spontaneous oscillation events per epoch at different gamma frequency ranges. The left panel represents the low gamma [21-40 Hz], the centre panel represents (mid) gamma [41-60 Hz], and the right panel represents the high gamma [61-120 Hz] band. (B) Oscillation responses to fTin stimulation with left and right plots comparing responses of evoked and induced gamma [41-60 Hz]. (C) fNIRS deoxy-Hb response to fRef stimulation in the left channel 14: Box plots display median, quartiles, and 5-95 percentile. (D) fNIRS deoxy-Hb changes in response to fRef, and oxy-Hb changes in response to fTin. Deoxy, deoxygenated haemoglobin; fRef, reference frequency stimulation; fTin, tinnitus frequency stimulation; oxy, oxygenated haemoglobin. Modified according to (Wertz et al., 2023).*

**In summary**, it is noteworthy that the T- and TH-group exhibit a reversed relation between the differences in spontaneous oscillation events and evoked gamma power.

## The left ventrolateral prefrontal region

In the left ventrolateral prefrontal region, we measured signals from BA44, 45, and the ventral part of BA46, regions involved in executive language and working memory (NIRS channels 4, 8, 9; electrode F7; **Figure 2**, **Table 4**, (Wertz et al., 2023)). The changes observed in the F7 electrode at rest correspond qualitatively to those described for the right AC. We noted significantly elevated spontaneous low gamma [21-40 Hz] oscillation events ($p = 0.04$, $d = 0.798$) and increased mid gamma [41-60 Hz] events ($p = 0.08$) in the T- compared to the C-group (**Figure 43A**, (Wertz et al., 2023)).

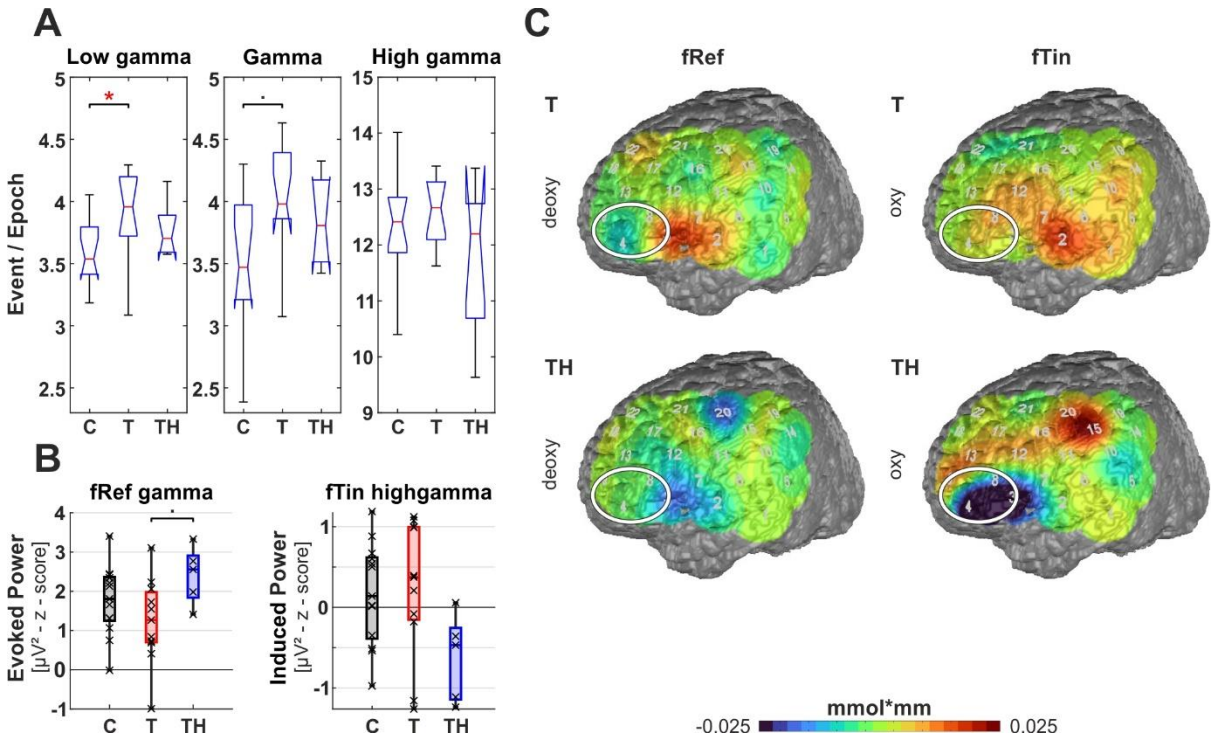


***Figure 43:*** *Oscillations and haemodynamic activity from the region of interest "F7": Box plots display median, quartiles, and range of measures derived from signals recorded at the F7 electrode for C- (n = 12), T- (n = 15), and TH-group (n = 6). (A) Spontaneous oscillation events per epoch at different gamma frequency ranges. The left panel represents the low gamma [21-40 Hz], the centre panel represents (mid) gamma [41-60 Hz], and the right panel represents the high gamma [61-120 Hz] band. (B) Evoked gamma [41-60 Hz] power, display responses to stimulation with fRef (left), and induced high gamma [61-120 Hz] power, display responses to stimulation with fTin (right). (C) fNIRS oxy- and deoxy-Hb changes in response to fRef (left column) and fTin (right column). Deoxy, deoxygenated haemoglobin; fRef, reference frequency stimulation; fTin, tinnitus frequency stimulation; oxy, oxygenated haemoglobin. Modified according to (Wertz et al., 2023).*

However, no such changes were observed in the TH-group. Similar to the T-group response in the AC, we could observe reduced gamma evoked by the two-tone discrimination task combined with the indicated increase in oscillatory events at rest. However, this fRef-evoked mid gamma [41-60 Hz] was more weakly expressed and showed a tendency of reduced responses in the T- compared to the TH-group ($p = 0.06$; **Figure 43B**, (Wertz et al., 2023), left panel). When stimulated at fTin, the post-tests showed a weak trend toward decreased high-induced gamma [61-120 Hz] in TH- compared to the T-group ($p = 0.099$; **Figure 43B**, (Wertz et al., 2023), right panel). Haemodynamic signals did not significantly affect the C-group on both hemispheres of the inferofrontal cortex. However, distinct reversed fNIRS responses were observed when comparing the T- and TH-group (**Figure 43C**, (Wertz et al., 2023)). The TH-group showed a substantial fTin-evoked decrease of oxy-Hb in the right hemispheric anterior convexity at BA47 and BA45; the T-group, in contrast, showed an oxy-Hb increase in both hemispheres (less pronounced on the right, see **Figure 39** for oxy, blue spots, (Wertz et al., 2023)).

The left dorsolateral prefrontal region

In the left dorsolateral prefrontal region, we observed signals from the dorsolateral part of BA9 (BA9DL) and the dorsolateral part of BA46, regions involved in attentional control and working memory (NIRS channels 4, 8, 9; electrode F3; **Figure 2**, **Table 4**, (Wertz et al., 2023)).

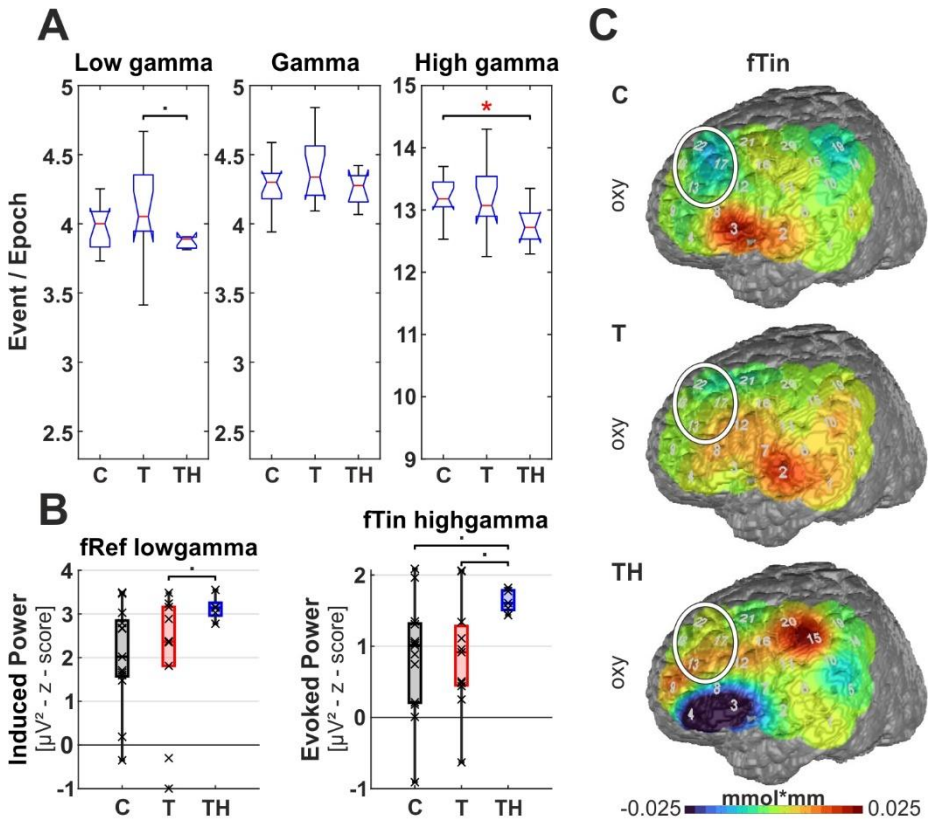


***Figure 44:*** *Oscillations and haemodynamic activity from the region of interest "F3": Box plots display median, quartiles, and range of measures derived from signals recorded at the F3 electrode for C- (n = 12), T- (n = 15), and TH-group (n = 6). (A) Spontaneous oscillation events per epoch at different gamma frequency ranges. The left panel represents the low gamma [21-40 Hz], the centre panel represents (mid) gamma [41-60 Hz], and the right panel represents the high gamma [61-120 Hz] band. (B) Induced low gamma [21-40 Hz] power displayed responses to stimulation with fRef (left) and evoked high gamma [61-120 Hz] power, showing responses to stimulation with fTin (right). (C) fNIRS oxy-Hb changes in response to fTin. Deoxy, deoxygenated haemoglobin; fRef, reference frequency stimulation; fTin, tinnitus frequency stimulation; oxy, oxygenated haemoglobin. Modified according to (Wertz et al., 2023).*

For the F3 electrode, we found a significant decrease in spontaneous high gamma events [61-120 Hz] in the TH- compared to the C-group ($p = 0.02$; **Figure 44A**, right panel, (Wertz et al., 2023)). In addition, the low gamma [21-40 Hz] events separated the TH- from the T-group by tending to occur reduced ($p = 0.077$; **Figure 44A**, left panel, (Wertz et al., 2023)). As noted for P3, we also detected decreased spontaneous gamma events associated with increased evoked gamma power for F3 in the TH-group. The reduced resting-state events were linked to a rise in fTin-induced high gamma [61-120 Hz] power

in the TH-group (**Figure 44B**, right panel, (Wertz et al., 2023)). However, this only reached a statistical trend toward the C- ($p = 0.075$) and T-group ($p = 0.094$). Also, there was a much smaller variance coupled with a noticeable increase in fRef-induced low gamma [21-40 Hz] power in the TH- compared to the T-group ($p = 0.09$). The hemodynamic activity indicated the most considerable difference in response to fTin stimulation in the oxy-Hb signal, which was reduced in the C-group, whereas the T- and TH-subjects exhibited an increase (**Figure 44C**, (Wertz et al., 2023)).

**In summary**, we again observed that the T- and TH-groups had a reversed relation between spontaneous and evoked gamma activity differences.

### Identified T- and TH-group specific biomarkers

Our observations indicate that subjects of the T-group show signs of reduced fast auditory processing, as evidenced by (i) reduced ABR wave V, (ii) reduced rs-fMRI functional connectivity between the auditory brainstem and MGB, (iii) as well as between MGB and AC. These findings are correlated with (iv) enhanced spontaneous gamma events, (v) reduced evoked gamma oscillations, (vi) and reduced deoxy-Hb activity in the left hemispheric temporal cortex in response to fRef stimulation (**Figure 36, 37, 40, 45**, (Wertz et al., 2023)). The TH-group, in contrast, exhibited differences in response to fTin primarily and demonstrated consistent alterations of spontaneous and evoked gamma oscillations in the left hemispheric parieto-temporal junction (P3) and left dorsolateral prefrontal cortex (F3; **Figure 42-45**, (Wertz et al., 2023)).

Associated haemodynamic fNIRS responses and rs-fMRI functional connectivity with AC-I were weak to both ventro- and dorsolateral prefrontal cortex (**Figure 45**, (Wertz et al., 2023)).

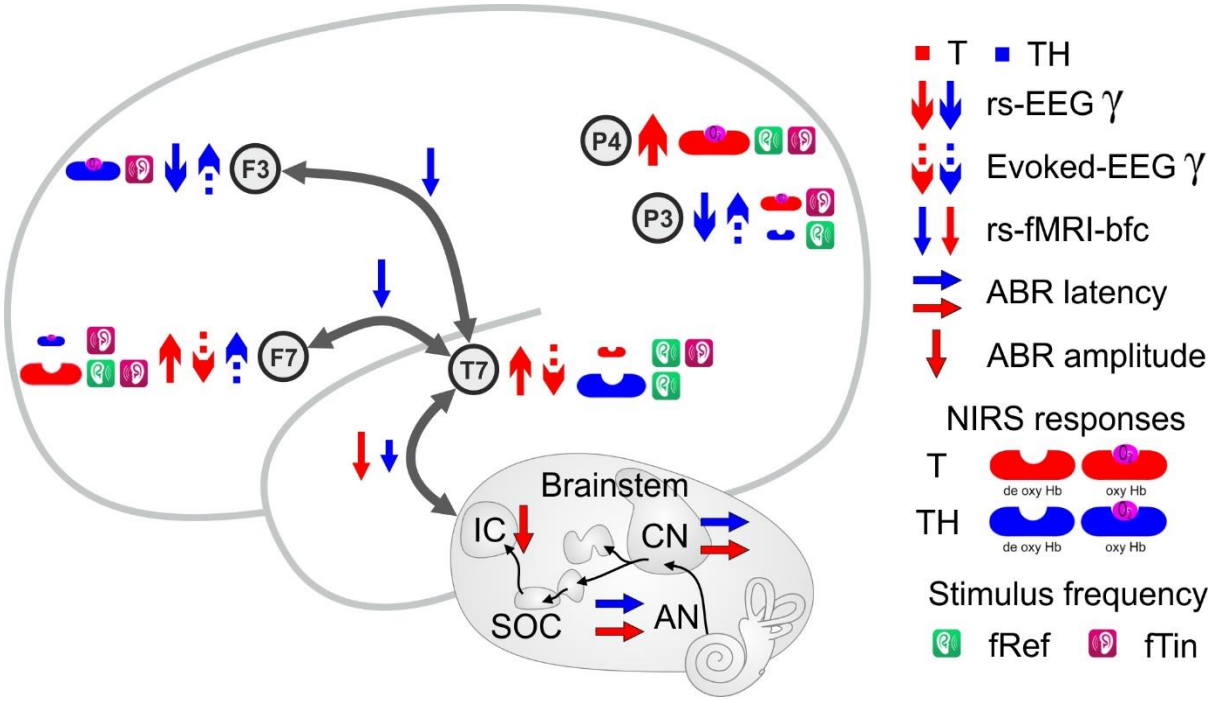


***Figure 45:*** *Overview of the characteristic functional electrical, and haemodynamic responses along subcortical (AN, CN, SOC, and IC) and cortical auditory pathways (Auditory cortex – T7, ventrolateral prefrontal cortex – F7, dorsolateral prefrontal cortex – F3, left temporo-parietal junction – P3, and right temporo-parietal junction – P4). Results are reduced to the arrows indicating the direction of parameter change when comparing T- or TH- to C-group. Group differences in oxy- and deoxy-Hb are shown as more prominent symbols (greater brain activity) and smaller symbols (lesser brain activity). The brain areas described with rs-fMRI-bfc are represented by grey arrows emanating from AC/T7. For abbreviations, see LIST OF ABBREVIATIONS.*

**In recap**, the analysis of spontaneous EEG displayed a rise in low or high gamma events at T7, P4, and F7 in the T-group. In contrast, the TH-group exhibited a decrease in low or high gamma events at P3 and F3. In the tone discrimination paradigm, we observed that fRef-evoked oscillations showed less power in the mid gamma band at T7 and F7 in the T-group. However, in the TH-group, the fTin-evoked gamma power was increased at P3 and F3. Yet, we found an exception for this pattern in the selected ROIs, as the F7 electrode was the only one in the TH-group to show a fRef-evoked increase in mid gamma. During simultaneous measurement of haemodynamic responses using fNIRS, we discovered that the left temporal region (T7) had a decrease in fRef-evoked deoxy-Hb responses, and both the T- and TH-group showed an increase in fRef-evoked deoxy-Hb activity in Wernicke's area (P3). In the following, these findings and other non-mentioned trends are discussed regarding the function of the cortical respective regions and attentional networks.

# 4. DISCUSSION

New approaches for finding a successful tinnitus therapy have been hampered for decades by the lack of knowledge on the neuronal mechanisms and neural correlates of tinnitus. This thesis provides a unique and novel multimodal approach to studying tinnitus with and without hyperacusis at different processing levels and under different attentional conditions, the latter providing important new cues for the differentiation of the T and TH subgroups. The main achievement indicates that the co-occurrence of hyperacusis masks key tinnitus-specific phenotype features. For tinnitus subjects without (T) and with hyperacusis (TH), we describe distinguishable (i) tinnitus distress-related biomarkers associated with tinnitus loudness, (ii) central auditory responsiveness at supra-threshold ABR, (iii) task-evoked BOLD fMRI/fNIRS responses in auditory and associated regions, (iv) impaired thalamocortical connectivity at rest based on BOLD rs-fMRI, (v) patterns of spontaneous and stimulus-dependent (evoked/induced) gamma-band brain oscillations in response to stimulation at reference and tinnitus frequencies which allowed for differential analysis both in stimulus and brain space (see also **Figure 22**, (Hofmeier et al., 2021); **Figure 45**, (Wertz et al., 2023)).

Naturally, we here begin with clinical standard methodologies, which are of particular interest because the ENT clinic benefits from the knowledge gained without additional expensive diagnostics. We will then continue with functional connectivity and telencephalic activity patterns, both in the spatial (fNIRS) and frequency (EEG) domain, which may, in the future, provide new diagnostic parameters for differentiating T- and TH-patients.

## 4.1. Insights gained from basic tinnitus diagnostics

According to the German clinical S3 guidelines (Hesse et al., 2022), basic diagnostic procedures for tinnitus auris include medical ENT examination (with anamneses, tympanon microscopy, tinnitus questionnaires), pure tone audiometry (PTA), extended high-frequency PTA, LDL, determination of tinnitus loudness (dB SL) and frequency, speech audiometry, TEOAE, DPOAE, and suprathreshold ABR.

### Audiometry – No hearing threshold differences in tinnitus patients with and without hyperacusis

Tinnitus was found to be significantly correlated with hearing loss (Chen et al., 2017b; Guest et al., 2017; Schecklmann et al., 2014). In order to eliminate this confounding factor

and to control for certain variables like recruitment, we put in a significant amount of work to select subjects with healthy PTA hearing thresholds. Our surveys demonstrate that there are many tinnitus subjects with good hearing. Still, in the TH-group, this was often accompanied by other comorbidities, such as moderate hearing loss, that led to exclusion. Studies have shown that the electromechanical properties of outer hair cells (OHCs) are responsible for hearing thresholds in cochlear/ sensory-neural hearing loss (Dallos and Harris, 1978; He et al., 1994), and there is no significant difference in these properties between T- (Knipper et al., 2013; Geven et al., 2011; Boyen et al., 2014; Guest et al., 2017; Gilles et al., 2016) or TH-group (Gu et al., 2010; Schecklmann et al., 2014; Hebert et al., 2013; Koops and van Dijk, 2020), and controls. Therefore, it is suggested that the loss of OHCs is not the cause of either tinnitus or hyperacusis. However, this does not rule out symptomatic hearing loss as an important risk factor for both diseases.

Based on the studies presented here, we found no evidence of corequisite hearing threshold reduction up to 10 kHz in the T- and TH-groups (**Figure 11**, (Hofmeier et al., 2021); **Figure 29**, (Refat et al., 2021)). However, this is not a novel discovery and has already been documented for hearing thresholds up to 8 kHz in the T- (Boyen et al., 2014; Geven et al., 2011; Gilles et al., 2016; Guest et al., 2017) and TH-group (Gu et al., 2010; Hebert et al., 2013; Schecklmann et al., 2014). As a novel observation, we add that no group differences in PTA hearing threshold were found at extended high frequencies up to 16 kHz (**Figure 29**, (Wertz et al., 2023)). Consequently, this convinced our research group that neither tinnitus nor hyperacusis is causally related to the loss of OHCs. However, an increase in thresholds within the EHF regions has been reported (Kim et al., 2011; Shim et al., 2009; Song et al., 2021; Peng et al., 2021; Sendesen et al., 2022), which may be caused by some degree of mechanical dysfunction of the cochlea in tinnitus patients that conventional audiometry may not detect (Jafari et al., 2022; Dewey and Dhar, 2017; Gilles et al., 2016). However, more accurate threshold measurements performed at the ENT clinic Tübingen using Békésy tracking audiometry up to 12 kHz or fine structure analysis of OHC function (Zelle et al., 2013) with pDPOAE recordings cannot convincingly support this finding yet. After all, if hearing threshold loss had a causal effect on perceived tinnitus frequency (Refat et al., 2021), one may anticipate that tinnitus frequency would shift to lower frequencies over time, as also occurs with hearing loss in presbycusis (Gates and Mills, 2005; Liberman, 2017). As far as the authors are aware, this feature has not been reported before, but our cohort, which is limited to individuals with mild hearing loss, is not able to provide evidence for this. (Refat et al., 2021).

## Tinnitus characterisation and distress – Differences in tinnitus patients with and without hyperacusis

Now that we have shown consistent hearing thresholds in the groups, it is essential to notice how stressed subjects were due to their brains' responses to their individual tinnitus frequencies. Our recent publications (Hofmeier et al., 2021; Refat et al., 2021) and **Figure 32** (Wertz et al., 2023) show that patients with additional hyperacusis are constantly exposed to more significant stress than tinnitus patients without hyperacusis (Ralli et al., 2017; Schecklmann et al., 2014; Gilles et al., 2014). From tinnitus onset, patients with the comorbidity of hyperacusis exhibit a significantly increased burden, as revealed by the GHS and HKI questionnaires (**Figure 9**, (Hofmeier et al., 2021); **Figure 32**, (Wertz et al., 2023)), due to bilateral tinnitus (**Figure 28**, (Refat et al., 2021)), and even due to subjective tinnitus loudness (dB SL) (**Figure 35C**, (Wertz et al., 2023)). In the T-group, however, tinnitus distress, assessed according to these markers, can be seen as a function of tinnitus duration. In contrast to the TH-group, the T subjects with more extended TD exhibit (i) increased burden according to HKI, (ii) possibly increased distress due to drastically increasing percentage of bilateral tinnitus as observed by (Ralli et al., 2017), (iii) increasing enhancement of the ABR wave III, a presumed feature of the co-occurrence of hyperacusis in TH-groups (**Figure 12**, (Hofmeier et al., 2021)). As this study cannot provide results from a longitudinal survey, we have only been able to gather cross sectional data from the medical anamnesis. Nevertheless, based on the different individual histories, we can assume that the general tendency of increasing burden in tinnitus patients is due to intensifying hyperacusis. In contrast to the markers mentioned above and associated with the burden caused by tinnitus loudness in dB HL, the latter rises with increasing tinnitus duration in the TH-group, while the burden decreases with time in the T-group. This development is particularly noteworthy because we expect tinnitus loudness in dB HL to decrease with tinnitus duration as the hearing threshold decreases. We assume that the tinnitus burden improves with time, but when hyperacusis is growing more severe, it will obscure tinnitus and could, therefore, become the primary clinical target in need of treatment (Refat et al., 2021).

The groups also responded rather differently to the distress caused by increasing tinnitus loudness. The T-group showed significant positive correlations of tinnitus loudness with (i) PTA thresholds (most robust at thresholds close to the tinnitus frequency; **Figure 34A-E**, (Wertz et al., 2023)), (ii) the dynamic range of LDLs (**Figure 34B**, (Wertz et al., 2023)), and (iii) the tinnitus distress (sub-)scores (**Figure 34F-I**, (Wertz et al., 2023)). The TH-group did not exhibit this correlation or even a negative correlation (**Figure 34G**, (Wertz et al., 2023)) because they show maximal distress already at low tinnitus intensities and

possibly because they have an overall increased threshold-adjusted tinnitus loudness (**Figure 34C**, (Wertz et al., 2023)). The TH-group did not exhibit this or even showed a negative correlation (**Figure 34G**, (Wertz et al., 2023)) because they already exhibited maximal distress at low tinnitus intensities (**Figure 10**, (Hofmeier et al., 2021); **Figure 34, 35A, B**, (Wertz et al., 2023)), possibly because they have an overall increased threshold-adjusted tinnitus loudness (**Figure 34C**, (Wertz et al., 2023)). These significant tinnitus subgroup differences in distress scores, along with the deviating correlation of tinnitus-loudness and distress or PTA thresholds, are consistent with the findings reported in studies conducted with significantly larger sample sizes (Schecklmann et al., 2015; Shin et al., 2022; Aazh et al., 2019; Tyler and Conrad-Armes, 1983; Ralli et al., 2017; Schecklmann et al., 2014; Refat et al., 2021; Hofmeier et al., 2021; Koops et al., 2021; Han et al., 2018). Therefore, we consider them reliable biomarkers for distinguishing the T- and TH-groups.

### Suprathreshold sound responsiveness differences in tinnitus patients with and without hyperacusis

Supra-threshold ABR measurements can reveal the fine structure of brain responses, both in the periphery and central regions (Ruttiger et al., 2017; Mohrle et al., 2019; Knipper et al., 2019; Knipper et al., 2015). Furthermore, the ABR wave amplitudes indicate synchronised neural activity along the nuclei of the ascending auditory pathway (Ruttiger et al., 2017; Johnson and Kiang, 1976). The distinct ABR waves originate from specific neuronal activities that can be spatially associated. For instance, the supra-threshold ABR (i) wave I is generated by the auditory nerve's distal peripheral portion (Portmann et al., 1980), (ii) wave III is generated by the spherical and globular cells of the CN connecting to the SOC (Melcher and Kiang, 1996), (iii) wave V is produced by the medial SOC and its projections to the nuclei in the lateral lemniscus and the IC, and (iv) wave VI arises from MGB or the IC output (Møller et al., 1994).

In the search for a specific neural correlate that distinguishes T- from TH-group, a significantly reduced and delayed suprathreshold ABR wave V (**Figure 12**, (Hofmeier et al., 2021); **Figure 30**, (Refat et al., 2021); **Figure 36**, (Wertz et al., 2023)) was identified as a characteristic feature of tinnitus in the T-group. These differences from the control are clearly distinguishable in ABR wave III and V (**Figure 12**, (Hofmeier et al., 2021); **Figure 30**, (Refat et al., 2021)), which in the first and second cohorts of the TH-group were significantly elevated and tendentially shortened in response to high sound levels. This most characteristic TH-group feature of enhanced and shorter latency waves V and III increased even further with tinnitus duration (**Figure 30**, (Refat et al., 2021)). As a further

difference between the groups, the ratio of suprathreshold ABR wave V to wave I amplitudes (V/I ratio), used to quantify central neural gain, was reduced in the T-group. In contrast, no difference to controls is observable in the TH-group (**Figure 13**, (Hofmeier et al., 2021); **Figure 31**, (Refat et al., 2021)). The group differences found in the ABR responses between the T- and TH-group indicate two aspects worth interpreting:

(1) The reduced auditory-specific responsiveness, evident through a reduced and delayed ABR wave V in the T-group (**Figure 12, 13**, (Hofmeier et al., 2021); **Figure 30, 31**, (Refat et al., 2021); **Figure 36**, (Wertz et al., 2023)), is best explained by critical deafferentation of high spontaneous firing rate fibres with low response thresholds (high-SR) and short response latencies (Liberman, 1978), defining perceptual hearing thresholds at distinct frequencies (Meddis, 2006; Heil et al., 2008). This concept is supported by previous studies demonstrating reduced and delayed ABR waves in animal models of tinnitus (Rüttiger et al., 2013; Singer et al., 2013) and in humans with tinnitus (Hofmeier et al., 2018; Knipper et al., 2020). The normal auditory thresholds accompanied by the reduced and delayed ABR wave V responses (**Figure 12, 13**, (Hofmeier et al., 2021); **Figure 30, 31**, (Refat et al., 2021); **Figure 36**, (Wertz et al., 2023)) strengthen the assumption that tinnitus is related to a loss of fast auditory processing. A critical loss of fast (high-SR) auditory nerve fibre (ANF) processing was previously suggested to re-emerge hyperexcitability through loss of tonic parvalbumin (PV+) interneuron in deprived regions, possibly through reversion of depolarising instead of inhibitory GABAergic signalling (Knipper et al., 2020). Some background information is necessary to fully assess the influence of high-SR fibres in this concept. High-SR auditory nerve fibres contribute significantly to (i) increased ANF compound action potential thresholds (Bourien et al., 2014), which might contribute to low perceptual thresholds by the increased action potential firing synchrony (Meddis, 2006; Heil et al., 2008), (ii) phase-locked responses for ANF (Huet et al., 2019), essential for envelope following response coding (Hunter et al., 2018), reflecting rising neural synchrony in the central auditory system, also evident in, i.e., frequency-following responses (Walton, 2010; Clinard et al., 2010; Anderson et al., 2012). These changes in envelope following responses (Encina-Llamas et al., 2019) are considered a potentially sensitive marker for cochlear synaptopathy (Marcher-Rorsted et al., 2022), when unaffected by dysfunction of outer hair cells. This re-emerged hyperexcitability and diminished memory-linked contrast amplification results in tinnitus patients failing to distinguish between relevant and irrelevant noise, causing constant alertness to phantom sounds (Knipper et al., 2020).

(2) It is possible to explain the enhanced amplitudes of ABR waves III and V in TH-group of cohort I and II (**Figure 12B, C**, (Hofmeier et al., 2021); **Figure 30**, (Refat et al., 2021))

by an unspecific overactivation of type-II cochlear afferents at the level of OHCs (Liu et al., 2015; Flores et al., 2015) or medial olivocochlear bundle (MOC) (Knudson et al., 2014; Sturm and Weisz, 2015). These studies indicate that increased ABR wave amplitudes in the TH-group in response to high stimuli are the compensatory response to noxious OHC/MOC overactivation. Thus, increased MOC activity is expected to suppress OHC activity, leading to a decrease in cochlear activity. The subsequent suppression of cochlear-nerve output may trigger – as hypothesised by (Knudson et al., 2014; Sturm and Weisz, 2015) – a compensating increase in evoked firing through disinhibition of brainstem regions such as the SOC complex, the cellular generator of ABR wave III (Melcher and Kiang, 1996). This compensation is also observed following acoustic trauma, e.g., in the ventral CN, dorsal CN, IC, and AC-I (Cai et al., 2009; Salvi et al., 2000; Middleton et al., 2011; Yang et al., 2011) and was suggested to possibly contribute to a lowering of loudness tolerance (Sturm and Weisz, 2015). As the MOC neurons are positioned in the SOC complex from which ABR wave III originates, the increased and (partly shortened) ABR wave III and V amplitudes measured in the TH-group (**Figure 12**, (Hofmeier et al., 2021); **Figure 30**, (Refat et al., 2021)) could also be attributed to acoustic trauma. However, this trend of increased ABR waves was not reproduced in the TH-group of the third cohort, possibly due to an older TH-group or the new measurement setup. We report that patients with tinnitus for over five years may show both reduced ABR wave V and enhanced ABR wave III (**Figure 30**, (Refat et al., 2021)), indicating hyperacusis characteristics progress in the T-group. Given the possible progressive co-occurrence of tinnitus and hyperacusis over time, it may be necessary to reassess the numerous controversial findings of altered central auditory responses in tinnitus (Schecklmann et al., 2014; Knipper et al., 2020; Sedley, 2019; Sheppard et al., 2020).

How MOC regions may become overactive is still highly speculative: As described above, an unspecific overactivation of type-II cochlear afferents at the level of outer hair cells triggered by loud sound levels has been considered (Liu et al., 2015). According to this view, type-II afferent fibres would contribute to MOC over-activation through hyperactivity of planar multipolar cells (T stellate cells) in the posteroventral CN (Flores et al., 2015), providing excitatory input to MOC neurons in the SOC complex (Darrow et al., 2012). Alternatively, it is hypothesised that over-activation of the auditory brainstem MOC regions occurs due to top-down influences during hyperacusis (Knudson et al., 2014; Sturm and Weisz, 2015). Regardless of whether bottom-up or top-down processes cause MOC hyperactivity in TH-groups, our research indicates that hyperacusis is linked to elevated distress and auditory perceptual difficulties (**Figure 9**, (Hofmeier et al., 2021); **Figure 32H, P**, (Refat et al., 2021)). The increased auditory perceptual difficulty score made the deficits in listening capacity particularly evident, in particular for TH patients

with tinnitus loudness scores below fifteen dB HL (**Figure 10C**, (Hofmeier et al., 2021); **Figure 35C**, (Wertz et al., 2023)). The following analysis of sound-induced BOLD fMRI activities in T- and TH-groups provides further insight into the origin group differences in distress and loudness sensitivity.

## 4.2. Insights gained based on altered BOLD fMRI haemodynamic responses

### Differences in auditory stimulus-evoked BOLD fMRI responses in tinnitus patients with and without hyperacusis

Subgroup-specific differences in evoked BOLD fMRI responses revealed an abnormal hyperactive central response pattern in the TH-group of the first cohort, which partially masks a tinnitus-specific reduction in auditory-associated regions. We observed a significant decrease in the evoked responses to music, LF-, and HF-chirp stimuli in auditory brainstem regions (CN or SOC) in both tinnitus subgroups compared to controls (**Figure 14**, (Hofmeier et al., 2021)). However, from the MGB upwards, we found differing evoked BOLD responses in the ascending auditory pathway, with reduced responses to music and HF-Chirp in the T-group, while the TH-group showed elevated responses to LF-chirps (**Figure 14**, (Hofmeier et al., 2021)). This indicates that elevated ABR wave III & V responses in the TH-group of the first cohort are reflected in reduced rather than elevated BOLD fMRI responses in CN and SOC, regions involved in generating ABR wave III (Melcher and Kiang, 1996). Based on these findings, we assume that these reduced sound-evoked responses in subcortical auditory regions are a characteristic tinnitus feature independent of hyperacusis. Further, our results suggest that increased BOLD fMRI activity in the MGB observed in the TH-group may cause enhanced AC-I, hippocampus, and posterior insula responses through spreading excitation (mainly observed in response to BB-chirp and music stimuli; **Figure 14-17**, (Hofmeier et al., 2021)). Regarding the increased BOLD fMRI activity in MGB, the posterior insula and hippocampus play a critical role in detecting sound (Sadaghiani et al., 2009) and shaping auditory signals for specific sound percepts (Kraus and White-Schwoch, 2015; Weinberger, 2015). Disproportionate activation of these regions may contribute to auditory perceptual difficulties and loudness hyper-sensation experienced by the TH-group. Finally, we focused on fear and pain pathways, including the mammillary body (Mam. Body) as part of the limbic system regulating, e.g., state-dependent fear (Bubb et al., 2017; Jiang et al., 2018), the insular and peri-insular regions, especially the dorsal posterior insula (DpIns) (Segerdahl et al., 2015), and the postcentral gyrus regions with the parietal operculum (PO1, PO2). It is essential to address the significant differences observed in

BOLD fMRI responses in the postcentral gyrus regions, particularly in the PO areas. Specifically, in these regions, BOLD fMRI responses were considerably reduced in the T-group but not in the TH-group when exposed to music stimuli (**Figure 17**, (Hofmeier et al., 2021); DpIns, PO1, PO2). The cortical areas PO1 and PO2 have been shown to be activated immediately after painful stimulation (Tracey and Mantyh, 2007; Garcia-Larrea and Peyron, 2013), with pain dominating even after all stimuli, such as heat or unpleasant sounds, are removed (Horing et al., 2019). This raises the question of whether the TH-group is unable to suppress acute pain perception due to insufficient suppression in response to music stimuli during BOLD fMRI, as is the case in the T-group.

Overall, the differences in evoked BOLD fMRI responses between T- and TH-groups may suggest that reduced evoked BOLD fMRI responses in the ascending auditory pathway, possibly dominating in the frequency channels of the tinnitus pitch, are rather a feature characteristic of tinnitus. With the co-occurrence of hyperacusis, it seems that a more widespread signal amplification process proceeds through an overactive thalamo-cortical activity that may trigger an excitation spread to limbic and pain regions and results in over-attention to increased loudness at all sound frequencies, as also previously suggested (Koops and van Dijk, 2020; Sedley, 2019).

### Differences in rs-fMRI BOLD functional connectivity in tinnitus patients with and without hyperacusis

Increased neural activity (evoked BOLD fMRI) during, e.g., sensory performance is correlated with enhanced synchronous positive correlations at rest (Haag et al., 2015). Moreover, it was suggested that a correlation between evoked fMRI and rs-fMRI reflects more strongly integrated brain regions during cognitive performance (Tagliazucchi et al., 2012; Goelman et al., 2014). This correlation, or lack thereof, between brain regions, may offer crucial information about altered/dysfunctional information transmission and changes in the structure of default networks (Chen et al., 2017b; Husain and Schmidt, 2014; Hullfish et al., 2018; Rosemann and Rauschecker, 2023). This would predict that a decreased BOLD fMRI response, linked to a decrease in positive BOLD rs-fMRI correlation, indicates less integration between brain regions during cognitive performance. If this hypothesis is correct, the significantly reduced evoked BOLD fMRI response in the subcortical and cortical auditory regions in the T-group (**Figure 14-16**, (Hofmeier et al., 2021)), together with a reduced number of connectivity between the auditory brainstem regions and MGB (**Figure 19A**, (Hofmeier et al., 2021)), between the MGB and AC-I (**Figure 19B**, (Hofmeier et al., 2021)), between the AC-I and emotional network (**Figure 20A**, anterior insula and amygdala, (Hofmeier et al., 2021)), and between the AC-I and

attention-controlling regions (**Figure 20B**, (Hofmeier et al., 2021), BA45, 46 (Cieslik et al., 2015)), as seen in the T-group of the first cohort, indicate less integrated brain regions. Although direct comparisons between rs-fMRI connectivity and evoked fMRI could not be calculated in the third cohort, the frequency of connectivity in the T-group also revealed a reduced frequency of significant connectivity (**Figure 37, 38**, (Wertz et al., 2023)). In contrast, in the TH-group, the number (**Figure 19, 20**, (Hofmeier et al., 2021) and frequency (**Figure 37**, (Wertz et al., 2023)) of connectivity diminishes significantly less pronounced than in the T-group but is still significantly reduced compared to the controls. Moreover, the reduced positive correlations of the amygdala and anterior insula to the pain network (**Figure 21A**, (Hofmeier et al., 2021) reflect a significantly more substantial loss of connectivity in the TH- than in the T-group. Reduced functional connectivity between the subcortical and cortical auditory regions may be reflected in reduced evoked BOLD fMRI response in auditory brainstem regions, such as the CN and SOC. In comparison, the increased evoked BOLD fMRI in the MGB, AC-I, and associated auditory regions exhibited in the TH-group were reflected in less reduced functional connections. Previous studies have shown decreased functional connectivity between the MGB and AC-I in tinnitus groups (Berlot et al., 2020; Kim et al., 2012; Hofmeier et al., 2018; Boyen et al., 2014). However, none of these studies examined the difference between the number and strength of resting-state correlations, which may have hindered the detection of group-specific correlation patterns.

Recent studies suggest that positive (Florin et al., 2015) and negative spontaneous correlations at rest, previously thought to lack a clear neural basis due to the complex interplay of neural and vascular parameters, may have a viable physiological basis (Zhang et al., 2020). The low number of significantly negatively correlated functional connections suggests that synchronised neuronal activity and homogeneous haemodynamic responses (Goelman et al., 2014), which positively correlate between ROIs, dominate our analysis. Whether negative spontaneous correlations at rest indicate less integration between brain regions remains to be seen. Currently, we can only make assumptions about the meaning of the negative correlations between the AC-I/ pain network and fronto-parietal medial BA9 and BA47 regions (**Figure 20C, 21C**, (Hofmeier et al., 2021), responsible for negative emotions such as fear, disgust, and anger (Ardila et al., 2017). Given that the puzzling anti-correlations could not be replicated in the third cohort, we refrain from interpreting them without additional evidence.

In the third cohort, we specifically assessed if the regions were correlated for each subject and compared the frequency of significant correlations across groups based on the individual level. The functional connectivity reduction was more prominent in the T- than

the TH-group, particularly between the temporal/ parietal areas and their respective input structures, the MGB and AC (**Figure 37A-C, 38A-C**, (Wertz et al., 2023)). However, between frontal areas and the AC, the TH-group subjects displayed a more substantial connectivity loss (**Figure 37D, E, 38D, E**, (Wertz et al., 2023)). Similar effects in the T-group were also found by previous studies, reporting that reduced and delayed ABR wave V are associated with reduced sound-evoked BOLD fMRI activity in the auditory cortex (Hofmeier et al., 2018; Koops and van Dijk, 2020), with reduced functional connectivity observed during sound-evoked responses (Boyen et al., 2014; Lanting et al., 2014), and with reduced rs-fMRI-bfc between auditory-specific brain regions and fronto-striatal regions (Hofmeier et al., 2018; Leaver et al., 2016b). Tinnitus patients with additional hyperacusis, on the other hand, were associated with partly increased (sub-) cortical responsiveness (Koops et al., 2021; Hofmeier et al., 2021). Since auditory responses were previously predicted to alter haemodynamic BOLD responses by altered phase-locking and changed oscillatory power in the mid/high gamma bands (Oya et al., 2018), we now consider the simultaneously measured EEG oscillations and haemodynamic responses in selected ROIs (**Figure 39-44**, (Wertz et al., 2023)).

## 4.3. Additional insights gained based on oscillatory events and haemodynamics

Based on the almost exclusively left-hemispheric group-specific resting-state gamma-band oscillation event patterns (**Figure 40-45**, (Wertz et al., 2023)), we selected ROIs for the following multimodal analysis. The ROIs, herein examined in more detail, include the (i) AC represented by electrode T7 with BA41, 42, 22, performing basic and higher hearing functions (Zatorre et al., 2002); (ii) Temporo-parietal junction/ Wernicke area represented by electrode P3 and P4 with BA39, 40 and ventral BA7, involved in sound detection and evaluation, i.e., language processing (Ardila et al., 2016; Coslett and Schwartz, 2018; Schwartz et al., 2012; Yantis et al., 2002); (iii) Ventrolateral prefrontal attention/stress-regulating areas represented by electrode F7 with BA45, 47 (Chen et al., 2017b; Husain, 2016; Leaver et al., 2016a) and BA46 (Cieslik et al., 2015); (iv) Dorsolateral prefrontal areas represented by electrode F3 with Dorsolateral BA9, among other things, involved in distress regulation (Lai et al., 2019; Li et al., 2022a). In addition to rs-fMRI, the measured fNIRS supply oxy- and deoxy-Hb concentrations in mmol*mm, interpreted as metabolic brain responses following neural activation. We have only analysed group-dependent changes in haemodynamic activity, as until now, there is no uniform interpretation of oxy-/ deoxy-Hb and BOLD fMRI responses (Steinbrink et al., 2006; Pinti et al., 2021). Here, the deoxy-Hb signal is interpreted as an indicator of reduced brain activity when there is

an increase in signal, while a decrease in signal is interpreted as an indicator of increased brain activity. Conversely, the oxy-Hb signal is interpreted in reverse; An increase in signal is taken as an indicator of increased brain activity, while a decrease in signal is taken as an indicator of reduced brain activity.

The T-group showed an increase in low or high gamma events at T7, P4, and F7 in the spontaneous EEG analysis. Conversely, the TH-group displayed a decrease in low or high gamma events at P3 and F3. Utilising the two-tone discrimination paradigm, the third cohort revealed that the fRef-evoked oscillations in the mid gamma band were less powerful in the T7 and F7 regions of the T-group. Conversely, the fTin-evoked gamma power was increased in the TH-group in the P3 and F3 regions. However, we noted an exception to this pattern in the selected ROIs: The F7 electrode in the TH-group exhibited a fRef-evoked increase in mid gamma. In addition, the simultaneous measured haemodynamic responses indicated that the left temporal region (T7) had a decrease in fRef-evoked deoxy-Hb responses, while both the T- and TH-group displayed an increase in fRef-evoked deoxy-Hb activity in Wernicke's area (P3). Subsequently, these results will be interpreted in the context of attention networks and the chosen ROIs described above.

### Functional connectivity and fast neural oscillation processes in left temporal cortex

It has been reported through various studies that slow EEG brain oscillation changes can be linked with tinnitus, especially alpha-band oscillation changes (Weisz et al., 2007; Leske et al., 2014; Ortmann et al., 2011; Sturm and Weisz, 2015; Li et al., 2022b). However, there is still some uncertainty and controversy regarding the role of gamma oscillations in the auditory cortex of tinnitus-affected individuals. This controversy is probably because previous EEG studies with tinnitus patients did not differentiate between those with and without hyperacusis. Furthermore, examining the differences in brain oscillations when tinnitus patients actively perceive auditory stimuli both within and outside their tinnitus frequency provides vital information that was missing up to date. The primary objective of the pitch discrimination task is to obtain group-specific differences in audibility level, attention, or working memory.

The analysis of oscillatory events in the left temporal cortex revealed a significant increase in spontaneous high gamma oscillation [61-120 Hz] events in the T- compared to the C-group. However, spontaneous low gamma oscillations [21-40 Hz], previously reported to be enhanced in tinnitus subjects (van der Loo et al., 2009; Vanneste et al., 2010; Vanneste et al., 2018), merely exhibited a non-significant trend towards increased activity in the T-group (**Figure 40A**, (Wertz et al., 2023)). In contrast, the power of fRef-evoked gamma

oscillations [41-60 Hz] was significantly lower in the T- than in the TH-group, while there was only a trend compared to the C-group (**Figure 40B**, (Wertz et al., 2023)). Those gamma-band differences in the temporal cortex were linked to differential haemodynamic fNIRS responses: The T-group indicated reduced but highly variable fRef-evoked deoxy-Hb activity, while the TH-group exhibited no distinction from the C-group (**Figure 40C, D**, (Wertz et al., 2023)). On the one hand, the increased spontaneous activity in the T-group, linked with decreased evoked gamma-band power in the AC, could arise from changes in synchronised activity in cortical representations of the tinnitus frequency, potentially affecting the representation of lower frequencies (Marcher-Rorsted et al., 2022), such as fRef. On the other hand, in the TH-group, which can be assumed to exhibit reduced fast auditory fibre processing, this effect is possibly masked by the proposed multiplicative neural gain driven by the deafferentation of OHCs (Knudson et al., 2014; Sturm and Weisz, 2015), which may result in inappropriately high attention.

It is worth noting that the increased occurrence of spontaneous gamma events in the auditory cortex, as observed in the T-group, is consistent with animal studies that have found a rapid increase in spontaneous neuronal firing linked to synchronised neuronal bursting (Noreña and Farley, 2013) due to induced chronic tinnitus. Presumably, this abnormal neuronal synchrony of neuronal populations in tinnitus patients is reflected by specific oscillatory frequency bands (Eggermont and Tass, 2015), particularly by enhanced spontaneous gamma band oscillations (Knipper et al., 2020). Indeed, previous studies in humans (Vanneste et al., 2019; Weisz et al., 2007; Ortmann et al., 2011) and animals (Tziridis et al., 2015) have shown that altered spontaneous gamma oscillations are associated with tinnitus. Until this work, most research groups have associated the heightened spontaneous gamma oscillations observed in tinnitus as the result of overactive feedback loops (De Ridder et al., 2015; Sedley, 2019; Vanneste et al., 2019). However, in contrast, our results imply that the observed increased cortical synchrony in tinnitus patients may result from underactive tonic feedback inhibition (Knipper et al., 2020). In addition to explaining the enhanced spontaneous gamma oscillations (**Figure 40A**, (Wertz et al., 2023)), this could also explain the decreased evoked gamma oscillations in AC (**Figure 40B**, (Wertz et al., 2023)), which are associated with reduced fNIRS deoxy-Hb activity observed in the T-group (**Figure 40C, D**, (Wertz et al., 2023)).

According to studies by (Cardin et al., 2009; Sohal et al., 2009; Chen et al., 2017a), PV+ inhibitory interneurons play a vital role in generating both gamma- (feed-forward inhibition) and beta-frequency oscillations (feed-back inhibition). Therefore, it can be concluded that in tinnitus patients, a critical reduction of fast (high-SR) auditory fibres in tinnitus frequency regions may result in a pathological reduction of tonic (perisomatic)

inhibition of pyramidal neurons through the monosynaptic coupling of PV+ interneurons in auditory cortical circuits (Knipper et al., 2020). If this applies, the signal-to-noise ratio of sensory transmission would decrease because the pyramidal neurons would fire synchronously and independently of input, as has been shown for cerebellar (Duguid et al., 2012) and cortical neurons in epilepsy (Rossignol et al., 2013; Hsieh et al., 2017). Strong evidence suggests that fast-spiking PV+ interneuron activity is directly linked to attention-driven contrast enhancement (Chen et al., 2017a; Kim et al., 2016), but whether a disruption in this "noise cancellation" contributes to the development of tinnitus, as suggested (Rauschecker et al., 2015; Knipper et al., 2020), remains to be verified. Overall, there is little scientifically supported evidence to date for the relief of tinnitus therapies, so one active repetitive transcranial magnetic stimulation study stands out as showing a reduction in tinnitus distress in the short and long term (6 months) after stimulation primarily of, i.e., the left auditory cortex (Lefebvre-Demers et al., 2021). This finding of eased tinnitus distress further supports confirmation of the importance of the left auditory cortex in understanding tinnitus and tinnitus hyperacusis.

We will now explore four additional cortical hubs that exhibited significant group effects between C-, T-, and TH-group, illustrating their relevance to our cohort. These hubs may be considered in light of previously observed tinnitus-related alterations in the connectivity of attentional (Husain, 2016; Schmidt et al., 2017), emotional-distress (Leaver et al., 2016a; Chen et al., 2017b; Husain, 2016), and temporo-frontal attentional networks (Leaver et al., 2016b; Rauschecker et al., 2015; Schlee et al., 2009; Schmidt et al., 2017; Vanneste and De Ridder, 2012). Indeed, many existing differences in functional connectivity, evoked/ induced haemodynamic responses, or gamma oscillatory power that are specific to the T- and TH-groups may have remained undetected because all the studies mentioned above have not distinguished between tinnitus subtypes and have primarily focused on only a limited number of methods.

### Functional connectivity and fast neural oscillation processes in parietal cortex

The only significant differences displayed on the right hemisphere were found in the lateral inferior parietal cortex (located close to the P4 electrode). This region showed significantly enhanced spontaneous low gamma (**Figure 41A**, (Wertz et al., 2023)), with the largest effect size (d = 1.258) among all the observed ROIs, combined with a substantial haemodynamic oxy-Hb increase in the T- compared to the C- and TH-group (**Figure 41C**, (Wertz et al., 2023)). Yet, no evoked gamma-band group differences were observed in this attention steering area. However, induced gamma oscillations [41-60 Hz] were lower in TH- than in the T-group (**Figure 41B**, (Wertz et al., 2023)), affirming that

the causality of induced gamma may differ from that of evoked gamma in the context of auditory processing. It is important to consider previous research identifying alterations in low brain oscillations within the right parietal cortex. According to (Deng et al., 2019), the right parietal cortex plays a role in top-down control of auditory attention during attention-requiring auditory tasks and can interfere with stimulation patterns of the opposite hemisphere. Furthermore, the P4 electrode also records signals from BA40, a region not only involved in language and classification decisions (Chen et al., 2019) but also plays a role in directing attention in the parietal region and contributing to limbic associational integration (Williams et al., 2000). These changes in brain oscillation and haemodynamic responses observed in the parietal cortex between the T- and TH-group need to be considered in light of previous papers reporting attention issues in tinnitus without subgroups (Roberts et al., 2013; Shore et al., 2016; Sedley, 2019).

In the opposite hemisphere, the left parieto-temporal junction, there was a reduction in rs-fMRI in both the T- and TH-groups (**Figure 37C, 38C**, (Wertz et al., 2023)). This reduction was associated with a differential increase (in mid gamma) and decrease (in low gamma) in spontaneous gamma-band events, as well as an increased evoked gamma power in the TH-group (**Figure 42A**, (Wertz et al., 2023)). Furthermore, the fNIRS oxy- and deoxy-Hb responses in the TH-group indicated increased brain activity (**Figure 42C, D**, (Wertz et al., 2023)). When comparing the observations with the right hemisphere, the complex findings in the extended Wernicke region can be attributed to its various functions, including mostly sound detection and language processing (Ardila et al., 2016). Possibly also to the specific role of BA39 that, if damaged, has been reported to be associated with dyslexia or semantic aphasia (Ardila et al., 2016). In summary, evidence suggests that our TH-subgroup can be distinguished by altered neural processing and impaired cognitive control mechanisms (Seeley et al., 2007; Vincent et al., 2008) in the left parietal cortex, part of the central executive frontoparietal network. Also, the observed increased spontaneous low gamma events expressed on the right side of the parietal cortex (**Figure 41A**, (Wertz et al., 2023)) could map processes that direct attention, converting the accompanying sensory processes into phantom percepts, as proposed by a computational model (Sedley, 2019).

### Functional connectivity and fast neural oscillation processes in left prefrontal cortex

In contrast to the above discussed ROIs, the rs-fMRI connectivity between ventrolateral/ dorsolateral prefrontal areas and the AC displayed more substantial connectivity loss in the TH-group (**Figure 37D, E, 38D, E**, (Wertz et al., 2023)). Also, prior research has

reported alterations in BOLD rs-fMRI function in the ventrolateral prefrontal area of tinnitus patients (Chen et al., 2018; Hussain et al., 2016; Leaver et al., 2016a). Nevertheless, none of these has investigated brain function modifications in a multimodal imaging study or differentiated between tinnitus participants with and without hyperacusis. This may explain some discrepancies in the results compared to previous studies. Additionally, to the reduced rs-fMRI connectivity variations (**Figure 37D**, (Wertz et al., 2023)) in the ventrolateral prefrontal area, we observed increased spontaneous low/mid gamma events (**Figure 43A**, (Wertz et al., 2023)) and reduced fRef-evoked gamma power in the T- compared to the TH-group (**Figure 43B**, (Wertz et al., 2023)). Again, as observed for the left temporal electrode, these findings indicate impaired neuronal synchronisation during active auditory discrimination when stimulated at lower frequency ranges (fRef) in the T- but not in the TH-group. To clarify this difference between tinnitus subgroups in the two-tone discrimination task (which requires attention and accurate recognition of categorical semantic information), it is necessary to briefly review some of the complex functions of the ventrolateral prefrontal cortex. Among other functions, the ventrolateral prefrontal cortex is responsible for sequencing acoustic stimuli (Gelfand and Bookheimer, 2003; Hickok and Poeppel, 2007) and semantic processing (Wagner et al., 2001). Based on our results, the functions of this ROI could imply that the T-group potentially experiences greater difficulty in processing rapid frequency transitions than the TH-group. This could be attributed to their comparatively lower evoked activation in brain regions necessary for efficient phonetic decoding (Gelfand and Bookheimer, 2003). While additional research is required to support this hypothesis, the current finding needs to be discussed regarding speech comprehension difficulties (Vielsmeier et al., 2016; Bures et al., 2019; Sendesen and Turkyilmaz, 2023; Zeng, 2020), impaired intensity discrimination (Epp et al., 2012), and mechanisms of involuntary attention to the tinnitus (Cuny et al., 2004). Furthermore, the differential activation may also relate to the high incidence of depression in tinnitus patients (Pattyn et al., 2016; Durai et al., 2019; Hebert, 2021) since several studies have shown that the BA46 and BA45 regions, as part of the ventrolateral PFC, are deactivated and functionally disconnected in tinnitus patients with a comorbid depressive disorder (Pizzagalli and Roberts, 2022).

Along with the described reduced rs-fMRI connectivity between AC and dorsolateral PFC in the TH-group (**Figure 37D, E**, (Wertz et al., 2023)), we observed decreased spontaneous high/low gamma events and a trend for increased evoked high gamma also confined to the left dorsolateral PFC of the TH-group (**Figure 44A, B**, (Wertz et al., 2023)). However, separating the rs-fMRI correlations between AC to BA9DL and BA9M (**Figure 38F, G**, (Wertz et al., 2023)) reveals that the decreased connectivity is confined to BA9DL, whereas the connectivity to BA9M appears to be increased in the TH-group. The reduced

spontaneous and enhanced evoked high gamma power is probably related to BA9M rather than BA9DL, but our current electrode array does not allow spatial differentiation at such a high resolution. This may redefine the accepted role of PFC region BA9 in distress regulation (Lai et al., 2019; Li et al., 2022a; Jacobs and Moghaddam, 2021; Kupferschmidt et al., 2022), implying positive regulation of BA9DL for stress balancing (Sullivan and Gratton, 2002) and BA9M for stress excitation (McKlveen et al., 2016; McKlveen et al., 2013; Utevsky and Platt, 2014).

In previous literature, the correlation strength of the frontoparietal executive resting-state network, involved in allocating top-down attentional resources (Fassbender et al., 2006), is reduced in tinnitus (Zhou et al., 2019; Kandeepan et al., 2019), especially with increased tinnitus distress (Kandeepan et al., 2019). Although the obtained results in both frontoparietal executive network regions (parietal P3 and frontal F3) brain regions are highly complex, high and low gamma events during resting EEG tend to be reduced in the TH-group. These findings indicate that the TH-group experiences an impaired cognitive control mechanism, apparent not only during rest but also in auditory tasks within the individual tinnitus frequency range. This again emphasises the importance of considering both resting-state and task-evoked conditions to comprehend the neural correlates of hyperacusis in tinnitus.

## 4.4. Conclusion

In summary, the results confirm our assumption that it is of utmost importance for the understanding and subsequent cure of tinnitus to consider each tinnitus patient individually. Although individual methods are not yet sufficient to identify the neural biomarkers underlying tinnitus and its sub-entities, we have been able to demonstrate accurately distinguishable biomarkers for the tinnitus subgroups, i.e. tinnitus duration, but more importantly, the presence of the common comorbidity of hyperacusis. We observed differential responses in auditory processing, cortical brain activity, and attentional/emotional circuits:

On the one hand, tinnitus patients without hyperacusis (T) exhibit delayed and reduced ABR wave responses, reduced evoked BOLD fMRI responses in auditory-associated regions, particularly in response to high-frequency stimuli, and a reduced frequency of positive correlations between them. On the other hand, tinnitus patients with co-occurring hyperacusis (TH) can best be distinguished through less reduced ABR wave V responses, enhanced evoked BOLD fMRI activity in, i.e., MGB, AC, hippocampus, and posterior Insula in response to low-frequency stimuli, and less reduced frequency of positive resting-state correlations in ascending cortical and subcortical auditory and associated regions (**Figure 22**, (Hofmeier et al., 2021); **Figure 45**, (Wertz et al., 2023)). In contrast to the T-group, which tended to exhibit differences in brain oscillations in the AC and Broca's area, the TH-group revealed differences in the left temporo-parietal and dorsolateral PFC, which might be related to arousal spread to limbic and pain/distress processing regions of the neocortex. In accordance with prior hypotheses (Knipper et al., 2020; Knudson et al., 2014; Sturm and Weisz, 2015; Sedley, 2019; Zeng, 2020), this could lead to an inadequately high attention to acoustic stimulation at all frequencies. These findings support the existence of distinct neural correlates for tinnitus and hyperacusis, emphasising the need for a sub-entity-specific differential diagnosis through a combination of psychometric tests, fine-structured audiometry, tinnitus pitch/loudness assessment, and an examination of the haemodynamic/ electrical activity of the brain. The insights gained here underscore the importance of revising current medical practices for tinnitus diagnosis and treatment, with the potential for personalised therapeutic interventions for both tinnitus with and without hyperacusis.

# 5. Summary

## 5.1. English Version

Tinnitus is a common condition caused by a dysfunction of the auditory system. The development of effective therapeutic interventions for tinnitus is challenging due to debate regarding its causative neural mechanisms. In Europe, approximately one in seven adults (14.7 %) report tinnitus symptoms (Biswas et al., 2022), resulting in significant personal distress and substantial socioeconomic costs. This thesis aimed to address the possible contribution of co-occurring hyperacusis as well as the tinnitus duration to the underlying neural mechanisms of tinnitus.

Three comprehensive studies were conducted with a total of 128 subjects: 45 tinnitus patients without hyperacusis (T-group), 26 tinnitus patients with hyperacusis (TH-group), and a control group of 57 subjects. In order to ensure the reliability of our findings, we adopted a multimodal approach to detect and exclude unwanted comorbidities. The multidimensional approach integrated questionnaire evaluations (Goebel-Hiller-Score and Hyperakusis-Inventar), audiological diagnostics (e.g., pure tone audiometry, speech audiometry, uncomfortable loudness level, tinnitus localisation, and supra-threshold auditory brainstem response (ABR)). Furthermore, I evaluated changes in neural activity using cortical haemodynamic responses (functional near-infrared spectroscopy (fNIRS) and blood oxygenation level-dependent (BOLD) functional magnetic resonance imaging (fMRI)) and electric potentials (electroencephalography (EEG)) in anatomically predefined brain regions.

The results distinguish or allow for differentiation between patients with recent onset of tinnitus and those with chronic tinnitus: TH patients reported higher levels of distress and annoyance from the beginning, with an increased tinnitus loudness in patients with long-term tinnitus, while in the T-group, the tinnitus loudness declined over time. In addition, the T-group experienced a shift from primarily unilateral (83 %) to utterly bilateral tinnitus percept, whereas the TH-group had bilateral tinnitus from early on (75 % bilateral). Moreover, the findings revealed distinct patterns emerging among tinnitus patients with and without hyperacusis, both at rest and in response to acoustic stimuli. Although no differences were observed in pure tone audiometry, the hearing threshold in the range of the individual tinnitus frequency correlated positively with the tinnitus loudness and distress in the T-group, whereas the TH-group experienced maximal distress levels already at minimal tinnitus loudness. The T-group exhibited delayed and reduced ABR

wave responses, diminished frequency of positive resting-state correlations and reduced evoked BOLD fMRI responses of auditory-associated regions, particularly in response to high-frequency stimuli. Conversely, the TH-group was distinguished based on less reduced ABR wave V responses, less reduced frequency of positive resting-state correlations in ascending (sub-) cortical auditory-associated regions, and enhanced BOLD fMRI responses of the thalamus, auditory cortex, hippocampus, and posterior insula, particularly in response to low-frequency stimuli. In addition to the group differences in slow cortical haemodynamic responses described above, the T-group exhibited increased spontaneous and reduced 1 kHz stimulus-evoked fast gamma-band oscillations in the Auditory Cortex and Broca's area. In contrast, the TH-group was characterised by distinctions in the left temporo-parietal and dorsolateral PFC, potentially associated with excessive auditory arousal spreading to attention and pain networks. In summary, these results support the tinnitus theory of reduced auditory responsiveness, best explained by hyperexcitability through the loss of tonic parvalbumin (PV) inhibitory interneurons in deprived regions due to the critical loss of high spontaneous firing rate fibres in the Organ of Corti. This interpretation would be consistent with the observed elevation in spontaneous gamma activity within the auditory cortex of the T-group, which could be attributed to the loss of tonic inhibition of pyramidal neurons through PV interneurons.

The present findings provide evidence for distinct neural correlates of tinnitus and tinnitus with co-occurring hyperacusis, emphasising the need for a sub-entity-specific differential diagnosis in therapy and research, as hyperacusis is one of the main causes of distress and tinnitus complaints over time. Furthermore, the identified characteristic neuronal profiles provide valuable functional biomarkers for the follow-up of therapeutic trials and should guide medical tinnitus practice towards personalised curative therapies.

## 5.2. German Version

Tinnitus, ein weitverbreitetes Symptom, das durch eine Fehlfunktion des auditorischen Systems verursacht wird, stellt aufgrund der anhaltenden Debatte über die ursächlichen neuronalen Korrelate eine große Herausforderung für die Entwicklung wirksamer therapeutischer Maßnahmen dar. In Europa leidet etwa jeder siebte Erwachsene (14,7 %) an Tinnitus-Symptomen (Biswas et al., 2022), wodurch ein erheblicher persönlicher Leidensdruck und umfangreiche sozioökonomische Kosten entstehen. Ziel dieser Arbeit war es, den möglichen Einfluss der Dauer des Tinnitus und der Komorbidität von Hyperakusis auf die zugrunde liegenden neuronalen Mechanismen des Tinnitus zu untersuchen.

Wir haben drei umfassende Studien mit insgesamt 128 Probanden durchgeführt: 45 Tinnitus-Patienten ohne Hyperakusis (T-Gruppe), 26 Tinnitus-Patienten mit Hyperakusis (TH-Gruppe) und 57 Kontrollprobanden. Um die Reliabilität unserer Befunde zu verbessern, haben wir einen multimodalen Ansatz zur Erkennung und zum Ausschluss unerwünschter Komorbiditäten verfolgt. Der multidimensionale Forschungsansatz umfasste die Auswertung von Fragebögen (Goebel-Hiller-Score und Hyperakusis-Inventar), audiologische Diagnostik (u. a. Reintonaudiometrie, Sprachaudiometrie, Unbehaglichkeitslautstärke, Tinnitus-Lokalisation und überschwellige Hirnstamm-audiometrie. Darüber hinaus bewerten wir Veränderungen der neuronalen Aktivität mit Hilfe von kortikalen hämodynamischen Reaktionen (funktionelle Nahinfrarotspektroskopie (fNIRS) und funktionelle Magnetresonanztomographie (fMRT)) und elektrischen Potenzialen (Elektroenzephalographie (EEG)).

Die Ergebnisse deuten auf vielversprechende Unterschiede zwischen Patienten mit akutem Tinnitus und solchen mit chronischem Tinnitus hin: Die TH-Patienten berichteten von Beginn an über einen starken Tinnitus Leidensdruck, gepaart mit einer erhöhten Tinnitus-Lautstärke bei Patienten mit chronischem Tinnitus, während Individuen der T-Gruppe mit längerer Tinnitus Dauer die Lautstärke als leiser empfanden. Parallel kam es in der T-Gruppe zu einer Verschiebung von einer primär unilateralen (83 %) zu einer hauptsächlich bilateralen Tinnitus Wahrnehmung, während in der TH-Gruppe von Anfang an bilateraler Tinnitus dominierte (75 % bilateral). Darüber hinaus enthüllen die Befunde unterschiedliche Muster zwischen Tinnitus-Patienten mit und ohne Hyperakusis, sowohl in Ruhe als auch als Reaktion auf akustische Reize. Obwohl bei der Reintonaudiometrie keine Unterschiede festgestellt werden konnten, korrelierte in der T-Gruppe die Hörschwelle im Bereich der individuellen Tinnitus-Frequenz positiv mit der Tinnitus-Lautstärke und dem Leidensdruck. In der TH-Gruppe hingegen wurde der maximale

Leidensdruck bereits bei minimaler Tinnitus-Lautstärke empfunden. Die T-Gruppe zeigte verzögerte und verringerte ABR-Wellen, eine verringerte Frequenz positiver Korrelationen im Ruhezustand und verringerte evozierte fMRI BOLD-Kontraste in auditiv assoziierten Regionen, insbesondere als Reaktion auf hochfrequente Stimuli. Im Gegensatz dazu unterschieden wir die TH-Gruppe anhand von weniger reduzierten ABR-Welle V Amplituden, einer weniger reduzierten Frequenz positiver Ruhezustands-Korrelationen in aufsteigenden (sub-) kortikalen auditiv-assoziierten Regionen und einen erhöhten fMRI BOLD-Kontrast in z. B. Thalamus, auditorischem Kortex, Hippocampus und posteriorer Insula, insbesondere als Reaktion auf niederfrequente Stimuli. Zusätzlich zu den oben beschriebenen Gruppenunterschieden langsamer kortikaler hämodynamischen Antworten wies die T-Gruppe erhöhte spontane und reduzierte evozierte schnelle Gamma-Band-Oszillationen als Antwort auf 1 kHz Stimuli im auditorischen Kortex und im Broca-Areal auf. Im Gegensatz dazu war die TH-Gruppe durch Differenzen im linken temporo-parietalen und dorsolateralen präfrontalen Kortex gekennzeichnet, möglicherweise assoziiert mit übermäßiger auditiver Erregung, die sich auf Aufmerksamkeits- und Schmerznetzwerke ausbreitet. Zusammenfassend unterstützen die Befunde die Tinnitus-Theorie einer verminderten auditorischen Reaktionsfähigkeit, die sich am besten durch eine Übererregbarkeit aufgrund des Verlusts tonischer hemmender Parvalbumin-(PV)-Interneuronen in beeinträchtigten Regionen infolge des kritischen Verlusts von Fasern mit hoher Spontanfeuerungsrate im Corti-Organ erklären lässt. Diese Interpretation steht im Einklang mit der beobachteten Erhöhung der spontanen Gamma-Aktivität im auditorischen Kortex der T-Gruppe, die durch den Verlust der tonischen Hemmung der Pyramidenneuronen mittels PV-Interneuronen begründet werden könnte.

Die vorliegenden Ergebnisse deuten auf unterschiedliche neuronale Korrelate für Tinnitus und Tinnitus mit koinzidenter Hyperakusis hin und unterstreichen die Notwendigkeit einer sub-entitätsspezifischen Differenzialdiagnose in Therapie und Forschung, da Hyperakusis ein Hauptfaktor für Tinnitus Beschwerden im zeitlichen Verlauf ist. Darüber hinaus liefern die identifizierten charakteristischen neuronalen Profile wertvolle funktionelle Biomarker für die Begleitung von Therapieversuchen und sollten die medizinische Tinnitus-Praxis in Richtung personalisierter Heilungstherapien lenken.

# 6. REFERENCES


AAZH, H., LANDGREBE, M., DANESH, A. A. & MOORE, B. C. 2019. Cognitive Behavioral Therapy For Alleviating The Distress Caused By Tinnitus, Hyperacusis And Misophonia: Current Perspectives. *Psychol Res Behav Manag,* 12**,** 991-1002.

AAZH, H., MCFERRAN, D., SALVI, R., PRASHER, D., JASTREBOFF, M. & JASTREBOFF, P. 2014. Insights from the First International Conference on Hyperacusis: causes, evaluation, diagnosis and treatment. *Noise Health,* 16**,** 123-6.

AMUNTS, K., MOHLBERG, H., BLUDAU, S., CASPERS, S., EICKHOFF, S. B. & PIEPERHOFF, P. 2020a. Whole-brain parcellation of the Julich-Brain Cytoarchitectonic Atlas *In:* EBRAINS (ed.) 2.0 ed.

AMUNTS, K., MOHLBERG, H., BLUDAU, S. & ZILLES, K. 2020b. Julich-Brain: A 3D probabilistic atlas of the human brain's cytoarchitecture. *Science,* 369**,** 988-992.

ANDERSON, S., PARBERY-CLARK, A., WHITE-SCHWOCH, T. & KRAUS, N. 2012. Aging affects neural precision of speech encoding. *J Neurosci,* 32**,** 14156-64.

ARDILA, A., BERNAL, B. & ROSSELLI, M. 2016. How Extended Is Wernicke's Area? Meta-Analytic Connectivity Study of BA20 and Integrative Proposal. *Neurosci J,* 2016**,** 4962562.

ARDILA, A., BERNAL, B. & ROSSELLI, M. 2017. Should Broca's area include Brodmann area 47? *Psicothema,* 29**,** 73-77.

BAGULEY, D., MCFERRAN, D. & HALL, D. 2013. Tinnitus. *Lancet,* 382**,** 1600-7.

BAGULEY, D. M. 2003. Hyperacusis. *J R Soc Med,* 96**,** 582-5.

BAUER, C. A., BROZOSKI, T. J. & MYERS, K. 2007. Primary afferent dendrite degeneration as a cause of tinnitus. *J Neurosci Res,* 85**,** 1489-98.

BEEBE PALUMBO, D., JOOS, K., DE RIDDER, D. & VANNESTE, S. 2015. The Management and Outcomes of Pharmacological Treatments for Tinnitus. *Curr Neuropharmacol,* 13**,** 692-700.

BERLOT, E., ARTS, R., SMIT, J., GEORGE, E., GULBAN, O. F., MOEREL, M., STOKROOS, R., FORMISANO, E. & DE MARTINO, F. 2020. A 7 Tesla fMRI investigation of human tinnitus percept in cortical and subcortical auditory areas. *Neuroimage Clin,* 25**,** 102166.

BERTHOLD-SCHOLZ, A. 2013. *Validierung von Selbsteinschätzungsinstrumenten (GÜF, Nelting und Finlayson, 2004 und HQ, Khalfa et al., 2002) in der Diagnostik der Geräuschüberempfindlichkeit - Entwicklung eines Hyperakusis-Inventar (HKI) zur Fremd- und Selbsteinschätzung.* Doktor der Medizin, Technischen Universität München.

BISWAS, R., GENITSARIDI, E., TRPCHEVSKA, N., LUGO, A., SCHLEE, W., CEDERROTH, C. R., GALLUS, S. & HALL, D. A. 2023. Low Evidence for Tinnitus Risk Factors: A Systematic Review and Meta-analysis. *J Assoc Res Otolaryngol,* 24**,** 81-94.

BISWAS, R., LUGO, A., AKEROYD, M. A., SCHLEE, W., GALLUS, S. & HALL, D. A. 2022. Tinnitus prevalence in Europe: a multi-country cross-sectional population study. *Lancet Reg Health Eur,* 12**,** 100250.

BOURIEN, J., TANG, Y., BATREL, C., HUET, A., LENOIR, M., LADRECH, S., DESMADRYL, G., NOUVIAN, R., PUEL, J. L. & WANG, J. 2014. Contribution of auditory nerve fibers to compound action potential of the auditory nerve. *J Neurophysiol,* 112**,** 1025-39.

BOYEN, K., DE KLEINE, E., VAN DIJK, P. & LANGERS, D. R. 2014. Tinnitus-related dissociation between cortical and subcortical neural activity in humans with mild to moderate sensorineural hearing loss. *Hear Res,* 312**,** 48-59.

BUBB, E. J., KINNAVANE, L. & AGGLETON, J. P. 2017. Hippocampal - diencephalic - cingulate networks for memory and emotion: An anatomical guide. *Brain Neurosci Adv,* 1.

BURES, Z., PROFANT, O., SVOBODOVA, V., TOTHOVA, D., VENCOVSKY, V. & SYKA, J. 2019. Speech Comprehension and Its Relation to Other Auditory Parameters in Elderly Patients With Tinnitus. *Front Aging Neurosci,* 11**,** 219.

CAI, S., MA, W. L. & YOUNG, E. D. 2009. Encoding intensity in ventral cochlear nucleus following acoustic trauma: implications for loudness recruitment. *J Assoc Res Otolaryngol,* 10**,** 5-22.

CARDIN, J. A., CARLEN, M., MELETIS, K., KNOBLICH, U., ZHANG, F., DEISSEROTH, K., TSAI, L. H. & MOORE, C. I. 2009. Driving fast-spiking cells induces gamma rhythm and controls sensory responses. *Nature,* 459**,** 663-7.

CEDERROTH, C. R., DYHRFJELD-JOHNSEN, J. & LANGGUTH, B. 2018. An update: emerging drugs for tinnitus. *Expert Opin Emerg Drugs,* 23**,** 251-260.

CHEN, G., ZHANG, Y., LI, X., ZHAO, X., YE, Q., LIN, Y., TAO, H. W., RASCH, M. J. & ZHANG, X. 2017a. Distinct Inhibitory Circuits Orchestrate Cortical beta and gamma Band Oscillations. *Neuron,* 96**,** 1403-1418 e6.

CHEN, H., PAN, X., BICKERTON, W. L., LAU, J. K., ZHOU, J., ZHOU, B., HARRIS, L. & ROTSHTEIN, P. 2019. Delineating the cognitive-neural substrates of writing: a large scale behavioral and voxel based morphometry study. *Sci Rep,* 9**,** 18881.

CHEN, Y. C., CHEN, H., BO, F., XU, J. J., DENG, Y., LV, H., CAI, Y., XIA, W., YIN, X., GU, J. P. & LU, G. 2018. Tinnitus distress is associated with enhanced resting-state functional connectivity within the default mode network. *Neuropsychiatr Dis Treat,* 14**,** 1919-1927.

CHEN, Y. C., XIA, W., CHEN, H., FENG, Y., XU, J. J., GU, J. P., SALVI, R. & YIN, X. 2017b. Tinnitus distress is linked to enhanced resting-state functional connectivity from the limbic system to the auditory cortex. *Hum Brain Mapp,* 38**,** 2384-2397.

CIESLIK, E. C., MUELLER, V. I., EICKHOFF, C. R., LANGNER, R. & EICKHOFF, S. B. 2015. Three key regions for supervisory attentional control: evidence from neuroimaging meta-analyses. *Neurosci Biobehav Rev,* 48**,** 22-34.

CLINARD, C. G., TREMBLAY, K. L. & KRISHNAN, A. R. 2010. Aging alters the perception and physiological representation of frequency: evidence from human frequency-following response recordings. *Hear Res,* 264**,** 48-55.

CONLON, B., HAMILTON, C., HUGHES, S., MEADE, E., HALL, D. A., VANNESTE, S., LANGGUTH, B. & LIM, H. H. 2019. Noninvasive Bimodal Neuromodulation for the Treatment of Tinnitus: Protocol for a Second Large-Scale Double-Blind Randomized Clinical Trial to Optimize Stimulation Parameters. *JMIR Res Protoc,* 8**,** e13176.

CONLON, B., LANGGUTH, B., HAMILTON, C., HUGHES, S., MEADE, E., CONNOR, C. O., SCHECKLMANN, M., HALL, D. A., VANNESTE, S., LEONG, S. L., SUBRAMANIAM, T., D'ARCY, S. & LIM, H. H. 2020. Bimodal neuromodulation combining sound and tongue

stimulation reduces tinnitus symptoms in a large randomized clinical study. *Sci Transl Med,* 12.

COSLETT, H. B. & SCHWARTZ, M. F. 2018. The parietal lobe and language. *Handb Clin Neurol,* 151**,** 365-375.

CUNY, C., NORENA, A., EL MASSIOUI, F. & CHERY-CROZE, S. 2004. Reduced attention shift in response to auditory changes in subjects with tinnitus. *Audiol Neurootol,* 9**,** 294-302.

DALLOS, P. & HARRIS, D. 1978. Properties of auditory nerve responses in absence of outer hair cells. *J Neurophysiol,* 41**,** 365-83.

DARROW, K. N., BENSON, T. E. & BROWN, M. C. 2012. Planar multipolar cells in the cochlear nucleus project to medial olivocochlear neurons in mouse. *J Comp Neurol,* 520**,** 1365-75.

DE CHEVEIGNE, A. & ARZOUNIAN, D. 2018. Robust detrending, rereferencing, outlier detection, and inpainting for multichannel data. *Neuroimage,* 172**,** 903-912.

DE RIDDER, D., VANNESTE, S., LANGGUTH, B. & LLINAS, R. 2015. Thalamocortical Dysrhythmia: A Theoretical Update in Tinnitus. *Front Neurol,* 6**,** 124.

DELORME, A. & MAKEIG, S. 2004. EEGLAB: an open source toolbox for analysis of single-trial EEG dynamics including independent component analysis. *J Neurosci Methods,* 134**,** 9-21.

DENG, Y., REINHART, R. M., CHOI, I. & SHINN-CUNNINGHAM, B. G. 2019. Causal links between parietal alpha activity and spatial auditory attention. *Elife,* 8.

DEWEY, J. B. & DHAR, S. 2017. Profiles of Stimulus-Frequency Otoacoustic Emissions from 0.5 to 20 kHz in Humans. *J Assoc Res Otolaryngol,* 18**,** 89-110.

DUGUID, I., BRANCO, T., LONDON, M., CHADDERTON, P. & HAUSSER, M. 2012. Tonic inhibition enhances fidelity of sensory information transmission in the cerebellar cortex. *J. Neurosci.,* 32**,** 11132-43.

DURAI, M., SANDERS, M., KOBAYASHI, K. & SEARCHFIELD, G. D. 2019. Auditory Streaming and Prediction in Tinnitus Sufferers. *Ear Hear,* 40**,** 345-357.

EGGERMONT, J. J. & TASS, P. A. 2015. Maladaptive neural synchrony in tinnitus: origin and restoration. *Front Neurol,* 6**,** 29.

ENCINA-LLAMAS, G., HARTE, J. M., DAU, T., SHINN-CUNNINGHAM, B. & EPP, B. 2019. Investigating the Effect of Cochlear Synaptopathy on Envelope Following Responses Using a Model of the Auditory Nerve. *J Assoc Res Otolaryngol,* 20**,** 363-382.

EPP, B., HOTS, J., VERHEY, J. L. & SCHAETTE, R. 2012. Increased intensity discrimination thresholds in tinnitus subjects with a normal audiogram. *J Acoust Soc Am,* 132**,** EL196-201.

FASSBENDER, C., SIMOES-FRANKLIN, C., MURPHY, K., HESTER, R., MEANEY, J., ROBERTSON, I. H. & GARAVAN, H. 2006. The Role of a Right Fronto-Parietal Network in Cognitive Control. *Journal of Psychophysiology,* 20.

FELDMANN, H. 1971. Homolateral and contralateral masking of tinnitus by noise-bands and by pure tones. *Audiology,* 10**,** 138-44.

FISCHER, A. 2013. Hyperakusis: Neues Screening-Instrument vorgestellt. *HNO Nachrichten,* 43**,** 38-38.

FISHBURN, F. A., LUDLUM, R. S., VAIDYA, C. J. & MEDVEDEV, A. V. 2019. Temporal Derivative Distribution Repair (TDDR): A motion correction method for fNIRS. *Neuroimage,* 184**,** 171-179.

FLORES, E. N., DUGGAN, A., MADATHANY, T., HOGAN, A. K., MARQUEZ, F. G., KUMAR, G., SEAL, R. P., EDWARDS, R. H., LIBERMAN, M. C. & GARCIA-ANOVEROS, J. 2015. A non-canonical pathway from cochlea to brain signals tissue-damaging noise. *Curr Biol,* 25**,** 606-12.

FLORIN, E., WATANABE, M. & LOGOTHETIS, N. K. 2015. The role of sub-second neural events in spontaneous brain activity. *Curr Opin Neurobiol,* 32**,** 24-30.

GARCIA-LARREA, L. & PEYRON, R. 2013. Pain matrices and neuropathic pain matrices: a review. *Pain,* 154 Suppl 1**,** S29-43.

GATES, G. A. & MILLS, J. H. 2005. Presbycusis. *Lancet,* 366**,** 1111-20.

GELFAND, J. R. & BOOKHEIMER, S. Y. 2003. Dissociating neural mechanisms of temporal sequencing and processing phonemes. *Neuron,* 38**,** 831-42.

GEVEN, L. I., DE KLEINE, E., FREE, R. H. & VAN DIJK, P. 2011. Contralateral suppression of otoacoustic emissions in tinnitus patients. *Otol Neurotol,* 32**,** 315-21.

GILLES, A., GOELEN, S. & VAN DE HEYNING, P. 2014. Tinnitus: a cross-sectional study on the audiologic characteristics. *Otol Neurotol,* 35**,** 401-6.

GILLES, A., SCHLEE, W., RABAU, S., WOUTERS, K., FRANSEN, E. & VAN DE HEYNING, P. 2016. Decreased Speech-In-Noise Understanding in Young Adults with Tinnitus. *Front Neurosci,* 10**,** 288.

GOEBEL, G. & HILLER, W. 1994. [The tinnitus questionnaire. A standard instrument for grading the degree of tinnitus. Results of a multicenter study with the tinnitus questionnaire]. *HNO,* 42**,** 166-72.

GOELMAN, G., GORDON, N. & BONNE, O. 2014. Maximizing negative correlations in resting-state functional connectivity MRI by time-lag. *PLoS One,* 9**,** e111554.

GOLDSTEIN, B. & SHULMAN, A. 1996. Tinnitus - Hyperacusis and the Loudness Discomfort Level Test - A Preliminary Report. *Int Tinnitus J,* 2**,** 83-89.

GROSSMANN, A. & MORLET, J. 1984. Decomposition of Hardy Functions into Square Integrable Wavelets of Constant Shape. *SIAM Journal on Mathematical Analysis,* 15.

GU, J. W., HALPIN, C. F., NAM, E. C., LEVINE, R. A. & MELCHER, J. R. 2010. Tinnitus, diminished sound-level tolerance, and elevated auditory activity in humans with clinically normal hearing sensitivity. *J Neurophysiol,* 104**,** 3361-70.

GUEST, H., MUNRO, K. J., PRENDERGAST, G., HOWE, S. & PLACK, C. J. 2017. Tinnitus with a normal audiogram: Relation to noise exposure but no evidence for cochlear synaptopathy. *Hear Res,* 344**,** 265-274.

GUIMARAES, A. R., MELCHER, J. R., TALAVAGE, T. M., BAKER, J. R., LEDDEN, P., ROSEN, B. R., KIANG, N. Y., FULLERTON, B. C. & WEISSKOFF, R. M. 1998. Imaging subcortical auditory activity in humans. *Hum Brain Mapp,* 6**,** 33-41.

HAAG, L. M., HEBA, S., LENZ, M., GLAUBITZ, B., HOFFKEN, O., KALISCH, T., PUTS, N. A., EDDEN, R. A., TEGENTHOFF, M., DINSE, H. & SCHMIDT-WILCKE, T. 2015. Resting BOLD

fluctuations in the primary somatosensory cortex correlate with tactile acuity. *Cortex,* 64**,** 20-8.

HAIDER, H. F., BOJIC, T., RIBEIRO, S. F., PACO, J., HALL, D. A. & SZCZEPEK, A. J. 2018. Pathophysiology of Subjective Tinnitus: Triggers and Maintenance. *Front Neurosci,* 12**,** 866.

HAN, J. J., JANG, J. H., RIDDER, D., VANNESTE, S., KOO, J. W. & SONG, J. J. 2018. Increased parietal circuit-breaker activity in delta frequency band and abnormal delta/theta band connectivity in salience network in hyperacusis subjects. *PLoS One,* 13**,** e0191858.

HE, D. Z., EVANS, B. N. & DALLOS, P. 1994. First appearance and development of electromotility in neonatal gerbil outer hair cells. *Hear Res,* 78**,** 77-90.

HEBERT, S. 2021. Psychological Comorbidities of Tinnitus. *Curr Top Behav Neurosci,* 51**,** 349-359.

HEBERT, S., FOURNIER, P. & NORENA, A. 2013. The auditory sensitivity is increased in tinnitus ears. *J Neurosci,* 33**,** 2356-64.

HEIL, P., NEUBAUER, H., BROWN, M. & IRVINE, D. R. 2008. Towards a unifying basis of auditory thresholds: distributions of the first-spike latencies of auditory-nerve fibers. *Hear Res,* 238**,** 25-38.

HESSE, G., KASTELLIS, G. & MAZUREK, B. 2022. S3-Leitlinie zu chronischem Tinnitus überarbeitet: Was derzeit zu Diagnostik und Therapie empfohlen wird und was nicht (S3 guideline on chronic tinnitus revised: What is currently recommended for diagnosis and therapy and what is not). *HNO Nachr,* 52**,** 32-37.

HICKOK, G. & POEPPEL, D. 2007. The cortical organization of speech processing. *Nat Rev Neurosci,* 8**,** 393-402.

HOFMEIER, B., WERTZ, J., REFAT, F., HINRICHS, P., SAEMISCH, J., SINGER, W., RUTTIGER, L., KLOSE, U., KNIPPER, M. & WOLPERT, S. 2021. Functional biomarkers that distinguish between tinnitus with and without hyperacusis. *Clin Transl Med,* 11**,** e378.

HOFMEIER, B., WOLPERT, S., ALDAMER, E. S., WALTER, M., THIERICKE, J., BRAUN, C., ZELLE, D., RUTTIGER, L., KLOSE, U. & KNIPPER, M. 2018. Reduced sound-evoked and resting-state BOLD fMRI connectivity in tinnitus. *Neuroimage Clin,* 20**,** 637-649.

HORING, B., SPRENGER, C. & BUCHEL, C. 2019. The parietal operculum preferentially encodes heat pain and not salience. *PLoS Biol,* 17**,** e3000205.

HÖRTECHGGMBH 2012. *Oldenburger Satztest. Handbuch und Hintergrundwissen,* Oldenburg.

HOTH, S. 2016. Der Freiburger Sprachtest. *HNO,* 540–548.

HSIEH, T. H., LEE, H. H. C., HAMEED, M. Q., PASCUAL-LEONE, A., HENSCH, T. K. & ROTENBERG, A. 2017. Trajectory of Parvalbumin Cell Impairment and Loss of Cortical Inhibition in Traumatic Brain Injury. *Cereb Cortex,* 27**,** 5509-5524.

HUET, A., BATREL, C., WANG, J., DESMADRYL, G., NOUVIAN, R., PUEL, J. L. & BOURIEN, J. 2019. Sound Coding in the Auditory Nerve: From Single Fiber Activity to Cochlear Mass Potentials in Gerbils. *Neuroscience,* 407**,** 83-92.

HULLFISH, J., ABENES, I., KOVACS, S., SUNAERT, S., DE RIDDER, D. & VANNESTE, S. 2018. Functional brain changes in auditory phantom perception evoked by different stimulus frequencies. *Neurosci Lett,* 683**,** 160-167.

HUSAIN, F. T. 2016. Neural networks of tinnitus in humans: Elucidating severity and habituation. *Hear Res,* 334**,** 37-48.

HUSAIN, F. T. & SCHMIDT, S. A. 2014. Using resting state functional connectivity to unravel networks of tinnitus. *Hear Res,* 307**,** 153-62.

HUSSAIN, R., O'LEARY, S., PACHECO, F. M., ZACHARIAS, T. E., LITVAK, P., SGUIGNA, P., MARDER, E., KIA, K., KOONER, K. & STUVE, O. 2016. Acute relapse after initiation of Siponimod in a patient with secondary progressive MS. *J Neurol,* 263**,** 606-10.

HYVARINEN, A. & OJA, E. 2000. Independent component analysis: algorithms and applications. *Neural Netw,* 13**,** 411-30.

IBARRA CHAOUL, A. & SIEGEL, M. 2021. Cortical correlation structure of aperiodic neuronal population activity. *Neuroimage,* 245**,** 118672.

JACOBS, D. S. & MOGHADDAM, B. 2021. Medial prefrontal cortex encoding of stress and anxiety. *Int Rev Neurobiol,* 158**,** 29-55.

JAFARI, Z., BAGULEY, D., KOLB, B. E. & MOHAJERANI, M. H. 2022. A Systematic Review and Meta-Analysis of Extended High-Frequency Hearing Thresholds in Tinnitus With a Normal Audiogram. *Ear Hear,* 43**,** 1643-1652.

JASPER, H. H. 1958. Report of the committee on methods of clinical examination in electroencephalography. *Electroencephalography and Clinical Neurophysiology,* 10**,** 370-375.

JASTREBOFF, P. J. & JASTREBOFF, M. M. 2015. Decreased sound tolerance: hyperacusis, misophonia, diplacousis, and polyacousis. *Handb Clin Neurol,* 129**,** 375-87.

JASTREBOFF, P. J. & JASTREBOFF, M. M. 2023. The neurophysiological approach to misophonia: Theory and treatment. *Front Neurosci,* 17**,** 895574.

JIANG, J., WANG, G. Y., LUO, W., XIE, H. & GUAN, J. S. 2018. Mammillary body regulates state-dependent fear by alternating cortical oscillations. *Sci Rep,* 8**,** 13471.

JOHNSON, D. H. & KIANG, N. Y. 1976. Analysis of discharges recorded simultaneously from pairs of auditory nerve fibers. *Biophys J,* 16**,** 719-34.

JOO, J. W., JEONG, Y. J., HAN, M. S., CHANG, Y. S., RAH, Y. C. & CHOI, J. 2020. Analysis of Auditory Brainstem Response Change, according to Tinnitus Duration, in Patients with Tinnitus with Normal Hearing. *J Int Adv Otol,* 16**,** 190-196.

JOSEPHS, O., TURNER, R. & FRISTON, K. 1997. Event-related f MRI. *Hum Brain Mapp,* 5**,** 243-8.

KANDEEPAN, S., MAUDOUX, A., RIBEIRO DE PAULA, D., ZHENG, J. Y., CABAY, J. E., GOMEZ, F., CHRONIK, B. A., RIDDER, D., VANNESTE, S. & SODDU, A. 2019. Tinnitus distress: a paradoxical attention to the sound? *J Neurol,* 266**,** 2197-2207.

KHALFA, S., DUBAL, S., VEUILLET, E., PEREZ-DIAZ, F., JOUVENT, R. & COLLET, L. 2002. Psychometric normalization of a hyperacusis questionnaire. *ORL J Otorhinolaryngol Relat Spec,* 64**,** 436-42.

KIM, D. K., PARK, S. N., KIM, H. M., SON, H. R., KIM, N. G., PARK, K. H. & YEO, S. W. 2011. Prevalence and significance of high-frequency hearing loss in subjectively normal-hearing patients with tinnitus. *Ann Otol Rhinol Laryngol,* 120**,** 523-8.

KIM, H., AHRLUND-RICHTER, S., WANG, X., DEISSEROTH, K. & CARLEN, M. 2016. Prefrontal Parvalbumin Neurons in Control of Attention. *Cell,* 164**,** 208-218.

KIM, H. J., LEE, H. J., AN, S. Y., SIM, S., PARK, B., KIM, S. W., LEE, J. S., HONG, S. K. & CHOI, H. G. 2015. Analysis of the prevalence and associated risk factors of tinnitus in adults. *PLoS One,* 10**,** e0127578.

KIM, J. Y., KIM, Y. H., LEE, S., SEO, J. H., SONG, H. J., CHO, J. H. & CHANG, Y. 2012. Alteration of functional connectivity in tinnitus brain revealed by resting-state fMRI? A pilot study. *Int J Audiol,* 51**,** 413-7.

KLEINJUNG, T. & LANGGUTH, B. 2020. Avenue for Future Tinnitus Treatments. *Otolaryngol Clin North Am,* 53**,** 667-683.

KLUG, M. & GRAMANN, K. 2021. Identifying key factors for improving ICA-based decomposition of EEG data in mobile and stationary experiments. *Eur J Neurosci,* 54**,** 8406-8420.

KNIPPER, M., HOFMEIER, B., SINGER, W., WOLPERT, S., KLOSE, U. & RUTTIGER, L. 2019. [Differentiating cochlear synaptopathies into different hearing disorders]. *HNO,* 67**,** 406-416.

KNIPPER, M., MAZUREK, B., VAN DIJK, P. & SCHULZE, H. 2021. Too Blind to See the Elephant? Why Neuroscientists Ought to Be Interested in Tinnitus. *J Assoc Res Otolaryngol,* 22**,** 609-621.

KNIPPER, M., PANFORD-WALSH, R., SINGER, W., RÜTTIGER, L. & ZIMMERMANN, U. 2015. Specific synaptopathies diversify brain responses and hearing disorders: you lose the gain from early life. *Cell Tissue Res,* 361**,** 77-93.

KNIPPER, M., VAN DIJK, P., NUNES, I., RÜTTIGER, L. & ZIMMERMANN, U. 2013. Advances in the neurobiology of hearing disorders: recent developments regarding the basis of tinnitus and hyperacusis. *Prog Neurobiol,* 111**,** 17-33.

KNIPPER, M., VAN DIJK, P., SCHULZE, H., MAZUREK, B., KRAUSS, P., SCHEPER, V., WARNECKE, A., SCHLEE, W., SCHWABE, K., SINGER, W., BRAUN, C., DELANO, P. H., FALLGATTER, A. J., EHLIS, A. C., SEARCHFIELD, G. D., MUNK, M. H. J., BAGULEY, D. M. & RUTTIGER, L. 2020. The Neural Bases of Tinnitus: Lessons from Deafness and Cochlear Implants. *J Neurosci,* 40**,** 7190-7202.

KNUDSON, I. M., SHERA, C. A. & MELCHER, J. R. 2014. Increased contralateral suppression of otoacoustic emissions indicates a hyperresponsive medial olivocochlear system in humans with tinnitus and hyperacusis. *J Neurophysiol,* 112**,** 3197-208.

KOOPS, E. A., HAYKAL, S. & VAN DIJK, P. 2021. Macrostructural Changes of the Acoustic Radiation in Humans with Hearing Loss and Tinnitus Revealed with Fixel-Based Analysis. *J Neurosci,* 41**,** 3958-3965.

KOOPS, E. A. & VAN DIJK, P. 2020. Hyperacusis in tinnitus patients relates to enlarged subcortical and cortical responses to sound except at the tinnitus frequency. *Hear Res,* 401**,** 108158.

KRAUS, N. & WHITE-SCHWOCH, T. 2015. Unraveling the Biology of Auditory Learning: A Cognitive-Sensorimotor-Reward Framework. *Trends Cogn Sci,* 19**,** 642-54.

KRONLAND-MARTINET, R., MORLET, J. & GROSSMANN, A. 1987. ANALYSIS OF SOUND PATTERNS THROUGH WAVELET TRANSFORMS. 01, No. 02**,** 273-302.

KUPFERSCHMIDT, D. A., CUMMINGS, K. A., JOFFE, M. E., MACASKILL, A., MALIK, R., SANCHEZ-BELLOT, C., TEJEDA, H. A. & YARUR CASTILLO, H. 2022. Prefrontal Interneurons: Populations, Pathways, and Plasticity Supporting Typical and Disordered Cognition in Rodent Models. *J Neurosci,* 42**,** 8468-8476.

LACADIE, C. M., FULBRIGHT, R. K., RAJEEVAN, N., CONSTABLE, R. T. & PAPADEMETRIS, X. 2008. More accurate Talairach coordinates for neuroimaging using non-linear registration. *Neuroimage,* 42**,** 717-25.

LAI, H., WANG, S., ZHAO, Y., ZHANG, L., YANG, C. & GONG, Q. 2019. Brain gray matter correlates of extraversion: A systematic review and meta-analysis of voxel-based morphometry studies. *Hum Brain Mapp,* 40**,** 4038-4057.

LANCASTER, J. L., WOLDORFF, M. G., PARSONS, L. M., LIOTTI, M., FREITAS, C. S., RAINEY, L., KOCHUNOV, P. V., NICKERSON, D., MIKITEN, S. A. & FOX, P. T. 2000. Automated Talairach atlas labels for functional brain mapping. *Hum Brain Mapp,* 10**,** 120-31.

LANTING, C. P., DE KLEINE, E., LANGERS, D. R. & VAN DIJK, P. 2014. Unilateral tinnitus: changes in connectivity and response lateralization measured with FMRI. *PLoS One,* 9**,** e110704.

LEAVER, A. M., SEYDELL-GREENWALD, A. & RAUSCHECKER, J. P. 2016a. Auditory-limbic interactions in chronic tinnitus: Challenges for neuroimaging research. *Hear Res,* 334**,** 49-57.

LEAVER, A. M., TURESKY, T. K., SEYDELL-GREENWALD, A., MORGAN, S., KIM, H. J. & RAUSCHECKER, J. P. 2016b. Intrinsic network activity in tinnitus investigated using functional MRI. *Hum Brain Mapp,* 37**,** 2717-35.

LEE, T. W., GIROLAMI, M. & SEJNOWSKI, T. J. 1999. Independent component analysis using an extended infomax algorithm for mixed subgaussian and supergaussian sources. *Neural Comput,* 11**,** 417-41.

LEFEBVRE-DEMERS, M., DOYON, N. & FECTEAU, S. 2021. Non-invasive neuromodulation for tinnitus: A meta-analysis and modeling studies. *Brain Stimul,* 14**,** 113-128.

LESKE, S., TSE, A., OOSTERHOF, N. N., HARTMANN, T., MULLER, N., KEIL, J. & WEISZ, N. 2014. The strength of alpha and beta oscillations parametrically scale with the strength of an illusory auditory percept. *Neuroimage,* 88**,** 69-78.

LI, L., ZHANG, Y., ZHAO, Y., LI, Z., KEMP, G. J., WU, M. & GONG, Q. 2022a. Cortical thickness abnormalities in patients with post-traumatic stress disorder: A vertex-based meta-analysis. *Neurosci Biobehav Rev,* 134**,** 104519.

LI, Y. H., CHI, T. S., SHIAO, A. S., LI, L. P. & HSIEH, J. C. 2022b. Pros and cons in tinnitus brain: Enhancement of global connectivity for alpha and delta waves. *Prog Neuropsychopharmacol Biol Psychiatry,* 115**,** 110497.

LIBERMAN, M. C. 1978. Auditory-nerve response from cats raised in a low-noise chamber. *J. Acoust. Soc. Am.,* 63**,** 442-55.

LIBERMAN, M. C. 2017. Noise-induced and age-related hearing loss: new perspectives and potential therapies. *F1000Res,* 6**,** 927.

LIU, C., GLOWATZKI, E. & FUCHS, P. A. 2015. Unmyelinated type II afferent neurons report cochlear damage. *Proc Natl Acad Sci U S A,* 112**,** 14723-7.

LOCKWOOD, A. H., SALVI, R. J. & BURKARD, R. F. 2002. Tinnitus. *N Engl J Med,* 347**,** 904-10.

MAI, J. K., MAJTANIK, M. & PAXINOS, G. 2016. *Atlas of the human brain,* Amsterdam, Elsevier Ltd.

MANCHE, S. K., MADHAVI, J., MEGANADH, K. R. & JYOTHY, A. 2016. Association of tinnitus and hearing loss in otological disorders: a decade-long epidemiological study in a South Indian population. *Braz J Otorhinolaryngol,* 82**,** 643-649.

MARCHER-RORSTED, J., ENCINA-LLAMAS, G., DAU, T., LIBERMAN, M. C., WU, P. Z. & HJORTKJAER, J. 2022. Age-related reduction in frequency-following responses as a potential marker of cochlear neural degeneration. *Hear Res,* 414**,** 108411.

MARGOLIS, R. H., SALY, G. L. & HUNTER, L. L. 2000. High-frequency hearing loss and wideband middle ear impedance in children with otitis media histories. *Ear Hear,* 21**,** 206-11.

MARKS, K. L., MARTEL, D. T., WU, C., BASURA, G. J., ROBERTS, L. E., SCHVARTZ-LEYZAC, K. C. & SHORE, S. E. 2018. Auditory-somatosensory bimodal stimulation desynchronizes brain circuitry to reduce tinnitus in guinea pigs and humans. *Sci Transl Med,* 10.

MCKLVEEN, J. M., MORANO, R. L., FITZGERALD, M., ZOUBOVSKY, S., CASSELLA, S. N., SCHEIMANN, J. R., GHOSAL, S., MAHBOD, P., PACKARD, B. A., MYERS, B., BACCEI, M. L. & HERMAN, J. P. 2016. Chronic Stress Increases Prefrontal Inhibition: A Mechanism for Stress-Induced Prefrontal Dysfunction. *Biol Psychiatry,* 80**,** 754-764.

MCKLVEEN, J. M., MYERS, B., FLAK, J. N., BUNDZIKOVA, J., SOLOMON, M. B., SEROOGY, K. B. & HERMAN, J. P. 2013. Role of prefrontal cortex glucocorticoid receptors in stress and emotion. *Biol Psychiatry,* 74**,** 672-9.

MEDDIS, R. 2006. Auditory-nerve first-spike latency and auditory absolute threshold: a computer model. *J Acoust Soc Am,* 119**,** 406-17.

MELCHER, J. R. & KIANG, N. Y. 1996. Generators of the brainstem auditory evoked potential in cat. III: Identified cell populations. *Hear Res,* 93**,** 52-71.

METZGER, F. G., SCHOPP, B., HAEUSSINGER, F. B., DEHNEN, K., SYNOFZIK, M., FALLGATTER, A. J. & EHLIS, A. C. 2016. Brain activation in frontotemporal and Alzheimer's dementia: a functional near-infrared spectroscopy study. *Alzheimers Res Ther,* 8**,** 56.

MICHIKAWA, T., NISHIWAKI, Y., KIKUCHI, Y., SAITO, H., MIZUTARI, K., OKAMOTO, M. & TAKEBAYASHI, T. 2010. Prevalence and factors associated with tinnitus: a community-based study of Japanese elders. *J Epidemiol,* 20**,** 271-6.

MIDDLETON, J. W., KIRITANI, T., PEDERSEN, C., TURNER, J. G., SHEPHERD, G. M. & TZOUNOPOULOS, T. 2011. Mice with behavioral evidence of tinnitus exhibit dorsal cochlear nucleus hyperactivity because of decreased GABAergic inhibition. *Proc Natl Acad Sci U S A,* 108**,** 7601-6.

MILLOY, V., FOURNIER, P., BENOIT, D., NORENA, A. & KORAVAND, A. 2017. Auditory Brainstem Responses in Tinnitus: A Review of Who, How, and What? *Front Aging Neurosci,* 9**,** 237.

MOHRLE, D., HOFMEIER, B., AMEND, M., WOLPERT, S., NI, K., BING, D., KLOSE, U., PICHLER, B., KNIPPER, M. & RUTTIGER, L. 2019. Enhanced Central Neural Gain Compensates Acoustic Trauma-induced Cochlear Impairment, but Unlikely Correlates with Tinnitus and Hyperacusis. *Neuroscience,* 407**,** 146-169.

MØLLER, A. R., JANNETTA, P. J. & JHO, H. D. 1994. Click-evoked responses from the cochlear nucleus: a study in human. *Electroencephalogr Clin Neurophysiol,* 92**,** 215-24.

MUHLAU, M., RAUSCHECKER, J. P., OESTREICHER, E., GASER, C., ROTTINGER, M., WOHLSCHLAGER, A. M., SIMON, F., ETGEN, T., CONRAD, B. & SANDER, D. 2006. Structural brain changes in tinnitus. *Cereb Cortex,* 16**,** 1283-8.

NELTING, M., RIENHOFF, N. K., HESSE, G. & LAMPARTER, U. 2002. [The assessment of subjective distress related to hyperacusis with a self-rating questionnaire on hypersensitivity to sound]. *Laryngorhinootologie,* 81**,** 327-34.

NEYMOTIN, S. A., TAL, I., BARCZAK, A., O'CONNELL, M. N., MCGINNIS, T., MARKOWITZ, N., ESPINAL, E., GRIFFITH, E., ANWAR, H., DURA-BERNAL, S., SCHROEDER, C. E., LYTTON, W. W., JONES, S. R., BICKEL, S. & LAKATOS, P. 2022. Detecting Spontaneous Neural Oscillation Events in Primate Auditory Cortex. *eNeuro,* 9.

NORENA, A. J. 2011. An integrative model of tinnitus based on a central gain controlling neural sensitivity. *Neurosci Biobehav Rev,* 35**,** 1089-109.

NOREÑA, A. J. 2015. Revisiting the cochlear and central mechanisms of tinnitus and therapeutic approaches. *Audiol Neurootol,* 20 Suppl 1**,** 53-9.

NOREÑA, A. J. & FARLEY, B. J. 2013. Tinnitus-related neural activity: theories of generation, propagation, and centralization. *Hear Res,* 295**,** 161-71.

ONUSKO, E. 2004. Tympanometry. *Am Fam Physician,* 70**,** 1713-20.

ORTMANN, M., MULLER, N., SCHLEE, W. & WEISZ, N. 2011. Rapid increases of gamma power in the auditory cortex following noise trauma in humans. *Eur J Neurosci,* 33**,** 568-75.

OYA, H., GANDER, P. E., PETKOV, C. I., ADOLPHS, R., NOURSKI, K. V., KAWASAKI, H., HOWARD, M. A. & GRIFFITHS, T. D. 2018. Neural phase locking predicts BOLD response in human auditory cortex. *Neuroimage,* 169**,** 286-301.

PATTYN, T., VAN DEN EEDE, F., VANNESTE, S., CASSIERS, L., VELTMAN, D. J., VAN DE HEYNING, P. & SABBE, B. C. G. 2016. Tinnitus and anxiety disorders: A review. *Hear Res,* 333**,** 255-265.

PELLEGRINI, F., HAWELLEK, D. J., PAPE, A. A., HIPP, J. F. & SIEGEL, M. 2021. Motion Coherence and Luminance Contrast Interact in Driving Visual Gamma-Band Activity. *Cereb Cortex,* 31**,** 1622-1631.

PENG, F., XIANG, Y., XU, H., YIN, Q., LI, J. & ZOU, Y. 2021. Systematic review and meta-analysis of extended high-frequency audiometry in tinnitus patients. *Ann Palliat Med,* 10**,** 12129-12139.

PINTI, P., SIDDIQUI, M. F., LEVY, A. D., JONES, E. J. H. & TACHTSIDIS, I. 2021. An analysis framework for the integration of broadband NIRS and EEG to assess neurovascular and neurometabolic coupling. *Sci Rep,* 11**,** 3977.

PION-TONACHINI, L., KREUTZ-DELGADO, K. & MAKEIG, S. 2019. ICLabel: An automated electroencephalographic independent component classifier, dataset, and website. *Neuroimage,* 198**,** 181-197.

PIZZAGALLI, D. A. & ROBERTS, A. C. 2022. Prefrontal cortex and depression. *Neuropsychopharmacology,* 47**,** 225-246.

PORTMANN, M., CAZALS, Y., NEGREVERGNE, M. & ARAN, J. M. 1980. Transtympanic and surface recordings in the diagnosis of retrocochlear disorders. *Acta Otolaryngol,* 89**,** 362-9.

RALLI, M., SALVI, R. J., GRECO, A., TURCHETTA, R., DE VIRGILIO, A., ALTISSIMI, G., ATTANASIO, G., CIANFRONE, G. & DE VINCENTIIS, M. 2017. Characteristics of somatic tinnitus patients with and without hyperacusis. *PLoS One,* 12**,** e0188255.

RAUSCHECKER, J. P., MAY, E. S., MAUDOUX, A. & PLONER, M. 2015. Frontostriatal Gating of Tinnitus and Chronic Pain. *Trends Cogn Sci,* 19**,** 567-578.

REFAT, F., WERTZ, J., HINRICHS, P., KLOSE, U., SAMY, H., ABDELKADER, R. M., SAEMISCH, J., HOFMEIER, B., SINGER, W., RUTTIGER, L., KNIPPER, M. & WOLPERT, S. 2021. Co-occurrence of Hyperacusis Accelerates With Tinnitus Burden Over Time and Requires Medical Care. *Front Neurol,* 12**,** 627522.

ROBERTS, L. E., EGGERMONT, J. J., CASPARY, D. M., SHORE, S. E., MELCHER, J. R. & KALTENBACH, J. A. 2010. Ringing ears: the neuroscience of tinnitus. *J Neurosci,* 30**,** 14972-9.

ROBERTS, L. E., HUSAIN, F. T. & EGGERMONT, J. J. 2013. Role of attention in the generation and modulation of tinnitus. *Neurosci Biobehav Rev,* 37**,** 1754-73.

ROBERTS, L. E. & SALVI, R. 2019. Overview: Hearing loss, tinnitus, hyperacusis, and the role of central gain. *Neuroscience*.

ROSEMANN, S. & RAUSCHECKER, J. P. 2023. Disruptions of default mode network and precuneus connectivity associated with cognitive dysfunctions in tinnitus. *Sci Rep,* 13**,** 5746.

ROSSIGNOL, E., KRUGLIKOV, I., VAN DEN MAAGDENBERG, A. M., RUDY, B. & FISHELL, G. 2013. CaV 2.1 ablation in cortical interneurons selectively impairs fast-spiking basket cells and causes generalized seizures. *Ann Neurol,* 74**,** 209-22.

RÜTTIGER, L., SINGER, W., PANFORD-WALSH, R., MATSUMOTO, M., LEE, S. C., ZUCCOTTI, A., ZIMMERMANN, U., JAUMANN, M., ROHBOCK, K., XIONG, H. & KNIPPER, M. 2013. The reduced cochlear output and the failure to adapt the central auditory response causes tinnitus in noise exposed rats. *PLoS One,* 8**,** e57247.

RUTTIGER, L., ZIMMERMANN, U. & KNIPPER, M. 2017. Biomarkers for Hearing Dysfunction: Facts and Outlook. *ORL J Otorhinolaryngol Relat Spec,* 79**,** 93-111.

SADAGHIANI, S., HESSELMANN, G. & KLEINSCHMIDT, A. 2009. Distributed and antagonistic contributions of ongoing activity fluctuations to auditory stimulus detection. *J Neurosci,* 29**,** 13410-7.

SALVI, R. J., WANG, J. & DING, D. 2000. Auditory plasticity and hyperactivity following cochlear damage. *Hear Res,* 147**,** 261-74.

SANTOSA, H., ZHAI, X., FISHBURN, F. & HUPPERT, T. 2018. The NIRS Brain AnalyzIR Toolbox. *Algorithms,* 11**,** 73.

SCHAETTE, R. & KEMPTER, R. 2012. Computational models of neurophysiological correlates of tinnitus. *Front Syst Neurosci,* 6**,** 34.

SCHAETTE, R. & MCALPINE, D. 2011. Tinnitus with a normal audiogram: physiological evidence for hidden hearing loss and computational model. *J Neurosci,* 31**,** 13452-7.

SCHECKLMANN, M., LANDGREBE, M., LANGGUTH, B. & GROUP, T. R. I. D. S. 2014. Phenotypic characteristics of hyperacusis in tinnitus. *PLoS One,* 9**,** e86944.

SCHECKLMANN, M., LEHNER, A., SCHLEE, W., VIELSMEIER, V., LANDGREBE, M. & LANGGUTH, B. 2015. Validation of Screening Questions for Hyperacusis in Chronic Tinnitus. *Biomed Res Int,* 2015**,** 191479.

SCHLEE, W., MUELLER, N., HARTMANN, T., KEIL, J., LORENZ, I. & WEISZ, N. 2009. Mapping cortical hubs in tinnitus. *BMC Biol,* 7**,** 80.

SCHMIDT, S. A., CARPENTER-THOMPSON, J. & HUSAIN, F. T. 2017. Connectivity of precuneus to the default mode and dorsal attention networks: A possible invariant marker of long-term tinnitus. *Neuroimage Clin,* 16**,** 196-204.

SCHWARTZ, M. F., FASEYITAN, O., KIM, J. & COSLETT, H. B. 2012. The dorsal stream contribution to phonological retrieval in object naming. *Brain,* 135**,** 3799-814.

SEDLEY, W. 2019. Tinnitus: Does gain explain? *Neuroscience*.

SEELEY, W. W., MENON, V., SCHATZBERG, A. F., KELLER, J., GLOVER, G. H., KENNA, H., REISS, A. L. & GREICIUS, M. D. 2007. Dissociable intrinsic connectivity networks for salience processing and executive control. *J Neurosci,* 27**,** 2349-56.

SEGERDAHL, A. R., MEZUE, M., OKELL, T. W., FARRAR, J. T. & TRACEY, I. 2015. The dorsal posterior insula subserves a fundamental role in human pain. *Nat Neurosci,* 18**,** 499-500.

SENDESEN, E., KAYNAKOGLU, B., VEZIROGLU, L. B. & TURKYILMAZ, M. D. 2022. Auditory brainstem response in unilateral tinnitus patients: does symmetrical hearing thresholds and within-subject comparison affect responses? *Eur Arch Otorhinolaryngol,* 279**,** 4687-4693.

SENDESEN, E. & TURKYILMAZ, D. 2023. Listening handicap in tinnitus patients by controlling extended high frequencies - Effort or fatigue? *Auris Nasus Larynx*.

SHEPPARD, A., STOCKING, C., RALLI, M. & SALVI, R. 2020. A review of auditory gain, low-level noise and sound therapy for tinnitus and hyperacusis. *Int J Audiol,* 59**,** 5-15.

SHIM, H. J., KIM, S. K., PARK, C. H., LEE, S. H., YOON, S. W., KI, A. R., CHUNG, D. H. & YEO, S. G. 2009. Hearing abilities at ultra-high frequency in patients with tinnitus. *Clin Exp Otorhinolaryngol,* 2**,** 169-74.

SHIN, S. H., BYUN, S. W., LEE, Z. Y., KIM, M. J., KIM, E. H. & LEE, H. Y. 2022. Clinical Findings That Differentiate Co-Occurrence of Hyperacusis and Tinnitus from Tinnitus Alone. *Yonsei Med J,* 63**,** 1035-1042.

SHORE, S. E., ROBERTS, L. E. & LANGGUTH, B. 2016. Maladaptive plasticity in tinnitus--triggers, mechanisms and treatment. *Nat Rev Neurol,* 12**,** 150-60.

SINGER, W., ZUCCOTTI, A., JAUMANN, M., LEE, S. C., PANFORD-WALSH, R., XIONG, H., ZIMMERMANN, U., FRANZ, C., GEISLER, H. S., KÖPSCHALL, I., ROHBOCK, K., VARAKINA, K., VERPOORTEN, S., REINBOTHE, T., SCHIMMANG, T., RÜTTIGER, L. & KNIPPER, M. 2013. Noise-induced inner hair cell ribbon loss disturbs central arc mobilization: a novel molecular paradigm for understanding tinnitus. *Mol Neurobiol,* 47**,** 261-79.

SISMANIS, A. 2003. Pulsatile tinnitus. *Otolaryngol Clin North Am,* 36**,** 389-402, viii.

SOHAL, V. S., ZHANG, F., YIZHAR, O. & DEISSEROTH, K. 2009. Parvalbumin neurons and gamma rhythms enhance cortical circuit performance. *Nature,* 459**,** 698-702.

SONG, Z., WU, Y., TANG, D., LU, X., QIAO, L., WANG, J. & LI, H. 2021. Tinnitus Is Associated With Extended High-frequency Hearing Loss and Hidden High-frequency Damage in Young Patients. *Otol Neurotol,* 42**,** 377-383.

STAPELLS, D. R. & PICTON, T. W. 1981. Technical aspects of brainstem evoked potential audiometry using tones. *Ear Hear,* 2**,** 20-9.

STEINBRINK, J., VILLRINGER, A., KEMPF, F., HAUX, D., BODEN, S. & OBRIG, H. 2006. Illuminating the BOLD signal: combined fMRI-fNIRS studies. *Magn Reson Imaging,* 24**,** 495-505.

STURM, J. J. & WEISZ, C. J. 2015. Hyperactivity in the medial olivocochlear efferent system is a common feature of tinnitus and hyperacusis in humans. *J Neurophysiol,* 114**,** 2551-4.

SULLIVAN, R. M. & GRATTON, A. 2002. Prefrontal cortical regulation of hypothalamic-pituitary-adrenal function in the rat and implications for psychopathology: side matters. *Psychoneuroendocrinology,* 27**,** 99-114.

TAGLIAZUCCHI, E., VON WEGNER, F., MORZELEWSKI, A., BRODBECK, V. & LAUFS, H. 2012. Dynamic BOLD functional connectivity in humans and its electrophysiological correlates. *Front Hum Neurosci,* 6**,** 339.

TRACEY, I. & MANTYH, P. W. 2007. The cerebral signature for pain perception and its modulation. *Neuron,* 55**,** 377-91.

TYLER, R. S. & CONRAD-ARMES, D. 1983. The determination of tinnitus loudness considering the effects of recruitment. *J Speech Hear Res,* 26**,** 59-72.

TZIRIDIS, K., AHLF, S., JESCHKE, M., HAPPEL, M. F., OHL, F. W. & SCHULZE, H. 2015. Noise Trauma Induced Neural Plasticity Throughout the Auditory System of Mongolian Gerbils: Differences between Tinnitus Developing and Non-Developing Animals. *Front Neurol,* 6**,** 22.

UTEVSKY, A. V. & PLATT, M. L. 2014. Status and the brain. *PLoS Biol,* 12**,** e1001941.

VAN DER LOO, E., GAIS, S., CONGEDO, M., VANNESTE, S., PLAZIER, M., MENOVSKY, T., VAN DE HEYNING, P. & DE RIDDER, D. 2009. Tinnitus intensity dependent gamma oscillations of the contralateral auditory cortex. *PLoS One,* 4**,** e7396.

VANNESTE, S. & DE RIDDER, D. 2012. The auditory and non-auditory brain areas involved in tinnitus. An emergent property of multiple parallel overlapping subnetworks. *Front Syst Neurosci,* 6**,** 31.

VANNESTE, S., JOOS, K., OST, J. & DE RIDDER, D. 2018. Influencing connectivity and cross-frequency coupling by real-time source localized neurofeedback of the posterior cingulate cortex reduces tinnitus related distress. *Neurobiol Stress,* 8**,** 211-224.

VANNESTE, S., PLAZIER, M., DER LOO, E., DE HEYNING, P. V., CONGEDO, M. & DE RIDDER, D. 2010. The neural correlates of tinnitus-related distress. *Neuroimage,* 52**,** 470-80.

VANNESTE, S., TO, W. T. & DE RIDDER, D. 2019. Tinnitus and neuropathic pain share a common neural substrate in the form of specific brain connectivity and microstate profiles. *Prog Neuropsychopharmacol Biol Psychiatry,* 88**,** 388-400.

VERNON, J. & FENWICK, J. 1984. Identification of Tinnitus: A Plea for Standardization. *The Journal of Laryngology & Otology,* Volume 98**,** 45 - 53.

VIELSMEIER, V., KREUZER, P. M., HAUBNER, F., STEFFENS, T., SEMMLER, P. R., KLEINJUNG, T., SCHLEE, W., LANGGUTH, B. & SCHECKLMANN, M. 2016. Speech Comprehension Difficulties in Chronic Tinnitus and Its Relation to Hyperacusis. *Front Aging Neurosci,* 8**,** 293.

VINCENT, J. L., KAHN, I., SNYDER, A. Z., RAICHLE, M. E. & BUCKNER, R. L. 2008. Evidence for a frontoparietal control system revealed by intrinsic functional connectivity. *J Neurophysiol,* 100**,** 3328-42.

VON GABLENZ, P. & HOLUBE, I. 2015. [Prevalence of hearing impairment in northwestern Germany. Results of an epidemiological study on hearing status (HORSTAT)]. *HNO,* 63**,** 195-214.

WAGENER, K., KOLLMEIER, B. & KUEHNEL, V. 1999. Entwicklung und Evaluation eines Satztests für die deutsche Sprache I: Design des Oldenburger Satztests. *Zeitschrift für Audiologie,* 38**,** 1-32.

WAGNER, A. D., PARE-BLAGOEV, E. J., CLARK, J. & POLDRACK, R. A. 2001. Recovering meaning: left prefrontal cortex guides controlled semantic retrieval. *Neuron,* 31**,** 329-38.

WALTON, J. P. 2010. Timing is everything: temporal processing deficits in the aged auditory brainstem. *Hear Res,* 264**,** 63-9.

WEINBERGER, N. M. 2015. New perspectives on the auditory cortex: learning and memory. *Handb Clin Neurol,* 129**,** 117-47.

WEISZ, N., HARTMANN, T., DOHRMANN, K., SCHLEE, W. & NOREÑA, A. 2006. High-frequency tinnitus without hearing loss does not mean absence of deafferentation. *Hear Res,* 222**,** 108-14.

WEISZ, N. & LANGGUTH, B. 2010. [Cortical plasticity and changes in tinnitus: treatment options]. *HNO,* 58**,** 983-9.

WEISZ, N., MULLER, S., SCHLEE, W., DOHRMANN, K., HARTMANN, T. & ELBERT, T. 2007. The neural code of auditory phantom perception. *J Neurosci,* 27**,** 1479-84.

WERTZ, J., RÜTTIGER, L., BENDER, B., KLOSE, U., STARK, R. S., DAPPER, K., SAEMISCH, J., BRAUN, C., SINGER, W., DALHOFF, E., BADER, K., WOLPERT, S.M., KNIPPER, M., MUNK, M.H.J. 2023. Differential cortical activation patterns: pioneering sub-classification of tinnitus with and without hyperacusis by combining audiometry, gamma oscillations, and hemodynamics. *Front. Neurosci.* 17, 1232446.

WILLIAMS, D., STOTT, C. M., GOODYER, I. M. & SAHAKIAN, B. J. 2000. Specific language impairment with or without hyperactivity: neuropsychological evidence for frontostriatal dysfunction. *Dev Med Child Neurol,* 42**,** 368-75.

WOBBROCK, J. O., FINDLATER, L., GERGLE, D. & HIGGINS, J. J. 2011. The Aligned Rank Transform for nonparametric factorial analyses using only ANOVA procedures. *CHI 2011 - 29th Annual CHI Conference on Human Factors in Computing Systems-Proceedings.* Vancouver, BC, Canada.

YAN, C. G., WANG, X. D., ZUO, X. N. & ZANG, Y. F. 2016. DPABI: Data Processing & Analysis for (Resting-State) Brain Imaging. *Neuroinformatics,* 14**,** 339-51.

YANG, S. & BAO, S. 2013. Homeostatic mechanisms and treatment of tinnitus. *Restor Neurol Neurosci,* 31**,** 99-108.

YANG, S., WEINER, B. D., ZHANG, L. S., CHO, S. J. & BAO, S. 2011. Homeostatic plasticity drives tinnitus perception in an animal model. *Proc Natl Acad Sci U S A,* 108**,** 14974-9.

YANTIS, S., SCHWARZBACH, J., SERENCES, J. T., CARLSON, R. L., STEINMETZ, M. A., PEKAR, J. J. & COURTNEY, S. M. 2002. Transient neural activity in human parietal cortex during spatial attention shifts. *Nat Neurosci,* 5**,** 995-1002.

ZATORRE, R. J., BELIN, P. & PENHUNE, V. B. 2002. Structure and function of auditory cortex: music and speech. *Trends Cogn Sci,* 6**,** 37-46.

ZELLE, D., GUMMER, A. W. & DALHOFF, E. 2013. Extraction of otoacoustic distortion product sources using pulse basis functions. *J Acoust Soc Am,* 134**,** EL64-9.

ZENG, F. G. 2013. An active loudness model suggesting tinnitus as increased central noise and hyperacusis as increased nonlinear gain. *Hear Res,* 295**,** 172-9.

ZENG, F. G. 2020. Tinnitus and hyperacusis: Central noise, gain and variance. *Curr Opin Physiol,* 18**,** 123-129.

ZENG, F. G., RICHARDSON, M., TRAN, P., LIN, H. & DJALILIAN, H. 2019. Tinnitus Treatment Using Noninvasive and Minimally Invasive Electric Stimulation: Experimental Design and Feasibility. *Trends Hear,* 23**,** 2331216518821449.

ZHANG, X., PAN, W. J. & KEILHOLZ, S. D. 2020. The relationship between BOLD and neural activity arises from temporally sparse events. *Neuroimage,* 207**,** 116390.

ZHOU, G. P., SHI, X. Y., WEI, H. L., QU, L. J., YU, Y. S., ZHOU, Q. Q., YIN, X., ZHANG, H. & TAO, Y. J. 2019. Disrupted Intraregional Brain Activity and Functional Connectivity in Unilateral Acute Tinnitus Patients With Hearing Loss. *Front Neurosci,* 13**,** 1010.

# 7. DECLARATION OF CONTRIBUTION

The present work was carried out under the supervision of:

Prof. Dr. rer. nat. Marlies Knipper, in the Tübingen Hearing Research Centre (THRC), Molecular Physiology of Hearing at the Department of Otolaryngology, Head and Neck Surgery Tübingen.
Prof. Dr. rer. nat. Uwe Klose, in the Department of Diagnostic and Interventional Neuroradiology Tübingen.
PD. Dr. Matthias H.J. Munk, in the Department of Psychiatry Tübingen.
Senior Physician Dr. med. Stephan Wolpert from the Department of Otolaryngology, Head and Neck Surgery Tübingen.

The conception of the study was carried out by Prof. Dr. rer. nat. Marlies Knipper, Prof. (Senior Investigator), Prof. Dr. rer. nat. Lukas Rüttiger (Audiometry, ENT), PD. Dr. Matthias H.J. Munk (Neurophysiology, EEG/fNIRS), Dr. rer. nat. Uwe Klose, Prof. (Functional imaging, fMRI), Dr. Ing. Ernst Dalhoff, Prof. Dr. rer. nat. Christoph Braun (Neurophysiology, MEG), Senior Physician Dr. med. Stephan Wolpert (Head of ENT Study Centre), and me, Jakob Wertz.

The audiological diagnostic experiments (Examination Day 1) for the first and second papers were (after initial instruction provided by laboratory members Dr. sc. hum. Benedikt Hofmeier and Senior Physician Dr. med. Stephan Wolpert) carried out by Ebrahim Aldamer (M.Sc.), Dr. sc. hum. Benedikt Hofmeier, cand. med. Pauline Hinrichs, and me, Jakob Wertz. Out of 96 subjects, my involvement in conducting the measurements, which included questionnaires, audiometry, and ABR, accounts for approximately 12 % (12 of 96 subjects). The statistical analysis was performed by me, Jakob Wertz (after guidance by Prof. Dr. rer. nat. Lukas Rüttiger).

The fMRI experiments (Examination Day 2) for the first paper were (after initial instruction provided by laboratory members Dr. sc. hum. Benedikt Hofmeier, Prof. Dr. rer. nat. Uwe Klose, and MTRA Silke Buschbach) carried out by Ebrahim Aldamer (M.Sc.), Dr. sc. hum. Benedikt Hofmeier, and me, Jakob Wertz. Out of 93 subjects, my involvement in conducting the measurements, which included stimulus-evoked fMRI and rs-fMRI, accounts for approximately 12 % (12 of 93 subjects). The statistical analysis of the rs-fMRI was performed by me, Jakob Wertz (after guidance by Prof. Dr. rer. nat. Uwe Klose and Prof. Dr. rer. nat. Lukas Rüttiger).

All audiological diagnostic experiments (Examination Day 1) for the last cohort were carried out by me, Jakob Wertz, with assistance from cand. med. Moritz Rühle. In 20 of 50 subjects' questionnaires, blood sample collection, and OLSA were performed by cand. med. Moritz Rühle. From these 50 participants, 40 were included in the study (Wertz et al., 2023) The statistical analysis was performed independently by me, Jakob Wertz (after consultation with Prof. Dr. rer. nat. Lukas Rüttiger).

The fMRI experiments (Examination Day 2) for the last cohort were (after initial instruction provided by Prof. Dr. rer. nat. Uwe Klose, MTRA Silke Buschbach, and me, Jakob Wertz) carried out by Konrad Dapper. The statistical analysis was performed by me, Jakob Wertz (after consultation with Prof. Dr. rer. nat. Uwe Klose and PD Dr. med. Benjamin Bender).

The EEG/fNIRS experiments (Examination Day 3) for the last cohort were (after initial instruction provided by PD. Dr. med. Matthias H.J. Munk, MTA Betti Schopp, MTA Ramona Täglich, and Dr. med. Robert Stark) carried out by me, Jakob Wertz. In 16 of 50 subjects, the measurement was assisted by MD Jörg Saemisch. The statistical analysis was performed by me, Jakob Wertz (after guidance by PD. Dr. med. Matthias H.J. Munk, Prof. Dr. rer. nat. Christoph Braun, Prof. Dr. rer. nat. Lukas Rüttiger, and Dr. med. Robert Stark)

I, Jakob Wertz, declare that I have created all the graphics independently.

I hereby declare that I have written this manuscript independently (according to the guidance of Prof. Dr. rer. nat. Marlies Knipper) and have not used any sources other than those I have indicated.

Tübingen, the

Signature: Jakob Wertz

# 8. PUBLICATIONS

Parts of this dissertation have been published in the following publications:

Hofmeier, B., **Wertz, J.**, Refat, F., Hinrichs, P., Saemisch, J., Singer, W., et al. (2021). "Functional biomarkers that distinguish between tinnitus with and without hyperacusis". Clin Transl Med 11(5), e378. doi: 10.1002/ctm2.378.

Refat, F., **Wertz, J.**, Hinrichs, P., Klose, U., Samy, H., Abdelkader, R.M., et al. (2021). „Co-occurrence of Hyperacusis Accelerates With Tinnitus Burden Over Time and Requires Medical Care". Front Neurol 12, 627522. doi: 10.3389/fneur.2021.627522.

**Wertz, J.**, Rüttiger, L., Bender, B., Klose, U., Stark, R. S., Dapper, K. (2023). „Differential cortical activation patterns: pioneering sub-classification of tinnitus with and without hyperacusis by combining audiometry, gamma oscillations, and hemodynamics". Front. Neurosci. 17, 1232446. doi: 10.3389/fnins.2023.1232446.

## ACKNOWLEDGMENTS

I would like to express my deepest gratitude to everyone who contributed to the completion of this dissertation. Their expertise, guidance, and support have been indispensable, and I am truly fortunate to have had the privilege of working with them.

First and foremost, I am profoundly thankful to my doctoral supervisor, Prof. Dr. Marlies Knipper, for their unwavering dedication, patience, and mentorship.

I would also like to extend my gratitude to Prof. Dr. Uwe Klose, PD. Dr. Matthias H.J. Munk, Prof. Dr. Lukas Rüttiger, Dr. Stephan Wolpert, Dr. Ernst Dalhoff, Prof. Dr. Christoph Braun, Dr. Robert Stark, and PD Dr. Benjamin Bender. Their expertise in their respective fields has been pivotal in providing me with valuable insights and perspectives that enriched the depth and breadth of my research.

Prof. Dr. Uwe Klose provided invaluable guidance and structured help on fMRI methodology and analysis.

Dr. Matthias H.J. Munk for his unwavering support, endless enthusiasm and valuable contributions with innovative ideas.

Prof. Dr. Lukas Rüttiger offered critical insights into each part of the thesis and never-ending patience for all questions, which greatly enhanced the theoretical framework and overall coherence of this dissertation.

Dr. Stephan Wolpert contributed significantly to the success of the thesis with his prompt and efficient support in resolving critical clinical issues. Thank you for the great mentoring.

I am also indebted to my fellow colleagues, who provided valuable input, support, and camaraderie throughout this academic journey. Your insights and friendship have been a source of motivation and inspiration.

Additionally, I would like to express my sincere appreciation to everyone who contributed to this dissertation in one way or another. Your support and belief in my abilities have been instrumental in bringing this research to a successful outcome.

Last but not least, I would like to thank my loved ones beyond work. Thank you for all the emotional support, understanding, and encouragement.

# CURRICULUM VITAE

# APPENDIX

**Checkliste für Probanden-Einschluss**

**Name:** _____

**Einschlusskriterien**

○ **Fallgruppe (mit Tinnitus, ohne Hyperakusis)**

○ **Kontrollgruppe (ohne Tinnitus, ohne Hyperakusis)**

○ **Fallgruppe (mit Tinnitus UND Hyperakusis)**

○ **Fallgruppe (ohne Tinnitus, MIT Hyperakusis)**

| Ja | Nein | | Ja | Nein | |
|---|---|---|---|---|---|
| O | O | kontinuierl. Tinnitus (>4 Wochen) | O | O | Kein Tinnitusleiden |
| O | O | nicht pulsatil | O | O | Keine Hyperakusis |
| O | O | Tinnitus nicht als Begleiterkrankung | | | |

Wenn Tinnitus, seit wann (Jahr):

Händigkeit (unzutreffendes bitte durchstreichen): rechts // links

**Ausschlusskriterien**

| Ja | Nein | **Hörsystem** |
|---|---|---|
| O | O | Hörverlust über 40dB |
| O | O | Knalltrauma |
| O | O | Jahrelange Lärmexposition |
| O | O | Chronische Gehörgang- oder Mittelohrentzündung |
| O | O | Ertaubung (ein-/beidseitig) |
| O | O | Morbus Menière |
| O | O | Retrocochleäre Hörstörung (Nachweis durch BERA) |
| O | O | Schallleitungsschwerhörigkeit (über 10dB bei mehreren Frequenzen) |

Ja Nein **Allgemeine Krankengeschichte**

O O Schädelhirntrauma(Grad II oder III)

O O Herz-Kreislauferkrankungen

O O Diabetes

O O Nierenerkrankungen

O O Behandlung von Krebsleiden (Leukämie)

O O Allergien (gegen Kontrastmittel)

O O Eingeschränkte Temperaturempfindung/erhöhte Empfindlichkeit gegenüber Erwärmung des Körpers

O O Ototox. Medikamente (Schleifendiuretika, Aminoglykoside, Chemo)

O O Behandlung von neurologischen oder psychiatrischen Erkrankungen (auch medikamentös: Neuroleptika, Haloperidol, L-Dopa)

O O Alkohol, Drogen

Ja Nein **Sonstiges**

O O Schwangerschaft

Ja Nein **Therapie Hörsystem**

O O Hörgeräteversorgung

O O Ohroperationen

O O Tinnitus Therapie (medikamentös, Masker/Noiser, HBO, Akupunktur)

Notiz:

Datum, Ort Unterschrift

***Appendix A:*** *List of inclusion/exclusion criteria.*

| Mini-Geräuschüberempfindlichkeits-Test | | | | |
|---|---|---|---|---|
| | *Stimmt immer* | *Stimmt oft* | *Stimmt manchmal* | *Stimmt nicht* |
| 1. Bestimmte Geräusche muss ich meiden. | | | | |
| 2. Ich habe sehr große Angst vor Lärm. | | | | |
| 3. Ich ärgere mich über Geräusche, die mir zu laut und unangenehm sind. | | | | |
| 4. Ich glaube, ich werde meinen Alltag nicht bewältigen können, wenn die Geräuschempfindlichkeit so schlimm bleibt. | | | | |
| 5. Bei lauten/unangenehmen Geräuschen ziehe ich mich sofort zurück. | | | | |
| 6. Haben Sie wegen der Geräuschempfindlichkeit Schwierigkeiten, an geräuschvollen Orten Gespräche zu führen? | | | | |
| 7. Empfinden Sie Lärm in manchen Umgebungen als unangenehm (zum Beispiel in Gaststätten, Lokalen, Konzerten, bei Feuerwerk)? | | | | |
| 8. Wenn Sie jemand bittet, mit Ihnen auszugehen (zum Beispiel ins Kino, ins Konzert, ins Restaurant), denken Sie dann als erstes an die Schwierigkeiten mit den Geräuschen? | | | | |
| 9. Können Sie sich in geräuschvollen Umgebungen schlechter konzentrieren, wenn Sie müde sind oder unter Stress stehen? | | | | |

*Mini-Geräuschüberempfindlichkeits-Test. Instruktion an den Patienten: Bitte beachten Sie, dass bei den hier abgefragten Beschwerden Außengeräusche jeglicher Art gemeint sind und nicht eventuell bestehende Innengeräusche wie zum Beispiel Ohrgeräusche (Tinnitus). Ziel der Aussagen ist es herauszufinden, ob Ihre Geräuschüberempfindlichkeit Einfluss auf Ihre Gefühle, Verhaltensweisen oder Einstellung hat. Kreuzen Sie bitte für jede Aussage die betreffende Antwort an. Es ist für jede Frage nur eine Antwort möglich.*
*Aus: Hyperakusis Inventar (HKI), Goebel und Berthold, 2012. © Goebel 2012*

| Mini-Geräuschüberempfindlichkeits-Test | | | | |
|---|---|---|---|---|
| | *Always correct* | *Often correct* | *Sometimes correct* | *Never correct* |
| 1. I have to avoid certain sounds. | | | | |
| 2. I am very afraid of noise. | | | | |
| 3. I get annoyed by noises that are too loud and unpleasant for me. | | | | |
| 4. I believe I won't be able to cope in everyday life if the hypersensitivity to sound continues to be this bad. | | | | |
| 5. I immediately withdraw when there are loud/uncomfortable sounds. | | | | |
| 6. Do you have difficulty having conversations in noisy places because of noise sensitivity? | | | | |
| 7. Do you find noise in some environments unpleasant (e.g., in restaurants, bars, concerts, fireworks)? | | | | |
| 8. When someone asks you to go out (for example, to the cinema, to a concert, to a restaurant), is the first thing that comes to your mind the difficulties with noise? | | | | |
| 9. Do you find it harder to concentrate when tired or stressed in noisy environments? | | | | |

***Appendix B:*** *The hyperacusis questionnaire is presented in the upper panel as the original German version and in the lower panel as a version translated into English by the author.*

| Control | | | | T-group | | | | TH-group | | | |
|---|---|---|---|---|---|---|---|---|---|---|---|
| **Subj.** | **Age** | **Sex** | **Handedness** | **Subj.** | **Age** | **Sex** | **Handedness** | **Subj.** | **Age** | **Sex** | **Handedness** |
| K002 | 27 | female | right | T001 | 36 | male | left | TN12 | 24 | male | right |
| K006 | 39 | male | right | T002 | 21 | male | right | TN13 | 21 | female | left |
| KN01 | 21 | female | right | T006 | 45 | female | right | TN17 | 26 | female | right |
| KN02 | 26 | female | right | T009 | 34 | male | right | TN19 | 34 | female | right |
| KN03 | 18 | male | right | TN01 | 26 | male | right | TN20 | 28 | female | right |
| KN04 | 32 | female | right | TN03 | 34 | male | left | TN21 | 24 | female | right |
| KN05 | 41 | female | left | TN04 | 23 | male | left | TN22 | 21 | female | right |
| KN06 | 21 | female | right | TN05 | 33 | male | right | TN23 | 24 | female | right |
| KN07 | 23 | female | right | TN08 | 27 | male | right | TN25 | 22 | female | right |
| KN08 | 18 | female | right | TN10 | 25 | female | right | TN28 | 30 | female | right |
| KN09 | 19 | male | right | TN11 | 25 | female | right | TS020 | 24 | female | right |
| KN10 | 20 | female | right | TN16 | 26 | male | left | TS033 | 49 | male | left |
| KN11 | 24 | female | right | TS004 | 44 | male | right | TS037 | 23 | female | right |
| KN14 | 20 | female | right | TS005 | 29 | male | right | TS040 | 23 | female | right |
| KN16 | 27 | male | left | TS008 | 20 | female | right | TS044 | 20 | male | left |
| KN17 | 24 | male | left | TS010 | 26 | male | right | TS048 | 27 | male | right |
| KN18 | 26 | male | right | TS017 | 29 | male | right | TS050 | 21 | female | right |
| KN20 | 27 | male | right | TS019 | 25 | male | right | TS057 | 33 | male | right |
| KN21 | 28 | male | right | TS021 | 27 | male | right | TS061 | 29 | male | right |
| KN22 | 26 | male | right | TS031 | 50 | male | right | TS067 | 36 | female | right |
| KN23 | 22 | male | right | TS032 | 24 | male | right | | | | |
| KN25 | 22 | female | right | TS036 | 27 | female | right | | | | |
| TS002 | 31 | male | right | TS049 | 26 | male | right | | | | |
| TS003 | 30 | female | right | TS053 | 29 | male | right | | | | |
| TS012 | 19 | male | right | TS054 | 21 | female | right | | | | |
| TS014 | 26 | male | right | TS059 | 35 | female | right | | | | |
| TS015 | 30 | female | right | TS062 | 36 | male | right | | | | |
| TS016 | 26 | female | right | TS068 | 25 | male | right | | | | |
| TS024 | 27 | male | right | TS070 | 20 | female | right | | | | |
| TS025 | 27 | male | right | TS073 | 44 | female | right | | | | |
| TS027 | 24 | female | right | | | | | | | | |
| TS028 | 26 | male | right | | | | | | | | |
| TS029 | 45 | female | right | | | | | | | | |
| TS030 | 27 | male | right | | | | | | | | |
| TS039 | 26 | female | right | | | | | | | | |
| TS041 | 25 | female | left | | | | | | | | |
| TS042 | 31 | male | right | | | | | | | | |
| TS047 | 28 | female | right | | | | | | | | |
| TS056 | 22 | male | right | | | | | | | | |
| TS060 | 24 | female | right | | | | | | | | |
| TS063 | 35 | female | right | | | | | | | | |
| TS071 | 27 | female | right | | | | | | | | |
| TS072 | 33 | male | right | | | | | | | | |

***Appendix C:*** *Participants demographic data – Study I. Modified according to (Hofmeier et al., 2021).*

| T-group | GHS Score | Right | Left | Both Sides | Right | | Left | |
|---|---|---|---|---|---|---|---|---|
| | | | | | Hz | dB | Hz | dB |
| T001 | 0 | low | moderate | moderate | 8000 | 15 | 8000 | 15 |
| T002 | 3 | low | low | --- | 10.000 | 6 | 10.000 | 4 |
| T006 | 21 | moderate | moderate | --- | 6000 | 27 | 6000 | 27 |
| T009 | 7 | --- | moderate | --- | --- | --- | 8000 | 34 |
| TN01 | 24 | moderate | --- | --- | 10.000 | 35 | --- | --- |
| TN03 | 48 | --- | low | --- | --- | --- | 10.000 | 31 |
| TN04 | 7 | inaudible | inaudible | --- | 4000 | 5 | 4000 | 6 |
| TN05 | 12 | very low | inaudible | --- | 10.000 | 28 | --- | --- |
| TN08 | 13 | inaudible | inaudible | very low | 10.000 | 13 | 10.000 | 10 |
| TN10 | 7 | inaudible | inaudible | inaudible | 4000 | 12 | 8000 | 7 |
| TN11 | 10 | very low | very low | very low | 6000 | 14 | 8000 | 7 |
| TN16 | 19 | high | low | moderate | 8000 | 15 | 6000 | 3 |
| TS004 | 22 | --- | low | --- | --- | --- | 10000 | 13 |
| TS005 | 7 | moderate | low | inaudible | 3000 | 15 | 3000 | 21 |
| TS008 | 19 | --- | moderate | --- | --- | --- | 500 | 10 |
| TS010 | 13 | --- | --- | low | 8000 | 14 | 8000 | 18 |
| TS017 | 18 | inaudible | low | low | 6000 | 18 | 6000 | 14 |
| TS019 | 7 | --- | --- | very low | 2000 | 14 | 2000 | 11 |
| TS021 | 10 | low | low | inaudible | 8000 | 13 | 8000 | 15 |
| TS031 | 38 | high | high | --- | 6000 | 34 | 6000 | 34 |
| TS032 | 4 | moderate | --- | inaudible | 8000 | 57 | --- | --- |
| TS036 | 5 | very low | --- | inaudible | 1500 | 15 | --- | --- |
| TS049 | 15 | low | very low | low | 4000 | 5 | 4000 | 1 |
| TS053 | 16 | --- | very low | --- | 6000 | 17 | 6000 | 17 |
| TS054 | 9 | low | very low | low | 6000 | 11 | 8000 | 9 |
| TS059 | 13 | moderate | low | --- | 3000 | 23 | 3000 | 26 |
| TS062 | 9 | --- | low | very low | --- | --- | 8000 | 8 |
| TS068 | 8 | low | --- | inaudible | 4000 | 24 | --- | --- |
| TS070 | 26 | inaudible | | inaudible | 500 | 16 | --- | --- |
| TS073 | 6 | very low | --- | --- | 125 | 11 | --- | --- |

| TH-group | GHS Score | Right | Left | Both Sides | Right | | Left | |
|---|---|---|---|---|---|---|---|---|
| | | | | | Hz | dB | Hz | dB |
| TN12 | 18 | low | very low | very low | 1000 | 11 | 8000 | 22 |
| TN13 | 9 | --- | very low | --- | --- | --- | 10000 | 5 |
| TN17 | 31 | very low | very low | very low | 8000 | 8 | 8000 | 8 |
| TN19 | 16 | low | --- | --- | 10000 | 20 | --- | --- |
| TN20 | 30 | low | high | inaudible | 10000 | 21 | 1000 | 16 |
| TN21 | 19 | very low | very low | moderate | 1000 | 11 | 750 | 13 |
| TN22 | 45 | moderate | moderate | --- | 6000 | 9 | 6000 | 10 |
| TN23 | 31 | low | low | --- | 1000 | 13 | 10000 | 9 |
| TN25 | 23 | low | moderate | inaudible | 4000 | 15 | 4000 | 15 |
| TN28 | 28 | high | moderate | inaudible | 8000 | 40 | 6000 | 23 |
| TS020 | 35 | --- | moderate | --- | --- | --- | 6000 | 20 |
| TS033 | 32 | low | moderate | low | 6000 | 10 | 6000 | 18 |
| TS037 | 53 | high | very low | low | 4000 | 15 | 4000 | 20 |
| TS040 | 27 | low | moderate | --- | 8000 | 9 | 6000 | 11 |
| TS044 | 23 | --- | inaudible | inaudible | --- | --- | 750 | 5 |
| TS048 | 32 | --- | --- | moderate | 8000 | 30 | 6000 | 9 |
| TS050 | 22 | low | low | --- | 6000 | 2 | 6000 | 1 |
| TS057 | 18 | moderate | moderate | inaudible | 6000 | 9 | 6000 | 25 |
| TS061 | 57 | moderate | moderate | inaudible | 10000 | 15 | 10000 | 16 |
| TS067 | 23 | very low | inaudible | inaudible | 1500 | 10 | 4000 | 12 |

***Appendix D:*** *Individual tinnitus localisation (frequency and loudness) – Study I. Modified according to (Hofmeier et al., 2021).*

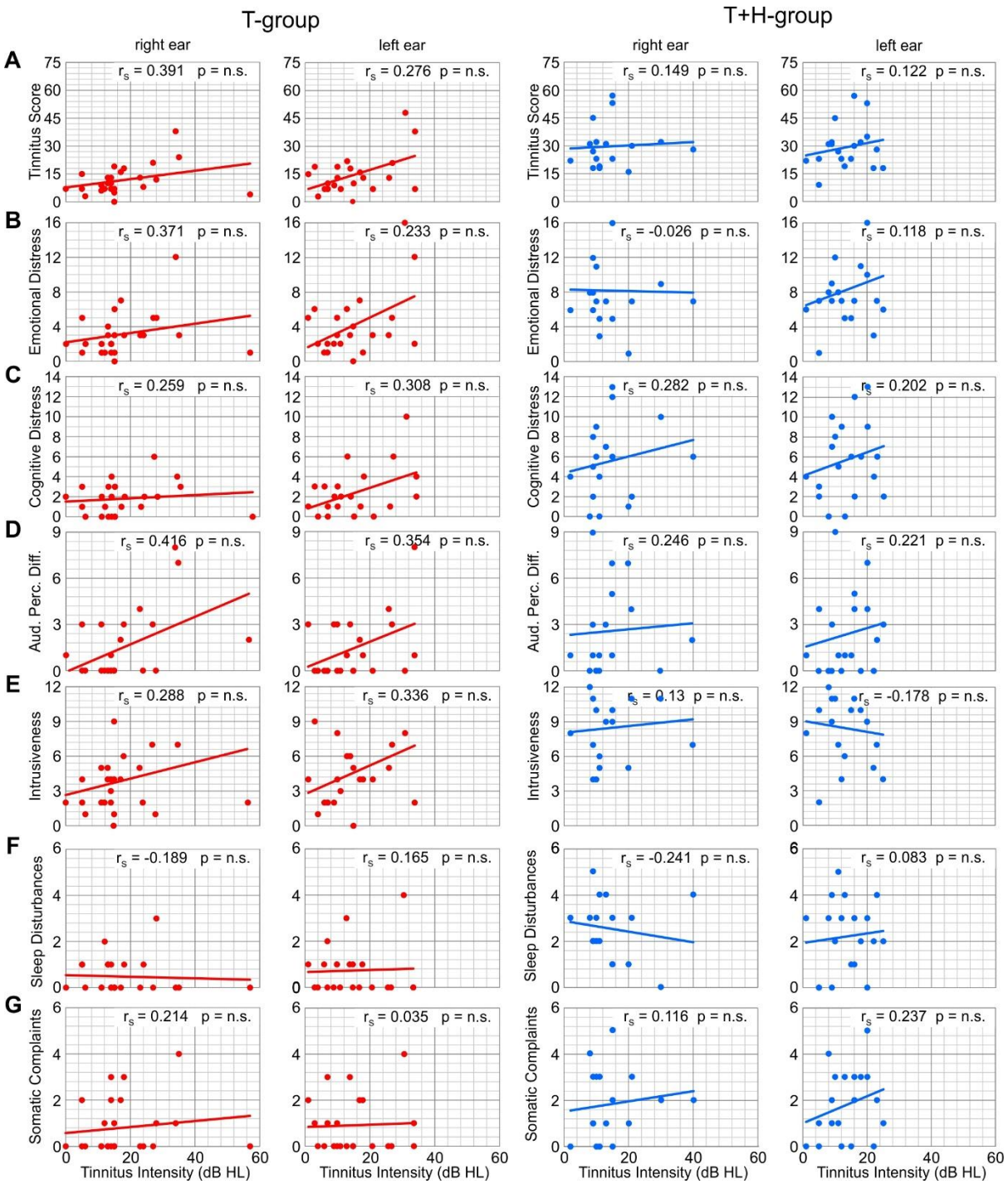


***Appendix E:*** *The correlation between the sub-scores of the (GHS) and tinnitus loudness. Two-tailed Spearman correlation of tinnitus loudness (n depends on the perception of tinnitus in the respective ear) with tinnitus questionnaire sub-scores (A-H) in T-group (n = 24 for the right and left ear, red) and TH-group (n = 17 for the right ear, n = 19 for the left ear, blue). Adjusted p values by FDR correction for multiple testing. (A) Total tinnitus score, (B) emotional distress, (C) cognitive distress, (D) auditory perceptual difficulties, (E) intrusiveness, (F) sleep disturbances and (G) somatic complaints.*

| C-group | | | | T-group <1yr | | | | | TH-group <1yr | | | | |
|---|---|---|---|---|---|---|---|---|---|---|---|---|---|
| No | age | sex | hand | No | age | sex | hand | duration | No | age | sex | hand | duration |
| C1 | 27 | m | r | T1 | 33 | m | r | 0.5 | TH1 | 24 | f | r | 0.25 |
| C2 | 41 | f | l | T2 | 27 | f | r | 0.5 | TH2 | 21 | f | r | 0.5 |
| C3 | 22 | m | r | T3 | 61 | m | r | 0.5 | TH3 | 49 | m | l | 0.5 |
| C4 | 27 | m | l | T4 | 25 | m | r | 0.6 | TH4 | 27 | m | r | 0.5 |
| C5 | 19 | m | r | T5 | 34 | m | l | 0.8 | TH5 | 21 | f | l | 0.8 |
| C6 | 18 | m | r | T6 | 31 | m | r | 1 | TH6 | 21 | f | r | 1 |
| C7 | 39 | m | r | | | | | | TH7 | 33 | m | r | 1 |
| C8 | 26 | m | r | | | | | | TH8 | 36 | f | r | 1 |
| C9 | 24 | f | r | | | | | | | | | | |
| C10 | 21 | f | r | T-group 1-5yr | | | | | TH-group 1-5 yr | | | | |
| C11 | 28 | m | r | No | age | f/m | hand | duration | No | age | sex | hand | duration |
| C12 | 31 | m | r | T7 | 26 | m | r | 1.5 | TH9 | 26 | f | r | 1.2 |
| C13 | 30 | f | r | T8 | 36 | m | r | 1.5 | TH10 | 20 | m | l | 1.5 |
| C14 | 19 | m | r | T9 | 50 | m | r | 1.6 | TH11 | 22 | f | r | 2.8 |
| C15 | 26 | m | r | T10 | 20 | f | r | 2 | TH12 | 29 | m | r | 3.5 |
| C16 | 26 | f | r | T11 | 31 | f | l | 2 | | | | | |
| C17 | 27 | m | r | T12 | 20 | f | r | 2.5 | | | | | |
| C18 | 27 | m | r | T13 | 56 | f | r | 2.5 | | | | | |
| C19 | 24 | f | r | T14 | 24 | m | r | 3 | | | | | |
| C20 | 26 | m | r | T15 | 44 | f | r | 3 | | | | | |
| C21 | 45 | f | r | | | | | | | | | | |
| C22 | 27 | f | r | T-group 5-10 years | | | | | TH-group 5-10 years | | | | |
| C23 | 26 | f | r | No | age | f/m | hand | duration | No | age | sex | hand | duration |
| C24 | 32 | f | r | T16 | 25 | f | r | 5 | TH14 | 24 | m | r | 5 |
| C25 | 21 | f | r | T17 | 44 | m | r | 6 | TH15 | 34 | f | r | 5 |
| C26 | 23 | f | r | T18 | 21 | f | r | 6 | TH16 | 24 | f | r | 6 |
| C27 | 18 | f | r | T19 | 23 | m | l | 6 | TH17 | 23 | f | r | 6 |
| C28 | 20 | f | r | T20 | 21 | m | r | 7 | TH14 | 30 | f | r | 8 |
| C29 | 20 | f | r | T21 | 26 | m | r | 7 | | | | | |
| C30 | 24 | m | l | T22 | 27 | m | r | 7 | | | | | |
| C31 | 26 | m | r | T23 | 49 | m | r | 7 | | | | | |
| C32 | 22 | f | r | T24 | 25 | f | r | 8 | | | | | |
| C33 | 26 | f | r | | | | | | | | | | |
| C34 | 25 | f | l | T-group >10yr | | | | | TH-group >10yr | | | | |
| C35 | 31 | m | r | No | age | sex | hand | duration | No | age | sex | hand | duration |
| C36 | 28 | f | r | T25 | 29 | m | r | 10 | TH18 | 24 | f | r | 12 |
| C37 | 22 | m | r | T26 | 36 | m | l | 11 | TH19 | 23 | f | r | 13 |
| C38 | 35 | f | r | T27 | 29 | m | r | 14 | TH20 | 28 | f | r | 18 |
| C39 | 30 | f | r | T28 | 26 | m | l | 15 | | | | | |
| C40 | 27 | m | r | T29 | 29 | m | r | 15 | | | | | |
| C41 | 24 | f | r | T30 | 61 | f | r | 15 | | | | | |
| C42 | 27 | f | r | T31 | 35 | f | r | 19 | | | | | |
| C43 | 33 | m | r | T32 | 27 | m | r | 21 | | | | | |
| | | | | T33 | 26 | m | r | 22 | | | | | |

***Appendix F:*** *Participants demographic data – Study II: f, female; m, male; hand, handedness; l, left-handed; r, right-handed; duration, time of tinnitus persistence. Modified according to (Refat et al., 2021).*

| Study group | GHS | HKI | Hz (right) | dB (right) | Hz (left) | dB (left) |
|---|---|---|---|---|---|---|
| T1 | 12 | 7 | 10.000 | 28 | --- | --- |
| T2 | 5 | 4 | 1500 | 15 | --- | --- |
| T3 | 10 | 7 | 4000 | 23 | --- | --- |
| T4 | 8 | 3 | 4000 | 24 | --- | --- |
| T5 | 48 | 5 | --- | --- | 10.000 | 31 |
| T6 | 17 | 5 | 6000 | 30 | 6000 | 70 |
| T7 | 13 | 7 | 8000 | 14 | 8000 | 18 |
| T8 | 9 | 3 | --- | --- | 8000 | 8 |
| T9 | 38 | 8 | 6000 | 34 | 6000 | 34 |
| T10 | 26 | 6 | 500 | 16 | | |
| T11 | 7 | 7 | 8000 | 31 | --- | --- |
| T12 | 19 | 6 | --- | --- | 500 | 10 |
| T13 | 6 | 3 | 6000 | 19 | 6000 | 38 |
| T14 | 4 | 1 | 8000 | 57 | --- | --- |
| T15 | 6 | 6 | 125 | 11 | --- | --- |
| T16 | 7 | 7 | 4000 | 12 | 8000 | 7 |
| T17 | 22 | 4 | --- | --- | 1000 | 13 |
| T18 | 9 | 9 | 6000 | 11 | 8000 | 9 |
| T19 | 7 | 11 | 4000 | 5 | 4000 | 6 |
| T20 | 3 | 3 | 10.000 | 6 | 10.000 | 4 |
| T21 | 24 | 8 | 10.000 | 35 | --- | --- |
| T22 | 10 | 2 | 8000 | 13 | 8000 | 15 |
| T23 | 4 | 6 | 10.000 | 47 | 10.000 | 48 |
| T24 | 10 | 7 | 6000 | 14 | 8000 | 7 |
| T25 | 18 | 9 | 6000 | 18 | 6000 | 14 |
| T26 | 0 | 0 | 8000 | 15 | 8000 | 15 |
| T27 | 16 | 11 | 6000 | 17 | 6000 | 17 |
| T28 | 19 | 9 | 8000 | 15 | 6000 | 3 |
| T29 | 7 | 6 | 3000 | 15 | 3000 | 21 |
| T30 | 44 | 8 | 4000 | 41 | 3000 | 26 |
| T31 | 13 | 11 | 3000 | 23 | 3000 | 26 |
| T32 | 13 | 8 | 10.000 | 13 | 10.000 | 10 |
| T33 | 15 | 5 | 4000 | 5 | 4000 | 1 |
| TH1 | 35 | 12 | --- | --- | 6000 | 20 |
| TH2 | 45 | 14 | 6000 | 9 | 6000 | 10 |
| TH3 | 32 | 15 | 6000 | 10 | 6000 | 18 |
| TH4 | 32 | 18 | 8000 | 30 | 6000 | 9 |
| TH5 | 9 | 12 | --- | --- | 10000 | 5 |
| TH6 | 22 | 15 | 6000 | 2 | 6000 | 1 |
| TH7 | 18 | 15 | 6000 | 9 | 6000 | 25 |
| TH8 | 23 | 25 | 1500 | 10 | 4000 | 12 |
| TH9 | 31 | 12 | 8000 | 8 | 8000 | 8 |
| TH10 | 23 | 17 | --- | --- | 750 | 5 |
| TH11 | 23 | 12 | 4000 | 15 | 4000 | 15 |
| TH12 | 57 | 20 | 10000 | 15 | 10000 | 16 |
| TH14 | 18 | 15 | 1000 | 11 | 8000 | 22 |
| TH15 | 16 | 18 | 10000 | 20 | --- | --- |
| TH16 | 19 | 14 | 1000 | 11 | 750 | 13 |
| TH17 | 53 | 22 | 4000 | 15 | 4000 | 20 |
| TH14 | 28 | 13 | 8000 | 40 | 6000 | 23 |
| TH18 | 31 | 19 | 1000 | 13 | 10000 | 9 |
| TH19 | 27 | 15 | 8000 | 9 | 6000 | 11 |
| TH20 | 30 | 19 | 10000 | 21 | 1000 | 16 |

***Appendix G:*** *Individual tinnitus localisation (frequency and loudness) – Study II. GHS, score from Goebel-Hiller tinnitus Questionnaire; ---, inaudible. Modified according to (Refat et al., 2021).*

| Subject | Age | Gender | Handedness | HKI | HKI [Quart] | LDL [Quart] |
|---|---|---|---|---|---|---|
| | | | C-group | | | |
| 'TS002' | 31 | male | right | 5 | None | Mild |
| 'TS003' | 30 | female | right | 3 | None | Moderate |
| 'TS012' | 19 | male | right | 4 | None | Mild |
| 'TS014' | 26 | male | right | 0 | None | Mild |
| 'TS015' | 30 | female | right | 9 | Mild | Mild |
| 'TS016' | 26 | female | right | 4 | None | Mild |
| 'TS024' | 27 | male | right | 4 | None | None |
| 'TS025' | 27 | male | right | 4 | None | Mild |
| 'TS027' | 24 | female | right | 2 | None | Mild |
| 'TS028' | 26 | male | right | 9 | Mild | Mild |
| 'TS029' | 45 | female | right | 7 | None | Mild |
| 'TS030' | 27 | male | right | 1 | None | Mild |
| 'TS039' | 26 | female | right | 7 | None | Mild |
| 'TS041' | 25 | female | left | 4 | None | Moderate |
| 'TS042' | 30 | male | right | 3 | None | Mild |
| 'TS047' | 28 | female | right | 7 | None | Mild |
| 'TS056' | 22 | male | right | 3 | None | Mild |
| 'TS060' | 24 | female | right | 3 | None | Mild |
| 'TS063' | 35 | female | right | 2 | None | Moderate |
| 'TS071' | 27 | female | right | 6 | None | Moderate |
| 'TS072' | 33 | male | right | 6 | None | Mild |
| 'TS074' | 36 | male | right | 1 | None | None |
| 'TS076' | 26 | male | right | 3 | None | Mild |
| 'TS077' | 31 | male | right | 11 | Mild | None |
| 'TS078' | 28 | female | right | 2 | None | Moderate |
| 'TS083' | 25 | female | right | 4 | None | None |
| 'TS084' | 30 | female | right | 2 | None | Mild |
| 'TS089' | 27 | female | right | 4 | None | Moderate |
| 'TS099' | 23 | male | right | 2 | None | None |
| 'TS100' | 28 | female | right | 2 | None | Moderate |
| 'TS103' | 25 | female | right | 1 | None | None |
| 'TS107' | 27 | female | right | 3 | None | None |
| 'TS131' | 39 | female | right | 3 | None | Moderate |
| 'TS145' | 25 | male | right | 6 | None | Moderate |
| 'TS146' | 25 | male | left | 3 | None | Mild |
| 'TS150' | 25 | female | right | 4 | None | Moderate |
| 'TS151' | 24 | female | left | 0 | None | None |
| 'TS153' | 25 | female | right | 4 | None | Mild |
| 'TS154' | 22 | male | right | 5 | None | Mild |
| 'TS004' | 44 | male | right | 4 | None | Moderate |
| 'TS005' | 29 | male | right | 6 | None | None |
| 'TS010' | 26 | male | right | 7 | None | None |
| 'TS017' | 29 | male | right | 9 | Mild | Mild |
| 'TS021' | 27 | male | right | 2 | None | Mild |

| Subject | Age | Gender | Handedness | HKI | HKI [Quart] | LDL [Quart] |
|---|---|---|---|---|---|---|
| | | | T-group | | | |
| 'TS031' | 50 | male | right | 8 | None | Moderate |
| 'TS036' | 27 | female | right | 4 | None | Mild |
| 'TS044' | 20 | male | right | 17 | Moderate | None |
| 'TS049' | 26 | male | right | 5 | None | None |
| 'TS054' | 21 | female | right | 9 | Mild | None |
| 'TS057' | 33 | male | right | 15 | Moderate | Moderate |
| 'TS059' | 35 | female | right | 11 | Mild | Mild |
| 'TS062' | 36 | male | right | 3 | None | None |
| 'TS068' | 25 | male | right | 3 | None | Moderate |
| 'TS070' | 20 | female | right | 6 | None | Mild |
| 'TS073' | 44 | female | right | 6 | None | Mild |
| 'TS079' | 25 | male | right | 2 | None | None |
| 'TS080' | 30 | male | right | 8 | None | None |
| 'TS082' | 27 | male | right | 6 | None | Mild |
| 'TS085' | 29 | male | right | 4 | None | Moderate |
| 'TS086' | 22 | female | right | 0 | None | Mild |
| 'TS087' | 28 | female | right | 6 | None | None |
| 'TS090' | 28 | female | right | 6 | None | Moderate |
| 'TS091' | 35 | male | right | 0 | None | None |
| 'TS094' | 28 | male | right | 11 | Mild | Mild |
| 'TS095' | 27 | male | right | 8 | None | Mild |
| 'TS097' | 33 | male | right | 10 | Mild | Mild |
| 'TS098' | 32 | female | right | 1 | None | Mild |
| 'TS121' | 51 | female | right | 13 | Mild | Mild |
| 'TS137' | 29 | male | right | 10 | Mild | Mild |

| Subject | Age | Gender | Handedness | HKI | HKI [Quart] | LDL [Quart] |
|---|---|---|---|---|---|---|
| | | | TH-group | | | |
| 'TS020' | 24 | female | right | 12 | Mild | Moderate |
| 'TS033' | 49 | male | left | 15 | Moderate | Moderate |
| 'TS037' | 23 | female | right | 22 | Severe | Mild |
| 'TS040' | 23 | female | right | 15 | Moderate | Severe |
| 'TS048' | 27 | male | right | 18 | Moderate | Severe |
| 'TS050' | 21 | female | right | 15 | Moderate | Severe |
| 'TS053' | 29 | female | right | 11 | Mild | Moderate |
| 'TS061' | 29 | male | right | 20 | Severe | Severe |
| 'TS067' | 36 | female | right | 25 | Severe | Severe |
| 'TS088' | 24 | male | right | 16 | Moderate | Moderate |
| 'TS102' | 36 | female | right | 10 | Mild | Moderate |
| 'TS104' | 55 | female | right | 16 | Moderate | Severe |
| 'TS105' | 57 | female | right | 10 | Mild | Severe |
| 'TS125' | 43 | female | left | 16 | Moderate | Severe |
| 'TS140' | 23 | female | right | 10 | Mild | Moderate |

| Subject | Age | Gender | Handedness | HKI | HKI [Quart] | LDL [Quart] |
|---|---|---|---|---|---|---|
| | | | TH-group | | | |
| 'TS141' | 25 | male | right | 14 | Moderate | Mild |
| 'TS147' | 20 | female | right | 9 | Mild | Severe |
| 'TS020' | 24 | female | right | 12 | Mild | Moderate |
| 'TS033' | 49 | male | left | 15 | Moderate | Moderate |
| 'TS037' | 23 | female | right | 22 | Severe | Mild |
| 'TS040' | 23 | female | right | 15 | Moderate | Severe |

***Appendix H:*** *Subject information to age, gender, handedness, hyperacusis self-report, and hyperacusis classification with Hyperacusis Inventory (HKI) and loudness discomfort level (LDL). HKI [Quart], quartile of hyperacusis burden (Goldstein and Shulman, 1996); LDL [Quart], quartile of LDL burden (Berthold-Scholz, 2013); T lateral., tinnitus laterality).*

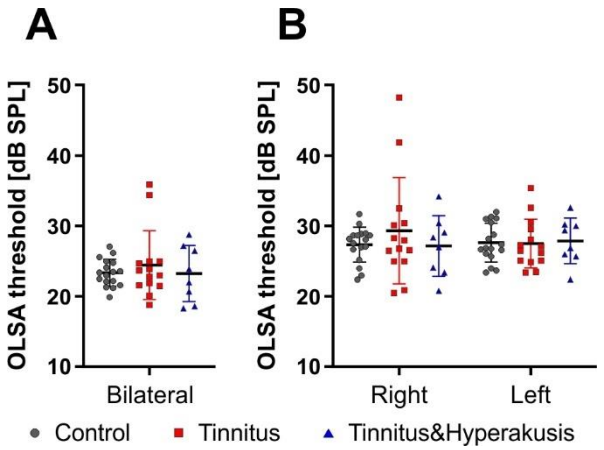


***Appendix I:*** *Speech perception is expressed as speech reception threshold at 50 % correct word recognition in individual values, mean and SD in dB HL for (A) bilateral stimulation without noise and (B) unilateral stimulation with contralateral 65 dB noise.*

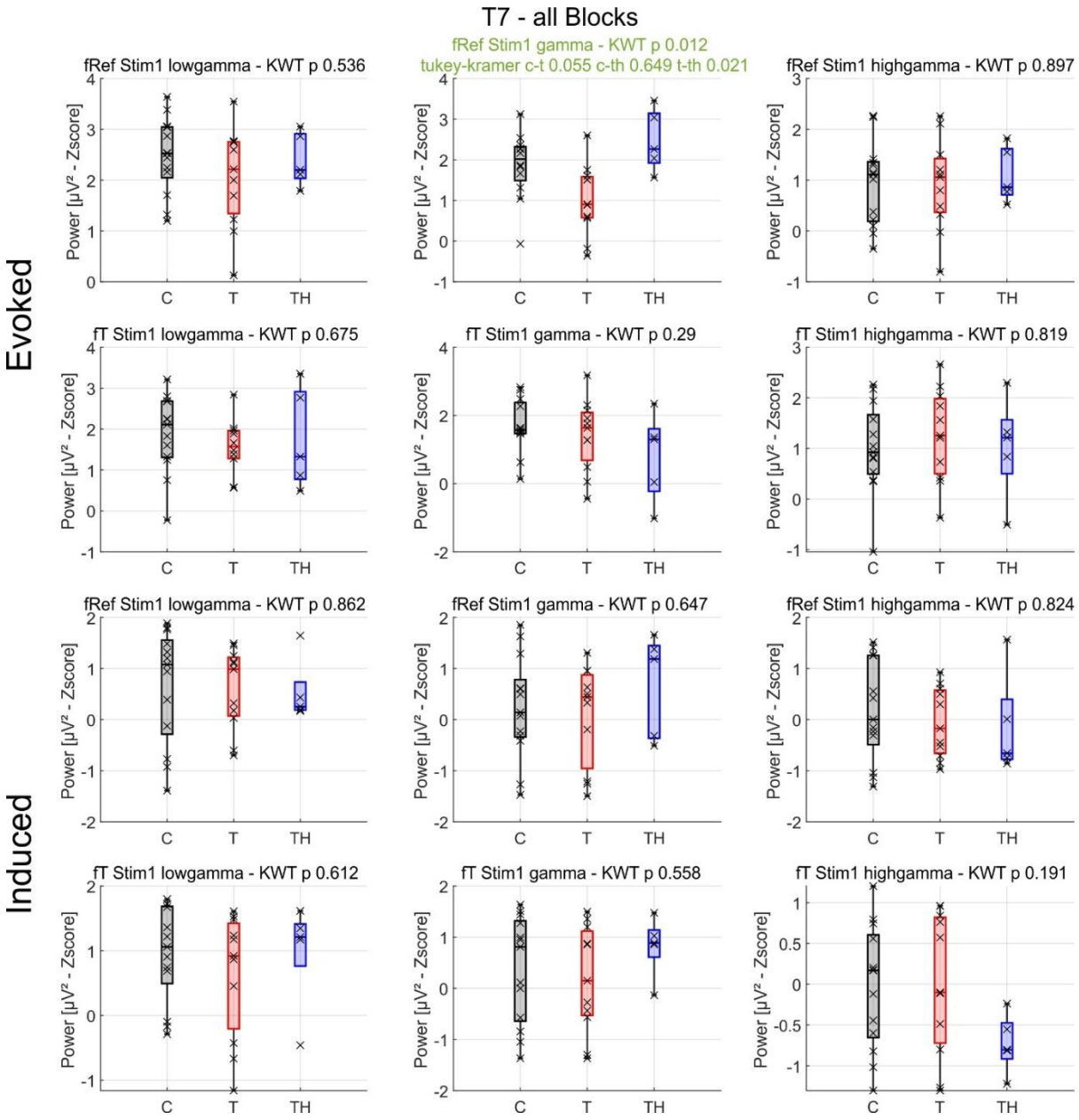


***Appendix J:*** *Evoked (first and second panels) and induced (third and fourth panels) power of low- (21-40 Hz), mid- (41-60 Hz), and high- (61-120 Hz) gamma in the T7 electrode position for the first stimulus in reference frequency (fRef) and individual tinnitus frequency (fTin). The bar charts depicted in the figure present the median and quartiles (box) for C- (grey), T- (red), and TH-group (blue). In case a statistical trend ($p < 0.1$) is observed through the Kruskal-Wallis test, p values of Dunn's multiple comparison tests are provided in the figure heading (highlighted in green).*

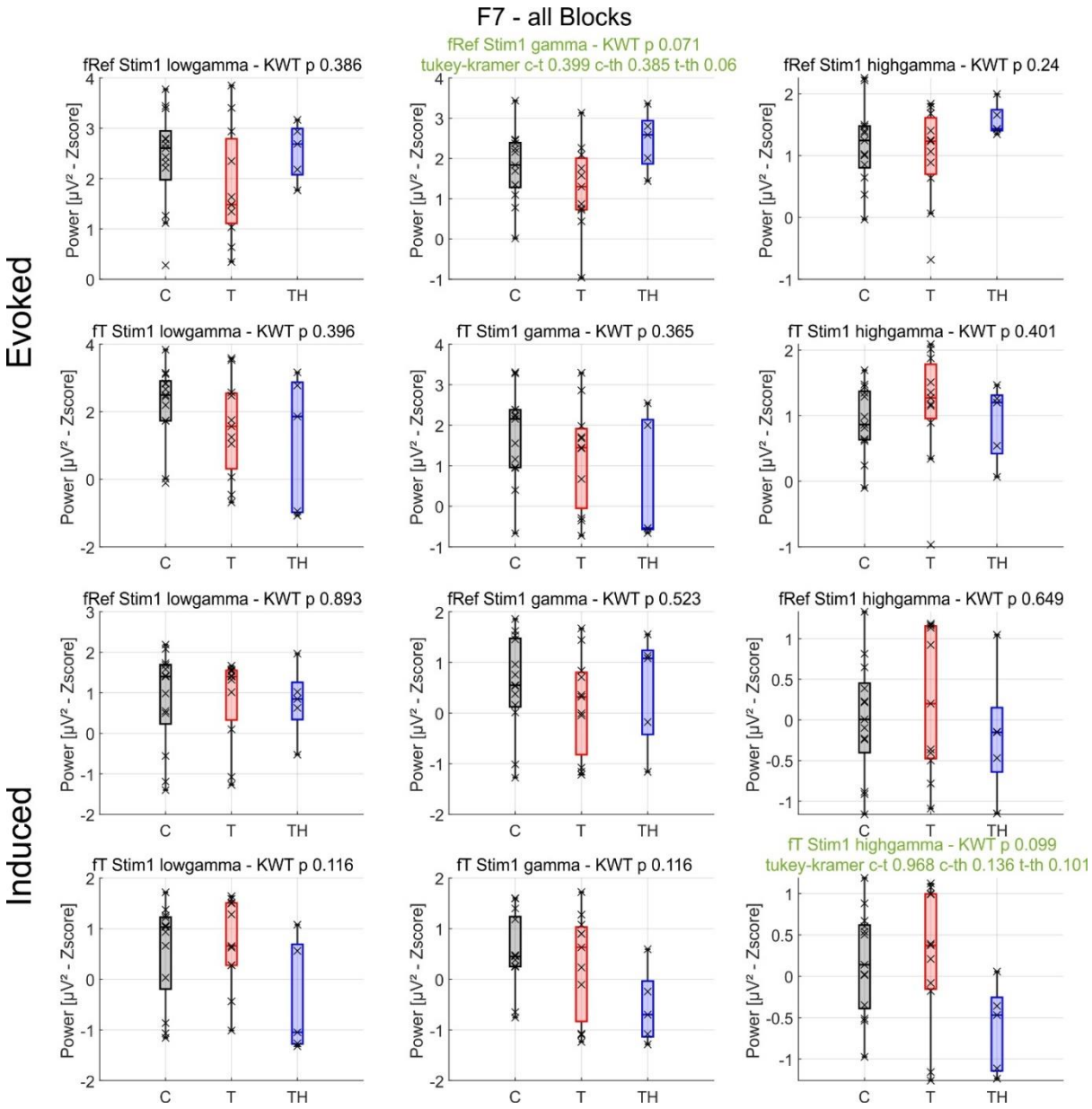


***Appendix K:*** *Evoked (first and second panels) and induced (third and fourth panels) power of low- (21-40 Hz), mid- (41-60 Hz), and high- (61-120 Hz) gamma in the F7 electrode position for the first stimulus in reference frequency (fRef) and individual tinnitus frequency (fTin). The bar charts depicted in the figure present the median and quartiles (box) for C- (grey), T- (red), and TH-group (blue). In case a statistical trend ($p < 0.1$) is observed through the Kruskal-Wallis test, p values of Dunn's multiple comparison tests are provided in the figure heading (highlighted in green).*

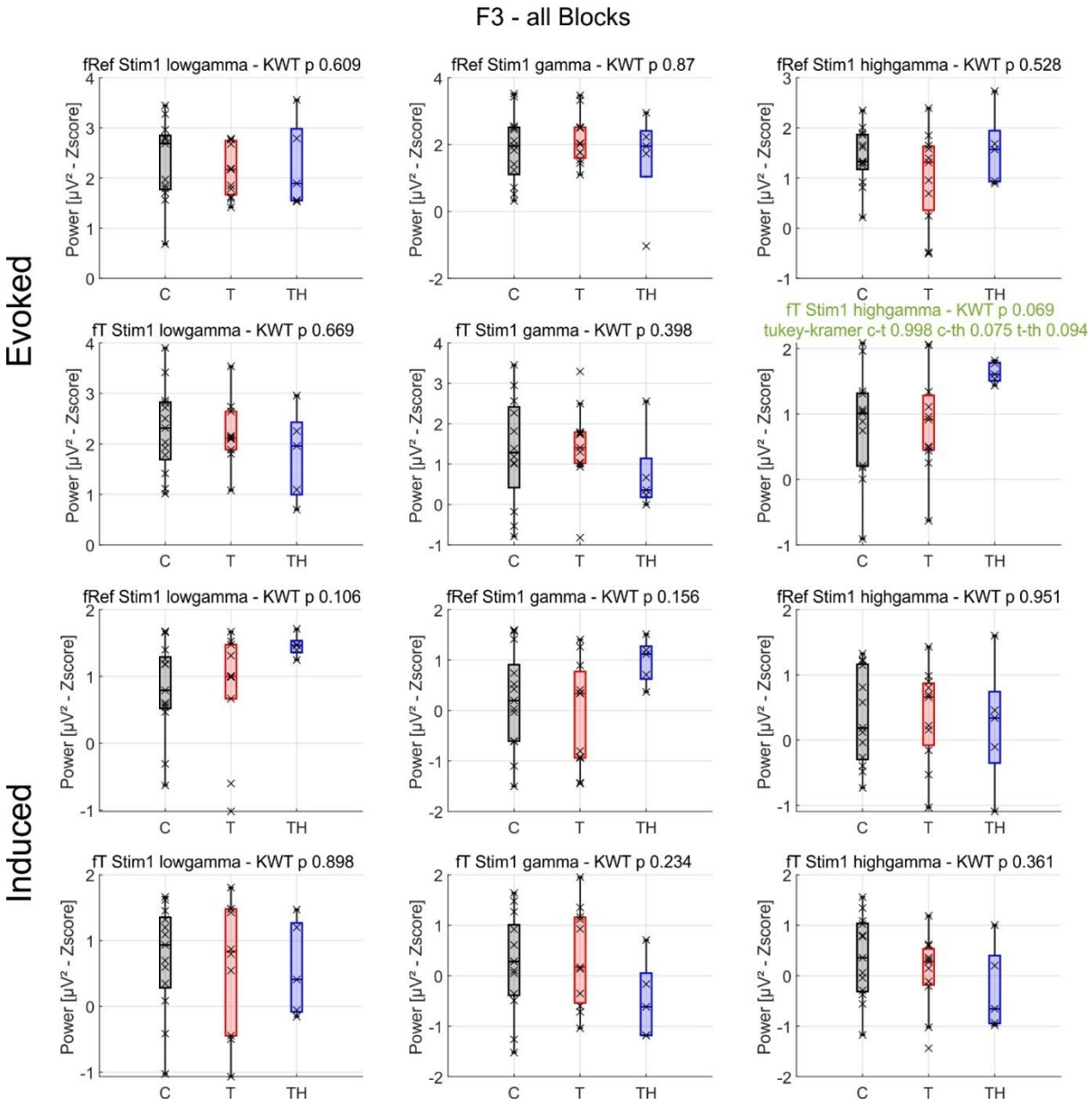


***Appendix L:*** *Evoked (first and second panels) and induced (third and fourth panels) power of low- (21-40 Hz), mid- (41-60 Hz), and high- (61-120 Hz) gamma in the F3 electrode position for the first stimulus in reference frequency (fRef) and individual tinnitus frequency (fTin). The bar charts depicted in the figure present the median and quartiles (box) for C- (grey), T- (red), and TH-group (blue). In case a statistical trend ($p < 0.1$) is observed through the Kruskal-Wallis test, p values of Dunn's multiple comparison tests are provided in the figure heading (highlighted in green).*

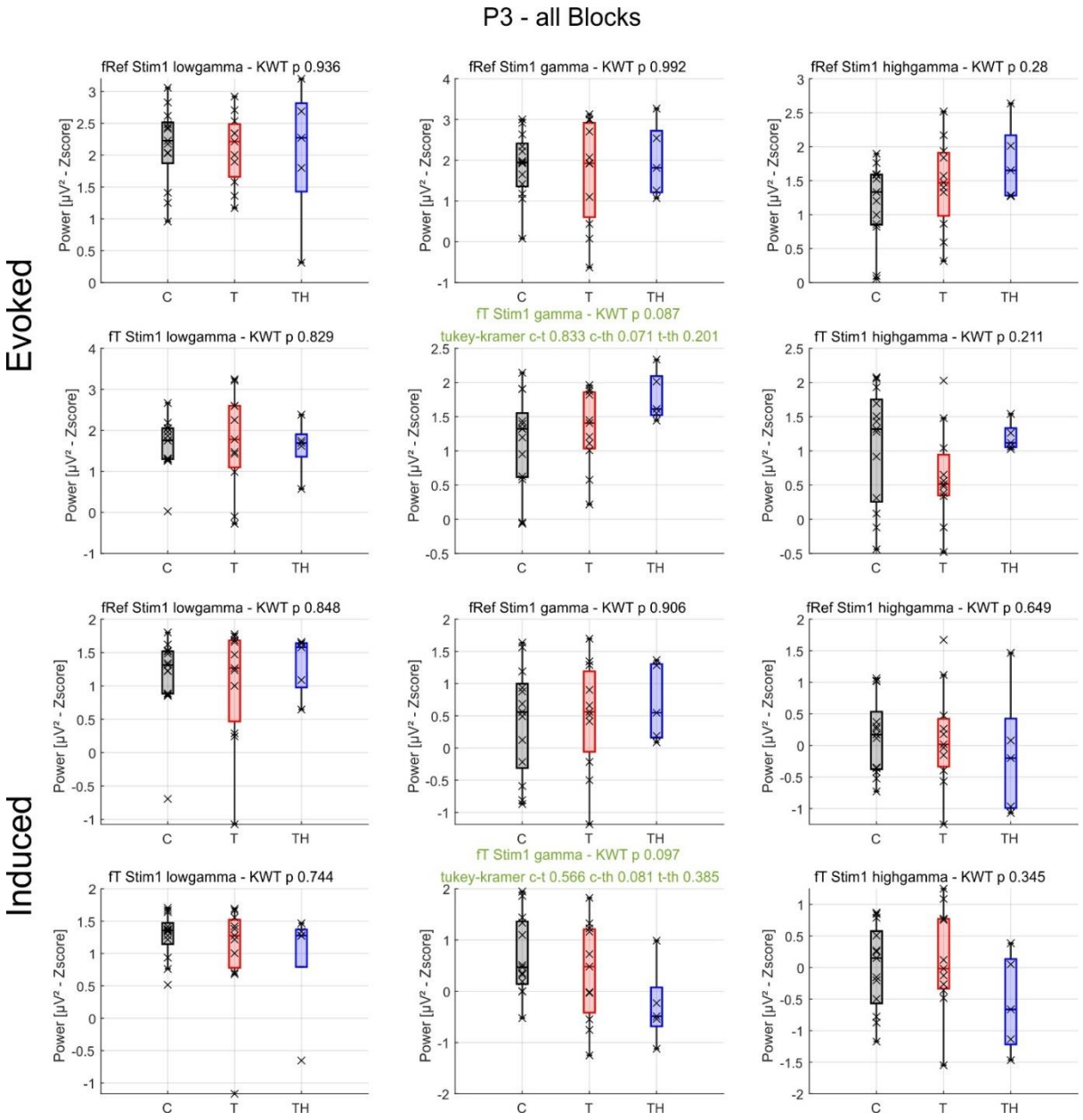


***Appendix M:*** *Evoked (first and second panels) and induced (third and fourth panels) power of low- (21-40 Hz), mid- (41-60 Hz), and high- (61-120 Hz) gamma in the P3 electrode position for the first stimulus in reference frequency (fRef) and individual tinnitus frequency (fTin). The bar charts depicted in the figure present the median and quartiles (box) for C- (grey), T- (red), and TH-group (blue). In case a statistical trend ($p < 0.1$) is observed through the Kruskal-Wallis test, p values of Dunn's multiple comparison tests are provided in the figure heading (highlighted in green).*